2021

Analytical Methods to Investigate Exact Solutions for Space-Time Fractional Differential Equations Arising in the Real Physical Phenomena of Mathematical Physics and Biology

Rahman, Zillur
University of Rajshahi, Rajshahi

Analytical Methods to Investigate Exact Solutions for Space-Time Fractional Differential Equations Arising in the Real Physical Phenomena of Mathematical Physics and Biology

Rajshahi University

Thesis submitted to the Department of Mathematics, University of Rajshahi, Rajshahi-6205, Bangladesh, for the partial fulfillment of the requirement for the degree of

MASTER OF PHILOSOPHY
IN
MATHEMATICS

Submitted By

Zillur Rahman

Id-1813021502
Session-2017-2018
Department of Mathematics
University of Rajshahi
Rajshahi-6205, Bangladesh.

Supervisor
Professor Dr. M. Zulfikar Ali
Department of Mathematics
University of Rajshahi
Rajshahi-6205

Co-Supervisor
Professor Dr. Harun-Or-Roshid
Department of Mathematics
Pabna University of Science and Technology
Pabna-6600

April-2021

Dedicated

To

My Parents and Beloved daughter

who are the main source of my inspiration to

walk forward.

ACKNOWLEDGEMENT

I am grateful to numerous persons who have contributed towards shaping this thesis.

At the outset, I would like to express my appreciation and deepest respect to my supervisor Professor Dr. M. Zulfikar Ali, Department of mathematics, University of Rajshahi, Rajshahi, Bangladesh for his advice during my M.Phil research. As my supervisor, he has constantly forced me to remain focused on achieving my goal. His observations and comments helped me to establish the overall direction of the research and to move forward with investigation in depth. I thank him for providing me with the opportunity to work with a talented team of researchers.

Secondly, I would also wish to express my gratitude to my Co-supervisor Dr. Harun-Or-Rashid, Associate Professor, Department of mathematics, Pabna University of Science and Technology, Pabna, Bangladesh for giving me unconditional time, extended discussions and valuable suggestions which have contributed greatly to the improvement of the thesis.

I wish to thanks the Chairman, Department of mathematics, University of Rajshahi, Rajshahi for providing all types of facilities during the course of my thesis work. I also wish to express my sincere admiration, appreciation and gratitude to all the teachers of the Department of mathematics, University of Rajshahi, Rajshahi for providing me invaluable suggestions during the period my research work.

A special thank will go to my colleagues at Comilla University, Cumilla for friendly support me to overcome the M.Phil program.

At the end, I am very grateful to my parents, beloved daughter and wife for their moral and constant blessing, good advice and encouragement.

(Zillur Rahman)

Department of Mathematics

CERTIFICATE

We are certified that the M.Phil. thesis entitled "**Analytical Methods to Investigate Exact Solutions for Space-Time Fractional Differential Equations Arising in the Real Physical Phenomena of Mathematical Physics and Biology**" submitted by **Zillur Rahman** in fulfillment of the requirement for the degree of M.Phil. in Mathematics from the Department of Mathematics, University of Rajshahi, Rajshahi-6205, Bangladesh has been completed under our supervision. We believe that the research work is an original one and it has not submitted elsewhere for any degree.

We wish him a bright future and every success in life.

23.3.2021

Prof. Dr. M. Zulfikar Ali
Supervisor
Department of Mathematics
University of Rajshahi
Rajshahi-6205, Bangladesh.

23.03.2021

Dr. Harun-or-Roshid
Co-Supervisor
Associate Professor
Department of Mathematics
Pabna University of Science and Technology
Pabna-6600, Bangladesh.

Statement of Originality

'I hereby declare that this submission is my own work and to the best of my knowledge it contains no materials previously published or written by another person, or substantial proportions of material which have been accepted for the award of any other degree or diploma at any other educational institution, except where due acknowledgement is made in the thesis. Any contribution made to the research by others, with whom I have worked at Rajshahi University, Rajshahi or elsewhere, is explicitly acknowledged in the thesis. I also declare that the intellectual content of this thesis is the product of my own work, except to the extent that assistance from others in the project's design and conception or in style, presentation and linguistic expression is acknowledged.'

Zillur 23.03.2021

Zillur Rahman

M.Phil Research Fellow

Rajshahi University, Rajshahi

March, 2021

Contents

Abstract

Fractional derivatives are most important to accurate nonlinear modeling of various real-world difficulties in applied nonlinear science and engineering incidents especially in the fields of crystal, optics and quantum mechanics even in biological phenomena. The investigation of exact solutions of such nonlinear models has great important to visualize the nonlinear dynamics. We consider the space-time fractional nonlinear differential equations for pulse narrowing transmission lines model, the space-time fractional Equal-width (s-tfEW) and the space-time fractional Wazwaz-Benjamin-Bona-Mahony (s-tfWBBM), complex Schrodinger and biological population models, the complex time fractional Schrodinger equation (FSE) and low-pass electrical transmission lines equation (ETLE) are studied with the effective unified method, Jacobi elliptic expansion function integral technique, generalized Kudryshov technique, modified simple equation (MSE) method respectively. As a result, we get some solitary wave solutions in the form of hyperbolic and combo hyperbolic-trigonometric functions including both stable and unstable cases. We obtain kink wave, bright bell wave, dark bell wave, combo periodic-rogue waves, combo M-W shaped periodic-rogue waves in stable cases, and singular kink type in unstable solitonic natures. Lastly, we proposed an Improved Kudryashov method for solving any nonlinear fractional differential models. We apply the proposed approach to the nonlinear space-time fractional model leading wave spread in electrical transmission lines (s-tfETL), the space-time M-fractional Schrodinger-Hirota (s-tM-fSH) and the time fractional complex Schrodinger (tfcS) models to verify the effectiveness of the propose approach. The implementations of the introduced new technique on the models provide us periodic envelope, exponentially changeable soliton envelope, rational, combo periodic-soliton and combo rational-soliton solutions, which are much interesting phenomena in the nonlinear sciences. Beside the scientific derivation of the analytical findings, we represent the results graphically for clear visualization of the dynamical properties.

Chapter-1

Introduction

Various real-world difficulties in applied nonlinear science and engineering are formed via nonlinear evolution equations. Finding the soliton solutions of such nonlinear equations is a vital field of experimentation. Nonlinear fractional differential equations are also taking deep consideration for accurate modeling of the scientist and researchers in recent year. The investigation of exact solutions of such nonlinear partial differential equations plays an important role in the study of physical phenomena in various scientific and engineering fields, such as of quantum mechanics [1-3], nonlinear optical communications [4-5], plasma physics [6], fluid mechanics [7-8], nonlinear electric-transmission line [9-13], superconductivity and Bose-Einstein condensates [14], signal processing [15], Biological dynamics [16], electro-magnetic waves [17], neuron networks [18], dust acoustic and dense electron-positron-ion wave [19], heat conduction [21], compact and non compact structure [22] and many others fields [22-24]. Numerous numbers of systematic techniques have proposed to achieve numerical or exact solutions of nonlinear or fractional nonlinear differential equations. Several powerful methods are as: Hirota bilinear [24-25], unified [26], Jacobi elliptic function expansion [27], generalized Kudryashov [28-29], modified simple equation method [30-31], Bäcklund transformations [32], tanh method [33], $\tan(\Theta/2)$-expansion [34], soliton ansatz [35-36], auxiliary equation [37], homogeneous balance [38], (G'/G)-expansion [39-40], Modified double sub-equation [41], variational iteration method [42], homotopy perturbation method [43], fractional sub-equation method [44] and so on.

Huge amount of integral schemes are introduced in the literature. Few of them are effective for both integrable and non-integrable models. Some schemes are not appropriate for non-integrable models. Among the above methods the Hirota bilinear [24-25], unified [26], Jacobi elliptic function expansion [27], generalized Kudryashov [28-29], modified simple equation method [30] are most useful, coincide, direct and attracted much more interest of researchers which are appropriate for both integrable and non-integrable.

Our main works start in the next chapter-two. In this chapter, we tried to investigate four influential non-linear evolutions equations namely, the first and second negative order integrable Burgers equation [45], the fifth order Korteweg-de-Vries equation [46], and the extended Sawada-Kotera [45] via Hirota bilinear method [24]. There solitons solutions consists diverse types of solitonic nature with different free parameters. Taking complex conjugate of free parameters on exact multi-soliton solutions, we illustrate the interaction between line and periodic soliton, line and rogue soliton, two rogue type solitons. We also provided some figures of the interaction of two, three and four soliton of the considered nonlinear models.

In third chapter, we explain the unified method [26] to solve nonlinear fractional partial differential equations. The method has applied on the space-time fractional nonlinear differential equations for pulse narrowing transmission lines model [11-13] to verify the effectiveness of the method. Different types of exact solution are derived. The derived results are innovative and noteworthy to disclose the relevant features of the physical phenomena.

A mathematical technique is discussed in the chapter four to find the exact solutions of the space-time fractional Equal-width [47] and the space-time fractional Wazwaz-Benjamin-Bona-Mahony models [49]. Presented Jacobi elliptic method [27] is a superb way to investigate and find exact solution of fractional nonlinear differential models.

Chapter five is devoted to search new exact solitary wave solutions for time fractional complex Schrodinger and time fractional biological population model [8] through the generalized Kudryshov method [28-29]. Considered models have successfully analyzed by this method. Finally some graphs of the exact solutions are presented in Fig-5.1 to Fig-5.6.

Chapter six uses the popular modified simple equation method [30-31]. The method applied on the complex time fractional Schrodinger [3] and space-time fractional differential equation governing wave propagation in low-pass electrical transmission lines equations.

The chapter seven covers a new class of fractional dynamical systems. Here, we proposed a new method namely Improved Kudryashov method for solving any nonlinear fractional differential models. We apply the proposed method to the nonlinear space-time fractional models leading wave spread in electrical transmission lines [11], the time fractional complex Schrodinger [3] and the space-time M-fractional Schrodinger-Hirota models [65] to bear out the effectiveness of the propose method. All the obtained solutions are illustrated graphically.

Finally, overall concluding remarks are in the last chapter-eight.

Chapter-2

Dynamics of interaction solutions of non-linear models

Acknowledgement

Based on the Hirota Bilinear Method, we study four influential non-linear evolutions equations and its different solitons solutions consisting of line soliton, periodic soliton, lump soliton, different type of breather type solitons with different free parameters. Taking complex conjugate of free parameters on exact multi-soliton solutions, we illustrate the interaction between line and periodic soliton, line and rogue soliton, two rogue type solitons. On the perspective of dynamical characteristics, it is found that the propagation directions, shapes and altitudes of waves are influenced by the exits parameters. The exact soliton interaction are also analyzed and illustrated graphically.

2.1 Introduction

The research on nonlinear equations has started on the past decades. Now this field is very important for its different character. There are different types of nonlinear equations that are deliberate in various areas of science, such as acoustics, continuous stochastic processes, and traffic system, dispersive of fluid, shock waves, heat conduction and instability of fluid flow in the field of applied mathematics, physics, and engineering science. Particularly the theory of solitons plays an significant role in nonlinear fields. Of particular interests are in the field of quantum mechanics [1-3], nonlinear optical fiber communications [4-5], plasma physics [6], water wave dynamics [7-8], nonlinear electric-transmission line [9-13], superconductivity and Bose-Einstein condensates [14], electrics signal processing [15], Biological dynamics [16], electro-magnetic waves [17], neuron networks [18], dust acoustic and dense electron-positron-ion wave [19], and in many aspect [20-24].

The study of multi-soliton solution and their analysis of non-linear equations played an important role and has become one of the most significant issues of such non-linear fields. Various techniques have been used to handle the non-linear models such as the the Hirota bilinear [25], Modified double sub-equation [26], Jacobi elliptic function expansion [27], generalized Kudryashov [28-29], modified simple equation method [30-31], Bäcklund transformations [32], tanh method [33], $\tan(\Theta/2)$-expansion approach [34], auxiliary equation [37], sine-cosine [38], homogeneous balance [38], (G'/G)-expansion [39,40], Modified double sub-equation method [41], variational iteration method [42], homotopy perturbation method [43]and so on. Some modified methods have been applied to solve and analyze non-linear partial differential equations with variable coefficients.

In this chapter, we want to investigate the interaction solutions and identify the solitonic phenomena for five non-linear partial differential equations. We consider five equations namely, the first and second negative order integrable Burgers equation [45], the fifth order Korteweg-de-Vries equation (KdV-5) [46], and the extended Sawada-Kotera equation [45]. These five equations have infinite sets of conservation laws. So the above five equations carry the N-soliton solutions.

The Hirota bilinear method [25] is an essential tool to gather multi-soliton solutions and its interaction with less computational efforts. This method is rather heuristic and significant to handle non-linear equation with constant coefficients even with variable coefficients. Hirota bilinear method posse powerful feathers that make it practical for the determination of single soliton and multiple solitons solutions for a wide class of non-linear evolution equations. By using the Hirota bilinear method, we shed light on the derivation of multi-solitonic solutions and its interactions, and the results will be investigated graphically as well. The computer symbolic systems such as Maple and Mathematica allow us to perform complicated and tedious calculations.

2.2. Applications

In this section, we are willing to determine solution of the interaction solutions of the first and second negative order integrable Burgers equation [45], the fifth order Korteweg-de-Vries equation (KdV-5) [46], and the extended Sawada-Kotera equation.

2.2.1 Integrable first negative-order Burger equation

The standard Burgers equation [45] reads

$$U_t + 2UU_x + U_{xx} = 0. \tag{2.1}$$

Which is the most important evolution equation arises in propagation of waves specially. The Burgers model holds the nonlinear UU_x and dissipative effects U_{xx}, which are two significant structures of solitonic propagation. The Burgers model was first presented in 1915 by Bateman [52], and after then further studied have done of the model in different structure in 1948 by Burgers. We have to know that the standard Burgers equation is the first equation in [52].

We initiate investigation of interaction solutions of the first negative-order integrable Burgers equation given by,

$$\Phi_{xxt} + \Phi_x\Phi_{xt} + \Phi_{xx}\Phi_t + \Phi_{xx} = 0. \tag{2.2}$$

At first consider a solution as a form of exponential

$$\Phi(x,t) = e^{l_j x - \gamma_j t}. \tag{2.3}$$

Using the Eq. (2.3) in the first and forth terms of Eq. (2.2) provides the dispersion relation:

$$\gamma_j = 1. \tag{2.4}$$

It is seen that the dispersion variable is a fixed with value one and not a variable alike the standard Burgers equation. Thus, we have the traveling variables

$$\eta_j = l_j x - t. \qquad (2.5).$$

The multi solitons solutions we can apply the following transformation,

$$\Phi(x,t) = r \ln f(x,t). \qquad (2.6)$$

Where the auxiliary function $f(x,t)$ for the different one or more than one soliton solution is given by,

$$f(x,t) = 1 + \sum_{j=1}^{N} e^{l_j x - t}. \qquad (2.7)$$

For single soliton, i.e, when $j=1$, setting Eq. (2.6) into Eq. (2.2) and solving for r, we find

$$r = 1. \qquad (2.8)$$

Case-1: To determine lump wave, we have to consider at least two soliton solutions by putting $j=2$ in Eq. (2.7), then the auxiliary function

$$f(x,t) = 1 + e^{\eta_1} + e^{\eta_2} = 1 + e^{l_1 x - t} + e^{l_2 x - t}. \qquad (2.9)$$

Suppose the constants are, $l_1 = a_1 + ib_1$, $l_2 = a_1 - ib_1$, then Eq. (2.9) reduce to

$$f(x,t) = 1 + e^{(a_1 + ib_1)x - t} + e^{(a_1 - ib_1)x - t}.$$

After some simplification, we get

$$f(x,t) = 1 + 2\cos(b_1 x) e^{(a_1 x - t)}. \qquad (2.10)$$

Substituting Eq. (2.10) into Eq. (2.6)

$$\Phi(x,t) = \ln(1 + 2\cos(b_1 x) e^{(a_1 x - t)}). \qquad (2.11)$$

The solution of Eq. (2.1) by using Eq. (2.11)

$$U(x,t) = \frac{2e^{(a_1 x - t)}\{a_1 \cos(b_1 x) - b_1 \sin(b_1 x)\}}{1 + 2\cos(b_1 x) e^{(a_1 x - t)}}. \qquad (2.12)$$

From two soliton, we get the solution Eq. (2.12) by considering the existing parameters in a complex conjugate and gives interaction of periodic lump waves and periodic line waves. Nature of solution Eq. (2.12) is depicted in 3D plot of Fig-2.1(a) and contour plot of 2.1(b) with the parametric values $a = 1, b = 1$.The corresponding 2D plots of Fig-(c) for $t = -1, t = 0, t = 1$. Figures show that lump wave of the interaction occurs along parallax of xt-plane and it is cleared that waves were disappeared when it goes to negative direction of space as time increases from the parallax. On the other hand, one can control the direction of the lump waves taking the parametric values as purely imaginary and propagate the wave along x-axis instead of parallax (see Fig-2.1(d), (e) and (f)). Actual shape of lump waves and line waves are clearly observed from its contour and 2D plots.

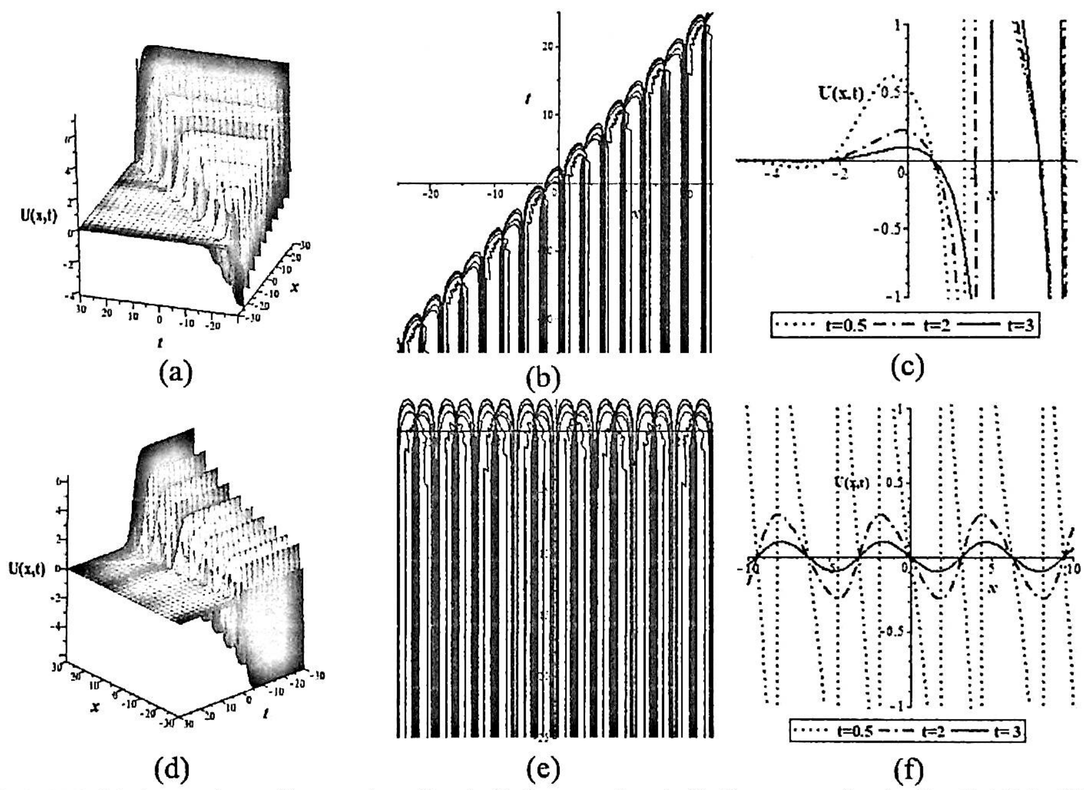

Fig-2.1(a),(b) shows plots of interaction of periodic lump and periodic line waves for the Eq. (2.12) in 3D and contour plot with the parametric values $a = 1$ and $b = 1$; 1(c) represents corresponding 2D plots for $t = -1, t = 0, t = 1$ and (d), (e) represent the interaction of breather type lump and periodic line waves for the Eq. (12) in 3D and contour with the parametric values $a = 0$ and $b = 1$; (f) represents corresponding 2D plot in Fig-(f).

Case-2: Putting $j = 3$ for three solitons solution in Eq. (2.7), then the assisting function

$$f(x,t)=1+e^{\eta_1}+e^{\eta_2}+e^{\eta_3}=1+e^{l_1x-t}+e^{l_2x-t}+e^{l_3x-t}. \qquad (2.13)$$

Let the constants, $l_1=a_1+ib_1, l_2=a_1-ib_1$ and $l_3=c$ (say)then Eq. (2.13) reduce to

$$f(x,t)=1+e^{l_1x-t}+e^{l_2x-t}+e^{l_3x-t}=1+e^{(a_1+ib_1)x-t}+e^{(a_1-ib_1x-t)}+e^{cx-t}. \qquad (2.14)$$

Simplifying the Eq. (2.14) we get

$$f(x,t)=1+2\cos(b_1x)e^{a_1x-t}+e^{cx-t}. \qquad (2.15)$$

Replacing Eq. (2.15) into the Eq. (2.6) gives

$$\Phi(x,t)=\ln(1+2\cos(b_1x)e^{a_1x-t}+e^{cx-t}). \qquad (2.16)$$

The solution of Eq. (2.1) by using Eq. (2.16) gives

$$U(x,t)=\frac{2e^{(a_1x-t)}\{a_1\cos(b_1x)\ -b_1\sin(b_1x)\}+ce^{cx-t}}{1+2\cos(b_1x)e^{a_1x-t}+e^{cx-t}}. \qquad (2.17)$$

The solution Eq. (2.17) comes from three soliton solutions considering two of the parameters in a complex conjugate and one as real valued. Resulting solution gives interaction of periodic lump waves with kink wave. Nature of solution Eq. (2.17) is depicted in 3D and contour plot of Fig-2.2(a), (b) with the parametric values $a_1=1, b_1=1$ and $c=-1$. 2D shape represent in Fig-2.2(c). Figures show that the periodic lump waves propagate along the parallax of xt-plane and interact with the kink wave orthogonally at the origin. It is observed that waves were disappear when it goes to negative direction of space as time increases and above the parallax but only kink type line wave exist there. On the other hand, one can control the direction of the periodic lump waves taking the parametric values as purely imaginary and propagate the lump wave along x-axis instead of parallax (see Fig-2.2(d), 2.2(e) and 2.2(f)) but direction of kink wave remain same. In this case angle between the lump and kink wave is 135°. Actual shape of periodic lump wave and kink type line wave are clearly observed from its contour plot.

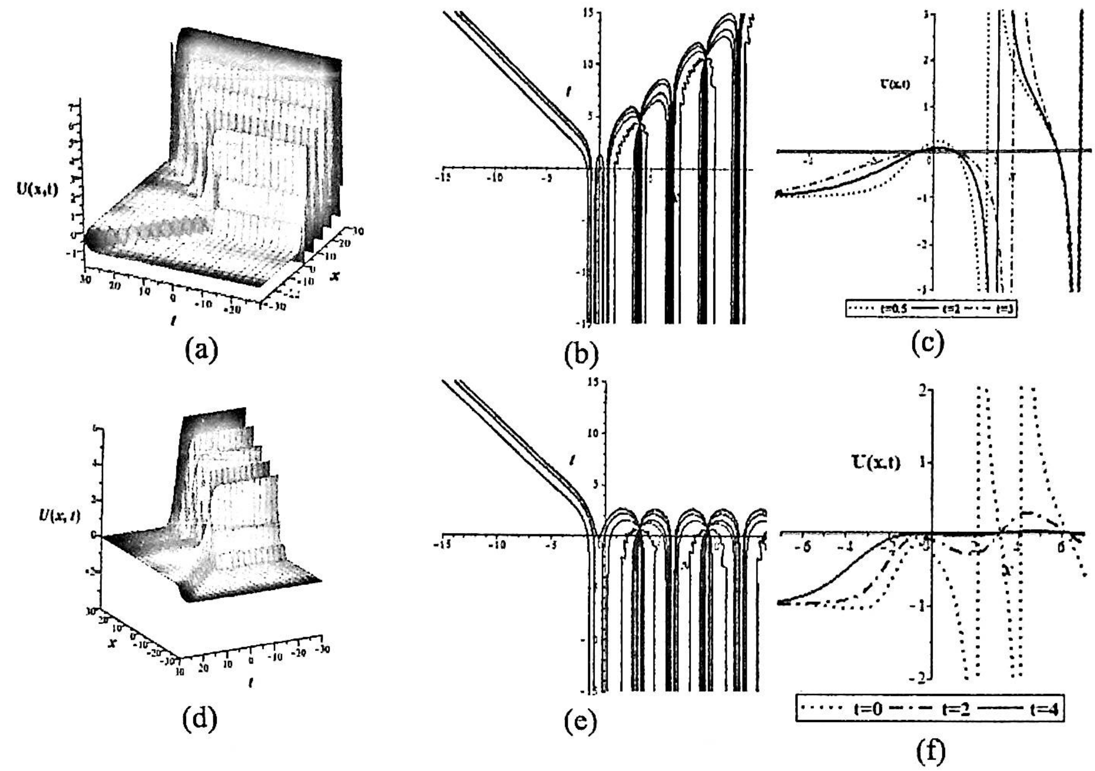

Fig-2.2(a), (b) shows plot of interaction of periodic lump wave with kink type line wave for the Eq. (2.17) in 3D and contour plots with the parametric values $a_1 = b_1 = 1, c = -1$; (c) represents the corresponding 2D plots for $t = 0.5, t = 2, t = 3$. (d),(e) depicted the interaction of lump and kink waves for the Eq. (2.17) in 3D and contour with the parametric values $a_1 = 0, b_1 = 1, c = -1$; (f) represents corresponding 2D plot of for $t = 0, t = 2, t = 4$.

Case-3: For four soliton solutions put $j = 4$ in Eq. (2.7), then the auxiliary function

$$f(x,t) = 1 + e^{\eta_1} + e^{\eta_2} + e^{\eta_3} + e^{\eta_4} = 1 + e^{l_1x-t} + e^{l_2x-t} + e^{l_3x-t} + e^{l_4x-t}. \quad (2.18)$$

Let us consider the constants, $l_1 = a_1 + ib_1$, $l_2 = a_1 - ib_1$, $l_3 = a_2 + ib_2$, and $l_4 = a_2 - ib_2$ then Eq. (2.6) reduce to

$$f(x,t) = 1 + e^{l_1x-t} + e^{l_2x-t} + e^{l_3x-t} + e^{l_4x-t}.$$

$$\Rightarrow f(x,t) = 1 + e^{(a_1+ib_1)x-t} + e^{(a_1-ib_1)x-t} + e^{(a_2+ib_2)x-t} + e^{(a_2-ib_2)x-t}. \quad (2.19)$$

After simplifying the Eq. (2.19)

$$f(x,t) = 1 + 2\cos(b_1x)e^{a_1x-t} + 2\cos(b_2x)e^{a_2x-t}. \quad (2.20)$$

Substituting Eq. (2.20) into Eq. (2.6)

$$\Phi(x,t) = \ln(1 + 2\cos(b_1x)e^{a_1x-t} + 2\cos(b_2x)e^{a_2x-t}). \quad (2.21)$$

The solution of Eq. (2.1) by using Eq. (2.21)gives

$$U(x,t)=\frac{2\{a_1\cos(b_1x)-b_1\sin(b_1x)\}e^{a_1x-t}+2\{a_2\cos(b_2x)-b_2\sin(b_2x)\}e^{a_2x-t}}{1+2\cos(b_1x)e^{a_1x-t}+2\cos(b_2x)e^{a_2x-t}}\quad,\ (2.22)$$

The solution Eq. (2.22) comes from four soliton solution considering the parameters in two pair of complex conjugates. Resulting solution gives interaction of two pair of periodic cross lump waves. Nature of the solution Eq. (2.22) is depicted in 3D plot of Fig-2.3(a) and contour plot of Fig-2.3(b) with the parametric values $a_1=1, b_1=1, a_2=-1$ and $b_2=1$. Figures show that two periodic lump wave propagate along opposite parallax of xt-plane. The interaction occurs at the origin and act orthogonally. On the other hand, one can control propagation direction of the lump waves taking the parametric values as purely imaginary. In that case, one lump wave propagate along x-axis instead of parallax and other lump wave propagate along the parallax and interact at the origin with angle 135° (see Fig-2.3(c) & 2.3(d)).Actual shape of interaction of the periodic lump waves are clearly identified from its contour plots.

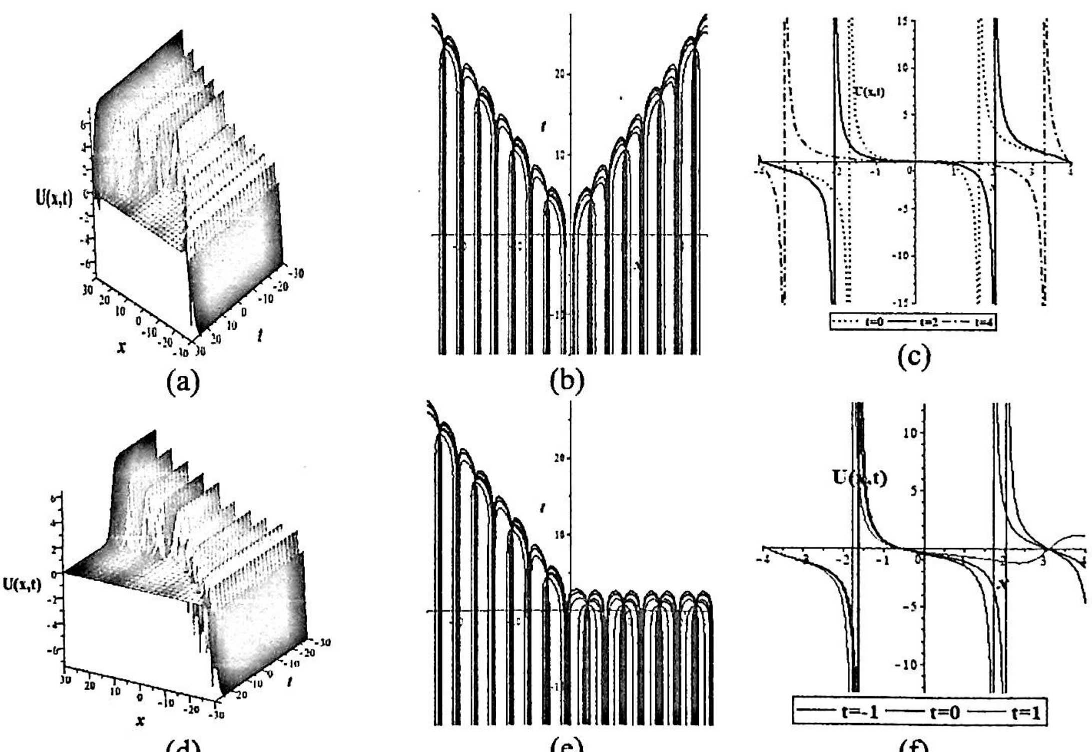

(a) (b) (c)

(d) (e) (f)

Fig-2.3(a), (b) plotted the interaction of two pair of the periodic lump waves for the Eq. (2.22) in 3D and contour with the unknown constants $a_1 = b_1 = b_2 = 1, a_2 = -1$;3(c) represents corresponding 2D shape for the time $t = 0, t = 2, t = 4$. and (d),(e) shows plot of interaction of lump and kink waves for the Eq. (2.22) in 3D and contour plot with the parametric values $a_1 = 0, b_1 = b_2 = 1, a_2 = -1$; (f) represents corresponding 2D plot for $t = -1, t = 0, t = 1$.

2.2.2. *Integrable second negative-order Burger's equation*

In this subsection, we analyse the second negative-order integrable Burger equation given by

$$\Phi_{xxt} + \Phi_x\Phi_{xt} + \Phi_{xx}\Phi_t + \Phi_{xxx} + 2\Phi_x\Phi_{xx} + \Phi_{xxx} = 0. \tag{2.23}$$

Here, firstly, consider a trial solution of second negative integrable burger's equation as an exponential form

$$\Phi(x,t) = e^{l_j x - \gamma_j t}. \tag{2.24}$$

Using the Eq. (2.24) in the first, fourth and sixth terms of Eq.(2.23) provides the dispersion relation:

$$\gamma_j = l_j. \tag{2.25}$$

It is seen that the dispersion variable is not fixed. Thus, we have the travelling variable as

$$\eta_j = l_j x - l_j t. \tag{2.26}$$

The multi solitons solutions can apply the following transformation

$$\Phi(x,t) = r \ln f(x,t). \tag{2.27}$$

Where the auxiliary function $f(x,t)$ for the different one or more than one soliton solution is given by,

$$f(x,t) = 1 + \sum_{j=1}^{N} e^{l_j x - l_j t}. \tag{2.28}$$

For single soliton i.e. when $j = 1$, setting Eq. (2.27) into Eq. (2.23) and solving for r, we find

$$r = 1. \tag{2.29}$$

Case-1: To determine breather type lump wave, put $j=2$ in Eq. (2.28), to consider at least two soliton solutions, then the auxiliary function,

$$f(x,t)=1+e^{\eta_1}+e^{\eta_2}=1+e^{l_1x-l_1t}+e^{l_2x-l_2t}. \tag{2.30}$$

Suppose the constants are, $l_1=a_1+ib_1$, $l_2=a_1-ib_1$, then Eq. (2.30) reduce to

$$f(x,t)=1+e^{(a_1+ib_1)(x-t)}+e^{(a_1-ib_1)(x-t)}.$$

After some simplification, we get

$$f(x,t)=1+2\cos(b_1(x-t))e^{a_1(x-t)}. \tag{2.31}$$

Inserting Eq. (2.31) into Eq. (2.27) gives

$$\Phi(x,t)=\ln(1+2\cos(b_1x)e^{a_1(x-t)}). \tag{2.32}$$

The solution of Eq. (2.1) by using Eq. (2.32)gives

$$U(x,t)=\frac{2e^{a_1(x-t)}\{a_1\cos(b_1(x-t))\ -b_1\sin(b_1(x-t))\}}{1+2\cos(b_1(x-t))e^{a_1(x-t)}}. \tag{2.33}$$

The solution Eq. (2.33) comes from two soliton solution considering exist parameters in a complex conjugate and provide lump type periodic breather wave. Nature of result in Eq. (2.33) is depicted in 3D plot of Fig-2.4(a) and contour plot of 2.4(b) with the parametric values $a=-0.5, \mathrm{b}=1.5$ .Fig-2.4(c) is the corresponding 2D shape for $t=-1, t=0, t=1$ .Figures show that breather waves occurs up to parallax of xt-plane and it is observed that waves disappear when it was in positive direction of space before interaction (as $t<0$).But, when we take the parametric values as purely imaginary, then we get the simple periodic waves comes in-terms of sinusoidal function (see Fig-2.4(c) & 2.4(d)). Actual shape of interaction of the periodic lump waves are clearly identified from its contour plots.

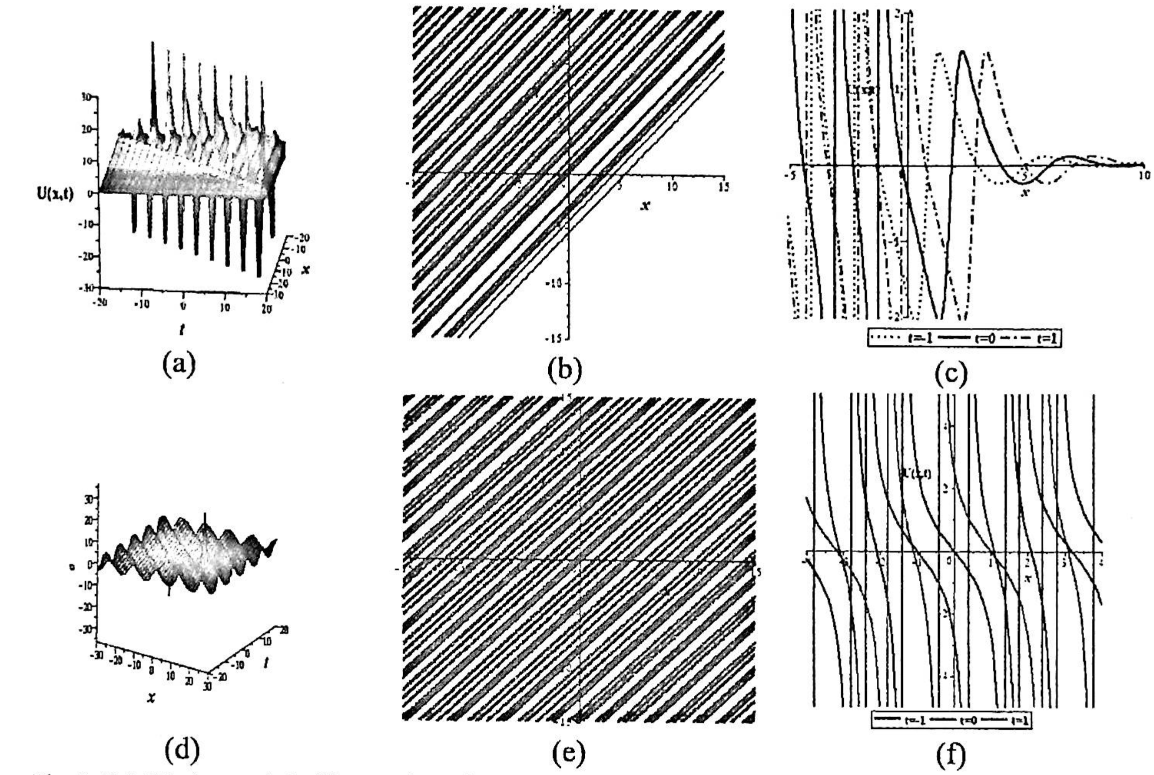

Fig-2.4(a),(b) shows plot of interaction of two pair of the lump type periodic breather wave for the Eq. (2.33) in 3D and contour plot with the parametric values $a=-0.5, \mathbf{b}=1.5$; (c) represents corresponding 2D plot for $t=-1, t=0, t=1$. Fig-(d),(e). Shows the simple periodic waves comes in-terms of sinusoidal function for the Eq. (2.33) in 3Dwith the parametric values $a=0$ and $b=1.5$; (f) represents corresponding 2D plot with $t=-1, t=0, t=1$.

Case-2: For kinky-lump type breather wave we have to consider three soliton solutions. In this regard, consider the three solitons solution by putting $j=3$ in Eq. (2.28), then the auxiliary function

$$f(x,t)=1+e^{\eta_1}+e^{\eta_2}+e^{\eta_3}=1+e^{l_1x-l_1t}+e^{l_2x-l_2t}+e^{l_3x-l_3t}. \tag{2.34}$$

Let the constants, $l_1=a_1+ib_1$, $l_2=a_1-ib_1$ and $l_3=c$ (say)then Eq. (34) reduce to

$$f(x,t)=1+e^{l_1x-t}+e^{l_2x-t}+e^{l_3x-t}=1+e^{(a_1+ib_1)(x-t)}+e^{(a_1-ib_1)(x-t)}+e^{c(x-t)}. \tag{2.35}$$

Simplifying the Eq. (2.35) we get

$$f(x,t)=1+2\cos(b_1(x-t))e^{a_1(x-t)}+e^{c(x-t)}. \tag{2.36}$$

Replacing Eq. (2.36) into Eq. (2.27)

$$\Phi(x,t)=\ln(1+2\cos(b_1(x-t))e^{a_1(x-t)}+e^{c(x-t)}). \tag{2.37}$$

The solution of Eq. (2.1) by using Eq. (2.37)

$$U(x,t)=\frac{2e^{a_1(x-t)}\{a_1\cos(b_1(x-t))\ -b_1\sin(b_1(x-t))\}+ce^{c(x-t)}}{1+2\cos(b_1(x-t))e^{a_1(x-t)}+e^{c(x-t)}}. \tag{2.38}$$

The solution Eq. (2.38) comes from three soliton solutions considering two of the parameters are in complex conjugate and one as real valued. Resulting wave solution gives kinky-lump type periodic breather wave. Nature of solution Eq. (2.38) is depicted in 3D plot of Fig-2.5(a) and contour plot of Fig-2.5(b) with the parametric values $a_1=-2,\mathbf{b}_1=1.5,c=4$. Figures show that kinky-lump type breather wave occurs up to parallax of xt-plane and it is observed that waves were disappear when it goes to positive direction of space before interaction (when $t<0$).The corresponding 2D plot for $t=-1,t=0,t=1$ in Fig-2.5(c). Fig-2.5(d), (e) represent the 3D and contour plots for $a_1=0,\mathbf{b}_1=1.5,c=4$. And Fig-2.5(f) represents the corresponding 2D plot.

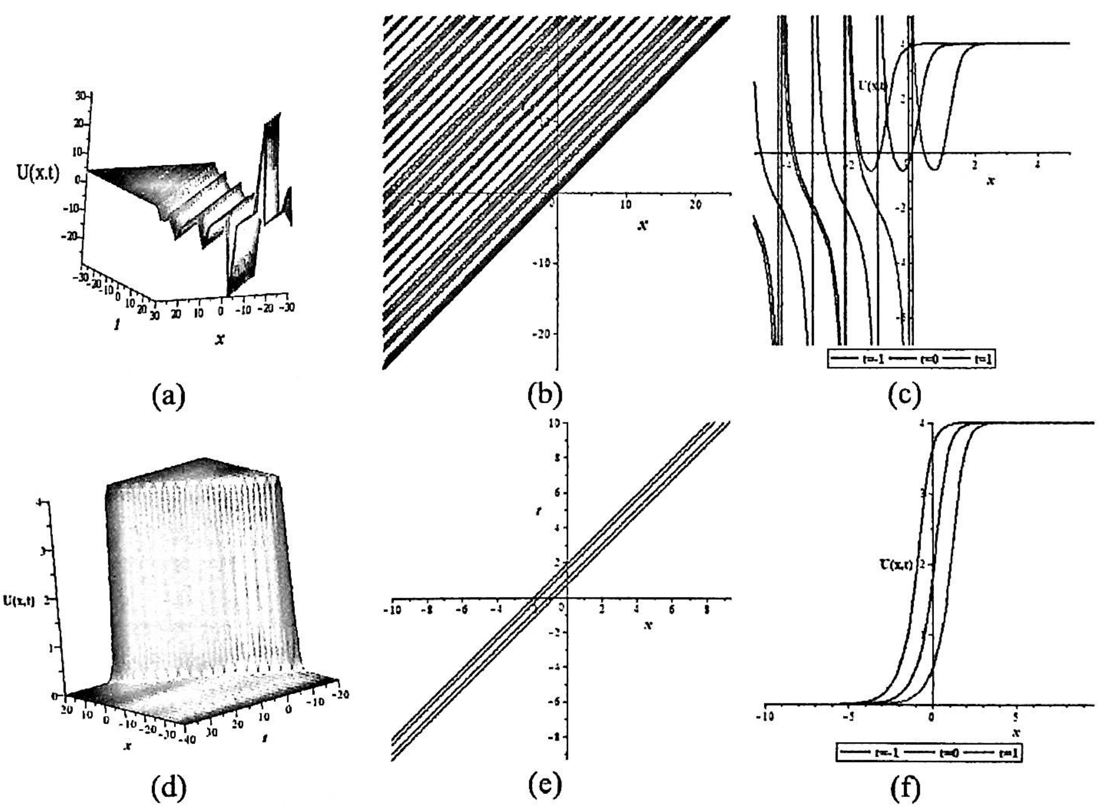

Fig-2.5(a) shows plot kinky-lump type breather wave for the Eq. (2.38) in 3D with the parametric values $a_1=-2,\mathbf{b}_1=1.5,c=4$; (b) represents corresponding contour plot. The corresponding 2D plot for

$t=-1, t=0, t=1$ in Fig-2.5(c). Fig-2.5(d) and (f) for the parametric values $a_1=0, \mathbf{b}_1=1.5, c=4$. Fig-(f) represents the 2D plot.

Case-3: To analysis periodic-lump type breather wave consider four soliton solutions. For the four solitons solution, put $j=4$ in Eq. (2.28), then the auxiliary function

$$f(x,t)=1+e^{\eta_1}+e^{\eta_2}+e^{\eta_3}+e^{\eta_4}=1+e^{l_1x-l_1t}+e^{l_2x-l_2t}+e^{l_3x-l_3t}+e^{l_4x-l_4t}. \quad (2.39)$$

Let us consider the constants, $l_1=a_1+ib_1$, $l_2=a_1-ib_1$, $l_3=a_2+ib_2$, and $l_4=a_2-ib_2$ then Eq. (2.39) reduce to

$$f(x,t)=1+e^{(a_1+ib_1)(x-t)}+e^{(a_1-ib_1)(x-t)}+e^{(a_2+ib_2)(x-t)}+e^{(a_2-ib_2)(x-t)}. \quad (2.40)$$

After simplifying the Eq. (2.40)

$$f(x,t)=1+2\cos(b_1(x-t))e^{a_1(x-t)}+2\cos(b_2(x-t))e^{a_2(x-t)}. \quad (2.41)$$

Substituting Eq. (2.41) into Eq. (2.27)

$$\Phi(x,t)=\ln(1+2\cos(b_1(x-t))e^{a_1(x-t)}+2\cos(b_2(x-t))e^{a_2(x-t)}). \quad (2.42)$$

The solution of Eq. (2.1) by using Eq. (2.42)

$$U(x,t)=\frac{2\{a_1\cos(b_1(x-t))-b_1\sin(b_1(x-t))\}e^{a_1(x-t)}+2\{a_2\cos(b_2(x-t))-b_2\sin(b_2(x-t))\}e^{a_2(x-t)}}{1+2\cos(b_1(x-t))e^{a_1(x-t)}+2\cos(b_2(x-t))e^{a_2(x-t)}}. \quad (2.43)$$

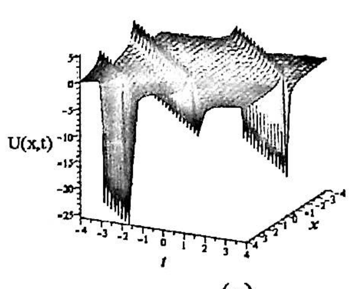

(a)

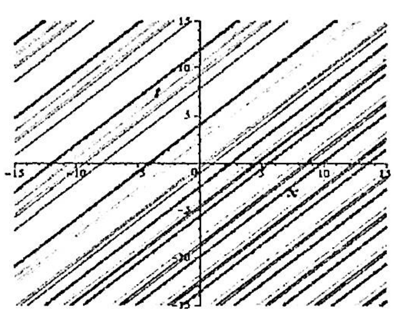

(b)

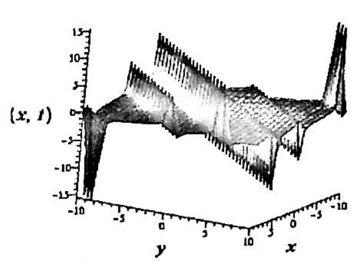

(c)

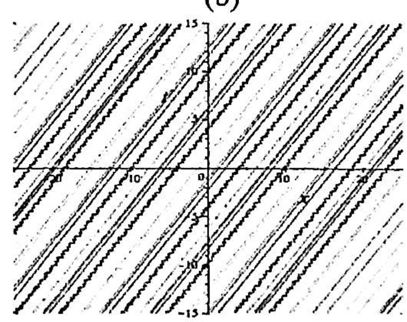

(d)

Fig-2.6(a) shows plot kinky-lump type breather wave for the Eq. (2.43) in 3D with the parametric values $a_1 = 0.2$; $b_1 = 0.8, a_2 = -0.5$ and $b_2 = 0.4$ (b) represents corresponding contour plot. Fig-(c) shows plot completely periodic waves for the Eq. (2.43) in 3Dwith the parametric values $a_1 = 0$; $b_1 = 0.8, a_2 = 0$ and $b_2 = 0.4$ (d) represents corresponding contour plot.

The solution Eq. (2.43) comes from four soliton solutions considering the parameters in two pair of complex conjugates. Resulting solution gives interaction of two pair of breather waves in the type of periodic-lump. Nature of the solution Eq. (2.43) is depicted in 3D plot of Fig-2.6(a) and contour plot of Fig-2.6(b) with the parametric values $a_1 = 0.2$,$b_1 = 0.8, a_2 = -0.5$ and $b_2 = 0.4$. Figures show that each breather wave of the interaction occurs up to parallax of xt-plane and the two pairs interact from opposite direction. But when we keep both pair of parameters as purely imaginary, then we achieved completely periodic waves in terms of sinusoidal functions (see Fig-2.6(c, d)). On the other hand, if we keep any one pair of complex conjugate as purely imaginary observed the dynamical nature of the waves like Fig-2.6(a). In that case density of waves may be different before or after parallax.

2.2.3. The fifth order Korteweg-de-Vries equation (KdV-5)

In this portion, we begin our analysis by studying extended KdV-5 [46] given by,

$$\begin{aligned}&\Psi_t + c\Psi_x + 3\Psi\Psi_x + 5\alpha^2(\Psi\Psi_{xxx} + 2\Psi_x\Psi_{xx}) + \frac{15\alpha^2}{2\beta}\Psi^2\Psi_x \\ &+ \beta(\alpha^2\Psi_{xxxxx} + \Psi_{xxx}) = 0, \quad \beta \neq 0\end{aligned} \tag{2.44}$$

At first consider a solution as a form of exponential

$$\Psi(x,t) = e^{v_i} = e^{\kappa_i x - \omega_i t}. \text{ Where } v_i = \kappa_i x - \omega_i t \tag{2.45}$$

From the linear term of Eq. (2.44) to solve dispersion relation

$$\omega_i = c\kappa_i + \beta(\kappa_i^3 + \alpha^2\kappa_i^5), \; i = 1,2,3,4 \tag{2.46}$$

And the corresponding phase variables,

$$v_i = \kappa_i x - \{c\kappa_i + \beta(\kappa_i^3 + \alpha^2\kappa_i^5)\}t. \tag{2.47}$$

The phase shift relation of Eq. (2.44),

$$A_{ij} = \frac{(\kappa_i - \kappa_j)^2}{(\kappa_i + \kappa_j)^2}, \text{ where } i, j = 1,2,3,.....N. \ (i < j). \tag{2.48}$$

The multi solitons solutions we can use the transformation

$$\Psi(x,t) = h(\ln f(x,t))_{xx}. \tag{2.49}$$

Where the auxiliary function $f(x,t)$ for the different one or more than one soliton solution is given by,

$$\begin{aligned} f(x,t) &= 1 + \sum_{i=1}^{N} \exp(v_i) + \sum_{i<j}^{N} A_{ij} \exp(v_i + v_j) \\ &+ \sum_{i<j<k}^{N} A_{ij} A_{jk} A_{ik} \exp(v_i + v_j + v_k) + ... + \prod_{i<j}^{N} A_{ij} (\sum_{i}^{N} \exp(v_i)) \end{aligned} \tag{2.50}$$

For single soliton, i.e., $N = 1$, then setting Eq. (2.49) into Eq. (2.44) and solving for h, we find

$$h = 4\beta. \tag{2.51}$$

Case-1: To determine lump wave, consider at two soliton solutions for $N = 2$. In this view, the auxiliary function from Eq. (2.50),

$$f(x,t) = 1 + e^{v_1} + e^{v_2} + A_{12} e^{v_1 + v_2}, \tag{2.52}$$

where $v_1 = \kappa_1 x - \omega_1 t$ and $v_2 = \kappa_2 x - \omega_2 t$

$\kappa_1 = p_1 + iq_1$ and $\kappa_2 = p_1 - iq_1$ then

$\omega_1 = m + in$ and $\omega_2 = m - in$,

where $m = a_1 c + \beta p_1^{\,3} + \alpha^2 \beta p_1^{\,5} - 10\alpha^2 \beta p_1^{\,3} q_1^{\,2} + 5\alpha^2 \beta p_1 q_1^{\,4})$,

$n = b_1 c + 3\beta p_1^{\,2} q_1 - 3\beta p_1 q_1^2 - \beta q_1^3 + 5\alpha^2 \beta p_1^{\,4} q_1 - 10\alpha^2 \beta p_1^{\,2} q_1^{\,3} + \alpha^2 \beta q_1^{\,5})$

and the term phase shift term from Eq. (2.48),

$$p_{12} = \frac{q_1^2}{p_1^2},$$

Simplifying the Eq. (2.50) by using the above terms

$$f(x,t)=1+2e^{\sigma_1}\cos(\xi_1)+A_{12}e^{2\sigma_1}, \tag{2.53}$$

where $\sigma_1 = p_1x-mt$ and $\xi_1 = q_1x-nt$

Replacing Eq. (2.53) in Eq. (2.49),

$$\Psi(x,t)=4\beta\{\ln(1+2e^{\sigma_1}\cos(\xi_1)+A_{12}e^{2\sigma_1})\}_{xx}. \tag{2.54}$$

The solution Eq. (2.54) comes via selecting complex form of exist parameters from two solitons solution and gives rogue type breather waves.

Nature of the solution Eq. (2.54) is illustrated in 3D shape Fig-2.7(a) and contour plot Fig-2.7(b) with the parametric values, $p_1=-1.3, q_1=2, c=0.02, \alpha=0.5, \beta=0.2$. Fig-2.7(c) represents 2D plots for time variation $t=-5, t=0$ and $t=5$. Graphical representation of the solution shows the multi-rogue type breather propagations along the paradox. Its rapidity, wideness and path are unchanged over all the dynamical structure and periodic rogues occur same distance from two wave. Actual shape, direction and distance among rogues of the wave are clearly observed from its contour plots. On the other hand, when we take the parameter as purely imaginary, then the solution Eq. (2.54) exhibits as a breather line waves. It portrayed 3D, contour and 2d plot in Fig-1(d), 1(e) and 1(f) respectively for the parametric values $p_1=0, q_1=1, c=-1, \alpha=2, \beta=1$ and $t=-1, t=0, t=1$.

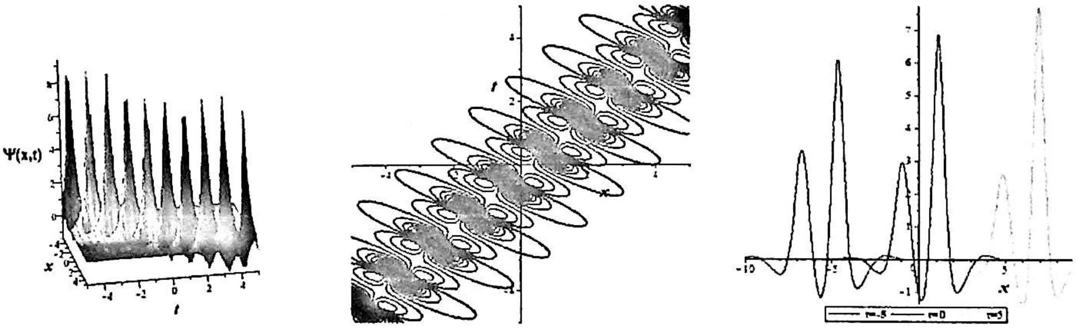

(a) (b) (c)

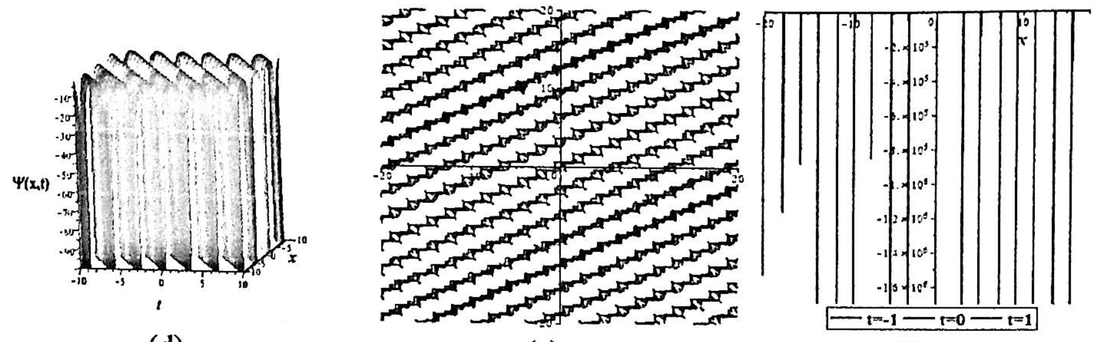

(d) (e) (f)

Fig-2.7(a) and (b) are outlook of the Eq. (2.54) in 3D, contour plots respectively with the parametric values $p_1 = -1.3, q_1 = 2, c = 0.02, \alpha = 0.5, \beta = 0.2$ (c) signifies corresponding 2D plot for the Eq. (2.54) for the values of $t = -5, t = 0, t = 5$; (d) and (d),(e) and (f) represent the outlook of the breather waves for the parameters $p_1 = 0, q_1 = 1, c = -1, \alpha = 2, \beta = 1$. (f) is corresponding 2D plot of breather wave for time $t = -1, t = 0$ and $t = 1$.

Case-2: Consider $N = 3$ in Eq. (2.50) to find three soliton solutions. Then the function $f(x,t)$ takes the form

$$f(x,t) = 1 + e^{\nu_1} + e^{\nu_2} + e^{\nu_3} + A_{12}e^{\nu_1+\nu_2} + A_{23}e^{\nu_2+\nu_3} + A_{13}e^{\nu_1+\nu_3} + A_{123}e^{\nu_1+\nu_2+\nu_3}. \quad (2.55)$$

Where $\nu_1 = \kappa_1 x - \omega_1 t$, $\nu_2 = \kappa_2 x - \omega_2 t$ and $\nu_3 = \kappa_3 x - \omega_3 t$,

Let $\kappa_1 = p_1 x + iq_1$, $\kappa_2 = p_1 x - iq_1$ and $\kappa_3 = \tau$.

$\omega_1 = m + in, \omega_2 = m - in$ and $\omega_3 = c + \alpha c^3 + \alpha^3 \beta c^5$,

where $m = p_1\tau + \beta p_1^3 + \alpha^2 \beta p_1^5 - 10\alpha^2 \beta p_1^3 q_1^2 + 5\alpha^2 \beta p_1 q_1^4)$,

$n = q_1\tau + 3\beta p_1^2 q_1 - 3\beta p_1 q_1^2 - \beta q_1^3 + 5\alpha^2 \beta p_1^4 q_1 - 10\alpha^2 \beta p_1^2 q_1^3 + \alpha^2 \beta q_1^5)$,

and phase shift terms from Eq. (2.48) ,

$$A_{12} = \frac{q_1^2}{p_1^2},$$

$$A_{23} = p_1 + iq_1 = \rho_1 \exp(i\theta_1)(say) \text{ and } A_{13} = p_1 - iq_1 = \rho_1 \exp(-i\theta_1),$$

where $\rho_1 = \sqrt{p_1^2 + q_1^2}$ and $\theta_1 = \tan^{-1}(\frac{q_1}{p_1})$.

Simplifying the Eq. (2.55) by using the above terms

$$\begin{aligned} f(x,t) &= 1 + 2e^{\sigma_1}\cos(\xi_1) + e^{\Lambda x - (c\Lambda + \beta\Lambda^3 + \alpha^2\beta\Lambda^5)t} + A_{12}e^{2\sigma_1} \\ &+ 2\rho_1 e^{(\sigma_1 + \Lambda x - (c\Lambda + \beta\Lambda^3 + \alpha^2\beta\Lambda^5)t}\cos(\xi_1 + \theta_1) + \rho_1^2 A_{12} e^{\{2\sigma_1 + \Lambda x - (c\Lambda + \beta\Lambda^3 + \alpha^2\beta\Lambda^5)t\}}, \end{aligned} \quad (2.56)$$

where $\sigma_1 = p_1 x - mt$ and $\xi_1 = q_1 x - nt$.

Replacing Eq. (2.56) in Eq. (2.49),

$$\Psi(x,t) = 4\beta\{\ln(1+2e^{\sigma_1}\cos(\xi_1) + e^{\Lambda x-(c\Lambda+\beta\Lambda^3+\alpha^2\beta\Lambda^5)t} + A_{12}e^{2\sigma_1} + 2\rho_1 e^{(\sigma_1+\Lambda x-(c\Lambda+\beta\Lambda^3+\alpha^2\beta\Lambda^5)t}\cos(\xi_1+\theta_1) + \rho_1^2 A_{12}e^{\{2\sigma_1+\Lambda x-(c\Lambda+\beta\Lambda^3+\alpha^2\beta\Lambda^5)t\}})\}_{xx} \tag{2.57}$$

In the Eq. (2.57), solution comes from the combination of exponential and periodic sinusoidal function exhibits collision of a periodic rogue type soliton and bell-shaped line soliton, as viewed in the Fig-2.8(a),(b),(c) with the values $p_1 = -1.3, q_1 = 0.2, c = 0.02, \alpha = 0.05, \beta = 2, \Lambda = -0.5$. It is interesting that before ($t < 0$) collision there are two waves (periodic rogue and bell shaped line soliton) interact at $t = 0$ and then rogue type soliton split into two part of rogue type waves (See Fig). It means that the collision is completely non-elastic. Actual shape of collision is clearly observed from its 3D plot Fig-2.8(a) and contour plots Fig-2.8(b). On the other hand, when we take the parameter as purely imaginary, then the solution Eq. (2.57) exhibits the interaction of a breather line solitons with kinky wave's provides kinky type breather waves. It portrayed in Fig-2.8(d),(e)(f) for the parametric values $p_1 = 0, q_1 = 0.35, c = 0.5, \alpha = 0.2, \beta = 0.5, \Lambda = 0.5$.

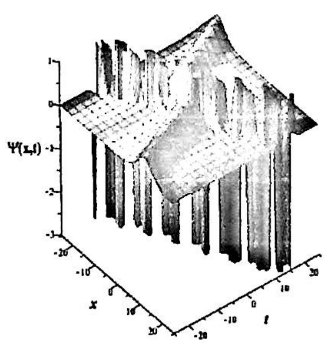

(a)

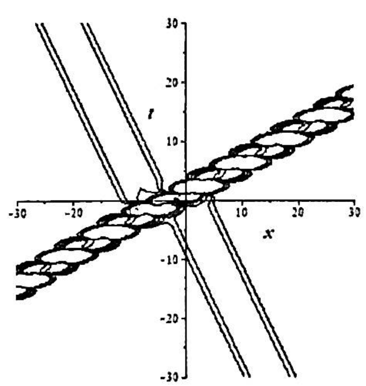

(b)

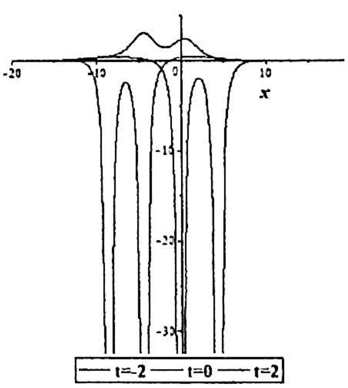

(c)

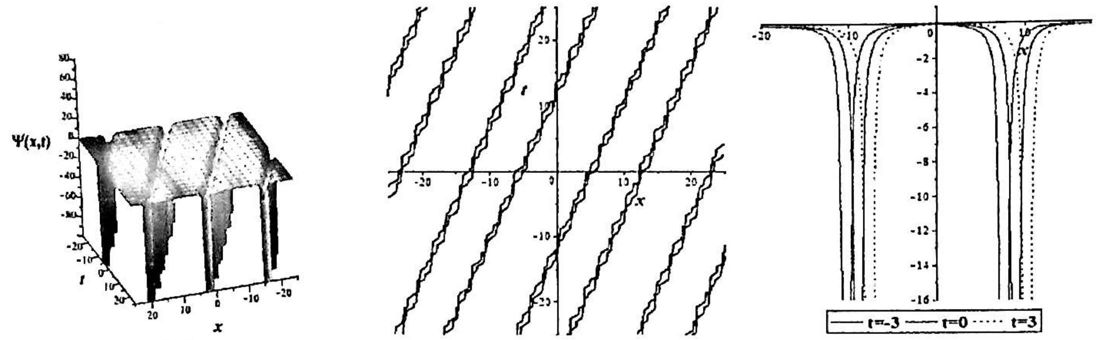

(d) (e) (f)

Fig-2.8(a),(b),(c) shows plot of interaction between a periodic rogue wave with a bell shape line soliton for the Eq. (2.57) in 3D with the parametric values $p_1 = -1.2, q_1 = 0.15, c = -1, \alpha = 0.005, \beta = 2, \Lambda = -0.5$ $t = -2, t = 0, t = 2$. Fig-2.8(d),(e) and 2(f) represents corresponding3D plot, contour plot and 2D plot respectively for the parametric values $p_1 = 0, q_1 = 0.35, c = 0.5, \alpha = 0.2, \beta = 0.5, \Lambda = 0.5$, $t = -3, t = 0, t = 3$.

Case-3: For $N = 4$, the four soliton solutions. The auxiliary function from Eq. (2.50) is,

$$\begin{aligned} f(x,t) &= 1 + e^{\nu_1} + e^{\nu_2} + e^{\nu_3} + e^{\nu_4} + A_{12}e^{\nu_1+\nu_2} + A_{13}e^{\nu_1+\nu_3} + \\ & A_{14}e^{\nu_1+\nu_4} + A_{23}e^{\nu_2+\nu_3} + A_{24}e^{\nu_2+\nu_4} + A_{34}e^{\nu_{31}+\nu_4} + A_{123}e^{\nu_1+\nu_2+\nu_3} + \\ & A_{234}e^{\nu_2+\nu_3+\nu_4} + A_{134}e^{\nu_1+\nu_3+\nu_4} + A_{1234}e^{\nu_1+\nu_2+\nu_3+\nu_4} \end{aligned} , \quad (2.58)$$

where $\nu_1 = \kappa_1 x - \omega_1 t, \nu_2 = \kappa_2 x - \omega_2 t, \nu_3 = \kappa_3 x - \omega_3 t$ and $\nu_4 = \kappa_4 x - \omega_4 t$.

Let $\kappa_1 = p_1 + iq_1, \kappa_2 = p_1 - iq_1, \kappa_3 = p_2 + iq_2$ and $\kappa_4 = p_2 - iq_2$,

$\omega_1 = m_1 + in_1, \omega_2 = m_1 - in_1, \omega_3 = m_2 + in_2$ and $\omega_4 = m_2 - in_2$,

where $m_1 = p_1 + \alpha(p_1^3 - 3p_1q_1^2) + \alpha^2\beta(p_1^5 - 10p_1^3q_1^2 + 5p_1q_1^4)$,

$$n_1 = q_1 + \alpha(3p_1^2q_1 - q_1^3) + \alpha^2\beta(5p_1^4q_1 - 10p_1^2q_1^3 + q_1^5)$$

$$m_2 = p_2 + \alpha(p_2^3 - 3p_2q_2^2) + \alpha^2\beta(p_2^5 - 10p_2^3q_2^2 + 5p_2q_2^4)$$

$$n_2 = q_2 + \alpha(3p_2^2q_2 - q_2^3) + \alpha^2\beta(5p_2^4q_2 - 10p_2^2q_2^3 + q_2^5).$$

The term phase shift terms of Eq. (2.44) from Eq. (2.48),

$$A_{12} = \frac{q_1^2}{p_1^2}, A_{23} = p_1 + iq_1 = \rho_1 \exp(i\theta_1)(say)$$

and $A_{13} = p_1 - iq_1 = \rho_1 \exp(-i\theta_1)$.

$$A_{14} = \frac{q_2^2}{p_2^2}, A_{14} = p_2 + iq_2 = \rho_2 \exp(i\theta_2)(say)$$

and $A_{23} = p_2 - iq_2 = \rho_2 \exp(-i\theta_2)$.

To find the values of ρ_1, ρ_2, θ_1 and θ_2 we will apply $\rho_i = \sqrt{p_i^{\,2} + q_i^{\,2}}$ and $\theta_i = \tan^{-1}(\frac{q_i}{p_i})$,

where $i = 1, 2$.

Simplifying the Eq. (2.58) by using the above terms

$$\begin{aligned}
f(x,t) &= 1 + 2e^{\sigma_1}\cos(\xi_1) + A_{12}e^{2\sigma_1} + 2e^{\sigma_2}\cos(\xi_2) + A_{34}e^{2\sigma_2} + \\
&2\rho_1 e^{(\sigma_1+\sigma_2)}\cos(\xi_1 + \xi_2 + \theta_1) + 2\rho_2 e^{(\sigma_1+\sigma_2)}\cos(\xi_1 - \xi_2 + \theta_2) + \\
&2a_{12}\rho_1\rho_2 e^{(2\sigma_1+\sigma_2)}\cos(\xi_2 + \theta_1 + \theta_2) + 2A_{34}\rho_1\rho_2 e^{(\sigma_1+2\sigma_2)}\cos(\xi_1 + \theta_1 - \theta_2) + \\
&a_{12}a_{34}\rho_1^{\,2}\rho_2^{\,2} e^{(2\sigma_1+2\sigma_2)}
\end{aligned} \tag{2.59}$$

Here $\sigma_1 = a_1 x - m_1 t$, $\xi_1 = b_1 x - n_1 t$, $\sigma_2 = a_2 x - m_2 t$ and $\xi_2 = b_2 x - n_2 t$

Replacing Eq. (2.59) in Eq. (2.49),

$$\begin{aligned}
\Psi(x,t) &= 4\beta \ln(1 + 2e^{\sigma_1}\cos(\xi_1) + A_{12}e^{2\sigma_1} + 2e^{\sigma_2}\cos(\xi_2) + A_{34}e^{2\sigma_2} + \\
&2\rho_1 e^{(\sigma_1+\sigma_2)}\cos(\xi_1 + \xi_2 + \theta_1) + 2\rho_2 e^{(\sigma_1+\sigma_2)}\cos(\xi_1 - \xi_2 + \theta_2) + \\
&2a_{12}\rho_1\rho_2 e^{(2\sigma_1+\sigma_2)}\cos(\xi_2 + \theta_1 + \theta_2) + 2A_{34}\rho_1\rho_2 e^{(\sigma_1+2\sigma_2)}\cos(\xi_1 + \theta_1 - \theta_2) \\
&+ a_{12}a_{34}\rho_1^{\,2}\rho_2^{\,2} e^{(2\sigma_1+2\sigma_2)})_{xx}
\end{aligned} \tag{2.60}$$

In the Eq. (2.60), solution comes from the exponential and periodic sinusoidal function exhibits crash of a pair of periodic rogue type solitons for $p_1 = -1.3, p_2 = 0.8, q_1 = 1, q_2 = 0.45, c = 2, \alpha = 0.25, \beta = 1$ viewed in the Fig-2.9(a),(b),(c). It is interesting that before ($t < 0$) and after ($t > 0$) collision each rogue shows same solitonic character and interact at $t = 0$ flowing all along reverse paradox (See Fig-2.9(a),(b),(c). It is observed that the some rogue waves periodically get into each soliton, being at equal distance from each other. Actual shape, direction and distance among rogues and their interaction wave are clearly observed from its 3D plot Fig-2.9(a) and contour plots Fig-2.9(b). On the other hand, when we take the parameters as purely imaginary, then the solution Eq. (2.60) exhibits the interaction of a pair of breather type line solitons with acute angle. It portrayed in Fig-2.9(d),(e),(f) for the parametric values $p_1 = 0, p_2 = 0, q_1 = 1, q_2 = 1, c = 1, \alpha = -1, \beta = 1$.

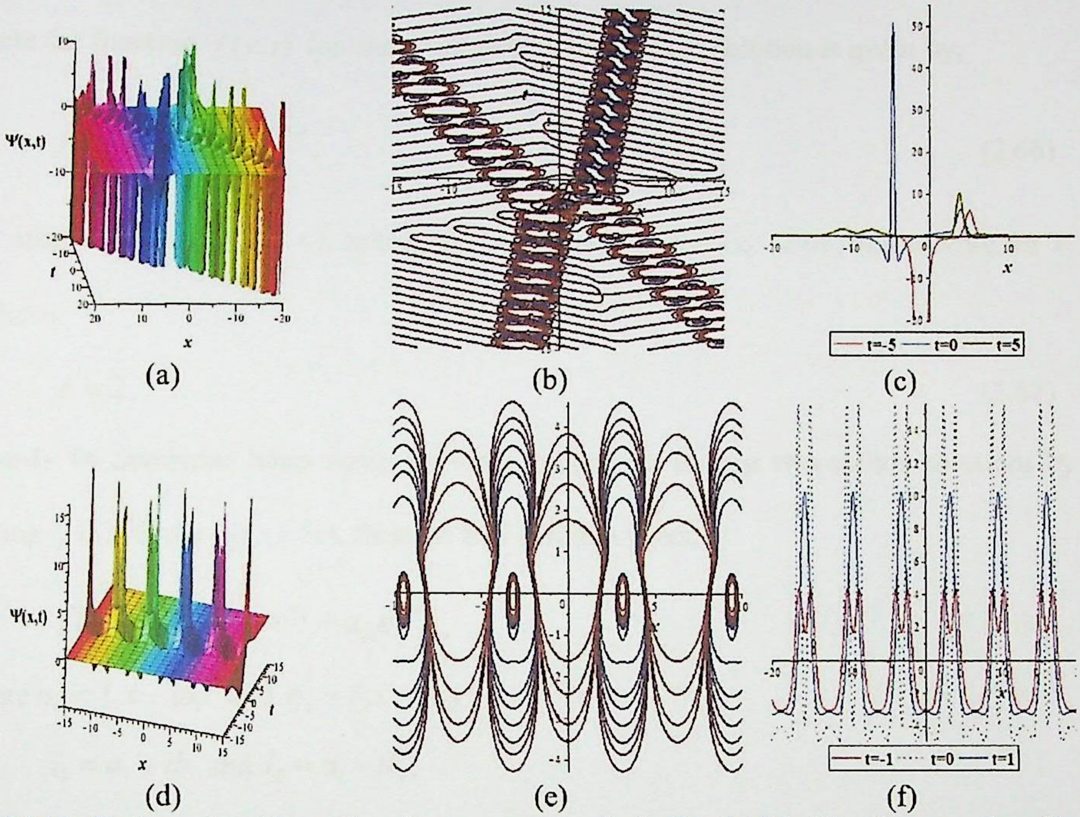

Fig-2.9 (a). (b) shows plot of interaction of two rogue waves for the Eq. (2.60) in 3D and contour plot with the parametric values $p_1 = -1.3, p_2 = 0.8, q_1 = 1, q_2 = 0.45, c = 2, \alpha = 0.25, \beta = 1$; Fig-2.9(d),(e),(f) represents breather wave with $p_1 = 0, p_2 = 0, q_1 = 1, q_2 = 1, c = 1, \alpha = -1, \beta = 1$.

2.2.4. The extended Sawada-Kotera equation

We start our investigation through the eSK equation,

$$\Phi_t + \Phi_x + \alpha(6\Phi\Phi_x + \Phi_{3x}) + \alpha^2\beta(45\Phi^2\Phi_x + 15\Phi_x\Phi_{2x} + 15\Phi\Phi_{3x} + \Phi_{5x}) = 0 \qquad (2.61)$$

At first consider a solution as a form of exponential

$$\Phi(x,t) = e^{\eta_i} = e^{l_j x - \omega_j t}, \text{ where } \eta_i = l_i x - \omega_i t \qquad (2.62)$$

The linear terms of the Eq. (2.61), gives the dispersion relation as

$$\omega_i = l_i + \alpha l_i^3 + \alpha^2 \beta l_i^5, \; i = 1,2,3,4. \qquad (2.63)$$

So, the corresponding phase variables can be written as

$$\eta_i = l_i x - (l_i + \alpha l_i^3 + \alpha^2 \beta l_i^5)t. \qquad (2.64)$$

To derive multi solitons solutions, we can use the transformation

$$\Phi(x,t)=r(\ln f(x,t))_{xx}. \tag{2.65}$$

Where the function $f(x,t)$ for one or more than one soliton solution is given by,

$$f(x,t)=1+\sum_{j=1}^{N} e^{l_j x-t}. \tag{2.66}$$

For single soliton (i.e. $j=1$), setting the Eq. (2.66) into the Eq. (2.61) and solving for r, we have

$$r=2. \tag{2.67}$$

Case-1- To determine lump wave, we have to consider at least two soliton solutions by putting $j=2$ in the Eq. (2.66), then the trail solution gives,

$$f(x,t)=1+e^{\eta_1}+e^{\eta_2}+a_{12}e^{\eta_1+\eta_2}, \tag{2.68}$$

where $\eta_1=l_1x-\omega_1 t$ and $\eta_2=l_2x-\omega_2 t$

Let $l_1=a_1+ib_1$ and $l_2=a_1-ib_1$,

$\omega_1=M+iN$ and $\omega_2=M-iN$,

where $M=a_1+\alpha(a_1^3-3a_1b_1^2)+\alpha^2\beta(a_1^5-10a_1^3b_1^2+5a_1b_1^4)$,

$N=b_1+\alpha(3a_1^2b_1-b_1^3)+\alpha^2\beta(5a_1^4b_1-10a_1^2b_1^3+b_1^5)$,

and the term,

$$a_{12}=-\frac{b_1^2\{5\alpha\beta(a_1^2-3b_1^2)+3\}}{a_1^2\{5\alpha\beta(3a_1^2-b_1^2)+3\}}.$$

Simplifying the Eq.(2.68) by using the above terms, we reach to

$$f(x,t)=1+2e^{\sigma_1}\cos(\xi_1)+a_{12}e^{2\sigma_1}, \tag{2.69}$$

where $\sigma_1=a_1x-Mt$ and $\xi_1=b_1x-Nt$

Replacing the Eq.(2.69) in the Eq.(2.65),

$$\Phi(x,t)=2\{\ln(1+2e^{\sigma_1}\cos(\xi_1)+a_{12}e^{2\sigma_1})\}_{xx}. \tag{2.70}$$

The solution Eq. (2.70) comes via selecting complex form of exist parameters from two soliton solution and gives rogue type breather waves from interaction of the solitons.

Nature of the solution Eq. (2.70) is illustrated in 3D shape Fig-2.10(a) and contour plot Fig-2.10(b) with the parametric values $a_1 = -1.3, b_1 = 2, \alpha = 0.2, \beta = 0.8$. 2D plot in Fig-2.10(c).Figures show that the solution exhibits as multi-rough type breather propagations along the paradox. Its swiftness, breadth and direction remain unchanged over all the dynamical system and periodic rogues occurs equidistance from each other. Actual shape, direction and distance among rogues of the wave are clearly observed from its contour plots. On the other hand, when we take the parameter as purely imaginary, then the solution Eq.(2.70) exhibits as a breather line waves. It portrayed in Fig-2.10(d),(e),(f) for the parametric values $a_1 = 0, b_1 = 0.5, \alpha = -0.8, \beta = 0.5$.

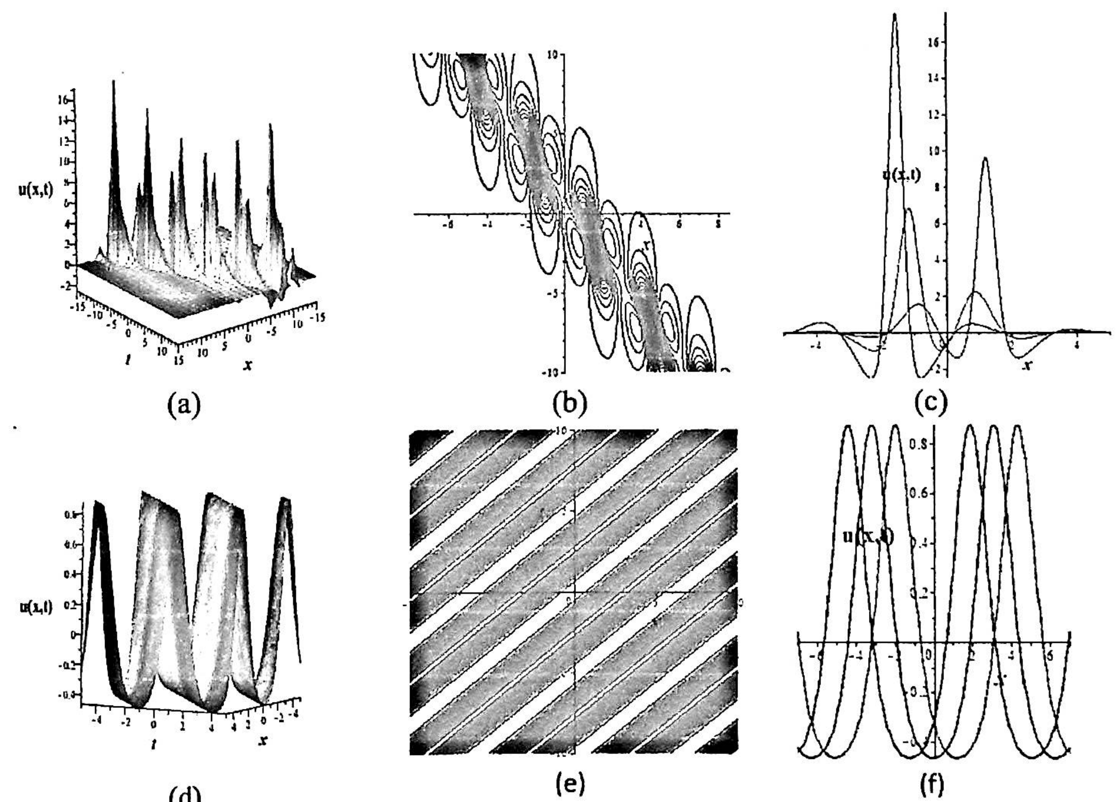

Fig-2.10(a) Represent rogue type breather waves of the Eq. (2.70) in 3D with the parametric values $a_1 = 1.3, b_1 = 2, \alpha = 0.2, \beta = 0.8$.; (b) signifies corresponding contour plot and (c) 2D plot. For the Eq. (2.70) the breather line waves for the parameters $a_1 = 0, b_1 = 0.5, \alpha = -0.8, \beta = 0.5$ in the Fig-2.10(d),(e),(f) .

Case-2: To determine interaction of rogue and a line soliton wave, we consider three soliton solutions. In this regard, consider the three solitons solution by putting $j=3$ in the Eq. (2.66), then the function

$$f(x,t)=1+e^{\eta_1}+e^{\eta_2}+e^{\eta_3}+a_{12}e^{\eta_1+\eta_2}+a_{23}e^{\eta_2+\eta_3}+a_{13}e^{\eta_1+\eta_3}+a_{123}e^{\eta_1+\eta_2+\eta_3}, \quad (2.71)$$

where $\eta_1=l_1x-\omega_1t, \eta_2=l_2x-\omega_2t$ and $\eta_3=l_3x-\omega_3t$.

Let $l_1=a_1+ib_1, l_2=a_1-ib_1, l_3=a_2+ib_2$ and $l_3=c$

and $\omega_1=M_1+iN_1, \omega_2=M_1-iN_1$ and $\omega_3=c+\alpha c^3+\alpha^2\beta c^5$,

where $M_1=a_1+\alpha(a_1^3-3a_1b_1^2)+\alpha^2\beta(a_1^5-10a_1^3b_1^2+5a_1b_1^4)$,

$N_1=b_1+\alpha(3a_1^2b_1-b_1^3)+\alpha^2\beta(5a_1^4b_1-10a_1^2b_1^3+b_1^5)$

and the term,

$$a_{12}=-\frac{b_1^2\{5\alpha\beta(a_1^2-3b_1^2)+3\}}{a_1^2\{5\alpha\beta(3a_1^2-b_1^2)+3\}}, a_{23}=p+iq=\rho\exp(i\theta)(say)$$

and $a_{13}=p-iq=\rho\exp(-i\theta)$,

in which $\rho=\sqrt{p^2+q^2}$ and $\theta=\tan^{-1}(\frac{q}{p})$.

Simplifying the Eq. (2.71) by using the above terms

$$\begin{aligned}f(x,t)=1+2e^{\sigma_1}\cos(\xi)+a_{12}e^{2\sigma_1}+2\rho e^{(\sigma_1+cx-(c+\alpha c^3+\alpha^2\beta c^5)t)}\cos(\xi_1+\theta)\\+\rho^2a_{12}e^{(2\sigma_1+cx-(c+\alpha c^3+\alpha^2\beta c^5)t)}\end{aligned}, \quad (2.72)$$

where $\sigma_1=a_1x-M_1t$ and $\xi_1=b_1x-N_1t$.

Inserting the Eq. (2.72) into the Eq. (2.65), we reach to

$$\begin{aligned}\Phi(x,t)=2\ln(1+2e^{\sigma_1}\cos(\xi)+a_{12}e^{2\sigma_1}+2\rho e^{(\sigma_1+cx-(c+\alpha c^3+\alpha^2\beta c^5)t)}\cos(\xi_1+\theta)\\+\rho^2a_{12}e^{(2\sigma_1+cx-(c+\alpha c^3+\alpha^2\beta c^5)t)})_{xx}\end{aligned}. \quad (2.73)$$

In the Eq. (2.73), solution comes from the combination of exponential and periodic sinusoidal function exhibits collision of a periodic rogue type soliton and bell-shaped line soliton, as viewed in the Fig-2.11(a),(b),(c) with the values $a_1=-1, b_1=1, c=-1, \alpha=0.5, \beta=0.5$. It is interesting (See Fig) that before ($t<0$) collision there are two waves (periodic rogue and bell shaped line soliton) interact at $t = 0$ and then rogue type soliton split into two part of rogue type waves. It means that the collision is completely non-elastic. Actual shape of collision are clearly observed from its 3D plot Fig-2.11(a) and contour plots Fig-2.11(b). On the other hand, when we take the parameter as purely imaginary, then the solution Eq.(2.73) exhibits the interaction of a breather line solitons with kinky waves provides kinky type breather waves. It portrayed in the Fig-2.11(d),(e),(f) for the parametric values $a_1 = 0, b_1 = -1, c = 1, \alpha = \beta = 0.5$.

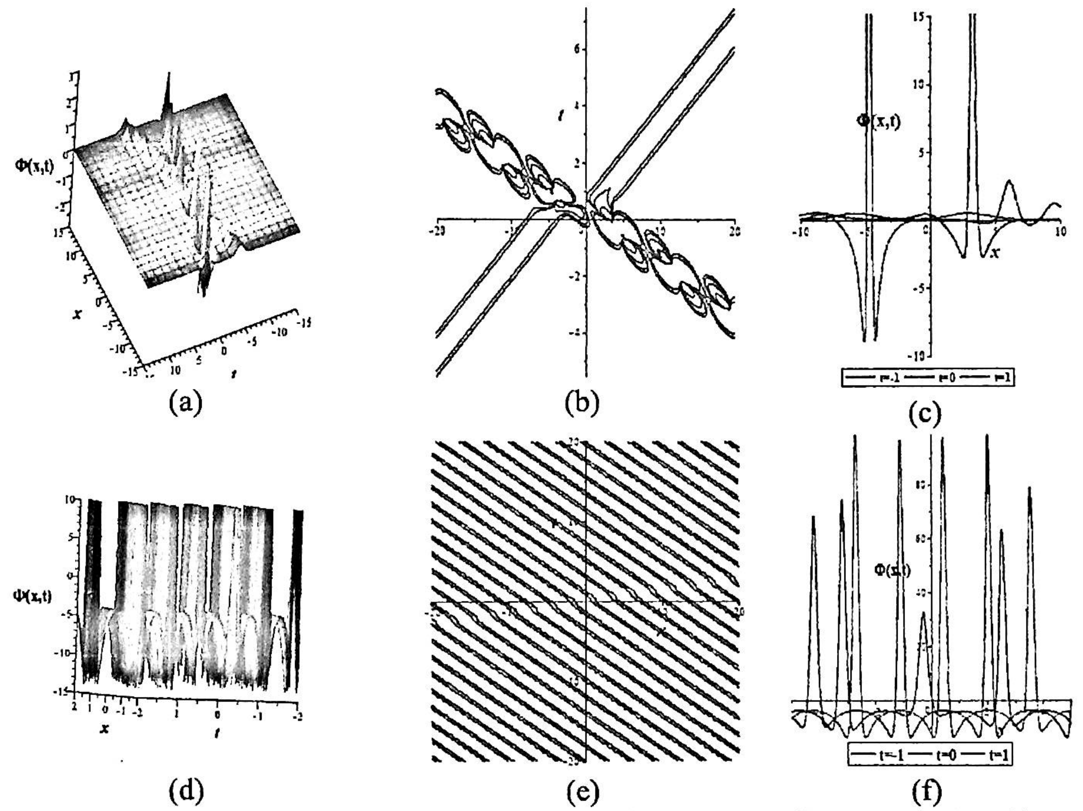

Fig-2.11(a),(b),(c) shows plot of interaction between a periodic rogue type soliton and bell-shaped line soliton for the Eq. (2.73) in 3D with the parametric values $a_1 = -1, b_1 = 1, c = -1, \alpha = 0.5, \beta = 0.5$. and Fig-2.11(d),(e),(f) represents the interaction of a breather line solitons with kinky waves for the Eq. (2.73) in 3D with the parametric values $a_1 = 0, b_1 = -1, c = 1, \alpha = \beta = 0.5$.

Case-3: Here, Let us consider the four solitons solution by putting $j = 4$ in the Eq. (2.66), then

$$\begin{aligned} f(x,t) = {} & 1 + e^{\eta_1} + e^{\eta_2} + e^{\eta_3} + e^{\eta_4} + a_{12}e^{\eta_1+\eta_2} + a_{13}e^{\eta_1+\eta_3} + a_{14}e^{\eta_1+\eta_4} + \\ & a_{23}e^{\eta_2+\eta_3} + a_{24}e^{\eta_2+\eta_4} + a_{34}e^{\eta_3+\eta_4} + a_{123}e^{\eta_1+\eta_2+\eta_3} + a_{234}e^{\eta_2+\eta_3+\eta_4} + \\ & a_{134}e^{\eta_1+\eta_3+\eta_4} + a_{1234}e^{\eta_1+\eta_2+\eta_3+\eta_4} \end{aligned} \tag{2.74}$$

where $\eta_1 = l_1 x - \omega_1 t, \eta_2 = l_2 x - \omega_2 t, \eta_3 = l_3 x - \omega_3 t$ and $\eta_4 = l_4 x - \omega_4 t$,

Let $l_1 = a_1 + ib_1, l_2 = a_1 - ib_1, l_3 = a_2 + ib_2$ and $l_4 = a_2 - ib_2$,

$\omega_1 = M_1 + iN_1, \omega_2 = M_1 - iN_1, \omega_3 = M_2 + iN_2$ and $\omega_4 = M_2 - iN_2$,

where $M_1 = a_1 + \alpha(a_1^3 - 3a_1 b_1^2) + \alpha^2 \beta(a_1^5 - 10a_1^3 b_1^2 + 5a_1 b_1^4)$,

$$N_1 = b_1 + \alpha(3a_1^2 b_1 - b_1^3) + \alpha^2 \beta(5a_1^4 b_1 - 10a_1^2 b_1^3 + b_1^5)$$

$$M_2 = a_2 + \alpha(a_2^3 - 3a_2 b_2^2) + \alpha^2 \beta(a_2^5 - 10a_2^3 b_2^2 + 5a_2 b_2^4)$$

$$N_2 = b_2 + \alpha(3a_2^2 b_2 - b_2^3) + \alpha^2 \beta(5a_2^4 b_2 - 10a_2^2 b_2^3 + b_2^5)$$

and the terms are:

$$a_{12} = -\frac{b_1^2\{5\alpha\beta(a_1^2 - 3b_1^2) + 3\}}{a_1^2\{5\alpha\beta(3a_1^2 - b_1^2) + 3\}},$$

$$a_{13} = -\frac{(a_1 + ib_1 - a_2 - ib_2)^2\{5\alpha\beta(a_1 + ib_1)^2 - (a_1 + ib_1)(a_2 + ib_2) + (a_2 + ib_2)^2 + 3\}}{(a_1 + ib_1 + a_2 + ib_2)^2\{5\alpha\beta(a_1 + ib_1)^2 + (a_1 + ib_1)(a_2 + ib_2) + (a_2 + ib_2)^2 + 3\}}$$

$$a_{13} = a_{24}^* = p_1 + iq_1 = \rho_1 \exp(i\theta_1)(say)$$

where $\rho_1 = \sqrt{p_1^2 + q_1^2}$, $\theta_1 = \tan^{-1}(q_1 / p_1)$,

$$a_{24} = -\frac{b_2^2\{5\alpha\beta(a_2^2 - 3b_2^2) + 3\}}{a_2^2\{5\alpha\beta(3a_2^2 - b_2^2) + 3\}},$$

$$a_{14} = -\frac{(a_1 + ib_1 - a_2 + ib_2)^2\{5\alpha\beta(a_1 + ib_1)^2 - (a_1 + ib_1)(a_2 - ib_2) + (a_2 - ib_2)^2 + 3\}}{(a_1 + ib_1 + a_2 - ib_2)^2\{5\alpha\beta(a_1 + ib_1)^2 + (a_1 + ib_1)(a_2 - ib_2) + (a_2 - ib_2)^2 + 3\}}$$

$$a_{14} = a_{23}^* = p_2 + iq_2 = \rho_2 \exp(i\theta_2)(say)$$

where $\rho_2 = \sqrt{p_2^2 + q_2^2}$, $\theta_2 = \tan^{-1}(q_2 / p_2)$.

Simplifying the Eq. (2.74) by using the above terms

$$\begin{aligned} f(x,t) = 1 + 2e^{\sigma_1}\cos(\xi_1) + a_{12}e^{2\sigma_1} + 2e^{\sigma_2}\cos(\xi_2) + a_{34}e^{2\sigma_2} + \\ 2\rho_1 e^{(\sigma_1+\sigma_2)}\cos(\xi_1 + \xi_2 + \theta_1) + 2\rho_2 e^{(\sigma_1+\sigma_2)}\cos(\xi_1 - \xi_2 + \theta_2) + \\ 2a_{12}\rho_1\rho_2 e^{(2\sigma_1+\sigma_2)}\cos(\xi_2 + \theta_1 + \theta_2) \\ + 2a_{34}\rho_1\rho_2 e^{(\sigma_1+2\sigma_2)}\cos(\xi_1 + \theta_1 - \theta_2) + a_{12}a_{34}\rho_1^2\rho_2^2 e^{(2\sigma_1+2\sigma_2)} \end{aligned} \quad (2.75)$$

Here $\sigma_1 = a_1 x - M_1 t$, $\xi_1 = b_1 x - N_1 t$, $\sigma_2 = a_2 x - M_2 t$ and $\xi_2 = b_2 x - N_2 t$

Inserting the Eq. (2.75) into the Eq. (2.65), we reach to

$$\Phi(x,t)=2\ln(1+2e^{\sigma_1}\cos(\xi_1)+a_{12}e^{2\sigma_1}+2e^{\sigma_2}\cos(\xi_2)+a_{34}e^{2\sigma_2}+ \\ 2\rho_1 e^{(\sigma_1+\sigma_2)}\cos(\xi_1+\xi_2+\theta_1)+2\rho_2 e^{(\sigma_1+\sigma_2)}\cos(\xi_1-\xi_2+\theta_2)+ \\ 2a_{12}\rho_1\rho_2 e^{(2\sigma_1+\sigma_2)}\cos(\xi_2+\theta_1+\theta_2)+2a_{34}\rho_1\rho_2 e^{(\sigma_1+2\sigma_2)}\cos(\xi_1+\theta_1-\theta_2) \\ +a_{12}a_{34}\rho_1^{\ 2}\rho_2^2 e^{(2\sigma_1+2\sigma_2)})_{xx} \tag{2.76}$$

In the Eq. (2.76), solution comes from the combination of exponential and periodic sinusoidal function exhibits collision of a pair of periodic rogue type solitons, as viewed in the Fig-2.12 with the values $a_1=-0.25, a_2=-1, b_1=b_2=\alpha=0.5, \beta=1/200$. It is interesting (See Fig) that before ($t<0$) and after ($t>0$) collision each rogue remains their same solitonic natures and interact at $t=0$ coming along opposite paradox. It is observed that the some rogue waves are periodically got into each soliton, being at equal distance from each other. Actual shape, direction and distance among rogues and their interaction wave are clearly observed from its 3D plot Fig-2.12(a), contour plots Fig-2.12(b) and corresponding 2D plot in Fig-2.12(c). On the other hand, when we consider one set of complex number as a purely imaginary and other as imaginary (i.e. only $a_1=0$), then the solution Eq. (2.76) exhibits collision of rogue type breather waves and breather line soliton which is observe Fig-2.12(d), (e), (f) for the parametric values $a_1=0, a_2=-1, b_1=0.5, b_2=0.5, \alpha=0.5, \beta=0.005$.

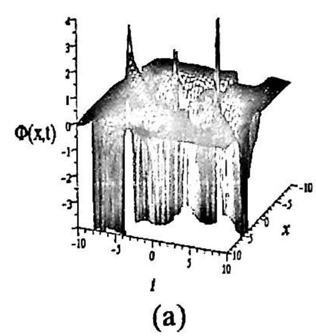

(a)

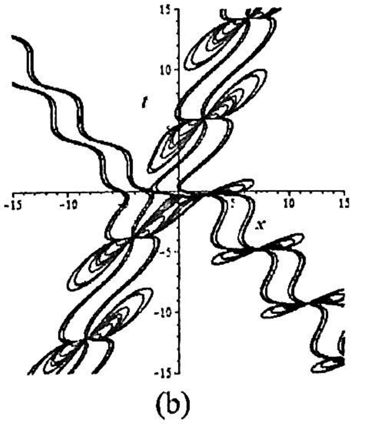

(b)

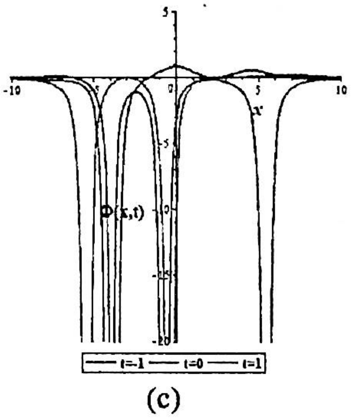

(c)

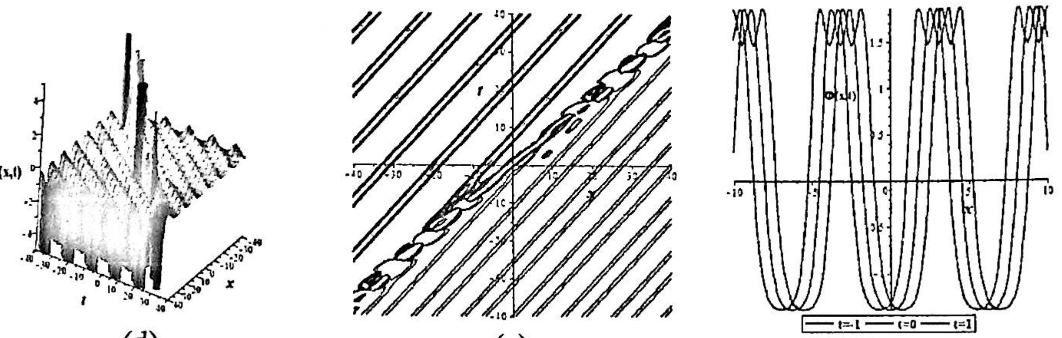

(d) (e) (f)

Fig-2.12(a) shows plot of interaction of periodic lump and periodic line waves for the Eq. (2.76) in 3D with the parametric values $a_1 = -0.25, a_2 = -1, b_1 = b_2 = \alpha = 0.5, \beta = 1/200$; 3(b)(c) represents corresponding contour and 2D plot. Fig-(d),(e), and (f) breather wave for the parametric values $a_1 = 0, a_2 = -1, b_1 = 0.5, b_2 = 0.5, \alpha = 0.5, \beta = 0.005$.

2.3. Conclusion

In this chapter, we have effectively apply the Hirota bilinear method to derive exact multi-soliton solutions of the first and second negative order integrable Burgers, KdV-5, the extended Sawada-Kotera equation and the extended Lax equations. Complex conjugates of parameters have settled to get distinguish dynamical interactions solutions from the multi soliton solutions of the nonlinear equations. By picking particular parametric values, we have shown different dynamical features of the multi soliton solutions (**Fig-2.1-2.12**). As a result, we obtained rogue type breather waves, breather line waves, periodic rogue type soliton and bell-shaped line soliton, breather line solitons with bell waves provides breather waves, a pair of X-shaped periodic rogue type solitons and a pair of breather type line solitons and cnoidal wave. This technique has their individual benefits: basic, concise, and it also can be used to other non-linear models. In this research, we can also investigate innovative approach to get further wide and exact result to the equations.

Chapter-3

The unified method and its application

Acknowledgement

In this chapter, the space-time fractional nonlinear differential equations for pulse narrowing transmission lines model is studied within the Jumarie's modified Riemann-Liouville derivative framework. By introducing the fractional complex transform, the effective unified method is used to find the explicit analytical solutions of the model. Abundant new exact solutions including the hyperbolic, trigonometric and rational functions are derived. These solutions are new and significant to reveal the pertinent features of the physical phenomena.

3.1. Introduction

In soliton theory of the fields: mathematical physics, control theory, fluid mechanics, optical fiber, plasma physics, biology and nonlinear transmission, the results of fractional nonlinear wave models presented an innovative success [1-24]. In fractional models, the pulse narrowing transmission lines differential model [11] is one of the model that extremely significance due to the capacity of representing electrical dynamics. Many scientists have exerted considerable efforts for determining various types of exact solutions of the fractional nonlinear transmission lines model [11-13]. Deriving exact solitary wave phenomena to fractional nonlinear models are an extremely vital task. In order to obtain the exact solitary wave solutions to nonlinear evolution equations, a number of effective methods have proposed, such as the unified method [26], The tanh method [33], homogenous balance method [38], variational iteration method[42], Adomian's decomposition method [42] the homotopy perturbation method[43], the fractional sub-equation method[44], and many more.

In this chapter, the unified method will be adopted to retrieve exact solutions of the governing equation. The details are exhibited in the upcoming sections.

3.2. Jumarie's modified Riemann-Liouville derivatives

We present the Jumarie's modified Riemann-Liouville derivative with some properties [53-54] for the continuous function $f:\Re \to \Re$ as follows;

$$D_x^{\eta} f(x)=\begin{cases}\dfrac{1}{\Gamma(1-\eta)}\dfrac{d}{dx}\displaystyle\int_0^x (x-t)^{-\eta}(f(t)-f(0))dt, & 0<\eta<1\\ (f^{(n)}(x))^{(\eta-n)}, \quad n\le\eta<n+1, & n\ge 1.\end{cases}$$

In this derivatives the well known Gamma function $\Gamma(x)$ is applied and The function is defined as

$$\Gamma(x)=\int_0^{\infty} e^{-t}t^{x-1}dx.$$

Some properties

(i). $D_x^{\eta}x^r=\dfrac{\Gamma(1+r)}{\Gamma(1+r-\eta)}x^{r-\eta}.$

(ii). $D_x^{\eta}(m\phi(x)+n\psi(x))=mD_x^{\eta}\phi(x)+nD_x^{\eta}\psi(x)$, where a and b are constants.

(iii). $D_x^{\eta}\phi(\xi)^{\xi=\psi(x)}=\dfrac{d\phi}{d\xi}D_x^{\eta}\xi.$

3.3. The Methodology of the unified method

We consider a nonlinear equation in general form in terms of x and t

$$\mathrm{H}(\chi,\chi_t^{\eta},\chi_x,\chi_{tx}^{\eta},\chi_{xx}\ldots)=0, x\in\Re, t>0, \tag{3.1}$$

where $\chi=\chi(x,t)$ is unknown function and H is a polynomial function, which carry nonlinear terms and highest order derivatives of the unknown function. The algorithm of the unified method is as [26]:

Step 1: Considering the transformation with traveling wave

$$\chi(x,t)=\chi(\zeta),\zeta=\frac{\ell}{\Gamma(1+\eta)}x^{\eta}+\frac{\wp}{\Gamma(1+\eta)}t^{\eta}+\zeta_0, \tag{3.2}$$

By using the above transformation Eq, (3.2) the nonlinear partial differential equation Eq. (3.1) is reduced to a nonlinear ordinary differential equation (ODE):

$$P(\chi,\chi',\chi'',...)=0, \tag{3.3}$$

where number of derivative of χ with respect to ζ indicated by the prime and P is a polynomial of $\chi(\zeta)$.

Step 2: In this step, we have to consider the solution of Eq. (3.3) as bellow:

$$\chi(\xi)=a_0+\sum_{i=1}^{n}a_iS^i(\zeta)+\sum_{i=1}^{n}b_iS^{-i}(\zeta), \tag{3.4}$$

Where $a_i(i=0,1,2,3,......n)$ and $b_i(i=0,1,2,3,......n)$ are constant to be consider in such a way that a_i and b_i cannot be zero at a time, and made its highest degree of Eq. (3.3) are

$$O(\chi(\zeta))=n,\ O(\frac{d\chi}{d\zeta})=n+1,\ O(\chi\frac{d\chi}{d\zeta})=2n+1,O(\frac{d^2\chi}{d\zeta^2})=n+2,......... \tag{3.5}$$

To solve Eq. (3.4) we taking an equation in ODE form, namely Riccati differential equation

$$S'=(S(\zeta))^2+\lambda. \tag{3.6}$$

Eq. (3.6) is satisfied by $\chi(\zeta)$. The solution of the Eq. (3.6) are given below,

Case-01: Hyperbolic function when, $\lambda<0$:

$$S(\zeta)=\frac{\sqrt{-(l^2+d^2)\lambda}-l\sqrt{-\lambda}\cosh(2\sqrt{-\lambda}(\zeta+E))}{l\sinh(2\sqrt{-\lambda}(\zeta+E))+d},$$
$$S(\zeta)=\frac{-\sqrt{-(l^2+d^2)\lambda}-l\sqrt{-\lambda}\cosh(2\sqrt{-\lambda}(\zeta+E))}{l\sinh(2\sqrt{-\lambda}(\zeta+E))+d},\qquad(3.7)$$
$$S(\zeta)=\sqrt{-\lambda}+\frac{2l\sqrt{-\lambda}}{l+\cosh(2\sqrt{-\lambda}(\zeta+E))-\sinh(2\sqrt{-\lambda}(\zeta+E))},$$
$$S(\zeta)=-\sqrt{-\lambda}+\frac{2l\sqrt{-\lambda}}{l+\cosh(2\sqrt{-\lambda}(\zeta+E))-\sinh(2\sqrt{-\lambda}(\zeta+E))}$$

Case-02: Trigonometric function when $\lambda>0$:

$$S(\zeta)=\frac{\sqrt{(l^2-d^2)\lambda}-l\sqrt{\lambda}\cos(2\sqrt{\lambda}(\zeta+E))}{l\sin(2\sqrt{\lambda}(\zeta+E))+d},$$
$$S(\zeta)=\frac{-\sqrt{(l^2+d^2)\lambda}-l\sqrt{\lambda}\cos(2\sqrt{\lambda}(\zeta+E))}{l\sin(2\sqrt{\lambda}(\zeta+E))+d},\qquad(3.8)$$
$$S(\zeta)=i\sqrt{\lambda}+\frac{-2il\sqrt{\lambda}}{l+\cos(2\sqrt{\lambda}(\zeta+E))-i\sin(2\sqrt{\lambda}(\zeta+E))},$$
$$S(\zeta)=-i\sqrt{\lambda}+\frac{2il\sqrt{\lambda}}{l+\cos(2\sqrt{\lambda}(\zeta+E))-i\sin(2\sqrt{\lambda}(\zeta+E))},$$

where $l\neq 0$ and d , E are real arbitrary constants.

Case-03: Rational function solution, when $\lambda=0$, then

$$S(\zeta)=\frac{1}{\zeta+E}.\qquad(3.9)$$

3.4. Implementation of the Unified method

In this portion, we apply the above effective method, in a realistic and efficient way, solve the nonlinear the space-time fractional nonlinear differential equations for pulse narrowing transmission lines models with time fractional derivatives.

3.4.1 The space-time fractional nonlinear differential equations for pulse narrowing transmission lines model

Picking the space-time fractional nonlinear differential equations for pulse narrowing transmission lines model [11]

$$D_{tt}^{2\eta}\Theta(x,t)-\frac{1}{Lh}D_{xx}^{2\eta}\Theta(x,t)-\frac{B}{2}D_{tt}^{2\eta}\Theta^{2}(x,t)-\frac{g}{12L}D_{xxxx}^{4\eta}\Theta(x,t)=0,0<\eta<1 . \tag{3.10}$$

Where $\Theta(x,t)$ is the voltage of the pulse and h,B,L and d are not variables. The physical detail of the Eq. (3.10) is elaborated in using the Kirchhoffs current law and Kirchhoffs voltage law.

Let us consider $\Theta(x,t)=\Theta(\zeta)$, $\zeta=\frac{\ell}{\Gamma(1+\eta)}x^{\eta}+\frac{\wp}{\Gamma(1+\eta)}t^{\eta}+\zeta_0$ where $\ell,\wp$ and ζ_0 are constants. Convert the Eq.(7) to the integer order.

$$(\wp-\frac{\ell^2}{Lh})\Theta-\frac{B}{2}\wp\Theta^2-\frac{g}{12Lh}\ell^4\Theta''=0 \tag{3.11}$$

By using the homogeneous balance theory in Eq. (3.11), which gives $\Rightarrow n=2$.

By using the Riccati Eq. (3.6), the Eq. (3.11) reduced to

$$\Theta(x,t)=a_0+a_1S(\zeta)+a_2S^2(\zeta)+b_1S^{-1}(\zeta)+b_2S^{-2}(\zeta) \tag{3.12}$$

Inserting Eq. (3.12) along with Eq. (3.5) into Eq. (3.11), we attain a polynomial of $S^k(\zeta),(k=0,1,2,...)$. Equating the coefficients of this polynomial of the same powers of $S(\zeta)$ to zero, we obtain a system of algebraic equations with the values for L,h,d,B,ℓ and $\wp$. Solving the system of algebraic equation with the help of Maple, we get the following solution set,

Set-1: $\wp=\pm\sqrt{\frac{(g^2\ell^2\lambda+3)}{3Lh}}\ell,\ a_0=\frac{2g^2\ell^2\lambda}{(4g^2\ell^2\lambda+3)B},\ a_2=\frac{3g^2\ell^2}{(4g^2\ell^2\lambda+3)B},\ b_2=\frac{3g^2\ell^2\lambda^2}{(4g^2\ell^2\lambda+3)B},\ a_1=b_1=0,$

Set-2: $\wp=\pm\sqrt{\frac{-(g^2\ell^2\lambda-3)}{3Lh}}\ell,\ a_0=\frac{6g^2\ell^2\lambda}{(4g^2\ell^2\lambda-3)B},\ a_2=\frac{3g^2\ell^2}{(4g^2\ell^2\lambda-3)B},\ b_2=\frac{3g^2\ell^2\lambda^2}{(4g^2\ell^2\lambda-3)B},\ a_1=b_1=0,$

Set-3: $\wp=\pm\sqrt{\frac{-(g^2\ell^2\lambda-3)}{3Lh}}\ell,\ a_0=\frac{3g^2\ell^2\lambda}{(g^2\ell^2\lambda-3)B},\ a_2=\frac{3g^2\ell^2}{(g^2\ell^2\lambda-3)B},\ a_1=b_1=b_2=0,$

Set-4: $\wp=\pm\sqrt{\frac{(g^2\ell^2\lambda+3)}{3Lh}}\ell,\ a_0=\frac{g^2\ell^2\lambda}{(g^2\ell^2\lambda+3)B},\ a_2=\frac{3g^2\ell^2\lambda^2}{(g^2\ell^2\lambda+3)B},\ a_1=b_1=b_2=0,$

Set-5: $\wp=\pm\sqrt{\frac{-(g^2\ell^2\lambda-3)}{3Lh}}\ell,\ a_0=\frac{3g^2\ell^2\lambda}{(g^2\ell^2\lambda-3)B},\ b_2=\frac{3g^2\ell^2\lambda^2}{(g^2\ell^2\lambda-3)B},\ a_1=a_2=b_1=0,$

Set-6: $\wp=\pm\sqrt{\frac{(g^2\ell^2\lambda+3)}{3Lh}}\ell,\ a_0=\frac{g^2\ell^2\lambda}{(g^2\ell^2\lambda+3)B},\ b_2=\frac{3g^2\ell^2\lambda^2}{(g^2\ell^2\lambda+3)B},\ a_1=a_2=b_1=0.$

Substitute the value of **set-1** in Eq. (3.10) with Eq. (3.7), Eq. (3.8) and Eq. (3.11), the solutions of Eq. (3.1) are follows,

If $\lambda<0$. The hyperbolic function solution

$$\Theta_{11}(x,t)=\frac{2g^2\ell^2\lambda}{(4g^2\ell^2\lambda+3)B}-\frac{3g^2\ell^2}{(4g^2\ell^2\lambda+3)B}\left\{\frac{\sqrt{-(l^2+d^2)\lambda}-l\sqrt{-\lambda}\cosh(2\sqrt{-\lambda}(\zeta+E))}{l\sinh(2\sqrt{-\lambda}(\zeta+E))+d}\right\}^2$$
$$-\frac{3g^2\ell^2\lambda^2}{(4g^2\ell^2\lambda+3)B}\left\{\frac{\sqrt{-(l^2+d^2)\lambda}-l\sqrt{-\lambda}\cosh(2\sqrt{-\lambda}(\zeta+E))}{l\sinh(2\sqrt{-\lambda}(\zeta+E))+d}\right\}^{-2}, \tag{3.13}$$

$$\Theta_{12}(x,t)=\frac{2g^2\ell^2\lambda}{(4g^2\ell^2\lambda+3)B}-\frac{3g^2\ell^2}{(4g^2\ell^2\lambda+3)B}\left\{\frac{-\sqrt{-(l^2+d^2)\lambda}-l\sqrt{-\lambda}\cosh(2\sqrt{-\lambda}(\zeta+E))}{l\sinh(2\sqrt{-\lambda}(\zeta+E))+d}\right\}^2$$
$$-\frac{3g^2\ell^2\lambda^2}{(4g^2\ell^2\lambda+3)B}\left\{\frac{-\sqrt{-(l^2+d^2)\lambda}-l\sqrt{-\lambda}\cosh(2\sqrt{-\lambda}(\zeta+E))}{l\sinh(2\sqrt{-\lambda}(\zeta+E))+d}\right\}^{-2}, \tag{3.14}$$

$$\Theta_{13}(x,t)=\frac{2g^2\ell^2\lambda}{(4g^2\ell^2\lambda+3)B}-\frac{3g^2\ell^2}{(4g^2\ell^2\lambda+3)B}\left\{\sqrt{-\lambda}+\frac{2l\sqrt{-\lambda}}{l+\cosh(2\sqrt{-\lambda}(\zeta+E))-\sinh(2\sqrt{-\lambda}(\zeta+E))}\right\}^2$$
$$\frac{3g^2\ell^2\lambda^2}{(4g^2\ell^2\lambda+3)B}\left\{\sqrt{-\lambda}+\frac{2l\sqrt{-\lambda}}{l+\cosh(2\sqrt{-\lambda}(\zeta+E))-\sinh(2\sqrt{-\lambda}(\zeta+E))}\right\}^{-2}, \tag{3.15}$$

$$\Theta_{14}(x,t)=\frac{2g^2\ell^2\lambda}{(4g^2\ell^2\lambda+3)B}-\frac{3g^2\ell^2}{(4g^2\ell^2\lambda+3)B}\{-\sqrt{-\lambda}+\frac{2l\sqrt{-\lambda}}{l+\cosh(2\sqrt{-\lambda}(\zeta+E))-\sinh(2\sqrt{-\lambda}(\zeta+E))}\}^2$$

$$-\frac{3g^2\ell^2\lambda^2}{(4g^2\ell^2\lambda+3)B}\left\{-\sqrt{-\lambda}+\frac{2l\sqrt{-\lambda}}{l+\cosh(2\sqrt{-\lambda}(\zeta+E))-\sinh(2\sqrt{-\lambda}(\zeta+E))}\right\}^{-2}. \quad (3.16)$$

If $\lambda > 0$, we get the trigonometric function solution,

$$\Theta_{15}(x,t)=\frac{2g^2\ell^2\lambda}{(4g^2\ell^2\lambda+3)B}-\frac{3g^2\ell^2}{(4g^2\ell^2\lambda+3)B}\{\frac{\sqrt{(l^2-d^2)\lambda}-l\sqrt{\lambda}\cos(2\sqrt{\lambda}(\zeta+E))}{l\sin(2\sqrt{\lambda}(\zeta+E))+d}\}^2$$

$$-\frac{3g^2\ell^2\lambda^2}{(4g^2\ell^2\lambda+3)B}\left\{\frac{\sqrt{(l^2-d^2)\lambda}-l\sqrt{\lambda}\cos(2\sqrt{\lambda}(\zeta+E))}{l\sin(2\sqrt{\lambda}(\zeta+E))+d}\right\}^{-2}, \quad (3.17)$$

$$\Theta_{16}(x,t)=\frac{2g^2\ell^2\lambda}{(4g^2\ell^2\lambda+3)B}-\frac{3g^2\ell^2}{(4g^2\ell^2\lambda+3)B}\{\frac{-\sqrt{(l^2+d^2)\lambda}-l\sqrt{\lambda}\cos(2\sqrt{\lambda}(\zeta+E))}{l\sin(2\sqrt{\lambda}(\zeta+E))+d}\}^2$$

$$-\frac{3g^2\ell^2\lambda^2}{(4g^2\ell^2\lambda+3)B}\left\{\frac{-\sqrt{(l^2+d^2)\lambda}-l\sqrt{\lambda}\cos(2\sqrt{\lambda}(\zeta+E))}{l\sin(2\sqrt{\lambda}(\zeta+E))+d}\right\}^{-2}, \quad (3.18)$$

$$\Theta_{17}(x,t)=\frac{2g^2\ell^2\lambda}{(4g^2\ell^2\lambda+3)B}-\frac{3g^2\ell^2}{(4g^2\ell^2\lambda+3)B}\{i\sqrt{\lambda}+\frac{-2il\sqrt{\lambda}}{l+\cos(2\sqrt{\lambda}(\zeta+E))-i\sin(2\sqrt{\lambda}(\zeta+E))}\}^2$$

$$-\frac{3g^2\ell^2\lambda^2}{(4g^2\ell^2\lambda+3)B}\left\{i\sqrt{\lambda}+\frac{-2il\sqrt{\lambda}}{l+\cos(2\sqrt{\lambda}(\zeta+E))-i\sin(2\sqrt{\lambda}(\zeta+E))}\right\}^{-2}, \quad (3.19)$$

$$\Theta_{18}(x,t)=\frac{2g^2\ell^2\lambda}{(4g^2\ell^2\lambda+3)B}-\frac{3g^2\ell^2}{(4g^2\ell^2\lambda+3)B}\{-i\sqrt{\lambda}+\frac{2il\sqrt{\lambda}}{l+\cos(2\sqrt{\lambda}(\zeta+E))-i\sin(2\sqrt{\lambda}(\zeta+E))}\}^2$$

$$-\frac{3g^2\ell^2\lambda^2}{(4g^2\ell^2\lambda+3)B}\left\{-i\sqrt{\lambda}+\frac{2il\sqrt{\lambda}}{l+\cos(2\sqrt{\lambda}(\zeta+E))-i\sin(2\sqrt{\lambda}(\zeta+E))}\right\}^{-2}, \quad (3.20)$$

If $\lambda = 0$, we get the rational function solution,

$$\Theta_{19}(x,t)=\frac{2g^2\ell^2\lambda}{(4g^2\ell^2\lambda+3)B}-\frac{3g^2\ell^2}{(4g^2\ell^2\lambda+3)B}\{\frac{1}{\zeta+E}\}^2-\frac{3g^2\ell^2\lambda^2}{(4g^2\ell^2\lambda+3)B}\left\{\frac{1}{\zeta+E}\right\}^{-2}. \quad (3.21)$$

Again substitute the value of **set-3** in Eq. (3.10) with Eq. (3.7), Eq. (3.8) and Eq. (3.11), the solutions of Eq. (3.1) are follows, If $\lambda < 0$. The hyperbolic function solution

$$\Theta_{31}(x,t)=\frac{3g^2\ell^2\lambda}{(g^2\ell^2\lambda-3)B}+\frac{3g^2\ell^2}{(g^2\ell^2\lambda-3)B}\{\frac{\sqrt{-(l^2+d^2)\lambda}-l\sqrt{-\lambda}\cosh(2\sqrt{-\lambda}(\zeta+E))}{l\sinh(2\sqrt{-\lambda}(\zeta+E))+d}\}^2, \quad (3.22)$$

$$\Theta_{32}(x,t)=\frac{3g^2\ell^2\lambda}{(g^2\ell^2\lambda-3)B}+\frac{3g^2\ell^2}{(g^2\ell^2\lambda-3)B}\{\frac{-\sqrt{-(l^2+d^2)\lambda}-l\sqrt{-\lambda}\cosh(2\sqrt{-\lambda}(\zeta+E))}{l\sinh(2\sqrt{-\lambda}(\zeta+E))+d}\}^2, \quad (3.23)$$

$$\Theta_{33}(x,t)=\frac{3g^2\ell^2\lambda}{(g^2\ell^2\lambda-3)B}+\frac{3g^2\ell^2}{(g^2\ell^2\lambda-3)B}\{\sqrt{-\lambda}+\frac{2l\sqrt{-\lambda}}{l+\cosh(2\sqrt{-\lambda}(\zeta+E))-\sinh(2\sqrt{-\lambda}(\zeta+E))}\}^2, \quad (3.24)$$

$$\Theta_{34}(x,t)=\frac{3g^2\ell^2\lambda}{(g^2\ell^2\lambda-3)B}+\frac{3g^2\ell^2}{(g^2\ell^2\lambda-3)B}\{-\sqrt{-\lambda}+\frac{2l\sqrt{-\lambda}}{l+\cosh(2\sqrt{-\lambda}(\zeta+E))-\sinh(2\sqrt{-\lambda}(\zeta+E))}\}^2, \quad (3.25)$$

If $\lambda > 0$, we get the trigonometric function solution,

$$\Theta_{35}(x,t)=\frac{3g^2\ell^2\lambda}{(g^2\ell^2\lambda-3)B}+\frac{3g^2\ell^2}{(g^2\ell^2\lambda-3)B}\{\frac{\sqrt{(l^2-d^2)\lambda}-l\sqrt{\lambda}\cos(2\sqrt{\lambda}(\zeta+E))}{l\sin(2\sqrt{\lambda}(\zeta+E))+d}\}^2, \quad (3.26)$$

$$\Theta_{36}(x,t)=\frac{3g^2\ell^2\lambda}{(g^2\ell^2\lambda-3)B}+\frac{3g^2\ell^2}{(g^2\ell^2\lambda-3)B}\{\frac{-\sqrt{(l^2+d^2)\lambda}-l\sqrt{\lambda}\cos(2\sqrt{\lambda}(\zeta+E))}{l\sin(2\sqrt{\lambda}(\zeta+E))+d}\}^2, \quad (3.27)$$

$$\Theta_{37}(x,t)=\frac{3g^2\ell^2\lambda}{(g^2\ell^2\lambda-3)B}+\frac{3g^2\ell^2}{(g^2\ell^2\lambda-3)B}\{i\sqrt{\lambda}+\frac{-2il\sqrt{\lambda}}{l+\cos(2\sqrt{\lambda}(\zeta+E))-i\sin(2\sqrt{\lambda}(\zeta+E))}\}^2, \quad (3.28)$$

$$\Theta_{38}(x,t)=\frac{3g^2\ell^2\lambda}{(g^2\ell^2\lambda-3)B}+\frac{3g^2\ell^2}{(g^2\ell^2\lambda-3)B}\{-i\sqrt{\lambda}+\frac{2il\sqrt{\lambda}}{l+\cos(2\sqrt{\lambda}(\zeta+E))-i\sin(2\sqrt{\lambda}(\zeta+E))}\}^2. \quad (3.29)$$

If $\lambda = 0$, then the rational function solution of Eq. (3.1) is,

$$\Theta_{39}(x,t)=\frac{3g^2\ell^2\lambda}{(g^2\ell^2\lambda-3)B}+\frac{3g^2\ell^2}{(g^2\ell^2\lambda-3)B}\{\frac{1}{\zeta+E}\}^2. \quad (3.30)$$

Replace with the value of **set-6** in Eq. (3.10) with Eq. (3.7), Eq. (3.8) and Eq. (3.11), the the solutions of Eq. (3.1) are follows,

If $\lambda < 0$. The hyperbolic function solution

$$\Theta_{61}(x,t)=-\frac{g^2\ell^2\lambda}{(g^2\ell^2\lambda+3)B}-\frac{3g^2\ell^2\lambda^2}{(g^2\ell^2\lambda+3)B}\{\frac{\sqrt{-(l^2+d^2)\lambda}-l\sqrt{-\lambda}\cosh(2\sqrt{-\lambda}(\zeta+E))}{l\sinh(2\sqrt{-\lambda}(\zeta+E))+d}\}^{-2}, \quad (3.31)$$

$$\Theta_{62}(x,t)=-\frac{g^2\ell^2\lambda}{(g^2\ell^2\lambda+3)B}-\frac{3g^2\ell^2\lambda^2}{(g^2\ell^2\lambda+3)B}\{\frac{-\sqrt{-(l^2+d^2)\lambda}-l\sqrt{-\lambda}\cosh(2\sqrt{-\lambda}(\zeta+E))}{l\sinh(2\sqrt{-\lambda}(\zeta+E))+d}\}^{-2}, \quad (3.32)$$

$$\Theta_{63}(x,t)=-\frac{g^2\ell^2\lambda}{(g^2\ell^2\lambda+3)B}-\frac{3g^2\ell^2\lambda^2}{(g^2\ell^2\lambda+3)B}\{\sqrt{-\lambda}+\frac{2l\sqrt{-\lambda}}{l+\cosh(2\sqrt{-\lambda}(\zeta+E))-\sinh(2\sqrt{-\lambda}(\zeta+E))}\}^{-2}, \quad (3.33)$$

$$\Theta_{64}(x,t)=\frac{g^2\ell^2\lambda}{(g^2\ell^2\lambda+3)B}-\frac{3g^2\ell^2\lambda^2}{(g^2\ell^2\lambda+3)B}\{-\sqrt{-\lambda}+\frac{2l\sqrt{-\lambda}}{l+\cosh(2\sqrt{-\lambda}(\zeta+E))-\sinh(2\sqrt{-\lambda}(\zeta+E))}\}^{-2}, \quad (3.34)$$

If $\lambda>0$, we get the trigonometric function solution,

$$\Theta_{65}(x,t)=-\frac{g^2\ell^2\lambda}{(g^2\ell^2\lambda+3)B}-\frac{3g^2\ell^2\lambda^2}{(g^2\ell^2\lambda+3)B}\{\frac{\sqrt{(l^2-d^2)\lambda}-l\sqrt{\lambda}\cos(2\sqrt{\lambda}(\zeta+E))}{l\sin(2\sqrt{\lambda}(\zeta+E))+d}\}^{-2}, \quad (3.35)$$

$$\Theta_{66}(x,t)=-\frac{g^2\ell^2\lambda}{(g^2\ell^2\lambda+3)B}-\frac{3g^2\ell^2\lambda^2}{(g^2\ell^2\lambda+3)B}\{\frac{-\sqrt{(l^2+d^2)\lambda}-l\sqrt{\lambda}\cos(2\sqrt{\lambda}(\zeta+E))}{l\sin(2\sqrt{\lambda}(\zeta+E))+d}\}^{-2}, \quad (3.36)$$

$$\Theta_{67}(x,t)=-\frac{g^2\ell^2\lambda}{(g^2\ell^2\lambda+3)B}-\frac{3g^2\ell^2\lambda^2}{(g^2\ell^2\lambda+3)B}\{i\sqrt{\lambda}+\frac{-2il\sqrt{\lambda}}{l+\cos(2\sqrt{\lambda}(\zeta+E))-i\sin(2\sqrt{\lambda}(\zeta+E))}\}^{-2}, \quad (3.37)$$

$$\Theta_{68}(x,t)=-\frac{g^2\ell^2\lambda}{(g^2\ell^2\lambda+3)B}+\frac{3g^2\ell^2}{(g^2\ell^2\lambda-3)B}\{-i\sqrt{\lambda}+\frac{2il\sqrt{\lambda}}{l+\cos(2\sqrt{\lambda}(\zeta+E))-i\sin(2\sqrt{\lambda}(\zeta+E))}\}^{-2}, \quad (3.38)$$

If $\lambda=0$, we get the rational function solution,

$$\Theta_{69}(x,t)=-\frac{g^2\ell^2\lambda}{(g^2\ell^2\lambda+3)B}-\frac{3g^2\ell^2\lambda^2}{(g^2\ell^2\lambda+3)B}\{\frac{1}{\zeta+E}\}^{-2}. \quad (3.39)$$

3.5. Graphical representations

In this part, we will provide some graphical representation of the exact solutions of The space-time fractional nonlinear differential equations for pulse narrowing transmission lines model (Eq.(3.10)). Graphical representations are portrayed below using the selected exact solutions of the considered model.

3.5.1. The space-time fractional nonlinear differential equations for pulse narrowing transmission lines model

Six solutions set are derived in the study. Each and every one of the derived solutions is analyzed and a few number of different types solution are illustrated here (Figs. 3.1–3.4). The graphs show the variation of amplitude, direction of flow and characteristics of the voltage of pulse for each derived solutions in space at time. Fig-(b) represents 2D plots of the voltage of the pulse $\Theta(x,t)$ for the values of inductance per unit length (L).

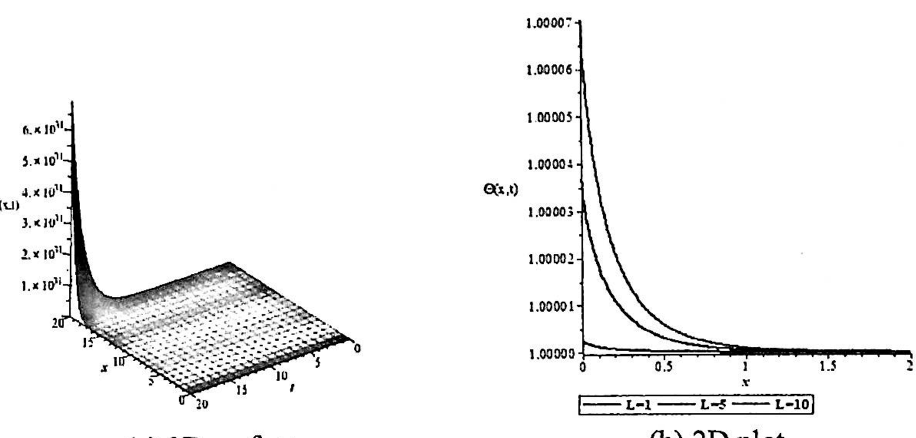

(a) 3D surface (b) 2D plot

Fig-3.1: Fig-(a) represent the solitary wave solution $\Theta(x,t)$ of Eq.(3.13) for the physical parametric values $g=1, l=1, \lambda=-1,\ B=2, d=1, L=10, E=2.h=0.5, \eta=0.8$ and for $L=1, L=5, L=10$ and $t=1$ 2D graph in Fig-(b)

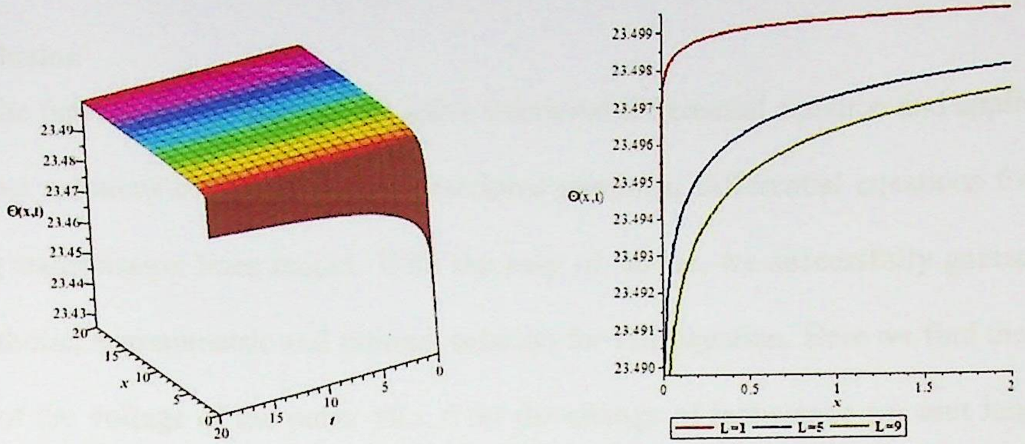

(a) 3D surface (b) 2D plot

Fig-3.2: Fig-(a) represent the solitary wave solution $\Theta(x,t)$ of Eq.(3.15) for the physical parametric values $g=1, l=1, \lambda=-1,\ B=2, d=1, L=9, E=2.h=0.5, \eta=0.2$ and for $L=1, L=5, L=9$ and $t=1$ 2D plot in Fig-(b).

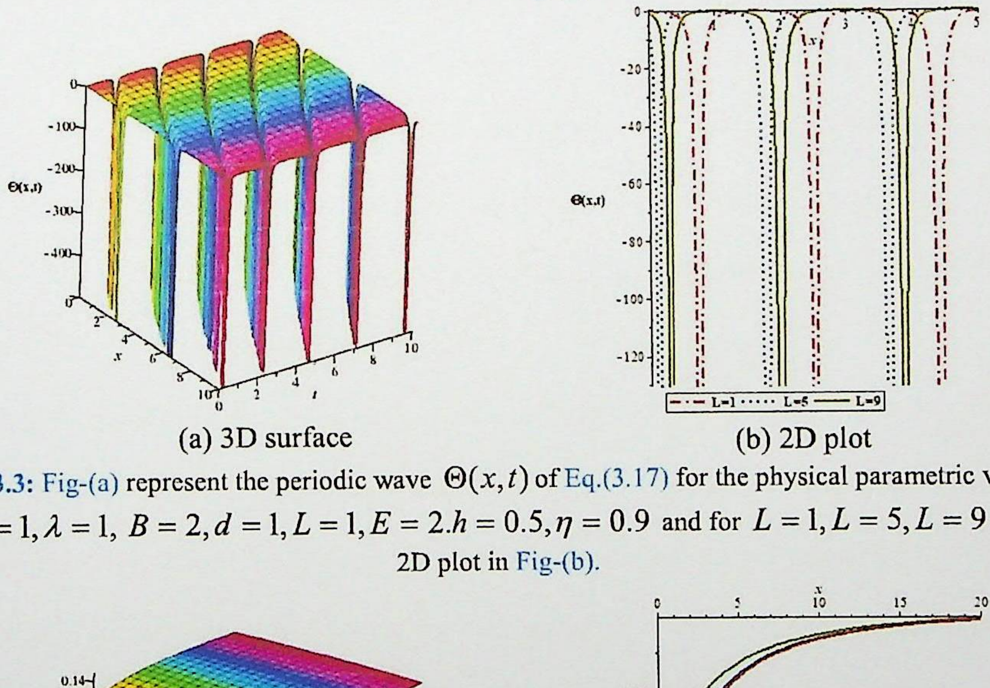

(a) 3D surface (b) 2D plot

Fig-3.3: Fig-(a) represent the periodic wave $\Theta(x,t)$ of Eq.(3.17) for the physical parametric values $g=1, l=1, \lambda=1,\ B=2, d=1, L=1, E=2.h=0.5, \eta=0.9$ and for $L=1, L=5, L=9$ and $t=1$ 2D plot in Fig-(b).

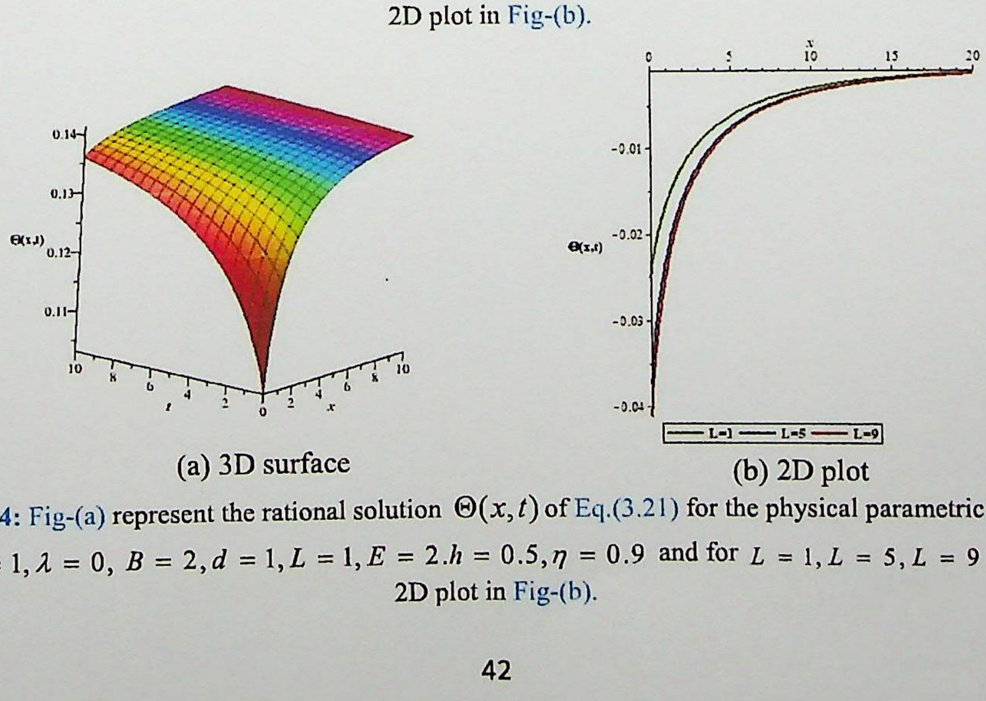

(a) 3D surface (b) 2D plot

Fig-3.4: Fig-(a) represent the rational solution $\Theta(x,t)$ of Eq.(3.21) for the physical parametric values $g=1, l=1, \lambda=0,\ B=2, d=1, L=1, E=2.h=0.5, \eta=0.9$ and for $L=1, L=5, L=9$ and $t=1$ 2D plot in Fig-(b).

3.6. Conclusion

We used the famous unified method for solve fractional differential equation and applied it to derive exact solutions of the space-time fractional nonlinear differential equations for pulse narrowing transmission lines model. With the help of Maple, we successfully gained some new hyperbolic, trigonometric and rational solution for this equation. Here we find the actual direction of the voltage of the pulse $\Theta(x,t)$ for the change of inductance per unit length (L) .So this method is more effective and can also be applied to other fractional differential equations.

Chapter-4

Analytical solutions of two space-time fractional nonlinear models using Jacobi elliptic expansion function method

Acknowledgement

In this chapter, the space-time fractional Equal-width(s-tfEW) and the space-time fractional Wazwaz-Benjamin-Bona-Mahony (s-tfWBBM) models have been investigated which are frequently arises in nonlinear optics, solid states, fluid mechanics and shallow water. Jacobi elliptic function expansion integral technique has been used to build more innovative exact solutions of the s-tfEW and s-tfWBBM nonlinear partial models. In this research fractional beta-derivatives are applied to convert the partial models to ordinary models. Several types of solutions have been derived for the models and performed some new solitary wave phenomena. The derived solutions have been presented in the form of Jacobi elliptic functions initially. Persevering different conditions on a parameter, we have achieved hyperbolic and trigonometric functions solutions from the Jacobi elliptic function solutions. Beside the scientific derivation of the analytical findings, the results have been illustrated graphically for clear identification of the dynamical properties. It is noticeable that the integral scheme is simplest, conventional and convenient in handling many nonlinear models arising in applied mathematics and the applied physics to derive diverse structural precise solutions.

4.1. Introduction

In current world, fractional derivatives have been applied to study the calculus of arbitrary order for modelling of nonlinear happening in different fields like fluid mechanics, signal processing, control theory, astrophysics, dynamical systems, plasma physics, non-linear biological systems, nanotechnology, and engineering [1-24]. Many real-life problems of the above areas can be modelled by PDE relating to the fractional derivatives. The concept of solitons, the top decisive way in applications to such models has played an important rule to identify the complex incident in various fields of sciences. Up to days, many techniques have introduced for deriving exact wave solutions of nonlinear models but the innovation reached is deficient. The precise mathematical methods to derive different classes of exact solutions namely; Jacobi elliptic function expansion [27], generalized Kudryashov [28], modified simple equation method [30-31], Bäcklund transformations [32], tanh method [33], $\tan(\Theta/2)$-expansion [34], soliton ansatz [35-36], auxiliary equation [37], sine-cosine [37], homogeneous balance [38], (G'/G)-expansion [39,40], Modified double sub-equation [41], and so on [42-44] and as well. Moreover, it is very problematic to derive the exact solution of nonlinear fractional PDE via the best possible method. So it is very top most significance to arise the explicit solutions which are exact for advance study of these nonlinear fractional models and have realizing the nonlinear phenomena. Many powerful and useful ways have introduced to solve the exact solution of nonlinear fractional equations [44]. The Jacobi elliptic method is an excellent way to integrate fractional nonlinear differential models.

In this research work, we start the research with s-tfEW [47] and sWBBM [55] models to analyse the nonlinear phenomena Hosseini and Ayati [47] presented exact solutions of the s-tfEW with the help of Kudrayshov method. Benjamin-Bona-Mohony introduces the BBM equation [49]. Then Wazwaz modified this equation to WBBM [48]. This script considers the Jacobi elliptic function expansion method to integrate the s-tfEW and s-tfWBBM models for deriving exact solutions. This technique also bases on the homogeneous balance method which is a influential procedure for achieving solutions of fractional PDE introduced by Zhang and Zhang [56]. According to this method, fractional complex transform and some useful formulas of fractional beta-derivative [57-58] are applied to transform the nonlinear s-tfEW equation to ordinary differential equation.

4.2. Beta-fractional derivative

Let us review the beta-derivative [57-58] as follows:

Definition-1. Let $\phi:[a,\infty)\to\Re$, then the fractional beta-derivative of ϕ of order β is defined as

$$D^{\eta}(\phi)(x)=\lim_{\varepsilon\to 0}\frac{\phi(x+\varepsilon(x+\frac{1}{\Gamma(\beta)})^{1-\beta})-\phi(x)}{\varepsilon},$$ for all $x\geq a,\beta\in(0,1]$. If the limit of the above exists, then ϕ (x) is said to be beta-differentiable.

Some properties of the derivative for the functions $\phi(x)$ and $\psi(x)$

(i). $D^{\beta}(m\phi(x)+n\psi(x))=mD^{\beta}\phi(x)+nD^{\beta}\psi(x)$, where a and b are constants.

(ii). $D^{\beta}x^{\alpha}=\alpha(x+\frac{1}{\Gamma(\beta)})^{\alpha-\beta}$. $\alpha\in\Re$.

(iii). $D^{\beta}(\phi\psi)=\phi D^{\beta}(\psi)+\psi D^{\beta}(\phi)$.

(iv). $D^{\beta}(\frac{\phi}{\psi})=\frac{\psi D^{\beta}(\phi)-\phi D^{\beta}(\psi)}{\psi^{2}}$, where $\psi\neq 0$.

(v). $D^{\beta}(c)=0$, where c is a constant.

Here $D^{\beta}(\psi(x))=(x+\frac{1}{\Gamma(\beta)})^{1-\beta}\frac{d\psi}{dx}$.

Definition-2. Let $\phi:[0,\infty)\to\Re$ such that ϕ is differentiable. Let $\psi(x)$ be another function defined the same range of $\phi(x)$ and also differentiable. Then the two functions satisfied the following rule :

$$D^{\beta}(\phi o\psi)=(x+\frac{1}{\Gamma(\beta)})^{1-\beta}\psi(x)'\phi'(\psi(x)).$$

4.3. The Jacobi elliptic function expansion method

Consider a given nonlinear wave equation

$$N(\varphi, D_t^{\gamma_2}\varphi, D_x^{\gamma_1}\varphi, D_t^{2\gamma_2}\varphi, D_x^{2\gamma_1}\varphi....) = 0. \quad (4.1)$$

The function $\varphi = \varphi(x,t)$ is unknown wave surface and N is a function of $\varphi = \varphi(x,t)$ and its highest order fractional derivatives.

We seek its wave transformation

$$\varphi = \varphi(\xi),\ \xi = \frac{k}{\Gamma(\gamma_1)}x^{\gamma_1} - \frac{c}{\Gamma(\gamma_2)}t^{\gamma_2}. \quad (4.2)$$

The symbols k the wave number and c wave speed.

By using the above Eq. (4.2), the fractional nonlinear Eq. (4.1) is converted to the following ODE;

$$P(\varphi, \varphi', \varphi'', \varphi'''.........). \quad (4.3)$$

In [56], $\varphi(\xi)$ is trail solution with $sn(\xi)$,

$$\varphi(\xi) = a_0 + \sum_{i=1}^{n} a_i sn^i(\xi) + \sum_{i=1}^{n} b_i sn^{-i}(\xi). \quad (4.4)$$

$sn(\xi)$ is Jacobi elliptic sine function.

is made and its highest degree is

$$P(\varphi(\xi)) = n. \quad (4.5)$$

$$P(\frac{d\varphi}{d\xi}) = n+1, P(\varphi\frac{d\varphi}{d\xi}) = 2n+1, P(\frac{d^2\varphi}{d\xi^2}) = n+2, \text{and } P(\frac{d^3\varphi}{d\xi^3}) = n+3. \quad (4.6)$$

Thus we can consider n in Eq. (4.3) to homogenous balance from the terms of the highest order of derivative term and nonlinear.

Here $cn(\xi)$ and $dn(\xi)$ are the Jacobi elliptic cosine function and the Jacobi elliptic functions respectively.

And

$$cn^2(\xi) = 1 - sn^2(\xi),\ dn^2(\xi) = 1 - m^2 sn^2(\xi), \text{ where } m\,(0 < m < 1). \quad (4.7)$$

$$\frac{d}{d\xi}(sn(\xi)) = cn(\xi)dn(\xi), \frac{d}{d\xi}(cn(\xi)) = -sn(\xi)dn(\xi). \tag{4.8}$$

$$\frac{d}{d\xi}(dn(\xi)) = -m^2 sn(\xi)cn(\xi). \tag{4.9}$$

We know that, when $m \to 1$, and $m \to 0$, then $sn(\xi) \to \tanh(\xi)$ and $sn(\xi) \to \sin(\xi)$ respectively. Thus, using Eq. (4.4) and its derivatives along with Eq. (4.7) and Eq. (4.8) into the Eq. (4.3), we achieve a set of equation with unknown parameters. Solving for unknown parameters. Using the parameters, series solution Eq. (4.4) is determined in-terms of Jacobi elliptic functions.

We can convert the Jacobi elliptic sine function to solitonic and periodic function by selecting the conditions $m \to 1$, and $m \to 0$ respectively.

4.4. Application of the method

In this section, we apply Jacobi Elliptic Expansion function method to the s-tfEW [47] and the s-tfWBBM models [55].

4.4.1: Solutions of s-tfEW equation

The space-time fractional EW(s-tfEW) equation [47] read as:

$$D_t^{\beta}\varphi(x,t) + \varepsilon D_x^{\beta}\varphi^2(x,t) - \delta D_{xxt}^{3\beta}\varphi(x,t) = 0, \quad t > 0, \; 0 < \beta \leq 1. \tag{4.10}$$

Introducing a travelling wave transformation for s-tfEW model Eq. (4.10)

$$\varphi(x,t) = f(\xi), \quad \xi = \frac{k}{\Gamma(\beta)}x^{\beta} - \frac{c}{\Gamma(\beta)}t^{\beta}. \tag{4.11}$$

Eq. (4.11) converts nonlinear partial differential Eq. (4.10) to the following nonlinear ODE,

$$-cf' + \varepsilon k(f^2)' + \delta ck^2 f''' = 0. \tag{4.12}$$

Integrating Eq. (4.12) with respect to ξ, then the equation converted to the nonlinear ODE Eq. (4.13),

$$-cf + \varepsilon kf^2 + \delta ck^2 f'' = 0. \tag{4.13}$$

Using the balance role (f^2 with f'') in Eq. (4.13) gives $n = 2$. Now choose an auxiliary solution for the balance number.

$$f(\xi) = a_0 + a_1 sn(\xi) + a_2 sn^2(\xi) + b_1 sn^{-1}(\xi) + b_2 sn^{-2}(\xi). \tag{4.14}$$

Inserting $f(\xi)$ from Eq. (4.14) to the Eq. (4.13), then equating adjacent terms of $sn^i(\xi)$ to zero and solve this terms for a_0, a_1, a_2, b_1 and b_2, we get

Case-1:

$$k=\frac{1}{2\sqrt{d}\sqrt[4]{m^4+14m^2+1}}, a_0=\frac{c\sqrt{d}(m^2+1-2\sqrt{(m^4+14m^2+1)})}{\varepsilon\sqrt[4]{m^4+14m^2+1}},$$
$$a_2=-\frac{3c\sqrt{d}m^2}{\sqrt[4]{m^4+14m^2+1}}, b_2=-\frac{3c\sqrt{d}}{\varepsilon\sqrt[4]{m^4+14m^2+1}}, a_1=0, b_1=0.$$

Case-2:

$$k=-\frac{1}{2\sqrt{d}\sqrt[4]{m^4+14m^2+1}}, a_0=-\frac{c\sqrt{d}(m^2+1-2\sqrt{(m^4+14m^2+1)})}{\varepsilon\sqrt[4]{m^4+14m^2+1}},$$
$$a_2=\frac{3c\sqrt{d}m^2}{\sqrt[4]{m^4+14m^2+1}}, b_2=\frac{3c\sqrt{d}}{\varepsilon\sqrt[4]{m^4-m^2+1}} a_1=0, b_1=0.$$

Case-3:

$$k=\frac{1}{2\sqrt{d}\sqrt[4]{m^4-m^2+1}}, a_0=\frac{c\sqrt{d}(m^2+1-2\sqrt{(m^4-m^2+1)})}{\varepsilon\sqrt[4]{m^4-m^2+1}},$$
$$b_2=-\frac{3c\sqrt{d}}{\varepsilon\sqrt[4]{m^4-m^2+1}}, a_1=0,\ a_2=0,\ b_1=0.$$

Case-4:

$$k=-\frac{1}{2\sqrt{d}\sqrt[4]{m^4-m^2+1}}, a_0=-\frac{c\sqrt{d}(m^2+1-2\sqrt{(m^4-m^2+1)})}{\varepsilon\sqrt[4]{m^4-m^2+1}},$$
$$b_2=\frac{3c\sqrt{d}}{\varepsilon\sqrt[4]{m^4-m^2+1}}, a_1=0,\ a_2=0,\ b_1=0.$$

Case:-5

$$k=\frac{1}{2\sqrt{d}\sqrt[4]{m^4-m^2+1}}, a_0=\frac{c\sqrt{d}(m^2+1-2\sqrt{(m^4-m^2+1)})}{\varepsilon\sqrt[4]{m^4-m^2+1}},$$
$$a_2=-\frac{3c\sqrt{d}m^2}{\varepsilon\sqrt[4]{m^4-m^2+1}}, a_1=0,\ b_1=0,\ b_2=0.$$

Case-6:

$$k=-\frac{1}{2\sqrt{d}\sqrt[4]{m^4-m^2+1}},a_0=-\frac{c\sqrt{d}(m^2+1-2\sqrt{(m^4-m^2+1)})}{\varepsilon\sqrt[4]{m^4-m^2+1}},$$

$$a_2=\frac{3c\sqrt{d}m^2}{\varepsilon\sqrt[4]{m^4-m^2+1}},a_1=0,\ b_1=0,\ b_2=0$$

Eq. (4.10) are reduced the following exact solutions by using (case-1-6)

$$\varphi(x,t)=\frac{c\sqrt{d}(m^2+1-2\sqrt{m^4+14m^2+1})}{\varepsilon\sqrt[4]{m^4+14m^2+1}}-\frac{3c\sqrt{d}m^2}{\sqrt[4]{m^4+14m^2+1}}sn^2(\frac{1}{2\sqrt{d}\sqrt[4]{m^4+14m^2+1}}\frac{1}{\Gamma(\beta)}x^\beta-\frac{c}{\Gamma(\beta)}t^\beta)-\frac{3c\sqrt{d}}{\varepsilon\sqrt[4]{m^4+14m^2+1}}sn^{-2}(\frac{1}{2\sqrt{d}\sqrt[4]{m^4+14m^2+1}}\frac{1}{\Gamma(\beta)}x^\beta-\frac{c}{\Gamma(\beta)}t^\beta)\quad (4.15)$$

$$\varphi(x,t)=-\frac{c\sqrt{d}(m^2+1-2\sqrt{m^4+14m^2+1})}{\varepsilon\sqrt[4]{m^4+14m^2+1}}+\frac{3c\sqrt{d}m^2}{\sqrt[4]{m^4+14m^2+1}}sn^2(-\frac{1}{2\sqrt{d}\sqrt[4]{m^4+14m^2+1}}\frac{1}{\Gamma(\beta)}x^\beta-\frac{c}{\Gamma(\beta)}t^\beta)+\frac{3c\sqrt{d}}{\varepsilon\sqrt[4]{m^4+14m^2+1}}sn^{-2}(-\frac{1}{2\sqrt{d}\sqrt[4]{m^4+14m^2+1}}\frac{1}{\Gamma(\beta)}x^\beta-\frac{c}{\Gamma(\beta)}t^\beta)\quad (4.16)$$

$$\varphi(x,t)=\frac{c\sqrt{d}(m^2+1-2\sqrt{m^4-m^2+1})}{\varepsilon\sqrt[4]{m^4-m^2+1}}-\frac{3c\sqrt{d}}{\varepsilon\sqrt[4]{m^4-m^2+1}}sn^{-2}(\frac{1}{2\sqrt{d}\sqrt[4]{m^4-m^2+1}}\frac{1}{\Gamma(\beta)}x^\beta-\frac{c}{\Gamma(\beta)}t^\beta)\quad (4.17)$$

$$\varphi(x,t)=-\frac{c\sqrt{d}(m^2+1-2\sqrt{m^4-m^2+1})}{\varepsilon\sqrt[4]{m^4-m^2+1}}+\frac{3c\sqrt{d}}{\varepsilon\sqrt[4]{m^4-m^2+1}}sn^{-2}(-\frac{1}{2\sqrt{d}\sqrt[4]{m^4-m^2+1}}\frac{1}{\Gamma(\beta)}x^\beta-\frac{c}{\Gamma(\beta)}t^\beta)\quad (4.18)$$

$$\varphi(x,t)=\frac{c\sqrt{d}(m^2+1+\sqrt{m^4-m^2+1})}{\varepsilon\sqrt[4]{m^4-m^2+1}}-\frac{3c\sqrt{d}m^2}{\varepsilon\sqrt[4]{m^4-m^2+1}}sn^2(\frac{1}{2\sqrt{d}\sqrt[4]{m^4-m^2+1}}\frac{1}{\Gamma(\beta)}x^\beta-\frac{c}{\Gamma(\beta)}t^\beta)\quad (4.19)$$

$$\varphi(x,t) = -\frac{c\sqrt{d}(m^2+1+\sqrt{m^4-m^2+1})}{\varepsilon\sqrt[4]{m^4-m^2+1}} + \frac{3c\sqrt{d}m^2}{\varepsilon\sqrt[4]{m^4-m^2+1}} sn^2(-\frac{1}{2\sqrt{d}\sqrt[4]{m^4-m^2+1}}\frac{1}{\Gamma(\beta)}x^\beta - \frac{c}{\Gamma(\beta)}t^\beta) \quad (4.20)$$

Eq. (4.15-4.20) represents the solutions in term of Jacobi elliptic function.

When $m \to 1$, the solutions Eq. (4.15-4.20) convert in the form,

$$\varphi(x,t) = -\frac{3c\sqrt{d}}{\varepsilon} - \frac{3c\sqrt{d}}{2}\tanh^2(\frac{1}{4\sqrt{d}}\frac{1}{\Gamma(\beta)}x^\beta - \frac{c}{\Gamma(\beta)}t^\beta) - \frac{3c\sqrt{d}}{2\varepsilon}\tanh^{-2}(\frac{1}{4\sqrt{d}}\frac{1}{\Gamma(\beta)}x^\beta - \frac{c}{\Gamma(\beta)}t^\beta) \quad (4.21)$$

$$\varphi(x,t) = \frac{3c\sqrt{d}}{\varepsilon} + \frac{3c\sqrt{d}}{2}\tanh^2(-\frac{1}{4}\frac{1}{\Gamma(\beta)}x^\beta - \frac{c}{\Gamma(\beta)}t^\beta) + \frac{3c\sqrt{d}}{2\varepsilon}\tanh^{-2}(-\frac{1}{4\sqrt{d}}\frac{1}{\Gamma(\beta)}x^\beta - \frac{c}{\Gamma(\beta)}t^\beta) \quad (4.22)$$

$$\varphi(x,t) = -\frac{3c\sqrt{d}}{\varepsilon}\tanh^{-2}(\frac{1}{2\sqrt{d}}\frac{1}{\Gamma(\beta)}x^\beta - \frac{c}{\Gamma(\beta)}t^\beta). \quad (4.23)$$

$$\varphi(x,t) = \frac{3c\sqrt{d}}{\varepsilon}\tanh^{-2}(-\frac{1}{2\sqrt{d}}\frac{1}{\Gamma(\beta)}x^\beta - \frac{c}{\Gamma(\beta)}t^\beta). \quad (4.24)$$

$$\varphi(x,t) = -\frac{3c\sqrt{d}}{\varepsilon}\tanh^{2}(\frac{1}{2\sqrt{d}}\frac{1}{\Gamma(\beta)}x^\beta - \frac{c}{\Gamma(\beta)}t^\beta). \quad (4.25)$$

$$\varphi(x,t) = \frac{3c\sqrt{d}}{\varepsilon}\tanh^{2}(-\frac{1}{2\sqrt{d}}\frac{1}{\Gamma(\beta)}x^\beta - \frac{c}{\Gamma(\beta)}t^\beta). \quad (4.26)$$

Solitary wave solutions Eq. (4.21-4.26) come in terms of hyperbolic functions form.

When $m \to 0$, the solutions Eq. (4.15-4.20) convert in the form,

$$\varphi(x,t) = -\frac{c\sqrt{d}}{\varepsilon} - \frac{3c\sqrt{d}}{\varepsilon}\sin^{-2}(\frac{1}{2\sqrt{d}}\frac{1}{\Gamma(\beta)}x^\beta - \frac{c}{\Gamma(\beta)}t^\beta). \quad (4.27)$$

$$\varphi(x,t) = \frac{c\sqrt{d}}{\varepsilon} + \frac{3c\sqrt{d}}{\varepsilon}\sin^{-2}(-\frac{1}{2\sqrt{d}}\frac{1}{\Gamma(\beta)}x^\beta - \frac{c}{\Gamma(\beta)}t^\beta). \quad (4.28)$$

$$\varphi(x,t) = -\frac{c\sqrt{d}}{\varepsilon} - \frac{3c\sqrt{d}}{\varepsilon}\sin^{-2}(\frac{1}{2\sqrt{d}}\frac{1}{\Gamma(\beta)}x^\beta - \frac{c}{\Gamma(\beta)}t^\beta). \quad (4.29)$$

$$\varphi(x,t)=\frac{c\sqrt{d}}{\varepsilon}+\frac{3c\sqrt{d}}{\varepsilon}\sin^{-2}\left(-\frac{1}{2\sqrt{d}}\frac{1}{\Gamma(\beta)}x^{\beta}-\frac{c}{\Gamma(\beta)}t^{\beta}\right). \tag{4.30}$$

These are periodic wave solution of the nonlinear s-tfEW model and the other two solutions (4.19), (4.20) give constants only.

4.4.2: Solutions of the WBBM model

The space-time fractional WBBM equation [49] read as:

$$\begin{aligned}&D_t^{\beta}\varphi(x,y,z,t)+D_x^{\beta}\varphi(x,y,z,t)+D_y^{\beta}\varphi(x,y,z,t)-D_{xzt}^{3\beta}\varphi(x,y,z.t)=0\\&t>0,\ 0<\beta\le 1\end{aligned}. \tag{4.31}$$

Considering a travelling wave transformation for space-time fractional 3D WBBM model Eq. (4.31)

$$\varphi(x,t)=\phi(\zeta),\quad \zeta=\frac{1}{\Gamma(\beta)}(\ell x^{\beta}+\wp y^{\beta}+cz^{\beta}-wt^{\beta}). \tag{4.32}$$

Eq. (4.32) transform to the WBBM Eq. (4.31) to the following nonlinear ODE,

$$(-w+\ell)\phi'+\wp(\phi^{3})'+\ell cw\phi'''=0. \tag{4.33}$$

Integrating Eq. (4.33) with respect to ζ , then Eq. (4.31) converted to the nonlinear ODE Eq. (4.34),

$$(-w+\ell)\phi+\wp\,\phi^{3}+\ell cw\phi''=0, \tag{4.34}$$

Using the balance role (ϕ^2 with ϕ'') in Eq. (4.34) gives $n=1$. Now choose an auxiliary solution for the balance number.

$$\phi(\zeta)=a_0+a_1 sn(\zeta)+b_1 sn^{-1}(\zeta). \tag{4.35}$$

Plugging $\phi(\zeta)$ from Eq. (4.35) to the Eq. (4.34), then comparing the adjacent terms of $sn^{i}(\zeta)$ to zero and solve this algebraic equations for a_0, a_1, w and b_1, we get four sets of solutions.

Case-1:

$$\begin{aligned}&w=\frac{\ell}{\ell cm^{2}-6\ell cm+\ell c+1},a_0=0,\\&a_1=\mp\ell m\sqrt{\frac{-2c}{\wp(\ell cm^{2}-6\ell cm+\ell c+1)}},b_2=\pm\ell\sqrt{\frac{-2c}{\wp(\ell cm^{2}-6\ell cm+\ell c+1)}}\end{aligned}.$$

Case-2:

$$\begin{aligned}&w=\frac{\ell}{\ell cm^{2}+6\ell cm+\ell c+1},a_0=0,\\&a_1=\pm\ell m\sqrt{\frac{-2c}{\wp(\ell cm^{2}+6\ell cm+\ell c+1)}},b_2=\pm\ell\sqrt{\frac{-2c}{\wp(\ell cm^{2}+6\ell cm+\ell c+1)}}\end{aligned}.$$

Case-3: $w=\dfrac{\ell}{\ell cm^2+\ell c+1}, a_0=0, a_1=0, b_2=\pm\ell\sqrt{\dfrac{-2c}{\wp(\ell cm^2+\ell c+1)}}$.

Case-4: $w=\dfrac{\ell}{\ell cm^2+\ell c+1}, a_0=0, b_1=0, a_1=\pm\ell m\sqrt{\dfrac{-2c}{\wp(\ell cm^2+\ell c+1)}}$

The exact solutions of Eq. (4.31) by using (case-1-4)

(4.36)

$$\varphi_{12}(x,t)=\ell\sqrt{\frac{-2c}{\wp(\ell cm^2-6\ell cm+\ell c+1)}}\left\{\begin{array}{l} msn(\frac{1}{\Gamma(\beta)}(\ell x^\beta+\wp y^\beta+cz^\beta-wt^\beta)) \\ -sn^{-1}(\frac{1}{\Gamma(\beta)}(\ell x^\beta+\wp y^\beta+cz^\beta-wt^\beta)) \end{array}\right\}, \quad (4.37)$$

In Eq. (4.36) and Eq. (4.37), $w=\dfrac{\ell}{\ell cm^2-6\ell cm+\ell c+1}$.

$$\varphi_{13}(x,t)=\ell\sqrt{\frac{-2c}{\wp(\ell cm^2+6\ell cm+\ell c+1)}}\left\{\begin{array}{l} msn(\frac{1}{\Gamma(\beta)}(\ell x^\beta+\wp y^\beta+cz^\beta-wt^\beta)) \\ +sn^{-1}(\frac{1}{\Gamma(\beta)}(\ell x^\beta+\wp y^\beta+cz^\beta-wt^\beta)) \end{array}\right\}, \quad (4.38)$$

$$\varphi_{14}(x,t)=-\ell\sqrt{\frac{-2c}{\wp(\ell cm^2+6\ell cm+\ell c+1)}}\left\{\begin{array}{l} msn(\frac{1}{\Gamma(\beta)}(\ell x^\beta+\wp y^\beta+cz^\beta-wt^\beta)) \\ +sn^{-1}(\frac{1}{\Gamma(\beta)}(\ell x^\beta+\wp y^\beta+cz^\beta-wt^\beta)) \end{array}\right\}. \quad (4.39)$$

In Eq. (4.38) and Eq. (4.39), $w=\dfrac{\ell}{\ell cm^2+6\ell cm+\ell c+1}$.

$$\varphi_{15}(x,t)=\ell\sqrt{\frac{-2c}{\wp(\ell cm^2+\ell c+1)}}sn^{-1}(\frac{1}{\Gamma(\beta)}(\ell x^\beta+\wp y^\beta+cz^\beta-wt^\beta)), \quad (4.40)$$

$$\varphi_{16}(x,t)=-\ell\sqrt{\frac{-2c}{\wp(\ell cm^2+\ell c+1)}}sn^{-1}(\frac{1}{\Gamma(\beta)}(\ell x^\beta+\wp y^\beta+cz^\beta-wt^\beta)), \quad (4.41)$$

$$\varphi_{17}(x,t)=\ell m\sqrt{\frac{-2c}{\wp(\ell cm^2+\ell c+1)}}sn(\frac{1}{\Gamma(\beta)}(\ell x^\beta+\wp y^\beta+cz^\beta-wt^\beta)), \quad (4.42)$$

$$\varphi_{18}(x,t)=-\ell m\sqrt{\frac{-2c}{\wp(\ell cm^2+\ell c+1)}}sn(\frac{1}{\Gamma(\beta)}(\ell x^\beta+\wp y^\beta+cz^\beta-wt^\beta)). \quad (4.43)$$

In Eq. (4.40), Eq. (4.41), Eq. (4.42) and Eq. (4.43), $w=\dfrac{\ell}{\ell cm^2+\ell c+1}$

Eq. (4.36-4.43) represents the Jacobi elliptic function solutions of Eq. (4.31).

When $m \to 1$, the solutions Eq. (4.36-4.43) convert in the form,

$$\varphi_{19}(x,t) = \ell\sqrt{\frac{-2c}{\wp(1-4\ell c)}}\left\{\begin{matrix} -\tanh(\frac{1}{\Gamma(\beta)}(\ell x^{\beta}+\wp y^{\beta}+cz^{\beta}-wt^{\beta})) \\ +\coth(\frac{1}{\Gamma(\beta)}(\ell x^{\beta}+\wp y^{\beta}+cz^{\beta}-wt^{\beta})) \end{matrix}\right\}, \quad (4.44)$$

$$\varphi_{19}(x,t) = \ell\sqrt{\frac{-2c}{\wp(1-4\ell c)}}\left\{\begin{matrix} \tanh(\frac{1}{\Gamma(\beta)}(\ell x^{\beta}+\wp y^{\beta}+cz^{\beta}-wt^{\beta})) \\ -\coth(\frac{1}{\Gamma(\beta)}(\ell x^{\beta}+\wp y^{\beta}+cz^{\beta}-wt^{\beta})) \end{matrix}\right\}. \quad (4.45)$$

In Eq. (4.44) and Eq. (4.45), $w=\frac{\ell}{(1-4\ell c)}$.

$$\varphi_{20}(x,t) = \ell\sqrt{\frac{-2c}{\wp(1+8\ell cm)}}\left\{\begin{matrix} \tanh(\frac{1}{\Gamma(\beta)}(\ell x^{\beta}+\wp y^{\beta}+cz^{\beta}-wt^{\beta})) \\ +\coth(\frac{1}{\Gamma(\beta)}(\ell x^{\beta}+\wp y^{\beta}+cz^{\beta}-wt^{\beta})) \end{matrix}\right\}, \quad (4.46)$$

$$\varphi_{21}(x,t) = -\ell\sqrt{\frac{-2c}{\wp(1+8\ell c)}}\left\{\begin{matrix} \tanh(\frac{1}{\Gamma(\beta)}(\ell x^{\beta}+\wp y^{\beta}+cz^{\beta}-wt^{\beta})) \\ +\coth(\frac{1}{\Gamma(\beta)}(\ell x^{\beta}+\wp y^{\beta}+cz^{\beta}-wt^{\beta})) \end{matrix}\right\}. \quad (4.47)$$

In Eq. (4.46) and Eq. (4.47) carry the value of $w=\frac{\ell}{(1+8\ell c)}$.

$$\varphi_{22}(x,t) = \ell\sqrt{\frac{-2c}{\wp(1+2\ell c)}}\coth(\frac{1}{\Gamma(\beta)}(\ell x^{\beta}+\wp y^{\beta}+cz^{\beta}-wt^{\beta})), \quad (4.48)$$

$$\varphi_{23}(x,t) = -\ell\sqrt{\frac{-2c}{\wp(1+2\ell c)}}\coth(\frac{1}{\Gamma(\beta)}(\ell x^{\beta}+\wp y^{\beta}+cz^{\beta}-wt^{\beta})), \quad (4.49)$$

$$\varphi_{25}(x,t) = -\ell\sqrt{\frac{-2c}{\wp(1+2\ell c)}}\tanh(\frac{1}{\Gamma(\beta)}(\ell x^{\beta}+\wp y^{\beta}+cz^{\beta}-wt^{\beta})). \quad (4.51)$$

In Eq. (4.48), Eq. (4.49), Eq. (4.50) and Eq. (4.51), $w=\frac{\ell}{(1+2\ell c)}$.

Solitary wave solutions Eq. (4.44-4.51) comes from the hyperbolic functions.

When $m \to 0$, the solutions Eq. (4.36-4.43) convert to the form,

$$\varphi_{25}(x,t)=\ell\sqrt{\frac{-2c}{\wp(1+\ell c)}}\left\{\operatorname{cosec}\left(\frac{1}{\Gamma(\beta)}(\ell x^{\beta}+\wp y^{\beta}+cz^{\beta}-wt^{\beta})\right)\right\}, \tag{4.52}$$

$$\varphi_{26}(x,t)=\ell\sqrt{\frac{-2c}{\wp(1+\ell c)}}\left\{-\operatorname{cosec}\left(\frac{1}{\Gamma(\beta)}(\ell x^{\beta}+\wp y^{\beta}+cz^{\beta}-wt^{\beta})\right)\right\}, \tag{4.53}$$

$$\varphi_{27}(x,t)=-\ell\sqrt{\frac{-2c}{\wp(1+\ell c)}}\left\{\operatorname{cosec}\left(\frac{1}{\Gamma(\beta)}(\ell x^{\beta}+\wp y^{\beta}+cz^{\beta}-wt^{\beta})\right)\right\}. \tag{4.54}$$

In Eq. (4.52), Eq. (4.53) and Eq. (4.54), $w=\frac{\ell}{(1+\ell c)}$.

Eq. (4.36)-Eq. (4.43) are Jacobi functions solution of the nonlinear WBBM model. Out of eight Jacobi elliptic functions, three of them are repeated and two results give zero solution. So these five solutions are neglected.

4.5. Graphical representation

In this section, we will provide some graphical representation of the exact solutions of the space-time fractional Equal Width (s-tfEW) equation (Eq. (4.10)) and the space-time fractional Wazwaz-Benjamin-Bona-Mahony (s-tfWBBM) model (Eq.(4.31)). Graphical representations are portrayed below using the selected exact solutions of EW and WBBM model.

4.5.1: Graphics of the solutions of s-tfEW equation

Three types of results are achieved for EW equation. Each and every one of the derived solutions is analyzed and a few number of different types solution are illustrated here **Figs-(4.1–4.3)**. All The graphs show the variation of amplitude, direction, shape of the derived wave solution to identify intrinsic nature of the model. The solution $\varphi(x,t)$ in Eq. (4.15-4.20) represent the Jacobi elliptic functions Eq. (4.21-4.26) shows the solitonic nature comes from hyperbolic function and Eq. (4.27-4.30) are trigonometric function exhibit as periodic waves.

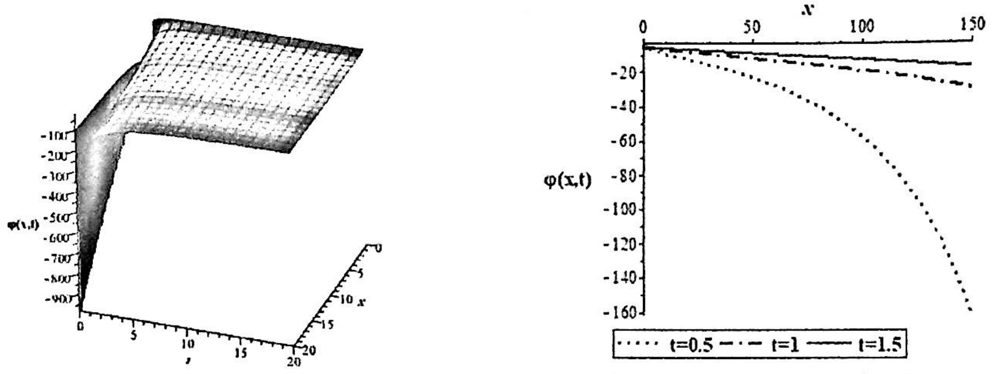

(a) 3D View of Eq.(4.21) (b) 2D View of Eq.(4.21)

Fig-4.1: Represent the function $\varphi(x,t)$ in Eq. (4.21) for the values; $d = 0.5, \beta = 1/6, c = 1, \varepsilon = 1$: **(a)** 3D surface, **(b)** 2D graphs at $t = 0.5, 1, 1.5$.

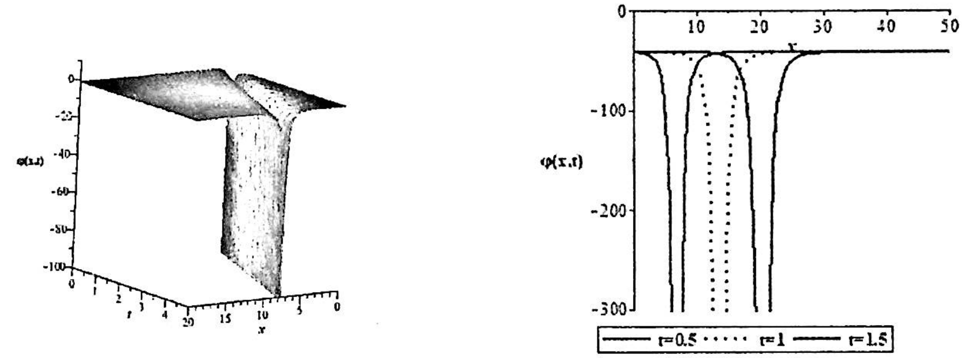

(a) 3D View of Eq.(4.23) (b) 2D View of Eq.(4.23)

Fig-4.2: Represent the function $\varphi(x,t)$ in Eq. (4.23) for : $d = 0.5, \beta = 3/4, c = 5, \varepsilon = 2$: **(a)** 3D surface and **(b)** 2D graphs at $t = 0.5, 1, 1.5$.

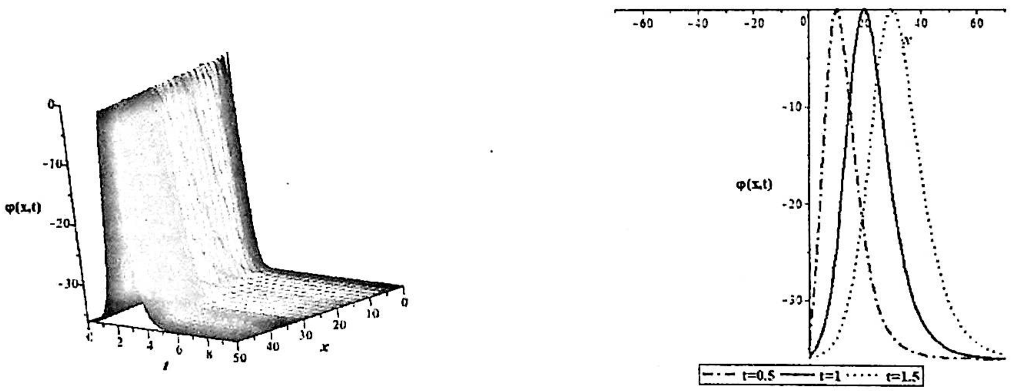

(a) 3D View of Eq.(4.25) (b)2D View of Eq.(4.25)

Fig-4.3: Represent the bell type wave $\varphi(x,t)$ in Eq. (4.25) for the parametric values, $d = 1, \beta = 3/5, c = 3, \varepsilon = 0.25$: **(a)** 3D surface and **(b)** 2D graphs for and $t = 0.5, 1, 1.5$.

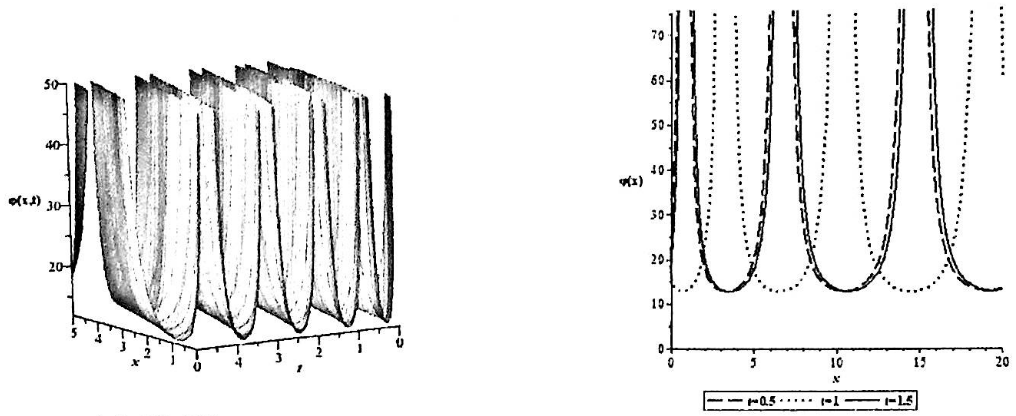

(a) 3D View of Eq.(3.27) (b) 2D View of Eq.(3.27)

Fig-4.4: Represent the periodic wave of $\varphi(x,t)$ in Eq. (4.27) for the physical parametric values, $d=0.5, \beta=3/4, c=-3, \varepsilon=1$: (a) 3D surface and (b) 2D graphs at $t=0.5,1,1.5$.

4.5.2: Graphics of the equation WBBM

The findings of the study on WBBM model are in the form of hyperbolic (Eq. (4.44-4.51)) and trigonometric (Eq. (4.52-4.55)) functions. Hyperbolic and trigonometric function represent solitonic and periodic solutions. All the derived functions are analyzed and two types function have shown graphically in the Fig-4.5 to Fig-4.6.

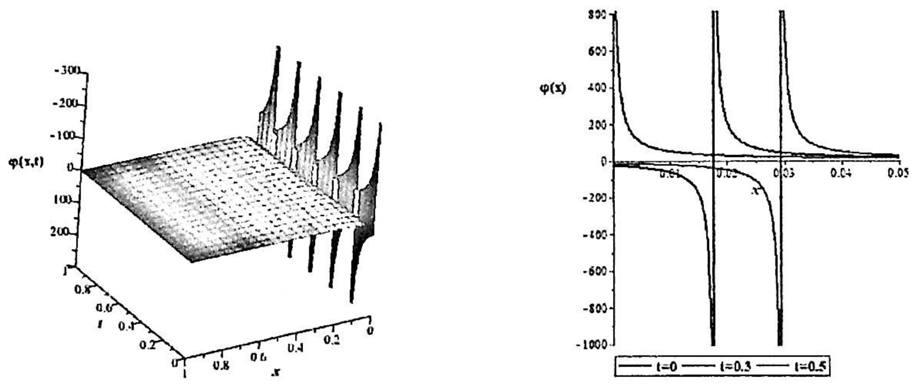

(a) 3D View of Eq.(4.48) (b) 2DView of Eq.(4.48)

Fig-4.5: Represent the solitary periodic wave $\varphi(x,t)$ in Eq. (4.48) for the physical parametric values, $\beta=1, \ell=2, c=-2, \wp=1, z=0, y=0$: (a) 3D surface, (b) 2D graphs at $t=0,1.03,0.5$.

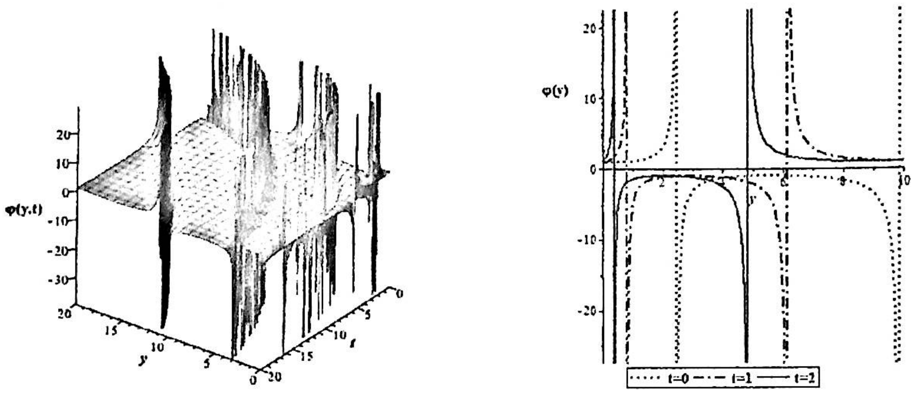

(a) 3D View of Eq.(4.52) (b) 3D View of Eq.(4.52)

Fig-4.6: Represent the periodic wave $\varphi(x,t)$ in Eq. (4.52) for the physical parametric values $\beta = 0.5, \ell = 2, c = -2, \wp = 1, z = 0, x = 0$: (a) 3D surface, (b) 2D graphs at $t = 0,1.2$.

Remarks: More other Jacobi function solutions to the s-tfEW and WBBM equation are derivable by keeping trial solution in terms of the Jacobi functions $cn(\xi)$ and $dn(\xi)$ as below;

$$u(\xi) = a_0 + \sum_{i-1}^{n} a_i cn^i(\xi) + \sum_{i-1}^{n} a_i cn^{-i}(\xi) \tag{4.55}$$

And

$$u(\xi) = a_0 + \sum_{i-1}^{n} a_i dn^i(\xi) + \sum_{i-1}^{n} a_i dn^{-i}(\xi) \tag{4.56}$$

In view of Eq. (4.55) and Eq. (4.56), we can add soliton and non-solitonic solutions describe via cnoidal, dnoidal waves and trigonometric functions.

4.6. Concluding remarks

In this chapter, the space-time fractional EW and WBBM equation has successfully integrated via Jacobi elliptic function expansion technique with modified Riemann-Liouville derivatives. By introducing a fractional transformation, the considered nonlinear partial travelling wave equation reduced to ordinary differential model. Then we successfully used Jacobi elliptic expansion method to integrate the model. At the end of our procedure, three types solutions are achieved namely, Jacobi elliptic, hyperbolic and trigonometric function with unknown parameters, which indicates that Jacobi elliptic expansion technique are very fruitful as well as appropriate to find the exact solutions of nonlinear fractional models. In addition, graphical illustration of the solutions has plotted with unknown parameters.

Researchers can undoubtedly use the technique to analyze the internal mechanism of nonlinear physical systems.

Chapter-5

New exact solitary wave solutions for Couple of models through the generalized Kudryshov method

Acknowledgement

Fractional derivatives are most important to accurate nonlinear modeling in the fields of crystal, optics and quantum mechanics even in biological phenomena. We present the generalized Kudryshov technique to integrate three nonlinear time fractional model namely; complex Schrodinger and biological population models. As a result, we get some solitary wave solutions in the form of hyperbolic and combo hyperbolic-trigonometric functions including both stable and unstable cases. We obtain kink wave, bright bell wave, dark bell wave, combo periodic-rogue waves, combo M-W shaped periodic-rogue waves in stable cases, and singular kink type in unstable solitonic natures. We analyzed the achieved results and illustrated graphically.

5.1. Introduction

The research of nonlinear partial differential equations has prepared huge effective work in the field of applied physics, manufacturing science and applied mathematics. After few decades ago most of the nonlinear research work based on the order of 1^{st}, 2^{nd} or any integer order. But what would be happen, when this order is fraction. To analysis the fractional order nonlinear problem, fractional calculus was developed. The new branch of calculus gives us huge opportunity to solve the exact solution of nonlinear science. It has a vast scope to form mathematical model by the new branch of mathematics in various fields such as, quantum mechanics [1-3], optics [5], Biological dynamics [8], electro-magnetic waves [10], superconductivity and Bose-Einstein condensates [14], electrics signal processing [15], dust acoustic and dense electron-positron-ion wave [19]control theory, astrophysics, dynamical systems, plasma physics, nanotechnology, acoustics and so on [20-24].

Time fractional evolution is most effective since it gives a the past of the example [26] and also, it takes care of the deliberate evolution. For example, if parametric values of the order of the fractional derivatives can be externally controlled, the evolution of the soliton is synthetically manifested. This is globally approved characteristics of the fractional derivatives that are being applied in several related fields. The practical example of the related filed is the temporal evolution of solitons in optical fibers which can be slowed to address internet bottleneck, that is growing problem in the internet industry.

Two models of NLEEs that are considered the fractional form of time fractional complex Schrodinger equation (FCSE) [2] and in population dynamics the time fractional biological population (FBP) model [8].

The Schrödinger model has describe the quantum transport, energy conservation law in quantum physics and identify the position of electron in its orbit. Schrodinger equation (SE) model was first developed by Laskin [50] which occurs in many important areas as water wave, fluid dynamics, bio-chemistry, optical pulses propagation into nonlinear fiber and plasma physics. Few researchers deliberated much more effort in investigation of the complex fractional Schrodinger model: Khater [2] studied by a supplementary equation and a (G′/G)-schemes. Alam and Li [3] presented exact solutions via modified (G′/G)-expansion method. The fractional biological population model describes the density of population in presences of birth and death with diverse effect of diseases [8]. This fractional model studied by many researchers for deriving exact solutions such as Bekir et. al. [59] by fractional complex transform and exp-function method. Also Lu [60] by Backlund transformation method.

The purpose of this chapter is to find stable and unstable soliton solutions of the FCSE and FBP models via the generalized Kudryashov method [28-29], which played a vital role in mathematical physics.

5.2. Conformable fractional derivative and its properties

Let, $\phi:(0,\infty)\rightarrow\Re$, the conformable fractional derivative of ϕ for order α is defined [57-58] as,

$$\frac{\partial^\alpha \phi}{\partial t^\alpha}=\lim_{\varepsilon\rightarrow 0^+}\frac{\phi(t+\varepsilon t^{1-\alpha})-\phi(t)}{\varepsilon},\ 0<\alpha\leq 1 \text{ and time } t \text{ is positive.}$$

Some mathematical postulate of the derivative is,

$$\frac{\partial^\alpha}{\partial t^\alpha}(a\phi+b\varphi)=a\frac{\partial^\alpha}{\partial t^\alpha}(\phi)+b\frac{\partial^\alpha}{\partial t^\alpha}(\varphi),\ \forall a,b\in\Re.$$

$$\frac{\partial^\alpha}{\partial t^\alpha}(t^\beta)=\beta t^{\beta-\alpha},\ \forall\beta\in\Re \text{ and } \frac{\partial^\alpha}{\partial t^\alpha}(\lambda)=0,\ \lambda=const.$$

$$\frac{\partial^\alpha}{\partial t^\alpha}(\phi\circ\varphi)(t)=t^{1-\alpha}\phi'(\varphi(t))\varphi'(t).$$

5.3. Summary of the method

Consider a general nonlinear partial differential equation,

$$\aleph(\chi,\chi_t^\alpha,\chi_x,\chi_{tx}^\alpha,\chi_{xx}\ldots)=0,, \tag{5.1}$$

where x is real and t is positive

where $\chi=\chi(x,t)$ is unknown surface and $\aleph$ is a polynomial of the function χ and its derivatives. The generalized Kudryashov method [28-29] can be summarized as follows:

Step 1: Consider the following traveling wave transformation

$$\chi(x,t) = \mathrm{B}(\zeta), \zeta = x - \frac{ct^{\alpha}}{\alpha}, \tag{5.2}$$

where c is the wave velocity. Eq. (5.1) converted to ODE with the wave transformation Eq. (5.2). The reduced ODE form as bellow:

$$\mathrm{P}(\mathrm{B}, \mathrm{B}', \mathrm{B}''', ...) = 0, \tag{5.3}$$

where prime indicate the derivation of B is with respect to ζ.

Step 2: Picking a trail solution of Eq. (5.3):

$$\mathrm{B}(\zeta) = \frac{\sum_{i=0}^{\mathrm{B}} \ell_i \phi^i(\zeta)}{\sum_{j=0}^{\mathrm{A}} \wp_j \phi^j(\zeta)}, \tag{5.4}$$

where ℓ_i and $\wp_j$ are unknown real parameters and $\phi(\zeta)$ satisfies the following Riccati type [62] ordinary differential equation:

$$\phi'(\zeta) = \phi^2(\zeta) - \phi(\zeta). \tag{5.5}$$

Eq. (5.5) is carrying the solution in the following form:

$$\phi(\zeta) = \frac{1}{1 + Ae^{\zeta}}, \tag{5.6}$$

where A is any unknown constant.

Step 3: By using the following homogenous balance role from the nonlinear and highest order term of Eq. (5.3).

The degree of $\mathrm{B}(\zeta)$ as $D(\mathrm{B}(\zeta)) = \mathrm{X} - \mathrm{A}$, which gives the degree of other term as

$$D(\frac{d^{\eta}\mathrm{B}}{d\zeta^{\eta}}) = \mathrm{X} - \mathrm{A} + \eta, D(\mathrm{B}^{\mu}(\frac{d^{\eta}\mathrm{B}}{d\zeta^{\eta}})^{s}) = (\mathrm{X} - \mathrm{A})\mu + s(\mathrm{X} - \mathrm{A} + \eta),$$

where μ, η, s are integer numbers.

Thus, we can evaluate the value of X and A in Eq. (5.3).

Step 4: Plugging Eq. (5.4) with Eq. (5.5) to Eq. (5.3). after collecting the expressions ϕ then setting each coefficients of ϕ to zero, we attain a arrangement of algebraic equations for $\ell_i, \wp_j$ and c .Solving for $\ell_i, \wp_j$ and c by Maple soft.

Step 5: Replacing gained parametric values into the Eq. (5.4), then the solutions of Eq. (5.1) can be constructed.

5.4. Implementation of the generalized Kudryashov method

In this section, we implement the above reliable technique, in a realistic and efficient way, to handle nonlinear time fractional complex Schrodinger and time fractional biological population models with time fractional derivatives.

5.4.1. The Time fractional complex Schrodinger model

Consider the Time fractional complex Schrodinger model

$$\frac{\partial^{\gamma}\varphi}{\partial t^{\gamma}}+i\frac{\partial^{2}\varphi}{\partial x^{2}}+\frac{\partial}{\partial x}(|\varphi|^{2}\varphi)=0, 0<\gamma<1, \tag{5.7}$$

Let us consider $\varphi(x,t)=\phi(\xi)\exp(i\tau)$, $\xi=ik(x-\frac{2g}{\gamma}.t^{\gamma})$, $\tau=(gx-\frac{h}{\gamma}.t^{\gamma})$ and convert this nonlinear complex FSE to the nonlinear integer order SE

$$\frac{\partial^{\gamma}\varphi}{\partial t^{\gamma}}=i(g\phi+2hk\phi')\exp(i\tau)$$

$$\frac{\partial^{2}\varphi}{\partial x^{2}}=-(h^{2}\phi+2hk\phi'+k^{2}\phi'')\exp(i\tau)$$

$$\frac{\partial}{\partial x}(|\varphi|^{2}\varphi)=i(h\phi^{3}+3k\phi^{2}\phi'')\exp(i\tau)$$

We obtain the nonlinear complex PSE by using the above equations,

$$(g-h^{2})\phi-k^{2}\phi''+h\phi^{3}+3k\phi^{2}\phi'=0 \tag{5.8}$$

Using the rule of homogenous balance on Eq. (5.8) (ϕ'' and $\phi^2\phi'$) $\Rightarrow$ ($\Rightarrow n = m+\frac{1}{2}$. Apply another transformation $\phi(\xi) = u^{\frac{1}{2}}(\xi)$ in Eq. (5.8), we get ordinary differential equations

$$4hu^3 + 4(g-h)u^2 + 6ku^2u' + k^2u'^2 - 2k^2uu'' = 0 \tag{5.9}$$

Case-1: using the homogenous balance role from term uu'' with term u^2u in Eq. (5.9) gives $\Rightarrow n = m+1$.

Setting $m = 1$, we have $n = 2$. Therefore Eq. (5.9) reduces to

$$u(\xi) = \frac{\ell_0 + \ell_1\phi + \ell_2\phi^2}{\wp_0 + \wp_1\phi} \tag{5.10}$$

Inserting Eq. (5.10) along with Eq. (5.5) into Eq. (5.9), we have a polynomial of $\phi^k, (k = 0,1,2,...)$. Equating the coefficients of this polynomial of the same powers of ϕ to zero, we obtain a system of equations yields the values for g, h, ℓ_0, ℓ_1 and $\wp_1$.

Set 1: $g = \frac{1}{2}k^2, h = -\frac{1}{2}k, \ell_0 = 0, \ell_1 = 0, \ell_2 = \frac{1}{2}k\wp_1, \wp_1 = \wp_1.\wp_0 = 0$

Set 2: $g = \frac{1}{2}k^2, h = \frac{1}{2}k, \ell_0 = 0, \ell_1 = -\frac{1}{2}k\ell_1, \ell_2 = \frac{1}{2}k\wp_1, \wp_1 = \wp_1.\wp_0 = 0$

, The time fractional complex PSE equations hold the solution for **set-1**,

$$\varphi_1 = [\frac{k}{2}.\frac{1}{1+\lambda\exp\{ik(x-\frac{k^2t^\gamma}{\gamma})\}}]^{\frac{1}{2}}\exp\{i(\frac{1}{2}kx + \frac{1}{2}\frac{kt^\gamma}{\gamma})\} \tag{5.11}$$

The time fractional complex PSE equations hold the solution for **set-2**,

$$\varphi_2 = \{-\frac{k}{2}\frac{1}{1+\lambda\exp\{ik(x+\frac{k^2t^\gamma}{\gamma})\}}\}^{\frac{1}{2}}\exp\{i(\frac{1}{2}kx + \frac{1}{2}\frac{kt^\gamma}{\gamma})\}, \tag{5.12}$$

5.4.2. The time fractional biological population model

We consider a time fractional biological population model of the form [8]:

$$\frac{\partial^\gamma P}{\partial t^\gamma}=\frac{\partial^2}{\partial x^2}(P^2)+\frac{\partial^2}{\partial y^2}(P^2)+\kappa(P^2-\rho),\ t>0,\ 0<\gamma<1,\ x,y\in R, \tag{5.13}$$

where P indicate the population density, $\kappa(P^2-\rho)$ presents the population supply owing to births and deaths, and κ,ρ are unknown parameters.

Use the transformation $\tau=vx+ivy-\dfrac{wt^\gamma}{\Gamma(1+\gamma)}$, (5.14)

In which w and v are free constants and $i=\sqrt{-1}$.

Eq. (5.14) converted to the Eq. (5.13) to an ODE as follows:

$$wp'+\kappa p^2-\kappa\rho=0. \tag{5.15}$$

Case-1: From the term p' and p^2 in Eq. (5.15), the homogenous balance number gives $\Rightarrow n=m+1$.

Setting $m=1$, we have $n=2$. Therefore Eq. (5.4) reduces to

$$u(\xi)=\frac{\ell_0+\ell_1 p+\ell_2 p^2}{\wp_0+\wp_1 p} \tag{5.16}$$

Inserting Eq. (5.16) along with Eq. (5.5) into Eq. (5.15), we have a polynomial of $p^k,(k=0,1,2,...)$. Equating the coefficients of this polynomial of the same powers of ϕ to zero, we obtain a system of equations yields the values for w,κ,ℓ_0,ℓ_1 and $\wp_1$.

Cluster-1: $w=\pm 2\kappa\sqrt{\rho},\ \ell_0=-(\ell_1\mp\wp_1\sqrt{\rho})/2,\ \ell_2=\mp 2\wp_1\sqrt{\rho},\ \wp_0=\dfrac{1}{2}(\wp_1\mp\dfrac{\ell_1}{\sqrt{\rho}}),\ell_1,\wp_1$

are constants.

Cluster-2: $w=\pm\kappa\sqrt{\rho},\ \ell_0=\mp\wp_1\sqrt{\rho}/2,\ \ell_1=\pm\wp_1\sqrt{\rho},\ \ell_2=\mp\wp_1\sqrt{\rho},\ \wp_0=-\wp_1/2.$ $\wp_1$ is constant.

For **cluster-1**, the time fractional biological population model holds the solution as:

$$P(x,y,t)=\frac{-(\ell_1\mp\wp_1\sqrt{\rho})(1+Ae^{\tau})^2\mp4\wp_1\sqrt{\rho}}{(\wp_1\mp\frac{\ell_1}{\sqrt{\rho}})(1+Ae^{\tau})^2+2\wp_1(1+Ae^{\tau})},\tag{5.17}$$

where, $\tau=vx+ivy\mp\dfrac{2\kappa\sqrt{\rho}t^{\gamma}}{\Gamma(1+\gamma)}$.

For **cluster-2**, the time fractional biological population model holds the solution as:

$$P(x,y,t)=\frac{\mp\sqrt{\rho}(1+Ae^{\tau})^2\pm2\sqrt{\rho}(1+Ae^{\tau})\mp2\sqrt{\rho}}{-(1+Ae^{\tau})^2+2(1+Ae^{\tau})},\tag{5.18}$$

where $\tau=vx+ivy\mp\dfrac{\kappa\sqrt{\rho}t^{\gamma}}{\Gamma(1+\gamma)}$

5.5. Graphical representations

In this section, we will provide some graphical representation of the exact solutions of time fractional complex Schrodinger equation (FCSE) (Eq. (5.7)) and in population dynamics the time fractional biological population (FBP) model (Eq. (5.13)).Graphical representations are portrayed below using the selected exact solutions of FCSE and FBP equations.

5.5.1. Graphs the Time fractional complex Schrodinger model

Two exact solutions are derived in this study. Both of them are analyzed and illustrate them in the Figs. 5.1–5.4. The grid indicates the change of all physical properties for each gained wave solutions. The solution $\varphi(x,t)$ of Eq. (5.11) for solution set-1, Eq. (5.12) for solution set-2 represented in Fig-5.1-5.2 and Fig-5.3-5.4 respectively

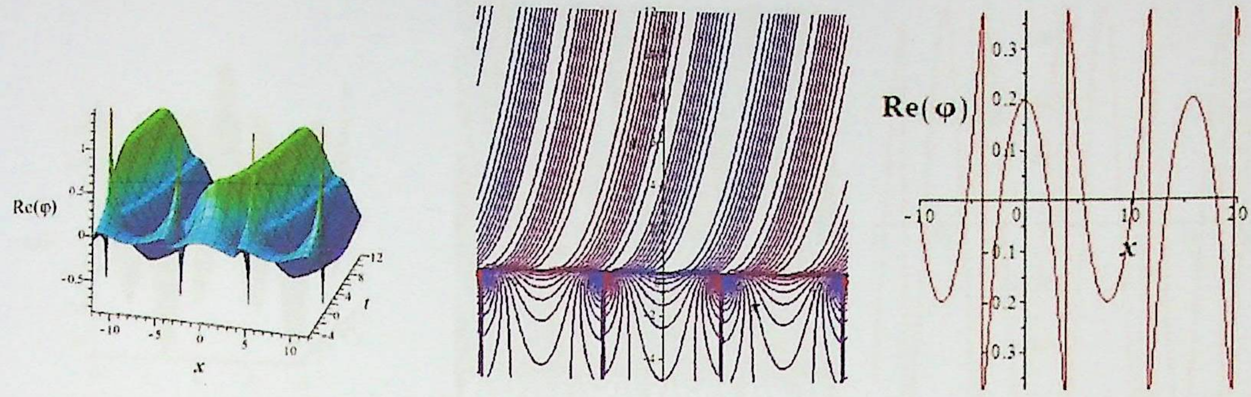

(a) Real 3D surface (b) Real contour shape (c) Real 2D shape

Fig-5.1: Represent the real part of the wave solution $\varphi(x,t)$ of Eq. (5.11) with $\lambda = 0.5$, $\gamma = 0.5$, $k = 0.8$ and $t = -1$ for 2D graph.

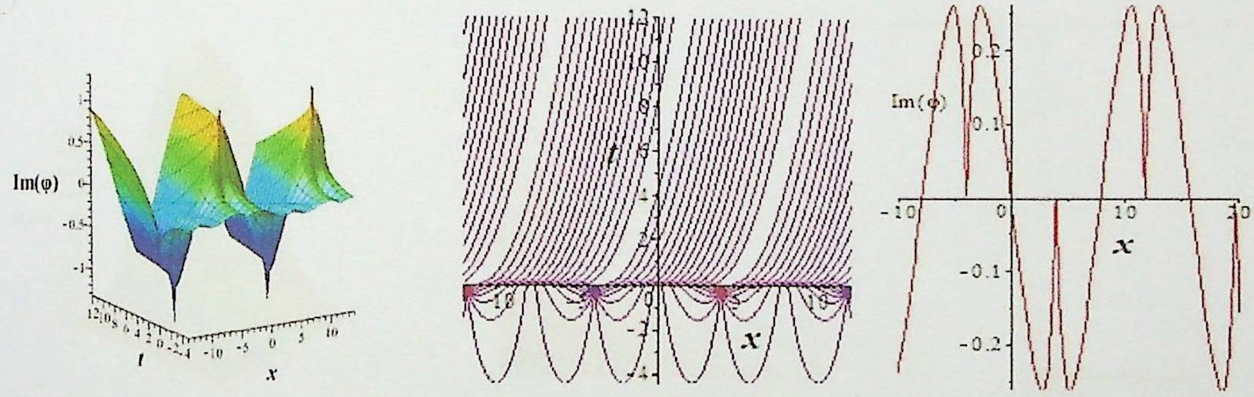

(a) Complex 3D surface (b) Complex contour shape (c) Complex 2D shape

Fig-5.2: Represent the imaginary part of the wave solution $\varphi(x,t)$ of Eq. (5.11) with $\lambda = 0.5$, $\gamma = 0.5$, $k = 0.8$ and $t = -1$ for 2D graph.

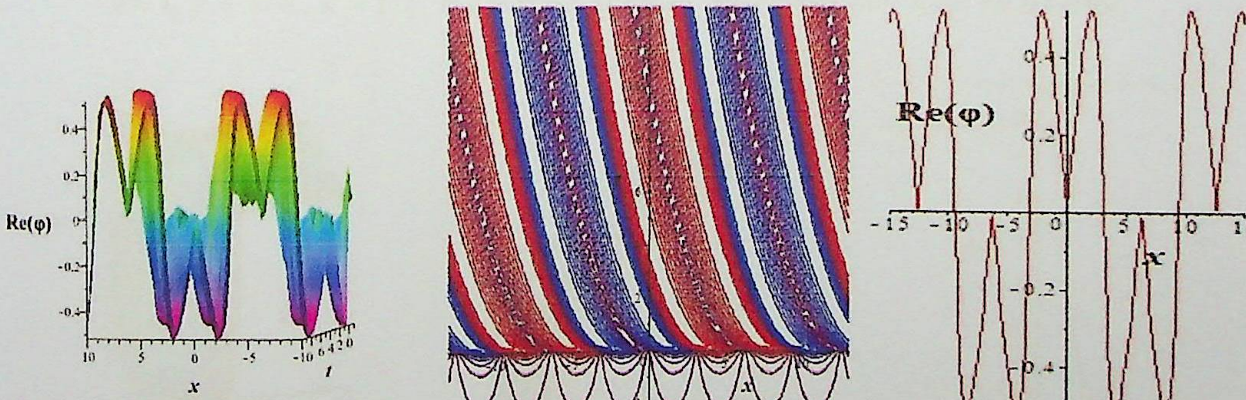

(a) Real 3D surface (b) Real contour shape (c) Real 2D shape

Fig-5.3: Represent the real part of the wave solution $\varphi(x,t)$ of Eq. (5.12) with $\lambda = 0.5$, $\gamma = 0.5$, $k = 1$ and $t = 0$ for 2D graph.

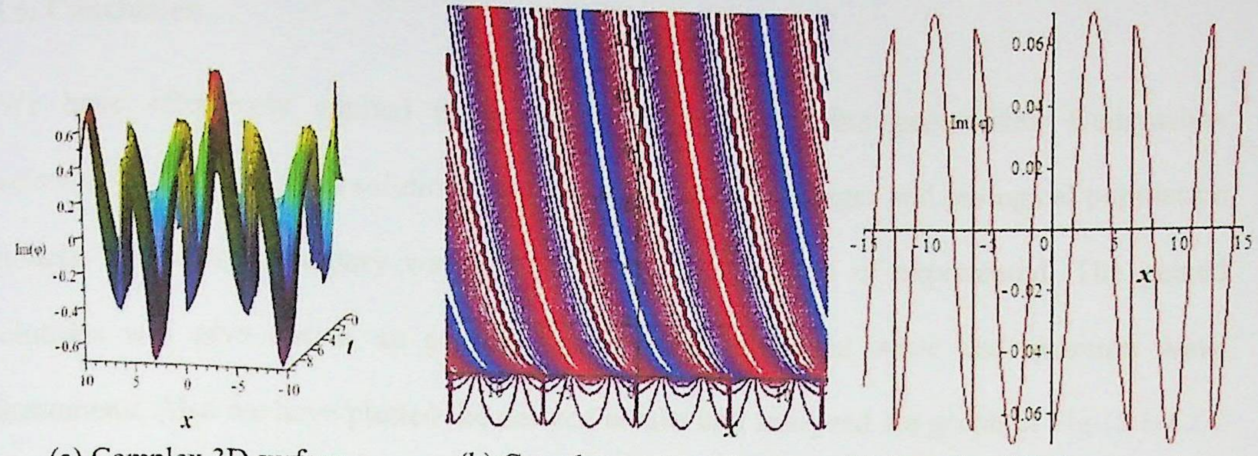

(a) Complex 3D surface (b) Complex contour shape (c) Complex 2D shape

Fig-5.4: Represent the imaginary part of the wave solution $\varphi(x,t)$ of Eq. (512) with $\lambda = 0.5$, $\gamma = 0.5$, $k = 1$ and $t = -1$ for 2D graph.

5.5.2: Graphs the time fractional biological population model

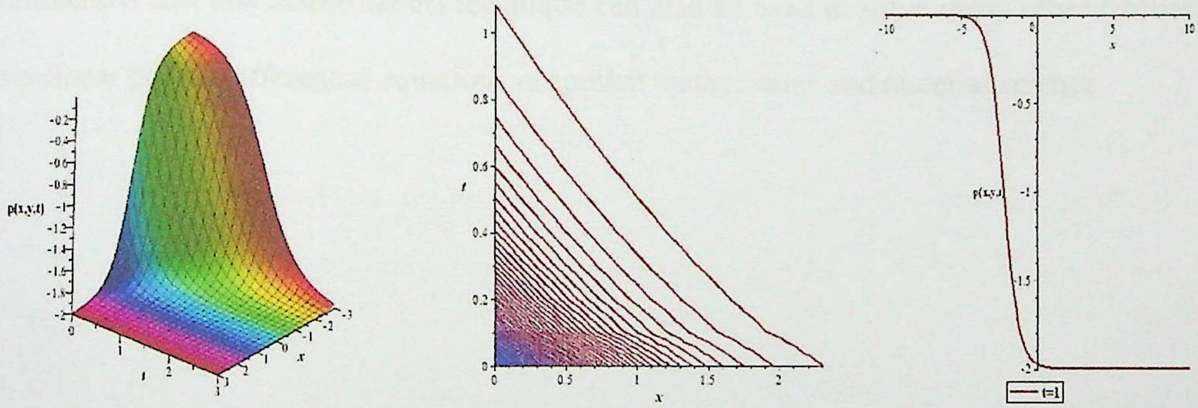

(a) (b) (c)

Fig-5.5: Represent the imaginary part of the solution $p(x,y,t)$ of Eq. (5.17) for the physical parametric values $A = 1$, $\gamma = 3/4$, $k = 2, \ell_1 = 1, \nu = -2, \rho = 1, \wp_1 = 1, y = 0$ and $t = 1$ for 2D graph.

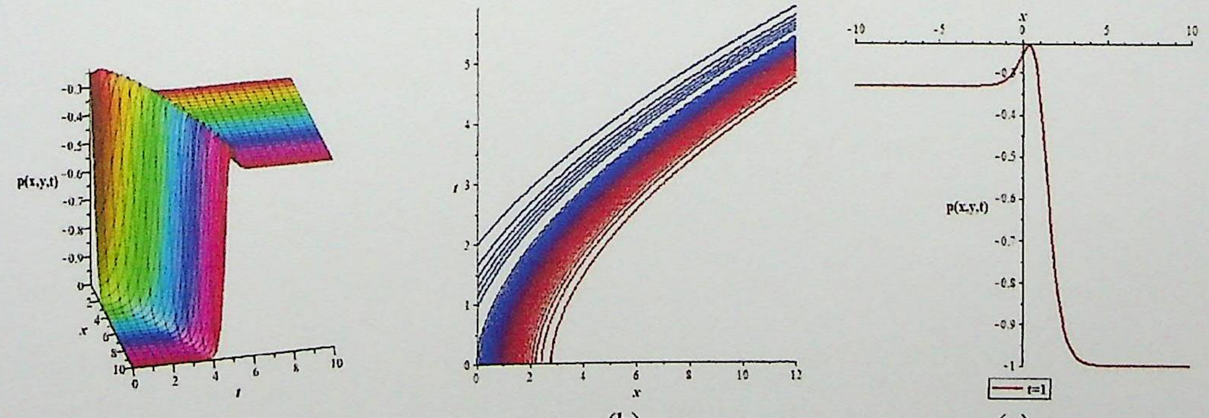

(a) (b) (c)

Fig-5.6: Represent the imaginary part of $p(x,y,t)$ of Eq. (5.18) for parametric values, $A = 1, \gamma = 7/4, k = 2, \ell_1 = 1, \nu = 2, \rho = 1, \wp_1 = -1, y = 0$ and $t = 1$ for 2D graph.

5.6. Conclusion

We have effectively applied mathematical tools named the generalized Kudryashov technique to find the exact solutions to the considered Schrodinger and biological population models. The derived solitary wave solutions are in the form of exponential. The gained solutions will give out as an awfully in the study a crystal wave and quantum wave phenomena. Also we have plotted the derived results and analyzed the graph in Fig-(5.1-5.6). The determined characteristics of the solutions are bright bell, dark bell, kink solitary wave, M- shape solitary wave, W- shape solitary wave. In the concluding remarks, finally we commented that this mathematical technique can also be used to solve many other fractional non-linear partial differential equations in applied mathematics and material science.

Chapter-6

Apply the Modified simple equation method for two non-linear time fractional models.

Acknowledgement

We establish new and exact travelling wave solutions of the complex time fractional Schrodinger equation (FSE) and low-pass electrical transmission lines equation (ETLE) with the help of modified simple equation (MSE) method. The approach provides us rational exponential function solutions with some free parameters. Few well-known solitary wave solutions are derived from the rational solutions choosing particular values of the free parameters. The exact solution obtained by the method indicate that the scheme is comparatively easier to implement and attractive on the view of results. Also we observed that the numerical results are very encouraging for the researchers for the further study on space-time fractional nonlinear partial evolution equations in mathematical physics.

6.1. Introduction

The technique of fractional differentiation is helpful in expressing the recollection and heritable character of materials and process. The Riemann-Liouville derivative or Grunwald-Letnokob derivative or Caputo derivative are the three way to defined the fractional derivative. In recent times, fractional nonlinear differential equations have played a vital rule to the modelling of internal mechanism of particles. This mathematical tools have been highlighted many research due to their numerous form in diverse applications in biological modelling, physical science, engineering, networking system, fractional dynamics, system detection, signal processing and finance [1-24]. Exact or numerical solutions for nonlinear fractional models are very essential to observe the physical character to the real-world physical problem. Recent five decades, dynamical researchers faced many complexities to finding the exact solutions for such models. Recently some effective new techniques have been proposed and improved the old methods for searching the exact solutions to the fractional nonlinear models. The proposed and improved techniques are: Jacobi elliptic function method [27], modified simple equation method [30-31], Bäcklund transformations [32], tanh method [33], $\tan(\Theta/2)$-expansion [34], soliton ansatz [35-36], auxiliary equation [37], sine-cosine [38], homogeneous balance [39], (G'/G)-expansion [40], Modified double sub-equation [41], and so on [41-43]. Among the techniques, MSE scheme [30-31] is more effective and concise for deriving solitonic nature of fractional and non-fractional nonlinear differential models. Besides this, Jumarie [54] proposed modified Riemann-Liouville fractional derivative to transform the fractional order partial differential equation (FPDE) to integer order ordinary differential equations (ODE). Many dynamical researchers have used the technique of conformable fractional derivative [57-58] as an accurate conversion way from FPDE to ODE for searching exact solutions of nonlinear fractional models.

The goal of this chapter is derive the exact solutions of the complex time fractional Schrodinger equation (FSE) [3] & low-pass electrical transmission lines equation (ETLE) [12] using the MSE method.

The complex time fractional Schrodinger equation (FSE) proposed by Nick Laskin [50] of the form:

$$\frac{\partial^{\gamma}\varphi}{\partial t^{\gamma}}+i\frac{\partial^{2}\varphi}{\partial x^{2}}+\frac{\partial}{\partial x}(|\varphi|^{2}\varphi)=0, 0<\gamma<1. \tag{6.1}$$

The above fractional model of nonlinear Schrodinger equation (FSE) is the most efficient universal model in quantum mechanics which describe various physical nonlinear systems. For example, nonlinear Schrodinger equation is used to explain the progress of low motion changing packets of quasi monochromatic waves in weakly nonlinear media with dispersion. The nonlinear Schrodinger equation never describes the time evolution of a quantum state. Nonlinear Schrodinger equation (NLSE) has found its various applications in wave transmission in dispersive and inhomogeneous media such as: dynamics in particle accelerators, non-uniform dielectric media, solitary waves in piezoelectric semiconductors, mean field theory of Bose-Einstein condensates hydrodynamics and plasma waves, nonlinear optical waves, quantum condensates and heat pulse in solids [59-68].

We also shed light on a fractional partial differential equation with the property of nonlinearity describing the wave propagation in nonlinear low–pass electrical transmission lines [12]:

$$\frac{\partial^{2\alpha}\varphi}{\partial t^2}-v\frac{\partial^{2\alpha}}{\partial t^2}(\varphi)^2+B\frac{\partial^{2\alpha}}{\partial t^2}(\varphi)^3-\rho^2\frac{\partial^{2\alpha}\varphi}{\partial x^2}-\frac{\rho^4}{12}\frac{\partial^{4\alpha}\varphi}{\partial x^4}=0;0<\alpha<1, \quad (6.2)$$

Solitary wave solutions and analysis of the nonlinear electrical transmission lines equation is very essential for diverse application of the areas like as linking wireless transmitters and receivers with their antennas, satellite signals processing, mobile networking system, computer networking and high-speed computer data buses. This model is describes the data carry and codify it in telecommunication system. Furthermore, a ETL is a main path or other structure designed to carry alternating current of radio frequency in electronic engineering. NLTLs are also ensuring an effective path to verify how the nonlinear excitations behave inside the nonlinear medium and to model the exotic properties of new systems.

6.2. Conformable fractional derivative and its properties

Now we want to go over the conformable fractional derivatives [57-58]:

Definition: Let the function $\phi:(0,\infty)\to\Re$, the conformable fractional derivative of ϕ for order γ is defined as $\lambda_\gamma(\phi)(t)=\lim_{\delta\to 0^+}\frac{\phi(t+\delta t^{1-\gamma})-\phi(t)}{\delta}, t>0$ and $0<\gamma\le 1$, where λ_γ is fractional differential operator.

Some important properties:

(i) $\lambda_\gamma(a\phi+b\varphi)=a\lambda_\gamma(\phi)+b\lambda_\gamma(\varphi)$, $\forall a,b\in\Re$.

(ii) $\lambda_\gamma(t^\beta)=\beta t^{\beta-\gamma}$, $\forall\beta\in\Re$

(iii) $\lambda_\gamma(\nu)=0$, $\nu=const.$

(iv) $\lambda_\gamma(\phi\circ\varphi)(t)=t^{1-\gamma}\phi'(\varphi(t))\varphi'(t)$.

(iii) $\lambda_\gamma(\frac{\phi}{\varphi})=\frac{\varphi\lambda_\gamma(\phi)-\phi\lambda_\gamma(\varphi)}{\varphi^2}$.

6.3. The fractional complex transformation

In this portion, we have discussed the fractional transformation for the fractional-order PDE,

$$P(\varphi,\frac{\partial^\gamma\varphi}{\partial t^\gamma},\frac{\partial\varphi}{\partial x},\frac{\partial\varphi}{\partial y},\frac{\partial^{2\gamma}\varphi}{\partial t^{2\gamma}},\frac{\partial^2\varphi}{\partial t^2})=0, t\ge 0, 0<\gamma\le 1, \tag{6.3}$$

where P is a polynomial of $\varphi(x,y,t)$ and its partial fractional derivative where in the maximum number of derivatives and the nonlinear term are drawn in. For the equation let

$\varphi=\varphi(\xi)=\varphi(x,y.z,t), \zeta=x+y+z-k\frac{t^\gamma}{\gamma}$ and

Find $\frac{\partial^\gamma}{\partial t^\gamma}=-k\frac{\partial}{\partial\zeta},\frac{\partial}{\partial x}=\frac{\partial}{\partial\zeta},\frac{\partial}{\partial y}=\frac{\partial}{\partial\zeta},\frac{\partial^{2\gamma}}{\partial t^{2\gamma}}=k^2\frac{\partial^{2\gamma}}{\partial\zeta^{2\gamma}}$.....where k indicates the travelling wave speed. The Eq. (6.3) becomes $R(\varphi,\frac{\partial\varphi}{\partial\zeta},\frac{\partial^2\varphi}{\partial\zeta^2}.....)=0$ (6.4)

6.4. Outline of the Modified Simple equation method

Let us picking a general nonlinear partial fractional evolution equation in x and t as

$$N(u, D_t^{\gamma} u, D_x^{\gamma} u, D_t^{2\gamma} u, D_x^{2\gamma} u....) = 0, \tag{6.5}$$

where the function $u = u(x,t)$ is unknown and N is a polynomial of the function u and its derivatives. To find the solution of Eq. (6.5) by modified simple equation (MSE) method [15]. We have executed some key steps of the MSE method. The steps are as follows,

Step 1: Assuming the bellows wave transformation for complex time fractional non-linear model,

$u(x,t) = u(\zeta)\exp(i\tau)$ with travelling wave variables

$$\zeta = ik(x - \frac{2gt^{\gamma}}{\gamma}) \text{ and } \tau = (gx - \frac{ht^{\gamma}}{\gamma}) \tag{6.6}$$

And without complex model $u(x,t) = u(\zeta)$ and travelling wave variable for space-time fractional model,

$$\zeta = \frac{k_1}{\Gamma(1+\gamma)}.t^{\gamma} + \frac{k_2}{\Gamma(1+\gamma)}.x^{\gamma}. \tag{6.7}$$

We can convert the nonlinear partial differential Eq. (6.5) to a nonlinear ordinary differential equation (ODE) by applying the above transformation:

$$G(u, u', u'', ...) = 0, \tag{6.8}$$

where u' and u'' are the 1st and 2nd time derivatives of u with respect to ζ and G is a polynomial of $u(\zeta)$.

Step 2: The solution of Eq. (6.8) can be considered by the following:

$$u(\zeta) = \sum_{i=0}^{N} a_i \left[\frac{s'(\zeta)}{s(\zeta)}\right]^i, \tag{6.9}$$

where $a_i(0,1,2,3....N)$ are unknown constants to be evaluated, such that $a_N \neq 0$ and $s(\zeta)$ is an unknown function to be estimated. Whereas the solutions are expres some well-known differential equation in (G'/G)-expansion method [39-40], Ricatti equation method [23]. But in MSE method $s(\zeta)$ is neither pre-defined nor a solution of pre-defined differential equation. These are the special characteristics of the MSE method. For that the solution is more useful and realistic by this method.

Step 3: The positive integers N in Eq. (6.9) can be determined by balancing the highest order derivative term and highest order nonlinear terms of $u(\zeta)$ in Eq. (6.9).

Step 4: Inserting Eq. (6.9) along with Eq. (6.7) and simplifying for the function $s(\zeta)$. After simplify we get a polynomial of $\left(\frac{1}{s(\zeta)}\right)$. Equating the adjacent terms of $s(\zeta)$ to zero. Then form a system of algebraic equations for $a_i(0,1,2,....N)$ and the other necessary parameters. Eq. (6.5) can solve by using this values.

Step 5: From these above algebraic relations, a_i can be determined and $u(\zeta)$ into the Eq. (6.5), then the solutions of Eq. (6.5) can be constructed.

6.5. Applications

In this section, we will apply the MSE method [30-31] to obtain the new exact solution to the complex time fractional Schrodinger equation (FSE) [59] and the space-time fractional differential equation governing wave propagation in low-pass electrical transmission lines equation (ETLE) [12].

6.5.1. The complex time fractional Schrodinger equation (FSE)

Consider the complex time fractional Schrodinger equation which is defined Eq. (6.1), Let us consider the transformation for complex FSE $\varphi(x,t)=s(\zeta)\exp(i\tau)$, and corresponding travelling variables are $\zeta=ik(x+\frac{2gt^{\gamma}}{\gamma})$, $\tau=(gx+\frac{ht^{\gamma}}{\gamma})$ and convert this nonlinear complex FSE to the nonlinear integer order SE

$$\begin{cases} \dfrac{\partial^{\gamma}\varphi}{\partial t^{\gamma}} = i(gs + 2hks')\exp(i\tau) \\ \dfrac{\partial^{2}\varphi}{\partial x^{2}} = -(h^{2}s + 2hks' + k^{2}s'')\exp(i\tau). \\ \dfrac{\partial}{\partial x}(|\varphi|^{2}\varphi) = i(h^{3}s + 3k^{2}s'')\exp(i\tau) \end{cases} \tag{6.10}$$

We obtain the nonlinear complex PSE by using the above Eq. (6.10),

$$(g - h^{2})s - k^{2}s'' + hs^{3} + 3ks^{2}s' = 0 \tag{6.11}$$

Using the rule of homogenous balance on Eq. (6.11) ($s''$and $s^{2}s'$) $\Rightarrow n = \frac{1}{2}$. Apply another transformation $s(\zeta) = u^{\frac{1}{2}}(\zeta)$ in Eq. (6.11), we get ordinary differential equations

$$4hu^{3} + 4(g - h)u^{2} + 6ku^{2}u' + k^{2}u'^{2} - 2k^{2}uu'' = 0 \tag{6.12}$$

Case1: By balancing the highest order derivative term uu'' with the nonlinear term $u^{2}u$ in Eq. (6.12) gives $\Rightarrow n = 1$.

Therefore Eq. (6.9) reduces to

$$u(\zeta) = \ell_{0} + \ell_{1}\left(\frac{s'(\zeta)}{s(\zeta)}\right), \tag{6.13}$$

Where ℓ_{0} and $\ell_{1} \neq 0$.

Differentiating Eq. (6.13) two times and putting Eq. (6.13) and its derivatives into the Eq. (6.12), we have a polynomial of $s^{k}, (k = 0,1,2,...)$. Considering the coefficients of s^{k} to zero, and some of algebraic equations yields the values for $\ell_{0}$and ℓ_{1}.

$$-4\ell_{0}^{2}h^{2} + 4h\ell_{0}^{3} + 4\ell_{0}^{2}g = 0, \tag{6.14}$$

$$\begin{aligned} &-8\ell_{0}\ell_{1}h^{2}s'(\zeta) + 12h\ell_{0}^{2}\ell_{1}s'(\zeta) + 6k\ell_{0}^{2}\ell_{1}s''(\zeta) - 2k^{2}\ell_{0}\ell_{1}s'''(\zeta) \\ &+ 8\ell_{0}\ell_{1}gs'(\zeta) = 0 \end{aligned}, \tag{6.15}$$

$$\begin{aligned} &-4\ell_{0}^{2}h^{2}(s'(\zeta))^{2} + 12h\ell_{0}\ell_{1}^{2}(s'(\zeta))^{2} - 6k\ell_{0}^{2}\ell_{1}(s'(\zeta))^{2} + 6k^{2}\ell_{0}\ell_{1}s'(\zeta)s''(\zeta) + \\ &12k\ell_{1}^{2}\ell_{0}s'(\zeta)s''(\zeta) - 2k^{2}\ell_{1}^{2}s'(\zeta)s'''(\zeta) + k^{2}\ell_{1}^{2}(s''(\zeta))^{2} + 4\ell_{1}^{2}g(s'(\zeta))^{3} = 0 \end{aligned}, \tag{6.16}$$

$$4h\ell_1^3(s'(\zeta))^3-4k^2\ell_0\ell_1(s'(\zeta))^3-12k\ell_0\ell_1^2(s'(\zeta))^3+4k^2\ell_1^2s''(\zeta)(s'(\zeta))^2+ \\ 6k\ell_1^3s''(\zeta)(s'(\zeta))^2=0 \quad , \quad (6.17)$$

$$-3k^2\ell_1^2(s'(\zeta))^4-6k\ell_1^3(s'(\zeta))^4=0. \quad (6.18)$$

From Eq. (6.14) implies

$$\ell_0=0,\frac{h^2-g}{h}$$

and from Eq. (6.18) , we attain

$$\ell_1=-\frac{k}{2}, \quad \because \ell_1\neq 0$$

Phase-1: $\ell_0=0,\ell_1=-\frac{k}{2}$

Eq. (6.17) together with phase-1, we obtain

$$s'(\zeta)=\frac{k}{2h}s''(\zeta). \quad (6.19)$$

Eq. (6.15) gives by using Eq. (6.19) then,

$$\frac{s''''(\zeta)}{s'''(\zeta)}=\frac{g}{k}, \quad (6.20)$$

Integrating Eq. (6.20) implies .

$$s'''=c_1\exp(\frac{g}{k}\zeta), \text{ where } c_1 \text{ is arbitrary constant.} \quad (6.21)$$

From Eq. (6.19) by putting the value of s''' from Eq. (6.21)

$$s''=\frac{k}{2h}c_1\exp(\frac{g}{k}\zeta), \quad (6.22)$$

Again integrating Eq. (6.22), then

$$s(\zeta)=c_2+\frac{k^2c_1}{2gh}\exp(\frac{g}{k}\zeta), \text{ where } c_1 \text{ and } c_2 \text{ is arbitrary constants.} \quad (6.23)$$

Thus the solution is

$$\varphi(x,t)=\left[-\frac{k}{2}\frac{\frac{k}{2h}c_1\exp(igk(x-\frac{kt^{\gamma}}{\gamma}))}{c_2+\frac{k^2c_1}{2gh}\exp(igk(x-\frac{kt^{\gamma}}{\gamma}))}\right]^{1/2}\exp\left[i(gx+\frac{ht^{\alpha}}{\gamma})\right]. \tag{6.24}$$

For the particular value $c_2=\frac{k^2c_1}{2gh}$, then the solution of Eq. (6.24) reduces to soliton solution

$$\varphi(x,t)=\left[-\frac{g}{4}(1+\tanh(\frac{igk}{2}(x+\frac{kt^{\gamma}}{\gamma})))\right]^{1/2}\exp\left[i(gx+\frac{ht^{\alpha}}{\gamma})\right]. \tag{6.25}$$

For the particular value $c_2=-\frac{k^2c_1}{2gh}$, then the solution of Eq. (6.24) reduces to soliton solution

$$\varphi(x,t)=\left[\frac{g}{4}\left\{1+\coth(\frac{igk}{2}(x+\frac{kt^{\gamma}}{\gamma}))\right\}\right]^{1/2}\exp\left[i(gx+\frac{ht^{\alpha}}{\gamma})\right]. \tag{6.26}$$

Phase-2: $\ell_0=\frac{h^2-g}{h},\ell_1=-\frac{1}{2}k,$

Eq. (6.17) together with phase-2 gives

$$s'(\zeta)=\frac{kh}{2(3h^2-2g)}s''(\zeta). \tag{6.27}$$

Eq. (6.15) gives by using Eq. (6.27) then,

$$\frac{s''''(\zeta)}{s'''(\zeta)}=\frac{10h^4+6g^2-16h^2g}{kh(3h^2-2g)}, \tag{6.28}$$

Integrating Eq. (6.28) implies

$$s'''=c_1\exp\left[(\frac{10h^4+6g^2-16h^2g}{kh(3h^2-2g)})\right], \text{ where } c_1 \text{ is arbitrary constant.} \tag{6.29}$$

From Eq. (6.27) and Eq. (6.29) implies the following,

$$s'(\zeta)=\frac{kh}{2(3h^2-2g)}\left[c_1\exp\left\{(\frac{10h^4+6g^2-16h^2g}{kh(3h^2-2g)})\right\}\right], \tag{6.30}$$

Again integrating Eq. (6.30), then

$$s(\zeta)=c_2+\frac{k^2h^2c_1}{2(10h^4+6g^2-16h^2g)}\exp\left[(\frac{10h^4+6g^2-16h^2g}{kh(3h^2-2g)})\right], \tag{6.31}$$

where c_1 and c_2 is arbitrary constants.

Thus the solution is

$$\varphi(x,t)=\left[\frac{h^2-g}{h}-\frac{\frac{k^2hc_1}{4(3h^2-2g)}\exp\{R\}}{c_2+\frac{k^2h^2c_1}{2(10h^4+6g^2-16h^2g)}\exp\{R\}}\right]^{1/2}\exp(i\tau), \tag{6.32}$$

where $R=\left[\frac{10h^4+6g^2-16h^2g}{kh(3h^2-2g)}\right]ik(x+\frac{2gt^{\gamma}}{\gamma})$ and $\tau=i(gx+\frac{ht^{\alpha}}{\gamma})$.

For the particular value $c_2=\frac{k^2h^2c_1}{2(10h^4+6g^2-16h^2g)}$, then the solution of Eq. (6.32) reduces to soliton solution

$$\varphi(x,t)=\left[\frac{h^2-g}{h}-\frac{(10h^4+6g^2-16h^2g)}{4(3h^2-2g)}(1+\tanh(\frac{R}{2}))\right]^{1/2}\exp\left[i(gx+\frac{ht^{\alpha}}{\gamma})\right]. \tag{6.33}$$

For the particular value $c_2=-\frac{k^2h^2c_1}{2(10h^4+6g^2-16h^2g)}$, then the solution of Eq. (6.32) reduces to soliton solution

$$\varphi(x,t)=\left[\frac{h^2-g}{h}+\frac{(10h^4+6g^2-16h^2g)}{4(3h^2-2g)}\left\{1+\coth(\frac{R}{2})\right\}\right]^{1/2}\exp\left[i(gx+\frac{ht^{\gamma}}{\gamma})\right]. \tag{6.34}$$

6.5.2. The space-time fractional differential equation governing wave propagation in low-pass electrical transmission lines equation

Let us consider the following space-time fractional differential equation governing wave propagation in low-pass electrical transmission lines equation, which is given in Eq. (6.2) where v,ρ,B are unknown constants and $\varphi(x,t)$ is the voltage in the transmission lines. The variable x is interpreted as the propagation distance and t is the slow time. T physical details of the derivation of Eq. (6.2) using the Kirchhoffs laws are given in .

Let us consider

$$\varphi(x,t)=u(\zeta)\,,\xi=\frac{k_1}{\Gamma(1+\alpha)}.t^{\alpha}+\frac{k_2}{\Gamma(1+\alpha)}.x^{\alpha}. \tag{6.35}$$

Convert this nonlinear complex ETL Eq. (6.2) to the nonlinear order ordinary differential ETL by using the above Eq. (6.35)

Then ETL Eq. (6.2) reduced to the following ordinary differential equations

$$(k_1^2-\rho k_2^2)u-k_1^2vu^2+Bk_1^2u^3-\frac{\rho^4}{12}k_2^2u''''=0. \tag{6.36}$$

By balancing the highest order derivative term $u''''(\xi)$ with the nonlinear term $u^3(\xi)$ in Eq. (6.36) gives $\Rightarrow n=1$.

We assumed the auxiliary solution of Eq. (6.36);

$$u(\xi)=a_0+a_1\left(\frac{s'(\xi)}{s(\xi)}\right), \tag{6.37}$$

where a_0 and $a_1\neq 0$ are constants.

Differentiating Eq. (6.37) two times and putting Eq. (6.37) and its derivatives into the Eq.(6.36). We have a polynomial of $s^k,(k=0,1,2,...)$. Comparing the coefficients of s^k of the equal powers of s to zero, we get a some of equations yields the values for a_0 and a_1.

$$Bk_1^2a_0^3-k_1^2va_0^2-a_0Ak_2^2+a_0k_1^2=0, \tag{6.38}$$

$$\begin{aligned}&-a_1Ak_2^2s''(\xi)+k_1^2a_1s''(\xi)-2vk_1^2a_0a_1s''(\xi)+3Bk_1^2a_0^2a_1s''(\xi)\\&-\frac{1}{12}a_1A^4k_2^2s''''(\xi)=0,\end{aligned} \tag{6.39}$$

$$-va_1k_1^2(s''(\xi))^2+3Bk_1^2a_0a_1^2(s''(\xi))^2+\frac{1}{4}A^4k_2^2a_1s'''(\xi)s''(\xi)=0, \tag{6.40}$$

$$Bk_1^2a_1^3(s''(\xi))^3-\frac{1}{6}A^4k_2^2a_1(s''(\xi))^3=0. \tag{6.41}$$

From Eq. (6.41) implies

$$a_1=0,\ a_1=\pm\frac{A^2k_2}{\sqrt{6Bk_1}}$$

Again from Eq. (6.38),

$$a_0=0,\ a_0=\frac{vk_1\pm\sqrt{L}}{2Bk_1},\ \text{where } L=4ABk_2^2+v^2k_1^2-4Bk_1^2.$$

Phase-1: $a_0=0, a_1=\frac{A^2k_2}{\sqrt{6Bk_1}}$

Eq. (6.40) together with **phase-1** gives

$$s'(\zeta)=\frac{\sqrt{6B}A^2k_2}{4vk_1}s''(\xi). \tag{6.42}$$

From Eq. (6.39) with phase-1 by using the Eq. (6.42),

$$\frac{s''''(\xi)}{s'''(\xi)}=\frac{3\sqrt{6B}}{vA^2k_1k_2}(k_1^2-A^2k_2). \tag{6.43}$$

Integrating Eq. (6.43) implies

$$s'''=c_1\exp(\frac{3\sqrt{6B}}{vA^2k_1k_2}(k_1^2-A^2k_2). \tag{6.44}$$

From Eq. (6.42)

$$s''=\frac{\sqrt{6B}A^2k_2}{4vk_1}c_1\exp(\frac{3\sqrt{6B}}{vA^2k_1k_2}(k_1^2-A^2k_2). \tag{6.45}$$

Again integrating Eq. (6.45), then

$$s(\xi)=c_2+c_1\frac{A^4k_2^2}{12(k_1^2-A^2k_2)}\exp(\frac{3\sqrt{6B}}{vA^2k_1k_2}(k_1^2-A^2k_2). \tag{6.46}$$

Thus the solution is

$$\varphi(x,t) = \frac{A^4 k_2^2 c_1}{4vk_1}\left[\frac{\exp(\pm\frac{3\sqrt{6B}}{vA^2k_1k_2}(k_1^2 - A^2k_2)}{c_2 + c_1\frac{A^4k_2^2}{12(k_1^2 - A^2k_2)}\exp(\pm\frac{3\sqrt{6B}}{vA^2k_1k_2}(k_1^2 - A^2k_2)}\right]. \quad (6.47)$$

For the particular value $c_2 = \frac{c_1 A^4 k_2^2}{12(k_1^2 - A^2k_2)}$, then the solution of Eq. (6.47) reduces to soliton solution

$$\phi(x,t) = \left[-\frac{3(k_1^2 - A^2k_2^2)}{2vk_1}\left\{1 \pm \tanh(\frac{3\sqrt{6B}}{2vA^2k_1k_2}(k_1^2 - A^2k_2)\right\}\right]. \quad (6.48)$$

For the particular value $c_2 = -\frac{k^2 c_1}{2gh}$, then the solution of Eq. (6.47) reduces to soliton solution

$$\phi(x,t) = \left[\frac{3(k_1^2 - A^2k_2^2)}{2vk_1}\left\{1 \pm \coth(\frac{3\sqrt{6B}}{2vA^2k_1k_2}(k_1^2 - A^2k_2)\right\}\right]. \quad (6.49)$$

Phase-2:

$$a_0 = \frac{vk_1 \pm \sqrt{L}}{2Bk_1}, \quad a_1 = \pm\frac{A^2k_2}{\sqrt{6B}k_1}$$

Eq. (6.40) together with **phase-2** gives

$$s'(\xi) = \frac{\sqrt{6B}A^2k_2}{2(-vk_1 \pm 3\sqrt{L})}s''(\xi). \quad (6.50)$$

From Eq. (6.40) with phase-3, then applying the Eq. (6.50),

$$\frac{s''''(\xi)}{s'''(\xi)} = \frac{3\sqrt{6B}A^2k_2\{4B(Ak_2^2 - k_1^2) + (vk_1 \pm \sqrt{L})(vk_1 \mp 3\sqrt{L})\}}{2BA^4k_2^2(vk_1 \pm 3\sqrt{L})}. \quad (6.51)$$

Integrating Eq. (6.51) implies

$s''' = c_1 \exp(\pm Q\xi)$ where

$$Q = \frac{3\sqrt{6B}A^2k_2\{4B(Ak_2^2 - k_1^2) + (vk_1 \pm \sqrt{L})(vk_1 \mp 3\sqrt{L})\}}{2BA^4k_2^2(vk_1 \pm 3\sqrt{L})} \quad (6.52)$$

From Eq. (6.50)

$$s'' = \frac{-\sqrt{6B}A^2k_2}{(vk_1 \pm 3\sqrt{L})} c_1 \exp(\pm Q\xi). \tag{6.53}$$

Again integrating Eq. (6.53), then

$$s(\xi) = c_2 - c_1 H \exp(Q\xi). \tag{6.54}$$

where $H = \dfrac{A^4Bk_2^2}{3\{4B(A^2k_2 - k_1^2) + (vk_1 \pm \sqrt{L})(vk_1 \mp 3\sqrt{L})\}}$

Thus the solution is

$$\varphi(x,t) = \frac{(vk_1 \pm \sqrt{L})}{2Bk_1} - \frac{A^4k_2^2c_1}{2k_1(vk_1 \pm 3\sqrt{L})}\left[\frac{\exp(\pm Q\xi)}{c_2 - c_1 H \exp(\pm Q\xi)}\right]. \tag{6.55}$$

For the particular value $c_2 = -c_1H$, then the solution of Eq. (6.55) reduces to soliton solution

$$\varphi(x,t) = \frac{(vk_1 \pm \sqrt{L})}{2Bk_1} + \frac{A^4k_2^2}{4k_1H(vk_1 \pm 3\sqrt{L})}\left[1 \pm \tanh(\frac{Q\xi}{2})\right]. \tag{6.56}$$

And for the particular value $c_2 = c_1H$, then the solution of Eq. (6.55) reduces to soliton solution

$$\varphi(x,t) = \frac{(vk_1 \pm \sqrt{L})}{2Bk_1} - \frac{A^4k_2^2}{4k_1H(vk_1 \pm 3\sqrt{L})}\left[1 \pm \coth(\frac{Q\xi}{2})\right]. \tag{6.57}$$

where $H = \dfrac{A^4Bk_2^2}{3\{4B(A^2k_2 - k_1^2) + (vk_1 \pm \sqrt{L})(vk_1 \mp 3\sqrt{L})\}}$,

$Q = \dfrac{3\sqrt{6B}A^2k_2\{4B(Ak_2^2 - k_1^2) + (vk_1 \pm \sqrt{L})(vk_1 \mp 3\sqrt{L})\}}{2BA^4k_2^2(vk_1 \pm 3\sqrt{L})}$ and $L = 4ABk_2^2 + v^2k_1^2 - 4Bk_1^2$.

6.6. Graphical representations

Here, we will represent some graphical illustration of the exact solutions of the complex time fractional Schrodinger equation (Eq. (6.1)) and the space-time fractional differential equation governing wave propagation in low-pass electrical transmission lines equation

(Eq.(6.2)). Graphical representations are portrayed below using the selected exact solutions of FSE and ETLE model.

6.6.1: The complex time fractional Schrodinger equation

In this subsection, we will illustrate one of results out of two. Derived results are examined and selected results are illustrated the real and complex part in Figs. 6.1–6.2 for the same unknown parametric values of $k = 0.5,\ \gamma = 0.5, h = 1, g = -2, t = 2$ respectively. The illustration of the result signify the variation of amplitude, direction, shape of flow and character of the solitary waves for each acquired wave solutions in space x at time t. The solution $\varphi(x,t)$ of Eq.(6.25) for solution **set-1**. For **set-2**, we get similar type of solution for that which is not illustrated below.

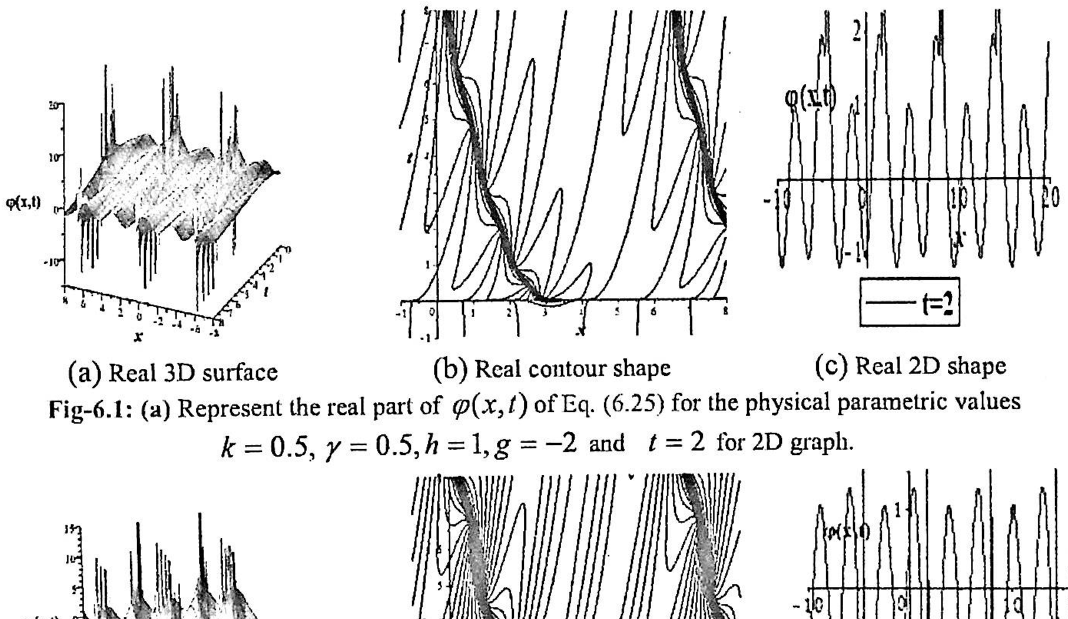

(a) Real 3D surface (b) Real contour shape (c) Real 2D shape

Fig-6.1: (a) Represent the real part of $\varphi(x,t)$ of Eq. (6.25) for the physical parametric values $k = 0.5,\ \gamma = 0.5, h = 1, g = -2$ and $t = 2$ for 2D graph.

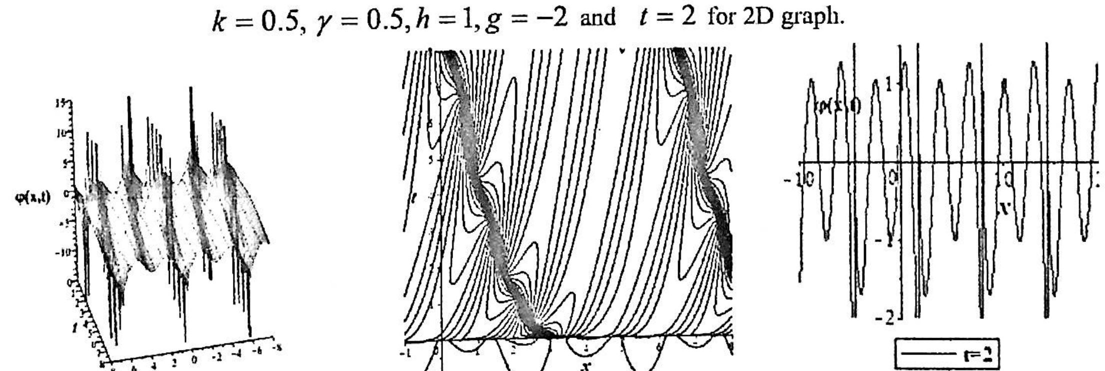

(a) Complex 3D surface (b) Complex contour shape (c) Complex 2D shape

Fig-6.2: (a) Represent the imaginary part of $\varphi(x,t)$ of Eq. (6.25) for the physical parametric values $k = 0.5,\ \gamma = 0.5, h = 1, g = -2, t = 2$.

6.6.2: The space-time fractional differential equation governing wave propagation in low-pass electrical transmission lines equation

Two set of outcome are derived in this study. Each and every results are examined and selected results are illustrated in the Fig-6.3 of Eq. (6.48).The illustration indicate the alteration of amplitude, direction, shape of wave and nature of the solitary waves for each acquired wave solutions in space x at time t. The solitary wave solution $\varphi(x,t)$ of Eq. (6.48) for solution set-1.Eq. (6.57) for solution set-2 represented in Fig-6.4.

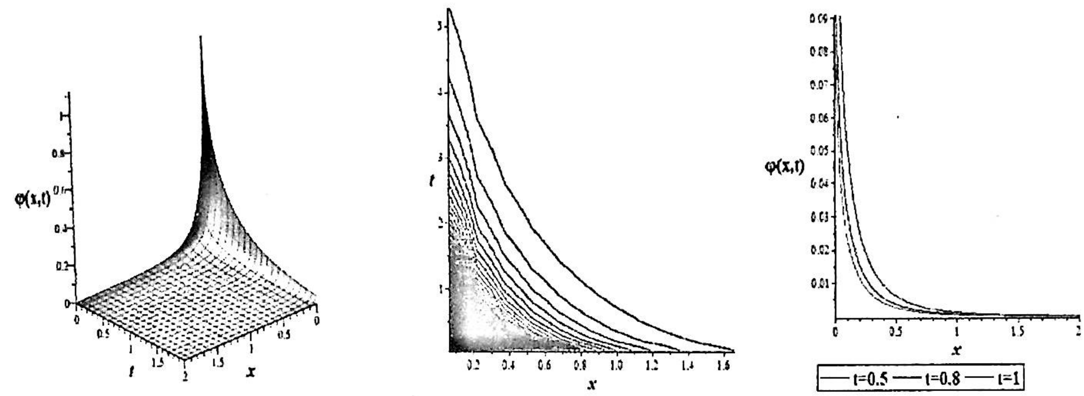

(a) (b) (c)

Fig-6.3: (a) Represent the solitary wave solution $\varphi(x,t)$ of Eq. (6.48) for the physical parametric values $\alpha = 0.5,\ k_1 = 0.5,\ k_2 = 1, \nu = 2, A = 1, B = 0.8$,and $t = 0.5, 0.8, 1$ for 2D graph.

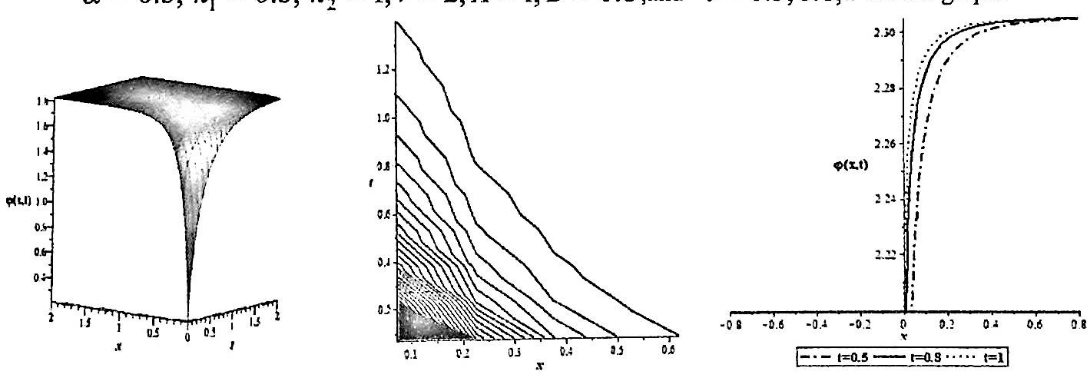

(a) (b) (c)

Fig-6.4: (a) Represent the imaginary part of the solitary wave solution $\varphi(x,t)$ of Eq. (6.57) for the physical parametric values $\alpha = 0.67,\ k_1 = 0.5,\ k_2 = 1, \nu = 2, A = 1, B = 2$ and $t = 0.5, 0.8, 1$ for 2D graph.

6.7. Concluding Remarks

We have applied the modified simple equation method on the complex time fractional Schrodinger equation and the space-time fractional differential equation governing wave propagation in low-pass electrical transmission lines equation to construct solitary wave solutions. We have retrieved rational exponential function solutions of the fractional order models including some arbitrary parameters. The obtained solutions with free parameters may be important to explain some physical phenomena including special solitonic behaviours. Finally, we conclude that the method can be implemented to various others nonlinear fractional evolution equations that occur in mathematical physics and engineering. We shall bring up it in our future investigations on various nonlinear fractional models.

Chapter-7

New soliton solutions of three nonlinear fractional models through an Improved Kudryashov method

Acknowledgement

Here inside this script, we introduce a new integral scheme namely Improved Kudryashov method for solving any nonlinear fractional differential models. We apply the approach to the nonlinear space-time fractional model leading wave spread in electrical transmission lines (s-tfETL), the space-time M-fractional Schrödinger -Hirota (s-tM-fSH) and the time fractional complex Schrödinger (tfcS) models to verify the effectiveness of the propose approach. The implementations of the introduced new technique on the models provide us periodic envelope, exponentially changeable soliton envelope, rational rogue wave, periodic rogue wave, combo periodic-soliton and combo rational-soliton solutions, which are much interesting phenomena in the nonlinear sciences. Thus the results disclose that the proposed technique is awfully effective, straight-forward, and such solutions of the models are much more fruitful than the generaliged Kudryashov and the Modified Kudryashov methods.

7.1. Introduction

The accurate modeling of nonlinear phenomena related to natural happening is really impossible without fractional derivatives. Now a day, fractional calculus has been frequently used to modeling of nonlinear systems in various fields such as quantum mechanics [2-3], optical communications [4-5], plasma physics [6], fluid dynamics [7-8], elec[illegible]smission line [9-13], superconductivity and Bose-Einstein condensates [14], electrics s[illegible]ng

[15], Biological dynamics [16], electro-magnetic waves [17], dust acoustic and dense electron-positron-ion wave [19], and in many aspect [20-24].

Various types of exact solutions including periodic and solitons are essential to realize intrinsic dynamical structure of such models even universe. Up to now, huge improvements have been done in the development of techniques to evaluate such exact solutions of the nonlinear models. Several powerful methods are as: generalized Kudryashov [28-29], modified simple equation method [30-31], Bäcklund transformations [32], $\tan(\Theta/2)$-expansion [34], soliton ansatz [35-36], auxiliary equation [37], sine-cosine [38], (G'/G)-expansion [39-40], Modified double sub-equation [41], variational iteration method [42],and so on [43-44]. It is obstruction that all the mentioned approaches have few advantages and disadvantages to integrate complex nonlinear systems. As we have known, no one approach is suitable for all equations. Thus, we willing to propose a new and active approach namely improved Kudryashov method (IKM) on the basis of the generalized Kudryashov method [28-29] changing its auxiliary equation.

Now, we shed light on the nonlinear space-time fractional electrical transmission lines (s-tfETL) [11], the time fractional complex Schrödinger (tcFSE) [2] and space-time M-fractional Schrödinger -Hirota (s-tM-fSH) [51] models via the proposed IKM. These models have been widely studied in many aspects for non-fractional differential case. Abdou and Soliman [11] only solved the fractional transmission lines equation thru the generalized $\exp(-\phi(\xi))$-expansion and generalized Kudryashov methods. But non-fractional transmission lines equation has been studied by Zayed and Alurrfi [63] using new Jacobi function expansion method; Kumar [64] using three schemes as modified Kudryashaov, Sine-Gordon- and extended Sinh-Gordon- expansion methods; Shahoot et. al. using

(G'/G)-expansion scheme. Beside this, the time fractional complex Schrodinger equation (FSE) is vital nonlinear model in solitonic field. The model describes collision of adjacent particles of identical mass to a lattice structure through a crystal and demonstrated fundamental properties of string dynamics with fixed curvature space [59]. This model was first developed by Laskin [50] which occurs in many important areas as water wave, fluid dynamics, bio-chemistry, optical pulses propagation into nonlinear fiber and plasma physics. Few researchers deliberated much more effort in investigation of the complex fractional Schrodinger model: Khater [2] studied by a supplementary equation as well as (G′/G)-schemes, Alam and Li [3] presented wave solutions through modified (G′/G)-expansion technique. Recent years, Sousa and Oliveira invented a M-fractional order derivative [65]. So, we also consider another model namely the space-time truncated M-fractional Schrodinger-Hirota model [51] which frequently arises in quantum hall-effect, optical fibers, heat pulses in solids and more areas. Sulaiman et. al. [51] investigated the M-fractional SH model to present optical solitons solutions with the help of a sinh-Gordon technique. But non-fractional SHE is investigated by many authors [66-68].

The intention of this research is to execute improved Kudryashov technique [69] to determine abundant exact solitonic solutions as periodic envelope, exponentially changeable soliton envelope, rational, combo periodic-soliton and combo rational-solitonic solutions of the s-tfETL [11], the tfcSE [50] and the s-tM-fSH [51] models, which take an essential part in nonlinear complex phenomena of physical sciences.

7.2. Conformable M-fractional and fractional derivatives with properties

The new M-fractional derivatives are given [51]:

Let $\wp:[0,\infty)\rightarrow\Re$ then M-fractional derivative $\wp$ with order α can be written

$$D_M^{\alpha,\beta}\{(\wp)(t)\} = \lim_{\varepsilon \to 0} \frac{\wp(t\mathrm{E}_\beta(\varepsilon t^{1-\gamma})) - \wp(t)}{\varepsilon}, \ \forall t > 0, 0 < \alpha < 1, \ \beta > 0,$$

where E_β is a truncated Mittag-Leffler function [52].

Properties of new M-fractional derivatives: When $t > 0, 0 < \alpha < 1, \ \beta > 0, \ m, n \in \Re$, Ψ and Ω are $\alpha-$differentiable, then

i) ${}_iD_M^{\alpha,\beta}\{(m\Psi + n\Omega)(t)\} = m\,{}_iD_M^{\alpha,\beta}\Psi(t) + n\,{}_iD_M^{\alpha,\beta}\Omega(t), \ \forall m, n \in \Re.$

ii) ${}_iD_M^{\alpha,\beta}(\Psi \cdot \Omega)(t) = \Psi(t)\,{}_iD_M^{\alpha,\beta}\Omega(t) + \Omega(t)\,{}_iD_M^{\alpha,\beta}\Psi(t), \ \forall \beta \in \Re,$

iii) ${}_iD_M^{\alpha,\beta}(\Psi / \Omega)(t) = \{\Omega(t)\,{}_iD_M^{\alpha,\beta}\Psi(t) - \Psi(t)\,{}_iD_M^{\alpha,\beta}\Omega(t)\} / \{\Omega(t)\}^2.$

iv) ${}_iD_M^{\alpha,\beta}(c) = 0,$ where $\Psi(t) = c$ is a constant.

v) (Chain rule) If is differentiable, then ${}_iD_M^{\alpha,\beta}\Psi(t) = \dfrac{t^{1-\alpha}}{\Gamma(1+\beta)} \dfrac{d\Psi(t)}{dt}.$

If a function defined by, $\phi : (0, \infty) \to \Re$, the conformable fractional derivative with order υ is defined [57-58] as $\dfrac{\partial^\upsilon \phi}{\partial t^\upsilon} = \lim_{\varepsilon \to 0^+} \dfrac{\phi(t + \varepsilon t^{1-\upsilon}) - \phi(t)}{\varepsilon}, t > 0$ and $0 < \upsilon \le 1$.

Properties:

i). $\dfrac{\partial^\upsilon}{\partial t^\upsilon}(m\Psi + n\Omega) = m\dfrac{\partial^\upsilon}{\partial t^\upsilon}(\Psi) + n\dfrac{\partial^\upsilon}{\partial t^\upsilon}(\Omega), \ \forall m, n \in \Re.$

ii). $\dfrac{\partial^\upsilon}{\partial t^\upsilon}(t^\tau) = \tau t^{\tau-\upsilon}, \ \forall \beta \in \Re$ and $\dfrac{\partial^\upsilon}{\partial t^\upsilon}(\nu) = 0, \ \nu = const.$

iii). $\dfrac{\partial^\upsilon}{\partial t^\upsilon}(\Psi \circ \Omega)(t) = t^{1-\upsilon}\Psi'(\Omega(t))\Omega'(t).$

This properties are also satisfies the all types of M-fractional derivatives.

7.3. Algorithm of the proposed method

The fundamental phases of the technique as follows:

Step-1: At first, bearing the subsequent fractional equation with the variables x and t,

$$N(Y, D_t^{\eta}Y, D_x^{\alpha}Y, D_t^{2\eta}Y, D_x^{2\alpha}Y....) = 0, \tag{7.1}$$

where the function $Y = Y(x,t)$ is unknown wave surface and N is a function of $Y(x,t)$ and its highest order fractional derivatives.

Step-2: For complex nonlinear model, take the transformation, $Y(x,t) = Y(\zeta)\exp(i\tau)$ with travelling wave variables for space-time fractional model

$$\zeta = ik\left(\frac{x^{\alpha}}{\Gamma(1+\alpha)} + \frac{gt^{\eta}}{\Gamma(1+\eta)}\right) \text{ and } \tau = \left(\frac{gx^{\alpha}}{\Gamma(1+\alpha)} + \frac{ht^{\eta}}{\Gamma(1+\eta)}\right), \tag{7.2}$$

and for without complex model $Y(x,t) = Y(\zeta)$ and travelling wave variable for space-time fractional model $\zeta = \frac{k_1}{\Gamma(1+\eta)}.t^{\eta} + \frac{k_2}{\Gamma(1+\alpha)}.x^{\alpha}$. (7.3)

Plugging the above Eq. (7.2) or Eq. (7.3) into the Eq. (7.1), it would be abridged to a ODE with the help of fractional complex transformation produce

$$\frac{\partial^{\eta}}{\partial t^{\eta}} = -\sigma\frac{\partial}{\partial \zeta}, \frac{\partial}{\partial x} = \frac{\partial}{\partial \zeta}, \frac{\partial^{2\eta}}{\partial t^{2\eta}} = \sigma^2\frac{\partial^{2\eta}}{\partial \zeta^{2\eta}}......, \tag{7.4}$$

then Eq. (7.1) turned to the following form,

$$\chi(Y, Y', Y'',...) = 0. \tag{7.5}$$

The prime of Y indicates the usual meaning of derivative.

Step-3: Picking a trial solution for Eq. (7.5) is

$$Y(\zeta) = \frac{\sum_{i=0}^{n} \ell_i \phi^i(\zeta)}{\sum_{j=0}^{m} \wp_j \phi^j(\zeta)}, \tag{7.6}$$

where ℓ_i, $\wp_j$ are real fixed values, and $n>0$, $m>0$ are integers with the restriction $\ell_n, \wp_m \neq 0$.

Here, we just need to take a different auxiliary equation which satisfies by $\phi(\zeta)$ as

$$\phi'(\zeta) = k - \phi^2(\zeta), \tag{7.7}$$

where k is an arbitrary constant. Some special solutions of the Riccati equation Eq. (7.7) are given by

$$\phi(\zeta) = \begin{cases} \sqrt{k}\tanh(\sqrt{k}\zeta), & k>0; \\ \sqrt{k}\coth(\sqrt{k}\zeta), & k>0; \\ \dfrac{1}{\zeta}, & k=0; \\ -\sqrt{-k}\tan(\sqrt{-k}\zeta), & k<0; \\ \sqrt{-k}\cot(\sqrt{-k}\zeta), & k<0. \end{cases} \tag{7.8}$$

Step-4: Combining Eq. (7.5), Eq. (7.6) and Eq. (7.7) through computational software, we can get polynomial in $\phi(\zeta)$. Taking zero of each coefficients of $\phi^{\kappa}(\zeta)(\kappa = 0,1,2,3......)$, and form some equations in-terms of unknown constants $\ell_{\kappa}, \wp_{\kappa}$. Solving this unknown constants then put into trial solution together with the solutions Eq. (7.8) completed the exact solution of Eq.(7.1).

Remark-1: It is noted that the auxiliary equation in the Generalized Kudryashov [11, 26] and the modified Kudryashov schemes [31] each are capable to provide only one solution in terms of exponential function. Consequently, the auxiliary Eq.(7.7) in the proposed IK scheme degenerate five different solutions involving hyperbolic, rational and trigonometric functions. In the concluding remark, we can say that the introduced scheme will be more useful than the other exiting schemes for its different types of solutions [26-31].

Remark-2: The propose technique is easier as it takes less calculations than the modified (G'/G)-expansion technique [28]. It is noticed that modified (G'/G)-expansion method takes double auxiliary equations while we consider only Riccati equation as auxiliary equation.

7.4. Applications

In this section, we check the validity of the proposed improved Kudryashov technique [69] by applying on the s-tfETL, the tfcSE and the s-tM-fSH models.

7.4.1. The space-time fractional electrical transmission lines equation (s-tfETLE)

General form of s-tfETLE can be written as follows [11]:

$$\frac{\partial^{2\beta}\phi}{\partial t^{2}}-v\frac{\partial^{2\beta}}{\partial t^{2}}(\phi)^{2}+B\frac{\partial^{2\beta}}{\partial t^{2}}(\phi)^{3}-A^{2}\frac{\partial^{2\beta}\phi}{\partial x^{2}}-\frac{A^{4}}{12}\frac{\partial^{4\beta}\phi}{\partial x^{4}}=0;0<\beta<1. \tag{7.9}$$

The s-tfETL Eq. (7.9) is one of the important equations in fractional electrical physics. The equation are describes data communication and codify it in telecommunication system.

Let us consider $\phi(x,t)=\varphi(\zeta),\zeta=\frac{k_1}{\Gamma(1+\beta)}t^{\beta}+\frac{k_2}{\Gamma(1+\beta)}x^{\beta}$ and convert this nonlinear s-tfETL partial evolution model to the nonlinear integer order ordinary differential ETL as follows:

$$(k_1^2-A^2k_2^2)\varphi(\zeta)-k_1^2v\varphi^2(\zeta)+Bk_1^2\varphi^3(\zeta)-\frac{A^4k_2^4\beta^2}{12\Gamma(1+\beta)^2}\varphi''(\zeta)=0. \tag{7.10}$$

It is well known that delicate balance between the height derivative and height nonlinear terms gives $n=m+1$. Consider a trial solution Eq. (7.6) in the following form $(m=1,\Rightarrow n=2)$

$$\varphi(\zeta)=\frac{\ell_0+\ell_1\varphi(\zeta)+\ell_2\varphi^2(\zeta)}{\wp_0+\wp_1\varphi(\zeta)}. \tag{7.11}$$

Where use the auxiliary equation,

$$\varphi'(\zeta) = k - \varphi^2(\zeta)$$

Inserting Eq. (7.11) with Eq. (7.7) into the reduced non-linear ordinary differential Eq. (7.11), we have a polynomial of $\varphi^i, (i = 0,1,2,...)$. All the adjacent terms of φ^i are equating to zero, and form some equations in-terms of unknown constants $\ell_0, \ell_1, \ell_2, \wp_0, \wp_1, k_1$ and k_2. Solving the equations via maple soft; we get the five sets of solution.

Set-1

$$\ell_0 = \frac{\nu \wp_1 \sqrt{-k}}{3\sqrt{2B}}, \ell_1 = \frac{\nu \wp_1}{3B}, \ell_2 = \frac{\nu \wp_1}{3B\sqrt{-2k}}, \wp_0 = 0, k_1 = \frac{3\nu L\sqrt{-3B}}{(9B-2\nu^2)\beta\sqrt{k}}, k_2 = \frac{\sqrt{3}\nu L}{\beta A\sqrt{2k\nu^2 - 9Bk}}$$

and $\wp_1$ is const.

Set-2

$$\ell_0 = \frac{\nu \wp_1 \sqrt{k}}{6B}, \ell_1 = \frac{\nu \wp_1}{3B}, \ell_2 = \frac{\nu \wp_1}{6B\sqrt{k}}, \wp_0 = 0, k_1 = \frac{3\nu L\sqrt{3B}}{(9B-2\nu^2)\beta\sqrt{2k}}, k_2 = \frac{\sqrt{3}\nu L}{\beta A\sqrt{18Bk - 4k\nu^2}}$$

and $\wp_1$ is const.

Set-3:

$$\ell_0 = \frac{\nu \wp_0}{3B}, \ell_1 = \frac{(3Bk\ell_2 + \nu \wp_0)}{3B\sqrt{k}}, \wp_1 = \frac{3B\ell_2\sqrt{k}}{\nu}, k_1 = \frac{3\nu L\sqrt{6B}}{(9B-2\nu^2)\beta\sqrt{k}}, k_2 = \frac{\sqrt{6}\nu L}{\beta A\sqrt{9Bk - 2k\nu^2}}$$

ℓ_2 and $\wp_0$ are const.

Set-4:

$$\ell_0 = -k\ell_2, \ell_1 = 0, \wp_0 = -\frac{2\ell_2\nu(A^2\beta^2k_2^2k + 3L^2)}{3\beta^2A^2k_2^2}, \wp_1 = \frac{\ell_2\sqrt{2A^2B\beta^2k_2^2k + 6BL^2}}{\beta A k_2},$$

$$k_1 = \frac{k_2A\sqrt{A^2\beta^2k_2^2k + 3L^2}}{\sqrt{3}L}$$

and ℓ_2 and $\wp_2$ are const.

The general solutions of s-tfETL equations for solution **set-1** are:

$$\phi_{11} = \frac{-\nu + \nu\sqrt{-2}\tanh(\sqrt{k}\zeta) + \nu\tanh^2(\sqrt{k}\zeta)}{3B\sqrt{-2}\tanh(\sqrt{k}\zeta)}, k > 0; \quad (7.12)$$

$$\phi_{12} = \frac{-\nu + \nu\sqrt{-2}\coth(\sqrt{k}\zeta) + \nu\coth^2(\sqrt{k}\zeta)}{3B\sqrt{-2}\coth(\sqrt{k}\zeta)}, k > 0; \quad (7.13)$$

$$\phi_{13} = \frac{-\nu k\zeta^2 + \nu\sqrt{-2k}\zeta + \nu}{3B\sqrt{-2k}\zeta}, k = 0; \quad (7.14)$$

$$\phi_{14} = \frac{\nu - \nu\sqrt{2}\tan(\sqrt{-k}\zeta) + \nu\tan^2(\sqrt{-k}\zeta)}{-3B\sqrt{2}\tan(\sqrt{-k}\zeta)}, k < 0; \quad (7.15)$$

$$\phi_{15} = \frac{\nu + \nu\sqrt{2}\cot(\sqrt{-k}\zeta) + \nu\cot^2(\sqrt{-k}\zeta)}{3B\sqrt{2}\cot(\sqrt{-k}\zeta)}, k < 0; \quad (7.16)$$

where $\zeta = \frac{3\nu L\sqrt{-3B}}{(9B - 2\nu^2)\beta\sqrt{k}\Gamma(1+\beta)} t^{\beta} + \frac{\nu L\sqrt{3}}{\sqrt{(2k\nu^2 - 9Bk)\beta A\Gamma(1+\beta)}} x^{\beta}$.

The general solutions of s-tfETL equations for solution **set-2** are:

$$\phi_{21} = \frac{\nu + 2\nu\tanh(\sqrt{k}\zeta) + \nu\tanh^2(\sqrt{k}\zeta)}{6B\tanh(\sqrt{k}\zeta)}, k > 0; \quad (7.17)$$

$$\phi_{22} = \frac{\nu + 2\nu\coth(\sqrt{k}\zeta) + \nu\coth^2(\sqrt{k}\zeta)}{6B\coth(\sqrt{k}\zeta)}, k > 0; \quad (7.18)$$

$$\phi_{23} = \frac{\nu d\zeta^2 + 2\nu\sqrt{k}\zeta + \nu}{6B\sqrt{k}\zeta}, k = 0; \quad (7.19)$$

$$\phi_{24} = \frac{\nu - 2\nu\sqrt{-1}\tan(\sqrt{-k}\zeta) - \nu\tan^2(\sqrt{-k}\zeta)}{6B\sqrt{-1}\tan(\sqrt{-k}\zeta)}, k < 0; \quad (7.20)$$

$$\phi_{25} = \frac{\nu - 2\nu\cot(\sqrt{-k}\zeta)\sqrt{-1} - \nu\cot^2(\sqrt{-k}\zeta)}{6B\cot(\sqrt{-k}\zeta)\sqrt{-1}}, k < 0; \quad (7.21)$$

where $\zeta = \frac{3\nu L\sqrt{3B}}{(9B-2\nu^2)\beta\sqrt{2k}\Gamma(1+\beta)}t^\beta + \frac{\nu L\sqrt{3}}{\sqrt{(18Bk-2k\nu^2)\beta A\Gamma(1+\beta)}}x^\beta$.

The general solutions of s-tfETL equations for solution **set-3** are:

$$\phi_{31} = \frac{\nu^2\wp_0 + (3B\nu k\ell_2 + \nu\wp_0)\nu\tanh(\sqrt{k}\zeta) + 3B\ell_2\nu k\tanh^2(\sqrt{k}\zeta)}{3B\nu\wp_0 + 9B^2\ell_2 k\tanh(\sqrt{k}\zeta)}, k>0; \quad (7.22)$$

$$\phi_{32} = \frac{\nu^2\wp_0 + (3B\nu k\ell_2 + \nu\wp_0)\nu\coth(\sqrt{k}\zeta) + 3B\ell_2\nu k\coth^2(\sqrt{k}\zeta)}{3B\nu\wp_0 + 9B^2\ell_2 k\coth(\sqrt{k}\zeta)}, k>0; \quad (7.23)$$

$$\phi_{33} = \frac{\nu^2\wp_0\sqrt{k}\zeta^2 + (3Bk\ell_2 + \nu\wp_0)\nu\zeta + 3B\nu\sqrt{k}\ell_2}{3B\sqrt{k}\zeta(\nu\wp_0\zeta + 3B\ell_2\sqrt{k})}, k=0; \quad (7.24)$$

$$\phi_{34} = \frac{\nu^2\wp_0 - (3B\nu k\ell_2 + \nu\wp_0)\nu\sqrt{-1}\tan(\sqrt{-k}\zeta) - 3B\ell_2\nu k\tan^2(\sqrt{-k}\zeta)}{3B\nu\wp_0 - 9B^2\ell_2 k\sqrt{-1}\tan(\sqrt{-k}\zeta)}, k<0; \quad (7.25)$$

$$\phi_{35} = \frac{\nu^2\wp_0 + (3B\nu k\ell_2 + \nu\wp_0)\nu\sqrt{-1}\cot(\sqrt{-k}\zeta) - 3B\ell_2\nu k\cot^2(\sqrt{-k}\zeta)}{3B\nu\wp_0 + 9B^2\ell_2 k\sqrt{-1}\cot(\sqrt{-k}\zeta)}, k<0; \quad (7.26)$$

where $\zeta = \frac{3\nu L\sqrt{6B}.}{(9B-2\nu^2)\beta\sqrt{k}\ \Gamma(1+\beta)}t^\beta + \frac{\nu L\sqrt{6}}{\beta A\sqrt{9Bk-2k\nu^2}\Gamma(1+\beta)}x^\beta$.

The general solutions of s-tfETL equations for solution **set-4** are:

$$\phi_{41} = \frac{3\beta^2A^2k_2^2(-k\ell_2 + \ell_2 k\tanh^2(\sqrt{k}\zeta))}{-2\ell_2\nu(A^2\beta^2kk_2^2 + 3L^2) + 3BA\ell_2\sqrt{2A^2B\beta^2kk_2^2 + 6BL^2}k_2\sqrt{k}\tanh(\sqrt{k}\zeta)}, k>0; \quad (7.27)$$

$$\phi_{42} = \frac{3\beta^2A^2k_2^2(-k\ell_2 + \ell_2 k\coth^2(\sqrt{k}\zeta))}{-2\ell_2\nu(A^2\beta^2kk_2^2 + 3L^2) + 3BA\ell_2\sqrt{2A^2B\beta^2kk_2^2 + 6BL^2}k_2\sqrt{k}\coth(\sqrt{k}\zeta)}, k>0; \quad (7.28)$$

$$\phi_{43} = \frac{3\beta^2A^2k_2^2(-k\ell_2\zeta^2 + \ell_2)}{-2\ell_2\nu(A^2\beta^2kk_2^2 + 3L^2)\zeta^2 + 3BA\ell_2\sqrt{2A^2B\beta^2kk_2^2 + 6BL^2}\zeta)}, k=0; \quad (7.29)$$

$$\phi_{44} = \frac{3\beta^2A^2k_2^2(-k\ell_2 - \ell_2 k\tan^2(\sqrt{-k}\zeta))}{-2\ell_2\nu(A^2\beta^2kk_2^2 + 3L^2) - 3BA\ell_2\sqrt{2A^2B\beta^2kk_2^2 + 6BL^2}k_2\sqrt{-k}\tan(\sqrt{-k}\zeta)}, k<0;$$

$$\phi_{45}=\frac{3\beta^2 A^2 k_2^2(-k\ell_2-\ell_2 k\cot^2(\sqrt{-k}\zeta))}{-2\ell_2 \nu(A^2\beta^2 kk_2^2+3L^2)+3BA\ell_2\sqrt{2A^2B\beta^2 kk_2^2+6BL^2}k_2\sqrt{-k}\cot(\sqrt{-k}\zeta)},k<0; \tag{7.31}$$

where $\zeta=\dfrac{k_2 A\sqrt{A^2\beta^2 kk_2^2+3L^2}}{\sqrt{3}L\Gamma(1+\beta)}t^{\beta}+\dfrac{k_2}{\Gamma(1+\beta)}x^{\beta}$.

7.4.2. The time fractional complex Schrödinger equation (tfcSE)

The section starts with the tfcSE in the form [50];

$$\frac{\partial^{\gamma}\varphi}{\partial t^{\gamma}}+i\frac{\partial^2\varphi}{\partial x^2}+\frac{\partial}{\partial x}(|\varphi|^2\varphi)=0, 0<\gamma<1. \tag{7.32}$$

For the purpose of mathematical conversion, bring the transformations: $\varphi(x,t)=\phi(\xi)\exp(i\tau)$ $,\xi=ik(x+\frac{2g}{\gamma}.t^{\gamma}),\tau=(gx+\frac{h}{\gamma}.t^{\gamma})$ and it convert this tfcSE to the without fractional order nonlinear SE:

$$\frac{\partial^{\gamma}\varphi}{\partial t^{\gamma}}=i(h\phi+2gk\phi')\exp(i\tau),$$

$$\frac{\partial^2\varphi}{\partial x^2}=-(g^2\phi+2gk\phi'+k^2\phi'')\exp(i\tau),$$

$$\frac{\partial}{\partial x}(|\varphi|^2\varphi)=i(g\phi^3+3k\phi^2\phi'')\exp(i\tau).$$

We obtain the nonlinear complex PSE by using the above expression,

$$(h-g^2)\phi-k^2\phi''+g\phi^3+3k\phi^2\phi'=0. \tag{7.33}$$

Using the rule of homogenous balance on Eq. (7.33)(ϕ'' and $\phi^2\phi'$) $\Rightarrow$ ($\Rightarrow n=m+\frac{1}{2}$. Apply another transformation $\phi(\xi)=u^{\frac{1}{2}}(\xi)$ in Eq. (7.33), we get ordinary differential equations

$$4gu^3+4(h-g^2)u^2+6ku^2u'+k^2u'^2-2k^2uu''=0. \tag{7.34}$$

Again using the rule of homogenous balance on Eq. (7.34)(uu'' and u^2u), we have $n = m+1$.

Therefore, the new form of Eq. (7.6) is by using the auxiliary equation $u'(\zeta) = d - u^2(\zeta)$,

$$u(\xi) = \frac{\ell_0 + \ell_1 u + \ell_2 u^2}{\wp_0 + \wp_1 u}. \tag{7.35}$$

Inserting Eq. (7.35) with Eq. (7) into the reduced non-linear ordinary differential Eq. (34), we have a polynomial of $u^i, (i = 0,1,2,...)$. All the adjacent terms of u^i are equating to zero, and form some equations in-terms of unknown constants g, h, ℓ_0, ℓ_1 and $\wp_1$ and its solutions are follows;

Set 1: $h = 2dk^2, g = \mp k\sqrt{d}, \ell_0 = \pm\frac{1}{2}\wp_0 k\sqrt{d}, \ell_1 = \frac{1}{2}k(\pm\wp_1\sqrt{d} - \wp_0), \ell_2 = -\frac{k\wp_1}{2}$.

Set 2: $h = 8dk^2, g = \mp 2k\sqrt{d}, \ell_0 = -\frac{1}{2}d\wp_1 k, \ell_1 = \pm k\wp_1\sqrt{d}, \ell_2 = -\frac{k\wp_1}{2}, \wp_0 = 0$.

For **set 1**, the solution sets of the considered equation hold as:

$$\varphi_1 = \left[\frac{\pm\wp_0 k\sqrt{d} + k(\pm\wp_1\sqrt{d} - \wp_0)(\sqrt{d}\tanh(\sqrt{d}\xi)) - k\wp_1 d(\tanh(\sqrt{d}\xi))^2}{2\{\wp_0 + \wp_1\sqrt{d}\tanh(\sqrt{d}\xi)\}}\right]^{\frac{1}{2}} \exp(i\tau); \tag{7.36}$$

$$\varphi_2 = \left[\frac{\pm\wp_0 k\sqrt{d} + k(\mp\wp_1\sqrt{d} - \wp_0)(\sqrt{d}\coth(\sqrt{d}\xi)) - k\wp_1 d(\coth(\sqrt{d}\xi))^2}{2\{\wp_0 + \wp_1\sqrt{d}\coth(\sqrt{d}\xi)\}}\right]^{\frac{1}{2}} \exp(i\tau); \tag{7.37}$$

$$\varphi_3 = \left[\frac{-k\wp_0\xi - k\wp_1}{2\{\wp_0\xi^2 + \wp_1\xi\}}\right]^{\frac{1}{2}} \exp(i\tau), d = 0; \tag{7.38}$$

$$\varphi_4 = \left[\frac{\pm\wp_0 k\sqrt{d} - k(\pm\wp_1\sqrt{d} - \wp_0)(\sqrt{-d}\tan(\sqrt{-d}\xi)) + k\wp_1 d(\tan(\sqrt{-d}\xi))^2}{2\{\wp_0 - \wp_1\sqrt{-d}\tan(\sqrt{-d}\xi)\}}\right]^{\frac{1}{2}} \exp(i\tau); \tag{7.39}$$

$$\varphi_5 = \left[\frac{\pm\wp_0 k\sqrt{d} + k(\pm\wp_1\sqrt{d} - \wp_0)(\sqrt{-d}\cot(\sqrt{-d}\xi)) + k\wp_1 d(\cot(\sqrt{-d}\xi))^2}{2\{\wp_0 + \wp_1\sqrt{-d}\cot(\sqrt{-d}\xi)\}}\right]^{\frac{1}{2}} \exp(i\tau); \tag{7.40}$$

where $\xi = ik(x \mp \frac{2k\sqrt{d}}{\gamma}.t^{\gamma})$ and $\tau = (\mp k\sqrt{d}x + \frac{2dk^2}{\gamma}.t^{\gamma})$.

For **set 2**, the tfcSE holds the solutions;

$$\varphi_6 = \left[\frac{dk\wp_1 \pm 2kd\wp_1 \tanh(\sqrt{d}\xi) - kd\wp_1(\tanh(\sqrt{d}\xi))^2}{2\wp_1\sqrt{d}\tanh(\sqrt{d}\xi)}\right]^{\frac{1}{2}} \exp(i\tau), d > 0; \tag{7.41}$$

$$\varphi_7 = \left[\frac{dk\wp_1 \pm 2kd\wp_1 \coth(\sqrt{d}\xi) - kd\wp_1(\coth(\sqrt{d}\xi))^2}{2\wp_1\sqrt{d}\coth(\sqrt{d}\xi)}\right]^{\frac{1}{2}} \exp(i\tau), d > 0; \tag{7.42}$$

$$\varphi_8 = \left[\frac{-k\wp_1}{2\wp_1\xi}\right]^{\frac{1}{2}} \exp(i\tau), d = 0; \tag{7.43}$$

$$\varphi_9 = \left[\frac{dk\wp_1 \mp 2kd\wp_1\sqrt{-d}\tan(\sqrt{-d}\xi) + kd\wp_1(\tan(\sqrt{-d}\xi))^2}{-2\wp_1\sqrt{-d}\tan(\sqrt{-d}\xi)}\right]^{\frac{1}{2}} \exp(i\tau), d < 0; \tag{7.44}$$

$$\varphi_{10} = \left[\frac{dk\wp_1 \pm 2kd\wp_1\sqrt{-d}\cot(\sqrt{-d}\xi) + kd\wp_1(\cot(\sqrt{-d}\xi))^2}{2\wp_1\sqrt{-d}\cot(\sqrt{-d}\xi)}\right]^{\frac{1}{2}} \exp(i\tau), d < 0; \tag{7.45}$$

where, $\xi = ik(x \mp \frac{4k\sqrt{d}}{\gamma}.t^{\gamma})$, $\tau = (\mp 2k\sqrt{d}x + \frac{8dk^2}{\gamma}.t^{\gamma})$.

7.4.3 The M-Fractional Schrodinger-Hirota equation (s-tM-fSH)

This subsection start with the Schrodinger-Hirota equation [52] with the form

$$\begin{aligned} &iD_{M,t}^{\alpha,\beta}\psi + \lambda D_{M,x}^{2\alpha,\beta}\psi + \Xi D_{M,t}^{\alpha,\beta}D_{M,x}^{\alpha,\beta}\psi + \rho|\psi|^2\psi + i(AD_{M,x}^{3\alpha,\beta}\psi + B|\psi|^2 D_{M,x}^{\alpha,\beta}\psi) \\ &= iCD_{M,x}^{\alpha,\beta}\psi + i\Theta D_{M,x}^{\alpha,\beta}(|\psi|^2\psi) + i\Omega D_{M,x}^{\alpha,\beta}(|\psi|^2)\psi,\ 0 < \alpha < 1, \beta > 0, i = \sqrt{-1} \end{aligned}, \tag{7.46}$$

where $\psi(x,t)$ is complex function, coefficients $\Theta, \lambda, \Xi, A,$ and C are the self-steepening, group velocity, spatiotemporal, 3rd dispersion and inter-modal dispersion terms respectively. Parameters B, Ω are nonlinear dispersions.

Plugging the complex wave transformation

$$\psi(x,t) = \mathrm{X}(\varsigma)\exp(i\tau), \varsigma = \frac{\Gamma(1+\beta)}{\alpha}n(x^\alpha - vt^\alpha), \tau = \frac{\Gamma(1+\beta)}{\alpha}(-\mathrm{K}x^\alpha + wt^\alpha + E),$$

into the Eq. (7.46), we attain to ODE with two conditions:

$$n^2(\lambda - \Xi v + 3A\mathrm{K})\mathrm{X}'' - (w + \lambda\mathrm{K}^2 - \Xi\mathrm{K}w + A\mathrm{K}^3 + C\mathrm{K})\mathrm{X} + (\rho + \mathrm{K}B - \mathrm{K}\Theta)\mathrm{X}^3 = 0, \qquad (7.47)$$

with $\Omega = \frac{(B-3\Theta)(\lambda - v\Xi) - 3A(2\mathrm{K}\Theta + \rho)}{2(3A\mathrm{K} + \lambda - \Xi v)}$,and

$$C = \frac{A(w + \mathrm{K}(-8\mathrm{K}\lambda + v(-3 + 6\mathrm{K}\Xi) + 2\Xi w)) - 8A^2\mathrm{K}^3 - (\lambda - v\Xi)(v + 2\mathrm{K}\lambda - v\mathrm{K}\lambda - \Xi w)}{2A\mathrm{K} + \lambda - \Xi v}.$$

The homogenous balance provide us, $n = m+1$. For $m = 1$, we have $n = 2$. So Eq. (7.6) reduces to the following by using $\mathrm{X}'(\zeta) = d - \mathrm{X}^2(\zeta)$,

$$\Psi(\xi) = \frac{\ell_0 + \ell_1\mathrm{X} + \ell_2\mathrm{X}^2}{\wp_0 + \wp_1\mathrm{X}}. \qquad (7.48)$$

Inserting Eq. (7.48) with Eq. (7.7) into the reduced non-linear ordinary differential Eq. (7.47), we have a polynomial of $\mathrm{X}^k, (k = 0,1,2,\ldots)$. All the adjacent terms of X^k are equating to zero, and form some equations with unknown constants $\ell_0, \ell_1, \ell_2, \wp_0, \wp_1, n$. Solving the equations with maple software and we get three sets of solution:

Set-1: $\ell_1 = \wp_0\sqrt{\frac{wK\Xi - A\mathrm{K}^3 - \mathrm{K}^2\lambda - C\mathrm{K} - w)}{d(\Theta\mathrm{K} - B\mathrm{K} - \rho)}}, \ell_2 = \wp_1\sqrt{\frac{wK\Xi - A\mathrm{K}^3 - \mathrm{K}^2\lambda - C\mathrm{K} - w)}{d(\Theta\mathrm{K} - B\mathrm{K} - \rho)}},$

$\ell_0 = 0, n = \sqrt{\frac{wK\Xi - A\mathrm{K}^3 - \mathrm{K}^2\lambda - C\mathrm{K} - w}{2d(3A\mathrm{K} - v\Xi + \lambda)}}.$

Set-2: $\ell_0 = -\frac{\wp_1}{2}\sqrt{\frac{d(wK\Xi - \mathrm{K}^2\lambda - C\mathrm{K} - w - A\mathrm{K}^3)}{\Theta\mathrm{K} - B\mathrm{K} - \rho}}, \ell_2 = \sqrt{\frac{wK\Xi - \mathrm{K}^2\lambda - C\mathrm{K} - w - A\mathrm{K}^3}{4d(\Theta\mathrm{K} - B\mathrm{K} - \rho)}},$

$\ell_1 = 0, \wp_0 = 0, n = \sqrt{\frac{wK\Xi - \mathrm{K}^2\lambda - C\mathrm{K} - w - A\mathrm{K}^3}{8d(3A\mathrm{K} - v\Xi + \lambda)}}.$

Set-3: $\ell_0 = -\frac{\wp_1}{2}\sqrt{\frac{2d(A\mathrm{K}^3 - w\mathrm{K}\Xi + \mathrm{K}^2\lambda + C\mathrm{K} + w)}{\Theta\mathrm{K} - B\mathrm{K} - \rho}}, \ell_2 = \sqrt{\frac{A\mathrm{K}^3 - w\mathrm{K}\Xi + \mathrm{K}^2\lambda + C\mathrm{K} + w}{2d(\Theta\mathrm{K} - B\mathrm{K} - \rho)}},$

$\ell_1 = 0, \wp_0 = 0, \; n = \sqrt{\frac{A\mathrm{K}^3 - w\mathrm{K}\Xi + \mathrm{K}^2\lambda + C\mathrm{K} + w}{4d(3A\mathrm{K} - v\Xi + \lambda)}}.$

For **set-1**, the space-time M-fractional SH equation holds the solutions

$$\psi(x,t) = \sqrt{\frac{w\mathrm{K}\Xi - A\mathrm{K}^3 - \mathrm{K}^2\lambda - C\mathrm{K} - w)}{d(\Theta\mathrm{K} - B\mathrm{K} - \rho)}}\sqrt{d}\tanh(\sqrt{d}\varsigma)e^{i\tau}, d > 0, \tag{7.49}$$

$$\psi(x,t) = \sqrt{\frac{w\mathrm{K}\Xi - A\mathrm{K}^3 - \mathrm{K}^2\lambda - C\mathrm{K} - w)}{d(\Theta\mathrm{K} - B\mathrm{K} - \rho)}}\sqrt{d}\coth(\sqrt{d}\varsigma)e^{i\tau}, d > 0, \tag{7.50}$$

$$\psi(x,t) = \sqrt{\frac{w\mathrm{K}\Xi - A\mathrm{K}^3 - \mathrm{K}^2\lambda - C\mathrm{K} - w)}{d(\Theta\mathrm{K} - B\mathrm{K} - \rho)}}\frac{e^{i\tau}}{\varsigma}, d = 0, \tag{7.51}$$

$$\psi(x,t) = -\sqrt{\frac{w\mathrm{K}\Xi - A\mathrm{K}^3 - \mathrm{K}^2\lambda - C\mathrm{K} - w)}{d(\Theta\mathrm{K} - B\mathrm{K} - \rho)}}\sqrt{-d}\tan(\sqrt{-d}\varsigma)e^{i\tau}, d < 0, \tag{7.52}$$

$$\psi(x,t) = \sqrt{\frac{w\mathrm{K}\Xi - A\mathrm{K}^3 - \mathrm{K}^2\lambda - C\mathrm{K} - w)}{d(\Theta\mathrm{K} - B\mathrm{K} - \rho)}}\sqrt{-d}\cot(\sqrt{-d}\varsigma)e^{i\tau}, d < 0, \tag{7.53}$$

where

$$\varsigma = \frac{\Gamma(1+\beta)}{\alpha}\sqrt{\frac{w\mathrm{K}\Xi - A\mathrm{K}^3 - \mathrm{K}^2\lambda - C\mathrm{K} - w}{2d(3A\mathrm{K} - v\Xi + \lambda)}}(x^\alpha - vt^\alpha), \tau = \frac{\Gamma(1+\beta)}{\alpha}(-\mathrm{K}x^\alpha + wt^\alpha + E).$$

For **set-2**, the space-time M-fractional SH model holds the solutions

$$\psi(x,t) = \sqrt{\frac{w\mathrm{K}\Xi - \mathrm{K}^2\lambda - C\mathrm{K} - w - A\mathrm{K}^3}{4d(\Theta\mathrm{K} - B\mathrm{K} - \rho)}}\left[\frac{-\wp_1 d + d\tanh^2(\sqrt{d}\varsigma)}{\wp_1\sqrt{d}\tanh(\sqrt{d}\zeta)}\right]e^{i\tau}, \; d > 0, \tag{7.54}$$

$$\psi(x,t) = \sqrt{\frac{w\mathrm{K}\Xi - \mathrm{K}^2\lambda - C\mathrm{K} - w - A\mathrm{K}^3}{4d(\Theta\mathrm{K} - B\mathrm{K} - \rho)}}\left[\frac{-\wp_1 d + d\coth^2(\sqrt{d}\varsigma)}{\wp_1\sqrt{d}\coth(\sqrt{d}\varsigma)}\right]e^{i\tau}, \; d > 0, \tag{7.55}$$

$$\psi(x,t) = \sqrt{\frac{w\mathrm{K}\Xi - \mathrm{K}^2\lambda - C\mathrm{K} - w - A\mathrm{K}^3}{4d(\Theta\mathrm{K} - B\mathrm{K} - \rho)}}\left[\frac{\wp_1 d + d\tan^2(\sqrt{-d}\varsigma)}{\wp_1\sqrt{-d}\tan(\sqrt{-d}\zeta)}\right]e^{i\tau}, \; d < 0, \tag{7.56}$$

$$\psi(x,t)=\sqrt{\frac{w\mathrm{K}\Xi-\mathrm{K}^2\lambda-C\mathrm{K}-w-A\mathrm{K}^3}{4d(\Theta\mathrm{K}-B\mathrm{K}-\rho)}}\left[\frac{-\wp_1 d-d\cot^2(\sqrt{-d}\varsigma)}{\wp_1\sqrt{-d}\cot(\sqrt{-d}\varsigma)}\right]e^{i\tau},\ d<0, \quad (7.57)$$

where

$$\varsigma=\frac{\Gamma(1+\beta)}{\alpha}\sqrt{\frac{w\mathrm{K}\Xi-\mathrm{K}^2\lambda-C\mathrm{K}-w-A\mathrm{K}^3}{8d(3A\mathrm{K}-v\Xi+\lambda)}}(x^\alpha-vt^\alpha),\tau=\frac{\Gamma(1+\beta)}{\alpha}(-\mathrm{K}x^\alpha+wt^\alpha+E).$$

For **set-3**, the space-time M-fractional SH equation holds the solutions

$$\psi(\xi)=\sqrt{\frac{A\mathrm{K}^3-w\mathrm{K}\Xi+\mathrm{K}^2\lambda+C\mathrm{K}+w}{2d(\Theta\mathrm{K}-B\mathrm{K}-\rho)}}\left[\frac{-\wp_1 d+d\tanh^2(\sqrt{d}\varsigma)}{\wp_1\sqrt{d}\tanh(\sqrt{d}\varsigma)}\right]e^{i\tau},d>0, \quad (7.58)$$

$$\psi(\xi)=\sqrt{\frac{A\mathrm{K}^3-w\mathrm{K}\Xi+\mathrm{K}^2\lambda+C\mathrm{K}+w}{2d(\Theta\mathrm{K}-B\mathrm{K}-\rho)}}\left[\frac{-\wp_1 d+d\coth^2(\sqrt{d}\varsigma)}{\wp_1\sqrt{d}\coth(\sqrt{d}\varsigma)}\right]e^{i\tau},d>0, \quad (7.59)$$

$$\psi(\xi)=\sqrt{\frac{A\mathrm{K}^3-w\mathrm{K}\Xi+\mathrm{K}^2\lambda+C\mathrm{K}+w}{2d(\Theta\mathrm{K}-B\mathrm{K}-\rho)}}\left[\frac{\wp_1 d+d\tan^2(\sqrt{-d}\varsigma)}{\wp_1\sqrt{-d}\tan(\sqrt{-d}\varsigma)}\right]e^{i\tau},d<0, \quad (7.60)$$

$$\psi(\xi)=\sqrt{\frac{A\mathrm{K}^3-w\mathrm{K}\Xi+\mathrm{K}^2\lambda+C\mathrm{K}+w}{2d(\Theta\mathrm{K}-B\mathrm{K}-\rho)}}\left[\frac{-\wp_1 d-d\cot^2(\sqrt{-d}\varsigma)}{\wp_1\sqrt{-d}\cot(\sqrt{-d}\varsigma)}\right]e^{i\tau},d<0, \quad (7.61)$$

where

$$\varsigma=\frac{\Gamma(1+\beta)}{\alpha}\sqrt{\frac{A\mathrm{K}^3-w\mathrm{K}\Xi+\mathrm{K}^2\lambda+C\mathrm{K}+w}{4d(3A\mathrm{K}-v\Xi+\lambda)}}(x^\alpha-vt^\alpha),\tau=\frac{\Gamma(1+\beta)}{\alpha}(-\mathrm{K}x^\alpha+wt^\alpha+E).$$

7.5. Graphical representations

In this part, we will plotted some graph of the exact solutions the nonlinear space-time fractional electrical transmission lines (s-tfETL) (Eq. (7.9)), the time fractional complex Schrödinger (tcFSE) (Eq. (7.32)) and space-time M-fractional Schrödinger -Hirota (s-tM-fSH) (Eq. (7.46)).

7.5.1 Graphical representation of the solutions for stFETL model

The findings of the research are in the types of hyperbolic, rational and trigonometric functions. All the results are analyzed and some of them have shown graphically in the Fig-7.1 to Fig-7.3.

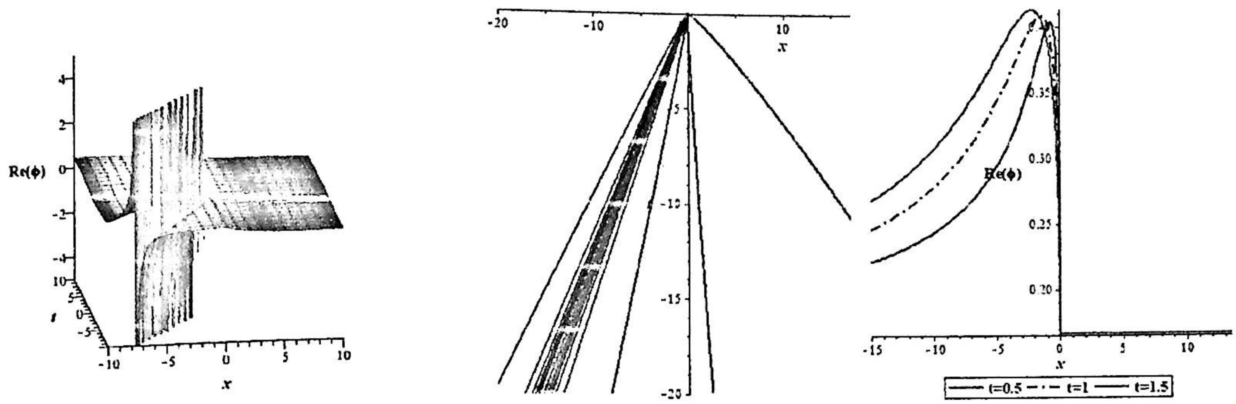

(a) Real 3D view (b) Real contour plot (c) Real 2D view

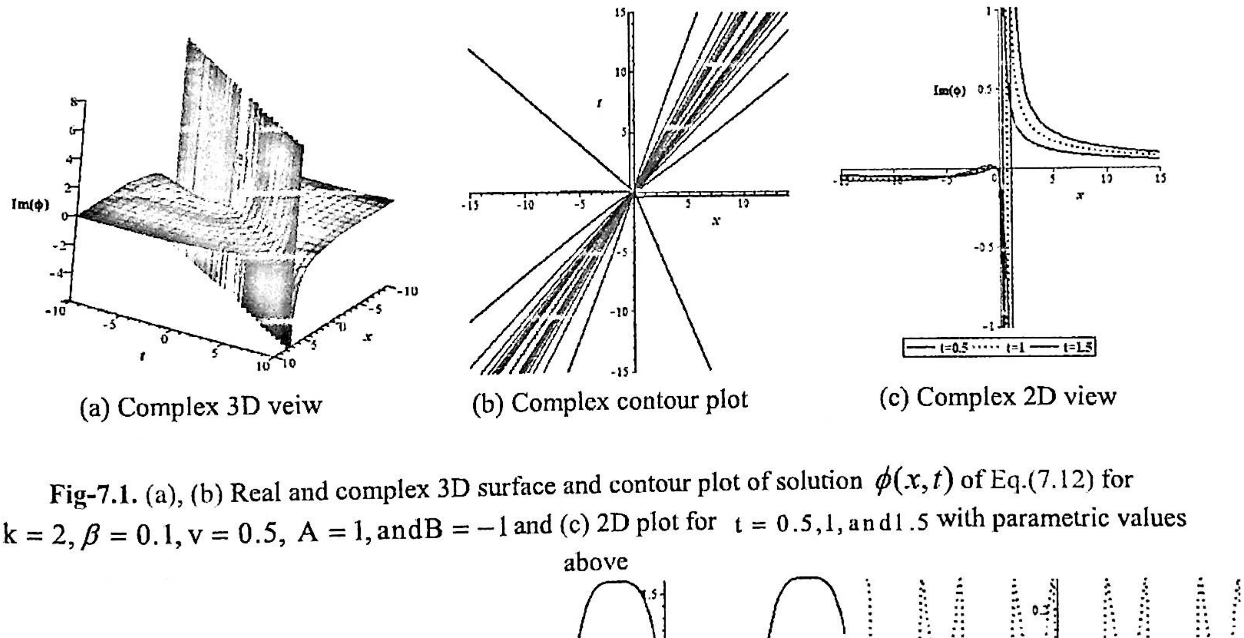

(a) Complex 3D veiw (b) Complex contour plot (c) Complex 2D view

Fig-7.1. (a), (b) Real and complex 3D surface and contour plot of solution $\phi(x,t)$ of Eq.(7.12) for $k = 2, \beta = 0.1, v = 0.5,\ A = 1, \text{and} B = -1$ and (c) 2D plot for $t = 0.5, 1, \text{and} 1.5$ with parametric values above

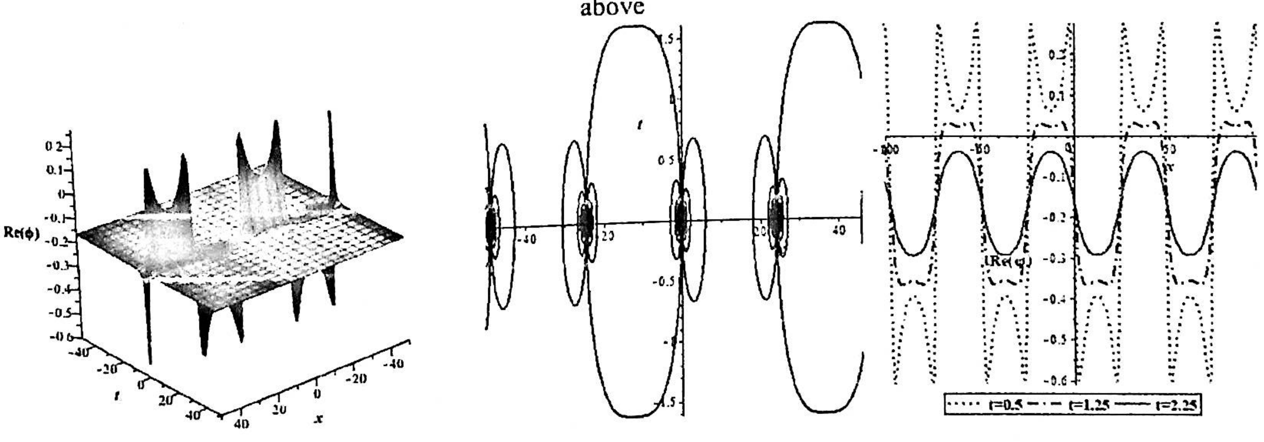

(a) Real 3D view (b) Real contour plot (c) Real 2D view

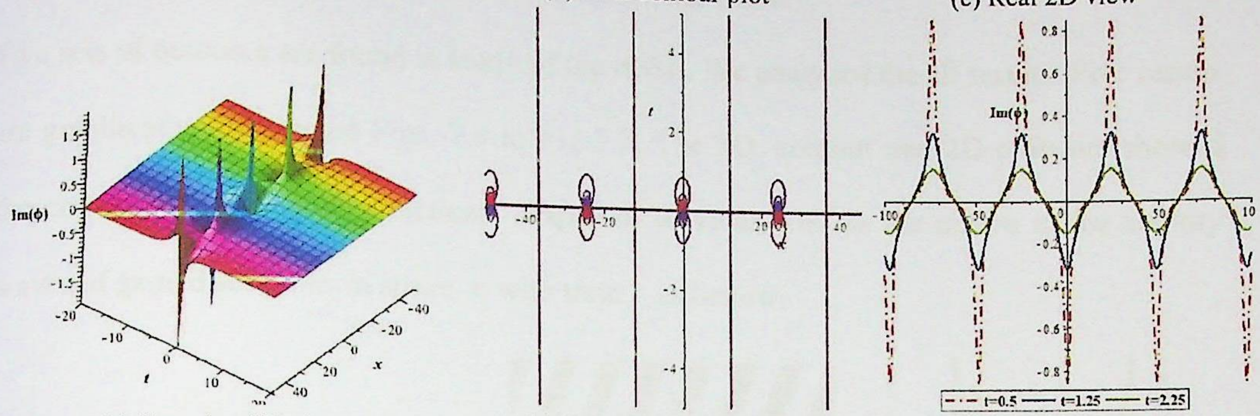

(a) Complex 3D view (b) Complex contour plot (c) Complex 2D view

Fig-7.2. (a), (b) Periodic rogue waves from real and complex 3D surface and contour plot of solution $\phi(x,t)$ of Eq.(7.15) for $k = -2, \beta = 1, v = 0.5, A = 1, \text{and} B = -1$ and Fig-(c) illustrates the 2D plot for $t = 0.5, 1.25, \text{and} 2.25$ with parametric values above

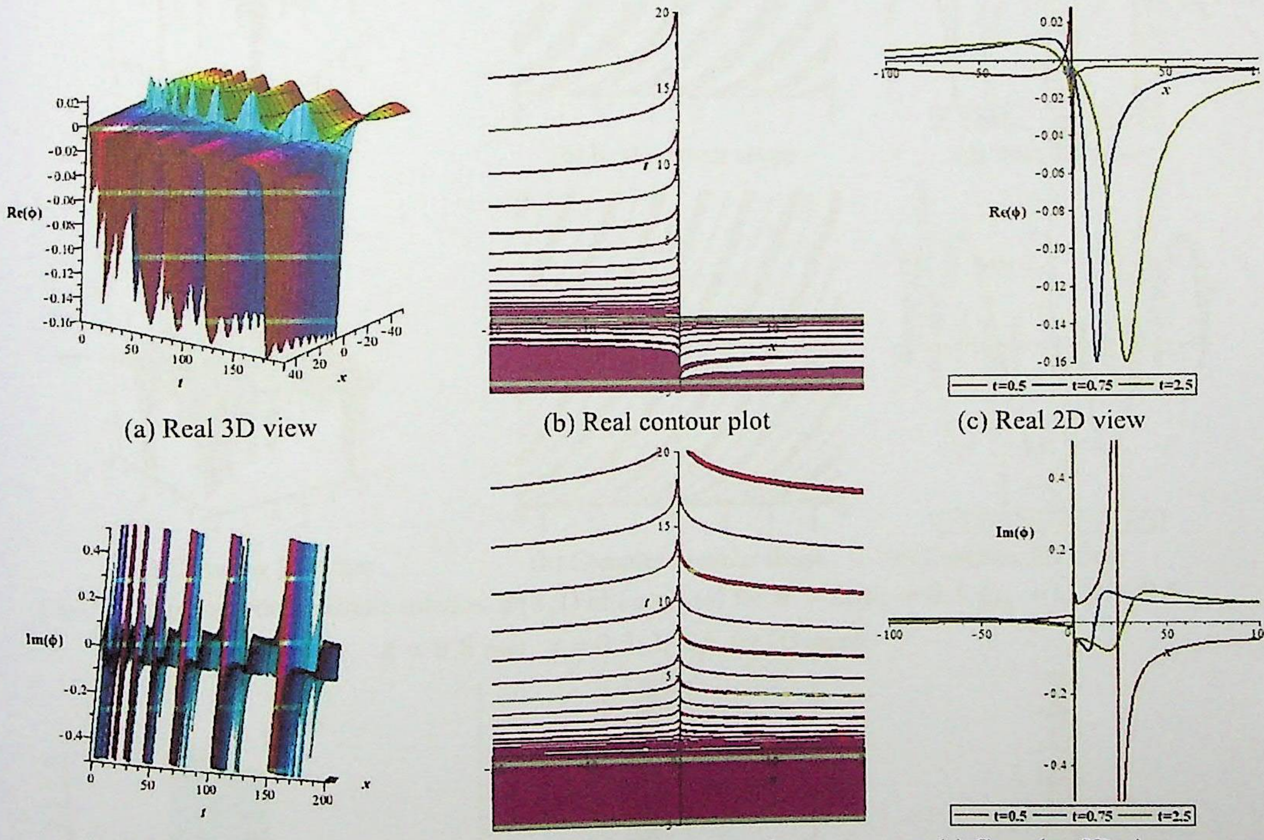

(a) Real 3D view (b) Real contour plot (c) Real 2D view

(a) Complex 3D view (b) Complex contour plot (c) Complex 2D view

Fig-3. (a), (b) Real and complex 3D surface and contour plot of solution $\phi(x,t)$ of Eq.(30) for $k = -2, \beta = 0.1, \ell_2 = 1, v = 3, A = 2, B = -1, \text{and} k_2 = 2$ and Fig-(c) illustrates the 2D plot for $t = 0.5, 0.75, \text{and} 2.5$ parametric values above.

7.5.2 Graphical representations of solutions for the tfcSE

Two sets of outcome are found in study of the tfcSE. We analyzed the all results .Five results are graphically represented Figs.-7.4 to Fig-7.7. The 3D, contour and 2D plots are showed the change of amplitudes, directions, shapes of wave as well as the nature of the solitary waves of gained solutions in space x with time t as bellow.

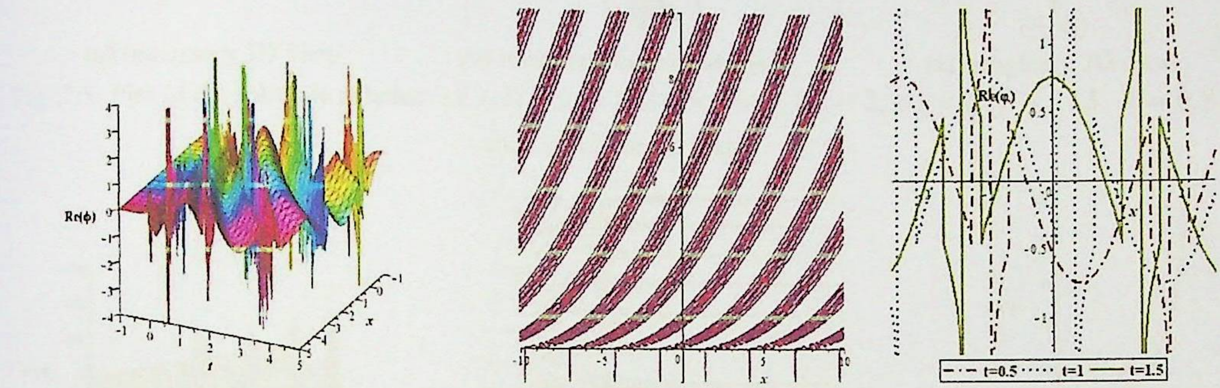

(a) Real 3D view (b) Real contour shape (c) Real 2D view

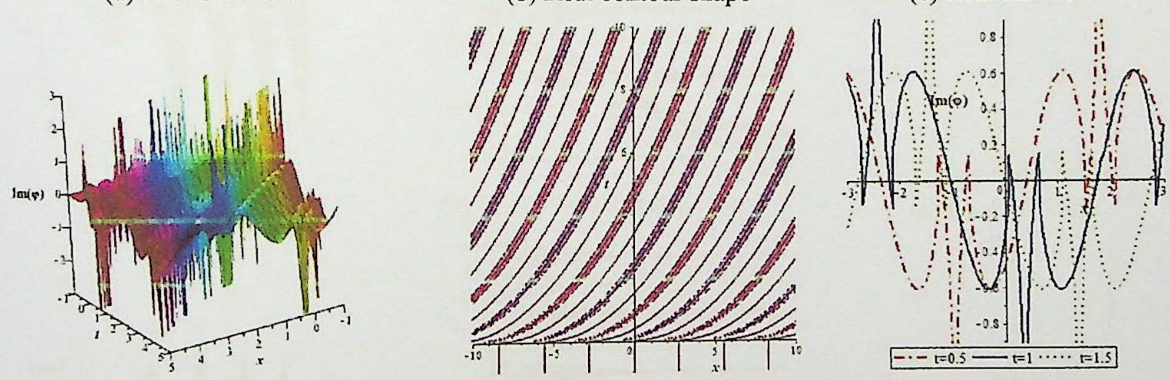

(a) Complex 3D view (b) Complex contour shape (c) Complex 2D view

Fig-7.4: Represent the solitonic solution $\varphi(x,t)$ of Eq. (7.36) for $d = 2, \wp_1 = 0.5, \wp_0 = 1,\ \gamma = 0.5$, $k = 0.8$ and $t = 0.5, 1, 1.5$ for 2D graph

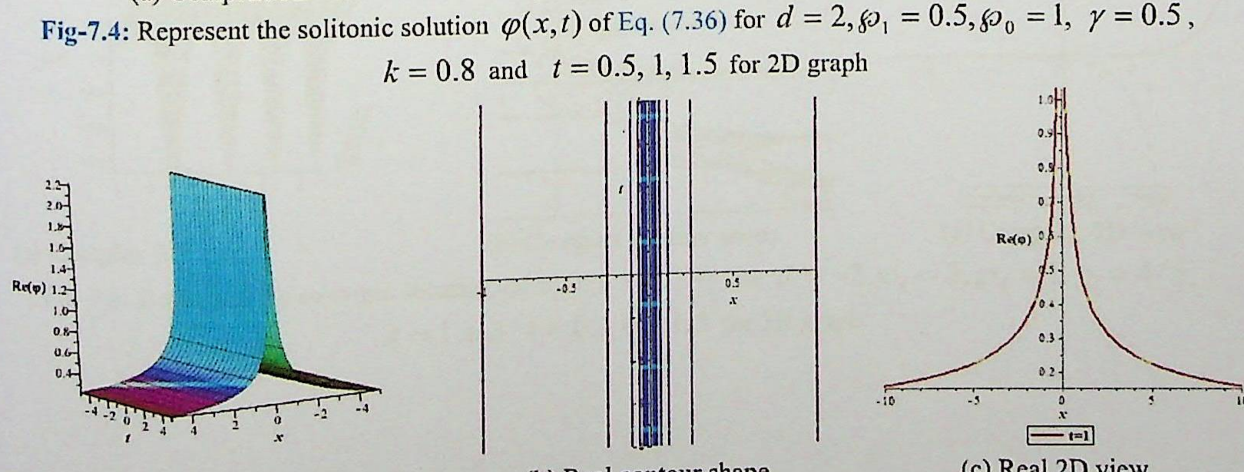

(a) Real 3D view (b) Real contour shape (c) Real 2D view

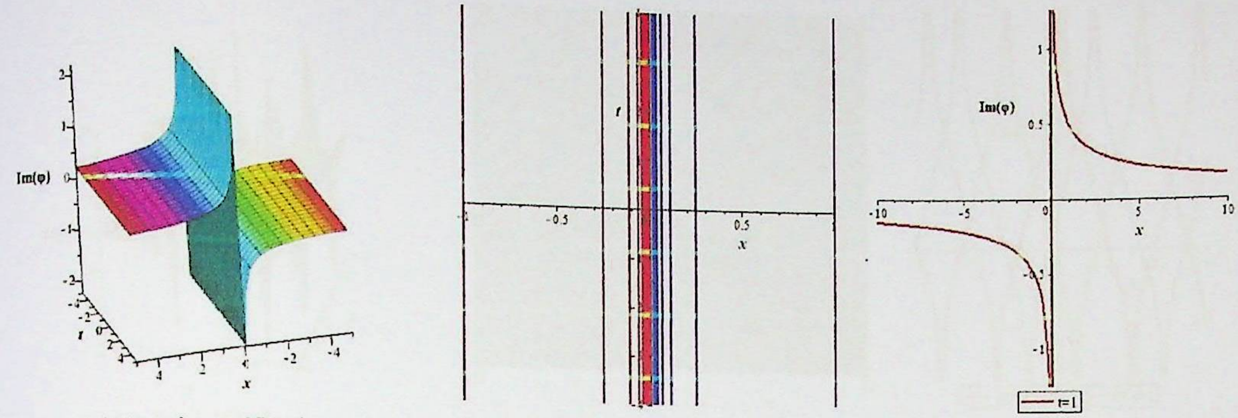

(a) Imaginary 3D view (b) Imaginary contour shape (c) Imaginary 2D view

Fig-.7.5: Plot of the solitonic solution $\varphi(x,t)$ of Eq. (7.38) for $d = 0, \wp_1 = 2, \wp_0 = 1,\ \gamma = 2/3,\ k = 0.8$ and $t = 1$ for 2D graph.

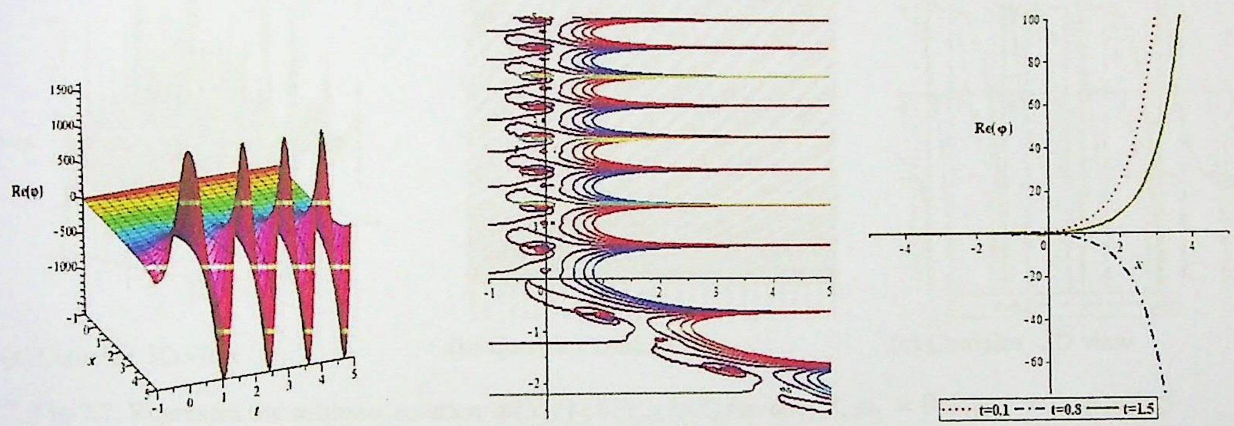

(a) Real 3D view (b) Real contour shape (c) Real 2D view

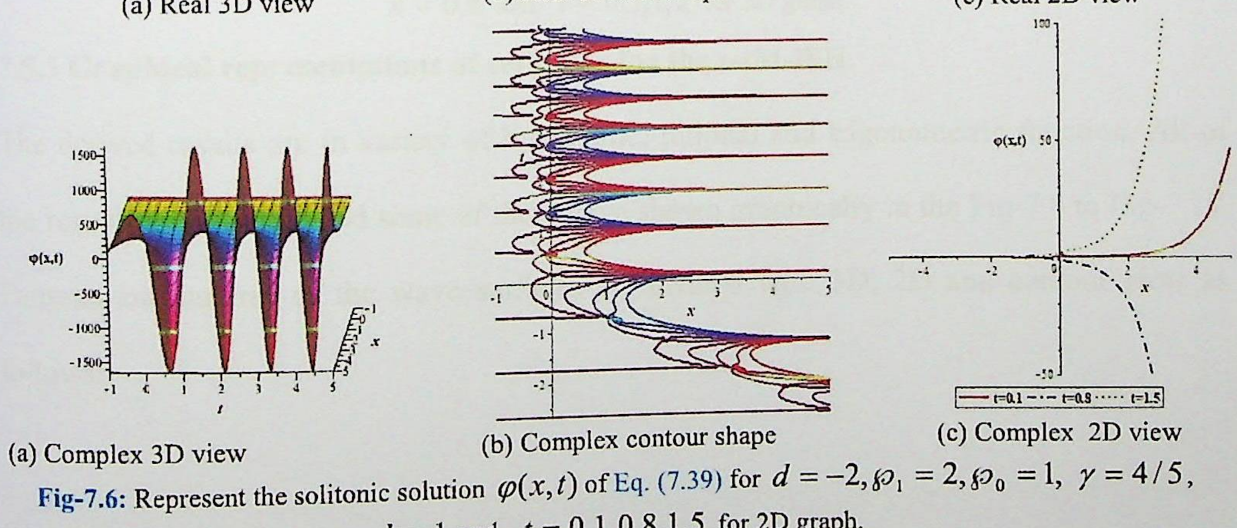

(a) Complex 3D view (b) Complex contour shape (c) Complex 2D view

Fig-7.6: Represent the solitonic solution $\varphi(x,t)$ of Eq. (7.39) for $d = -2, \wp_1 = 2, \wp_0 = 1,\ \gamma = 4/5$, $k = 1$ and $t = 0.1, 0.8, 1.5$ for 2D graph.

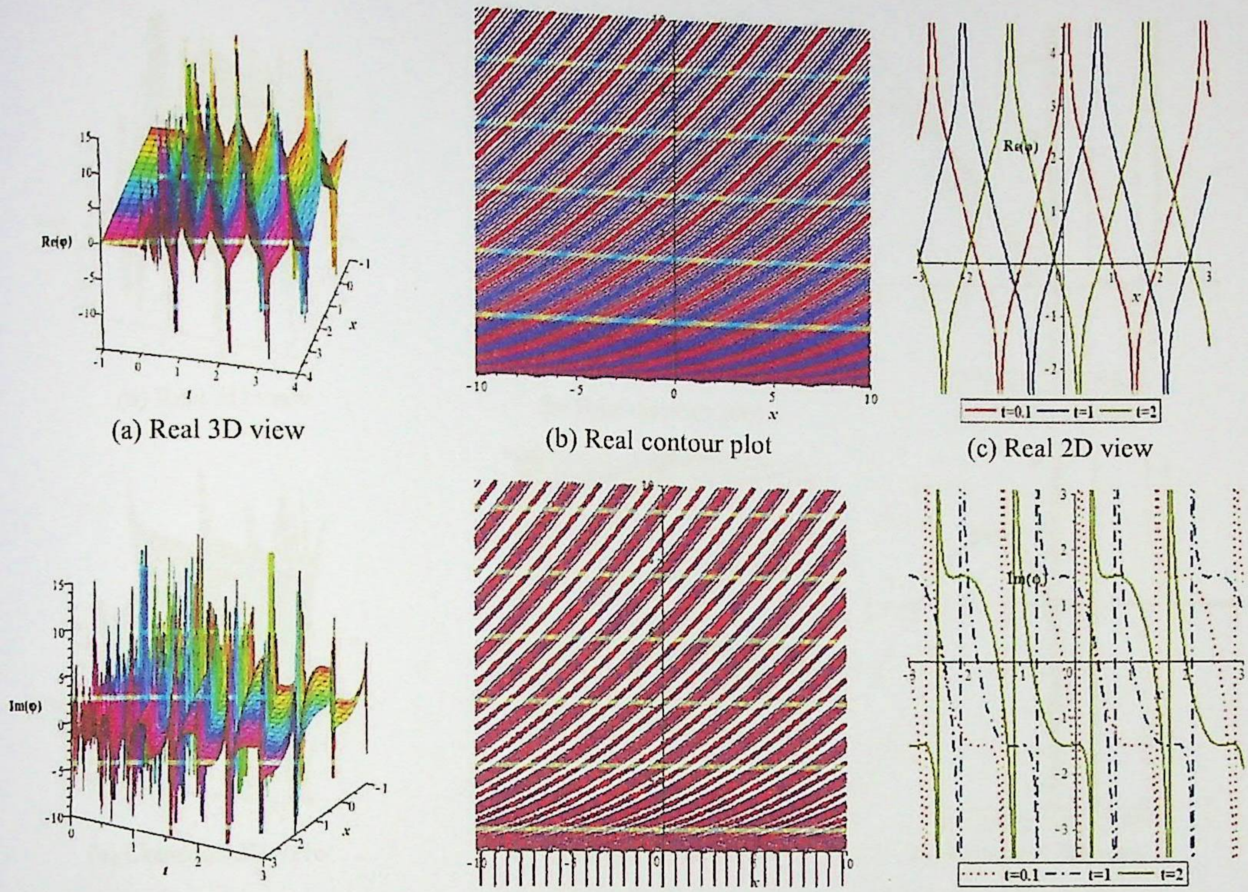

(a) Real 3D view (b) Real contour plot (c) Real 2D view

(a) Complex 3D view (b) Complex contour plot (c) Complex 2D view

Fig-7.7: Represent the solitonic solution $\varphi(x,t)$ of Eq. (7.42) for $d = 2, \wp_1 = 0.5, \wp_0 = 1,\ \gamma = 0.5$, $k = 0.8$ and $t = 0.1, 1, 2$ for 2D graph.

7.5.3 Graphical representations of solutions for the s-tM-fSH.

The derived results are in variety of hyperbolic, rational and trigonometric function. All of the results are analyzed and some of them have shown graphically in the Fig-7.8 to Fig-7.13. Patterns and natures of the wave surfaces are cleared with 3D, 2D and contour plots as follows:

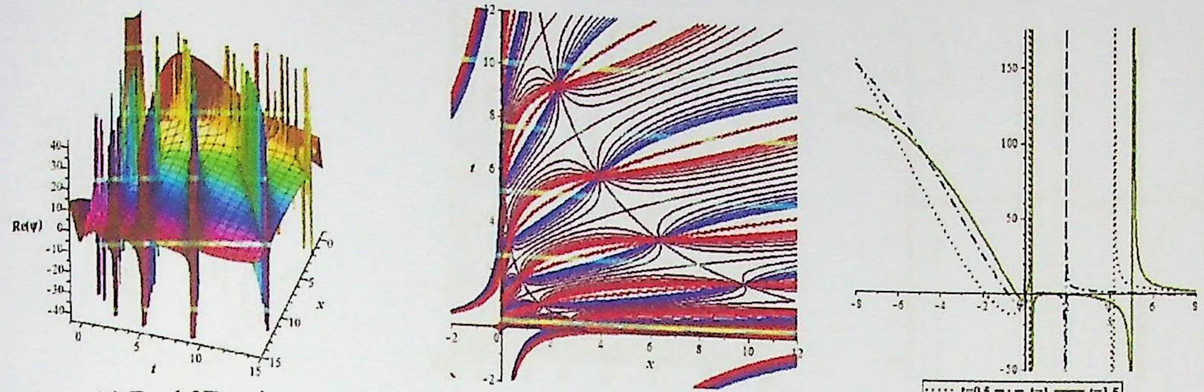

(a) Real 3D veiw (b) Real contour plot (c) Real 2D veiw

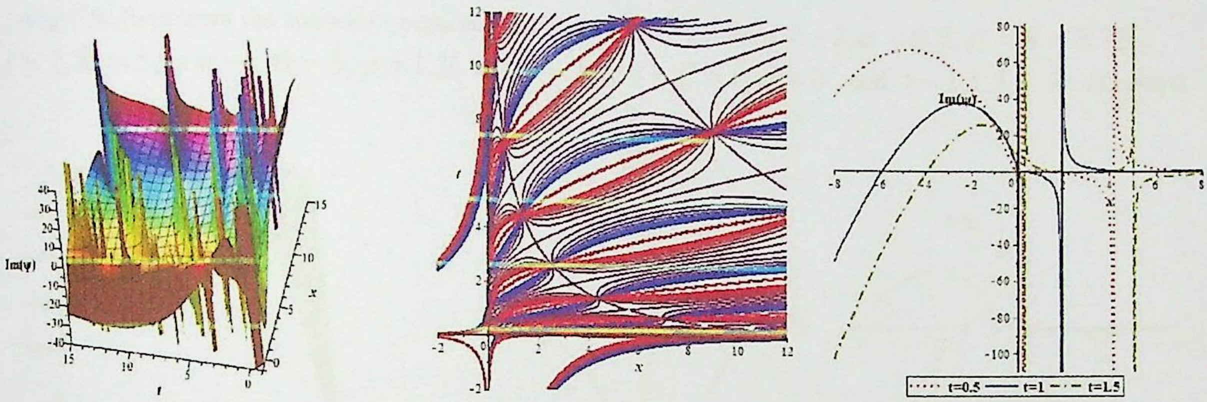

(a) Complex 3D veiw (b) Complex contour plot (c) Complex 2D veiw

Fig-7.8: Illustrate the solitary wave solution $\psi(x,t)$ of Eq. (7.49) for $d = 2, \alpha = \beta = 0.25,$ $A = K = \lambda = \Theta = \sigma = 1, w = -1,, \rho = 2, \Xi = 2, \nu = 3,\ E = 6$,and $t = 0.5, 1,\ 1.5$ for 2D graph.

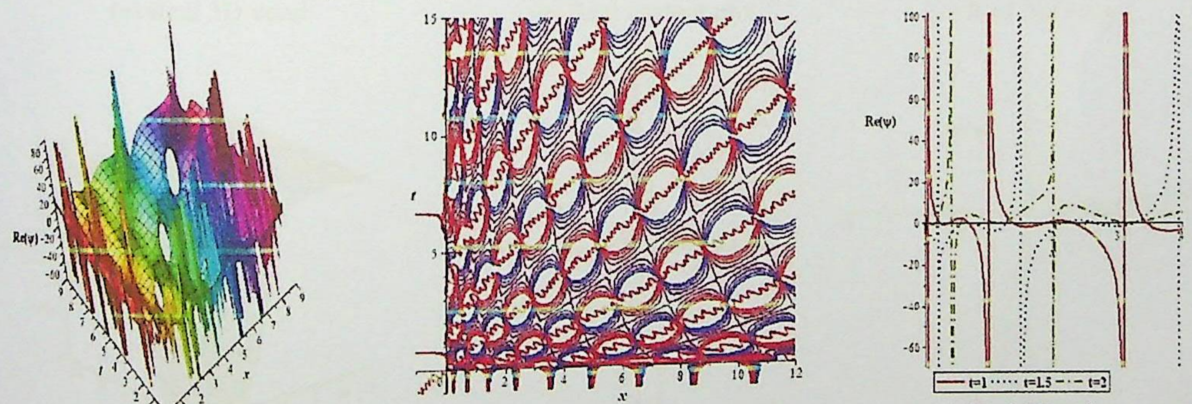

(a) Real 3D view (b) Real contour plot (c) Real 2D veiw

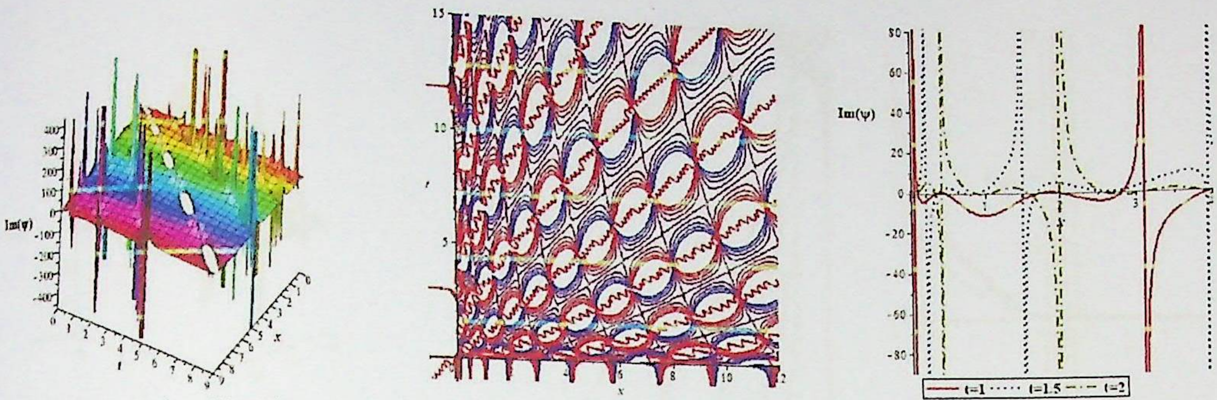

(a) Complex 3D veiw (b) Complex contour Plot (c) Complex 2D veiw

Fig-7.9: Represent the solitonic solution $\psi(x,t)$ of Eq. (7.52) for $d=-2, \alpha=0.5, \beta=B=0.75$, $A=2, \mathrm{K}=5, w=-1, \Theta=3, \rho=1, \Xi=4, \nu=1, \lambda=1, E=6, \sigma=3$, and $t=1,1.5,2$ for 2D graph.

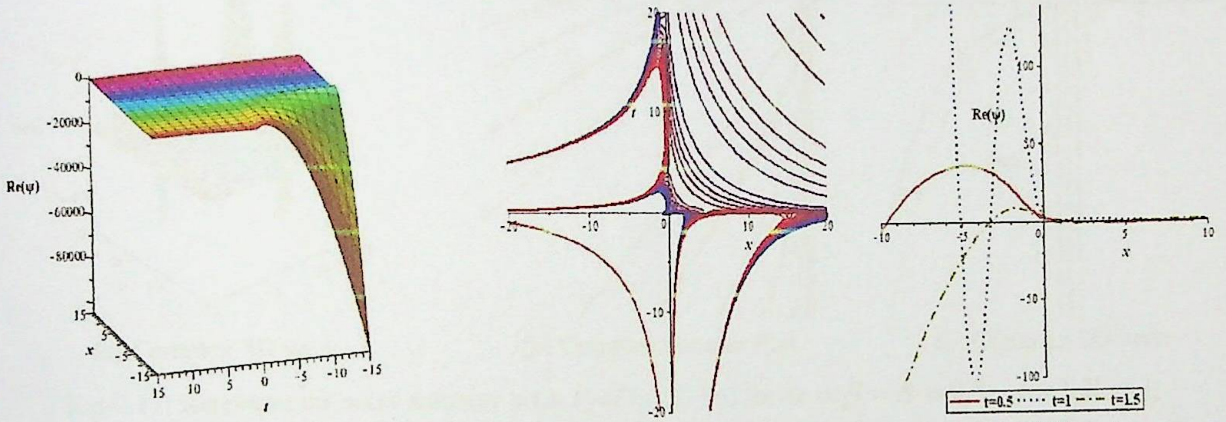

(a) Real 3D veiw (b) Real contour plot (c) Real 2D veiw

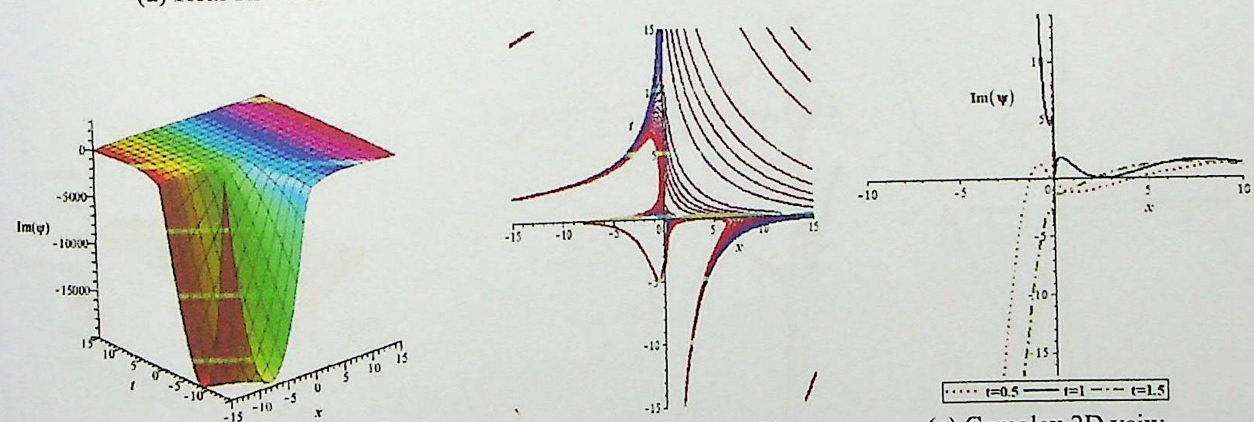

(a) Complex 3D veiw (b) Complex contour Plot (c) Complex 2D veiw

Fig-7.10: Represent the solitonic solution $\psi(x,t)$ of Eq. (7.54) for $\alpha=0/3, \beta=B=0.5, A=1$, $\mathrm{K}=1, w=-1, \Theta=1, \rho=2, \Xi=2, \nu=0, \lambda=1, E=6$ and for 2D graph $t=0.5, 1, 1.5$.

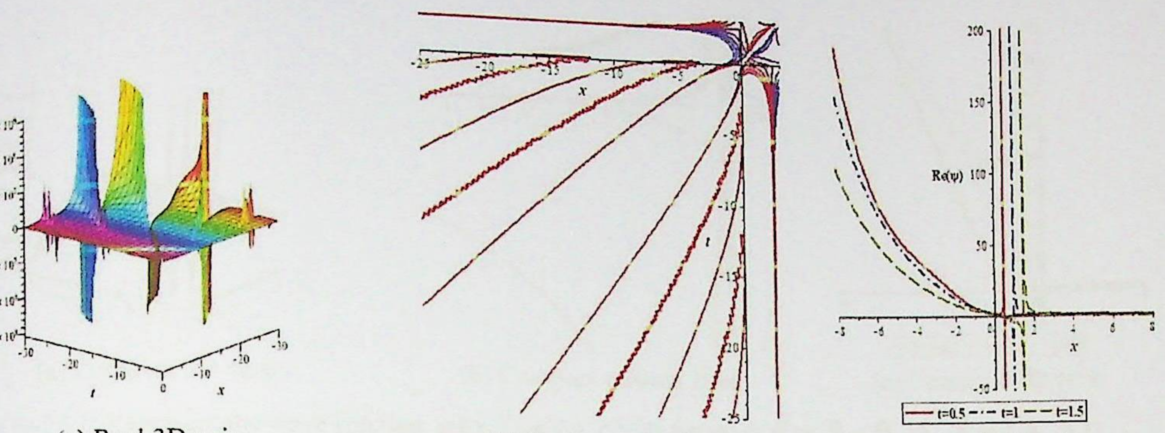

(a) Real 3D veiw (b) Real contour plot (c) Real 2D veiw

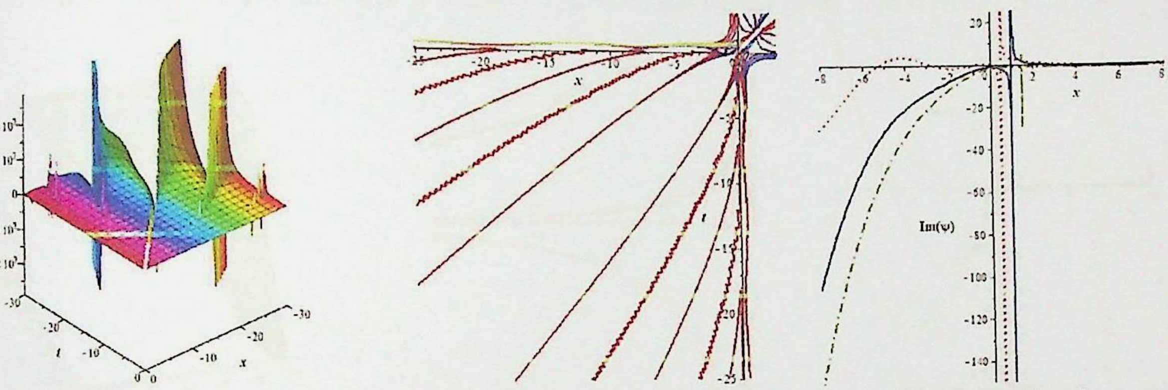

(a) Complex 3D veiw (b) Complex contour Plot (c) Complex 2D veiw

Fig-7.11: Represent the wave solution $\psi(x,t)$ of Eq. (7.56) for $\alpha = \beta = B = 0.5,\ A = 1, \mathrm{K} = 1,$ $w = -1, \Theta = 1, \rho = 1, \Xi = 2, \nu = 1, \lambda = 1, E = 6$, and for 2D graph $t = 0.5\ 1, 10.5$.

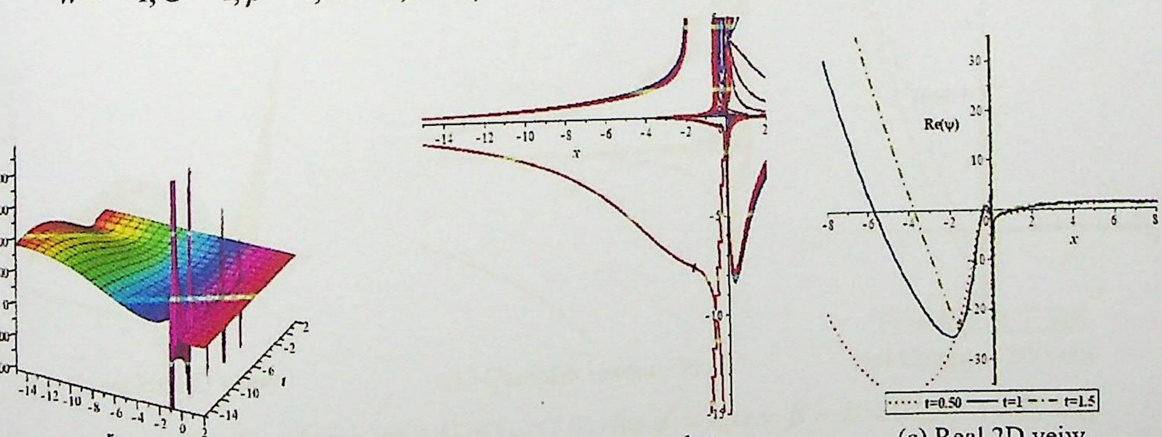

(a) Real 3D veiw (b) Real contour plot (c) Real 2D veiw

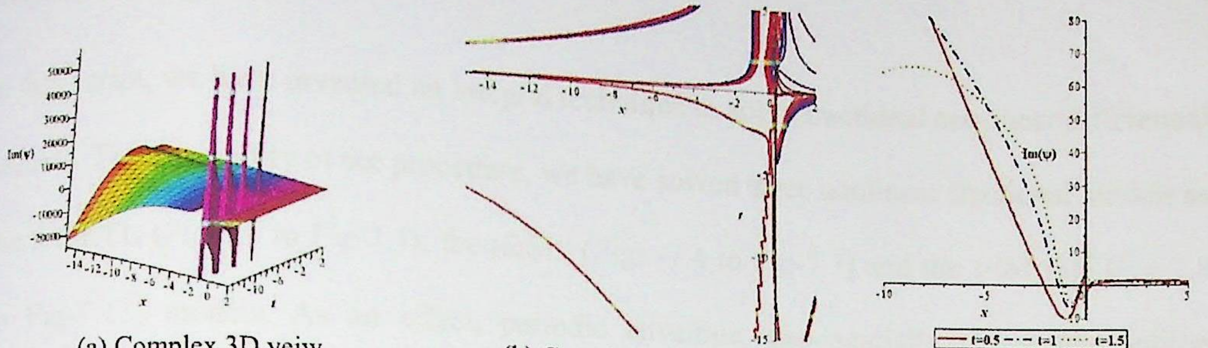

(a) Complex 3D veiw (b) Complex contour Plot (c) Complex 2D veiw

Fig-7.12: Represent the wave solution $\psi(x,t)$ of Eq. (7.59) for $\alpha=\beta=B=0.25,\ A=1, \mathrm{K}=1,$ $w=-1, \Theta=1, \rho=\Xi=2, \nu=0.5, \lambda=1, E=6$, and for 2D graph $t=0.5,\ 1,\ 1.5$.

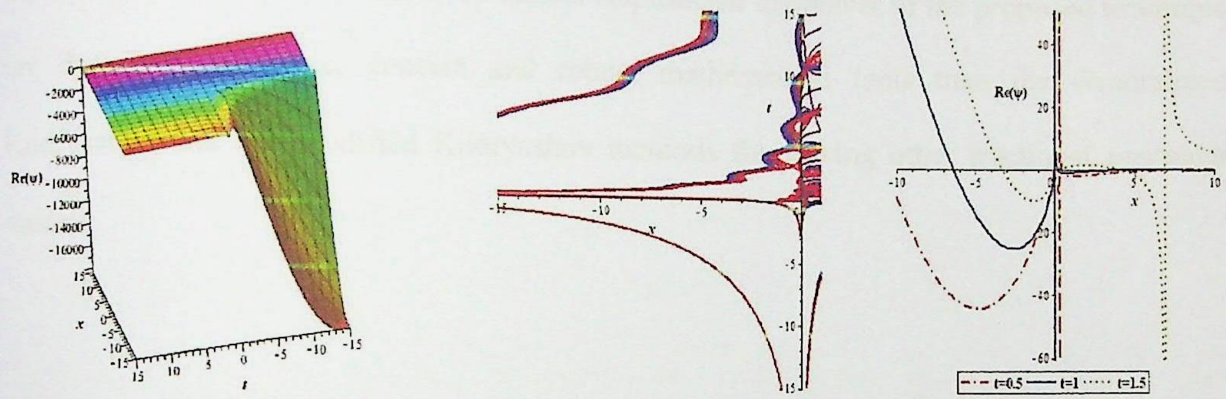

(a) Real 3D veiw (b) Real contour plot (c) Real 2D veiw

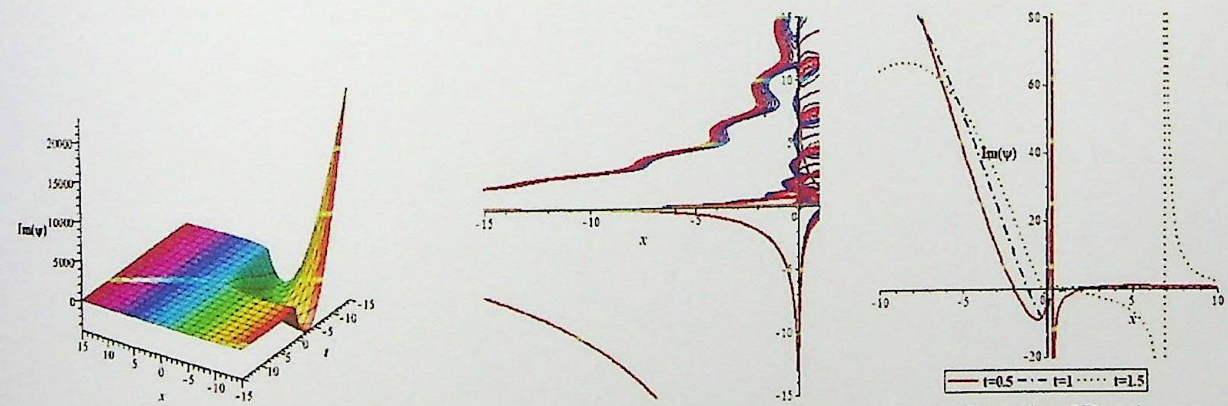

(a) Complex 3D veiw (b) Complex contour Plot (c) Complex 2D veiw

Fig-7.13: Represent the solution $\psi(x,t)$ of Eq. (7.61) for $d=2, \alpha=\beta=B=0.25,\ A=\mathrm{K}=1,$ $w=-1, \Theta=1, \rho=\Xi=2, \nu=12, \lambda=1, E=6$, and for 2D graph $t=0.5,\ 1,\ 1.5$

7.6. Concluding Remark

In this script, we have invented an integral technique to solve fractional nonlinear differential models. To test validity of the procedure, we have solved three nonlinear fractional models as the s-tFETL (Fig-7.1 to Fig-7.3); the tfcSE, (Figs.-7.4 to Fig-7.7) and the s-tM-fSH (Fig-7.8 to Fig-7.13) models. As an effect, periodic envelope, exponentially changeable soliton envelope, rational, combo periodic-soliton and combo rational-soliton solutions are formally derived of the models. The achieved results emphasized the power of the proposed technique are dreadfully effective, concise and robust mathematical tools than the Generalized Kudryashov and the Modified Kudryashov methods for solving other fractional nonlinear models.

Chapter-8

Conclusions

We have successfully used Hirota bilinear method to derive exact multi-soliton solutions of the first and second negative order integrable Burgers, the KdV-5, the extended Sawada-Kotera equation and the extended Lax equations in Chapter two. Complex conjugates of parameters have settled to get distinguish dynamical interactions solutions from the multi-soliton solutions of the nonlinear models. By picking particular parametric values, we have shown different dynamical features of the multi soliton solutions. As a result, we obtained rogue type breather waves, breather line waves, periodic rogue type soliton and bell-shaped line soliton, breather line solitons with bell waves provides breather waves, a pair of X-shaped periodic rogue type solitons and a pair of breather type line solitons and cnoidal wave.

In chapter three, we used the famous unified method to solve fractional differential equation and applied it to derive exact solutions of the space-time fractional nonlinear differential equations for pulse narrowing transmission lines model. Here we find the actual direction of the voltage of the pulse $\Theta(x,t)$ for the change of inductance per unit length (L). So this method is more effective and can also be applied to other fractional differential equations.

The space-time fractional EW and WBBM equation has successfully integrated via Jacobi elliptic function expansion technique with modified Riemann-Liouville derivatives in chapter four. At the end of the procedure, three types of solutions are achieved namely, Jacobi elliptic, hyperbolic and trigonometric function with unknown parameters, which indicates that Jacobi elliptic expansion technique are very fruitful as well as appropriate to find the exact solutions of nonlinear fractional models.

We have effectively applied a mathematical apparatus named the generalized Kudryashov method to find the exact wave solutions to the considered Schrodinger and biological population models in chapter five. The derived solitary wave solutions are expressed in an exponential form. The gained solutions will give out as an awfully in the study a crystal wave and quantum wave phenomena. The determined characteristics of the solutions are bright bell, dark bell, kink solitary wave, M- shape solitary wave, W- shape solitary wave.

The modified simple equation method is applied on the complex time fractional Schrodinger equation and the space-time fractional differential equation which govern wave propagation in low-pass electrical transmission lines equation to construct solitary wave solutions in chapter six. We have retrieved rational exponential function solutions of the fractional order models including some arbitrary parameters.

Lastly in chapter seven, we have invented an integral technique as IKM to solve fractional nonlinear differential models. To test validity of the procedure, we have applied it on three nonlinear fractional models such as the s-tFETL; the tfcSE and the s-tM-fSH models. As an effect, periodic envelope, exponentially changeable soliton envelope, rational, combo periodic-soliton and combo rational-soliton solutions are formally derived of the models. The achieved results emphasized the power of the proposed technique are dreadfully effective, concise and robust mathematical tools than the Generalized Kudryashov and the Modified Kudryashov methods for solving other fractional nonlinear models.

In addition, graphical illustration of the solutions has plotted with unknown parameters in each chapter. Researchers can undoubtedly use the above techniques to analyze the internal mechanism of nonlinear fractional evolution systems in mathematical physics and engineering.

References

1. A. Biswas, Soliton solutions of the perturbed resonant nonlinear schrodingers equation with full nonlinearity by semi-inverse variational principle. Quant. Phys. Lett. 1, 79–83, 2012.
2. M. A. Khater, A. R. Seadawy and D Lu, New optical soliton solutions for nonlinear complex fractional Schrödinger equation via new auxiliary equation method and novel (G'/G)-expansion method. Pramana J. Phys. 90(5), 59, 2018.
3. M. N. Alam and A. Li, New solitons to the nonlinear complex fractional Schrodinger equation and the conformable time-fractional Klein-Gordon equation with quadratic and cubic nonlinearity. Phys. Scr. 95, 045224, 2020.
4. A. Biswas and D. Milovic, Optical solitons in 1 + 2 dimensions with time-dependent dispersion, nonlinearity and attenuation in a Kerr-law media. J. Electromagn. Waves Appl. 22:1801– 1808, 2008.
5. Q. Zhou and Q. Zhu, Optical solitons in medium with parabolic law nonlinearity and higher order dispersion. Waves Rand. Complex Media. 25:52–59, 2015.
6. Q. Zhou, L. Liu, H Zhang, M. Mirzazadeh, A Bhrawy, E Zerrad and S Moshokoa, A Biswas, Dark and singular optical solitons with competing nonlocal nonlinearities. Opt. Appl. 46, 79-86, 2016.
7. Z. Dahmani, M. M Mesmoudi and R. Bebbouchi, The foam drainage equation with time and spacefractional derivatives solved by the Adomain method. Elect. J. Qual. Theory Diff. Equ. 31, 1-10, 2008
8. A. R. Seadawy, D. Lu and M. M. A. Khater, New wave solutions for the fractional order biological population model, time fractional Burgers, Drinfeld-Sokolov-Wilson and

system of shallow water wave equations and their applications. Euro. J. Comput. Mech. 26, 5-6, 2017.

9. D. L. Sekulic, M. V. Sataric, M. B. Zibanov and J. S. Bajic, Soliton-like pulses along electrical nonlinear transmission line. Electron Electr. Eng. 5, 121, 2012.

10. E. Afshari and A. Hajimiri, Nonlinear transmission lines for pulse shaping in Silicon. IEEE J Solid State Circuits. 40: 744–752, 2005.

11. M. A. Abdoua and A. A. Soliman, New exact travelling wave solutions for space-time fractional nonlinear equations describing nonlinear transmission lines. Result in Phy. 9, 1497-1501, 2018.

12. S. Abdoulkary, T. Beda, O. Dafounamassou, E. W. Tafo and A. Mohamadou, Dynamics of solitary pulses in the nonlinear low-pass electrical transmission lines through the auxiliary equation method. J. Mod. Phys. Appl. 2, 69-87, 2013.

13. D. S. Ricketts, X. Li and D. Ham, Electrical soliton oscillator IEEE transactions on microwave theory and techniques. IEEE Microwave Theory Tech. Sos. 54, 373-382, 2006.

14. A. Patra, On comparison of two reliable techniques for the Riesz fractional complex ginzburg-landau-schrodinger equation in modelling superconductivity. Prog Fractional Differ Appl. 5, 125-141, 2019.

15. M. Salinas, R. Salas, D. Mellado, A. Graria and C. Saavedra, A computational fractional signal derivative method. Modelling and Simulation in Engineering. Article Id- 7280306, 2018.

16. R. L. Magin, Fractional calculus models of complex dynamics in Biological tissues. Comput. Math. Appl. 59, 1586-1593, 2010.

17. F. A. A. El-Salam, Fractional approach of Maxwell equation s in curved space time. J Taibah Uni. Sci. 7, 173-179, 2013.

18. S. Zhou. H, li and Z. Zhu, Chaos control and synchronization in a fractional neuron network system. Chaos Solitons & Fractals. 36, 973-984, 2008

19. M. A. Abdou, An analytical method for space-time fractional nonlinear differential equations arising in plasma physics. Journal of Ocean Engineering and Sciences. 2(4), 288-292, 2017.

20. M. Mirzazadeh, M. Eslami and A. Biswas, Solitons and periodic solutions to a couple of fractional nonlinear evolution equations. Pramana J. Phys. 82, 465-476, 2014.

21. A. M. Wazwaz, The tanh method for generalized forms of nonlinear heat conduction and Burgers–Fisher equations. Appl. Math. Comput. 169, 321-338, 2005.

22. A. M. Wazwaz, The sine-cosine method for obtaining solutions with compact and non compact structures. Applied Mathematics and Computation. 159 (2), 559-576, 2004.

23. M. R. Fedele, G. Miele, L. Palumbo and V. G. Vaccaro, Thermal wave model for nonlinear longitudinal dynamics in particle accelerators. Phys. Lett. A. 179, 407, 1993.

24. A.M. Wazwaz, Multiple-soliton solutions for the KP equation by Hirota's bilinear method and by the tanh-coth method. Appl. Math. Comput. 190, 633–640, 2007.

25. L. L. Feng and T.T. Zhang, Breather wave, rogue wave and solitary wave solutions of a coupled nonlinear Schrodinger equation. Appl. Math. Lett. 78, 133-140, 2018.

26. M. S. Osmana, A. Korkmazc, H. Rezazadeh, M. Mirzazadeh, M. Eslami and Q. Zhou, The unified method for conformable time fractional schrodinger equation with perturbation terms. Chinese J. Phys. 56, 2500-2506, 2018.

27. S. K. Liu, Z. T. Fu and S. D. Liu, Jacobi elliptic function expansion method and periodic wave solutions of nonlinear wave equations. Physical Letters A. 289, 69-74, 2001.

28. A.A Gaber, A. F. Alijohani, A. Ebaid and J. T. Machado, The generalized Kudryshov method for nonlinear space-time fractional differential equations of Burgers type. Nonlinear Dynamics. 95, 361-368, 2019.

29. S. T. Demiray, Y. Pandir, and H. Bulut, Generalized Kudryashov Method for Time-Fractional Differential Equations. Abstract and Applied Analysis. Article Id- 901540, 13, 2014.

30. H. O. Roshid, Novel solitary wave solution in shallow water and ion acoustic plasma waves in-terms of two nonlinear models via MSE method. Journal of Ocean Engineering and Science. 2 (3), 196-202, 2017.

31. J. M. Jawad, A. M. D. Petkovic, and A. Biswas, Modified simple equation method for nonlinear evolution equations. Appl Math. Comput. 217, 869-77, 2010.

32. H.A. Zedan, E. Alaidarous and S. Shapll, Erratum to: Exact solutions for a perturbed nonlinear Shrödinger equation by using Bäcklund transformations. Nonlinear Dyn. 74(4) 1153-1153, 2013.

33. A. M. Wazwaz, The tanh method for generalized forms of nonlinear heat conduction and Burgers–Fisher equations. Appl. Math. Comput. 169, 321-338, 2005.

34. M. F. Hoque and H. O. Roshid, Optical soliton solutions of the Biswas-Arshed model by the $\tan(\Theta/2)$-expansion approach. Phys. Scr. 95 (7), 075219, 2020.

35. H. O. Roshid and W. X. Ma, Dynamics of mixed lump-solitary waves of an extended $(2+1)$-dimensional shallow water wave model. Physics Letters A. 382(45), 3262-3268, 2018.

36. M. B. Hossen, H. O. Roshid and M. Z. Ali, Characteristics of the solitary waves and rogue waves with interaction phenomena in a (2+ 1)-dimensional Breaking Soliton equation. Phys. Lett. A. 382, 1268-1274, 2018.

37. Sirendaoreji and J.Sun, Auxiliary equation method for solving nonlinear partial differential equations. Phys. Letter. A. 309, 387-396, 2003.

38. M.L. Wang, Exact solutions for a compound KdV-Burgers equation. Phys. Letter A. 213, 279-287, 1996.

39. Zhenya Yan, Abundant families of Jacobi elliptic function solutions of the (G'/G)-dimensional integrable Davey-Stewartson- type equation via a new method. Chaos, Solitons and Fractals. 18(2), 299-309, 2003.

40. H. O. Roshid, M.N. Alam, M.F. Hoque and M.A. Akbar, A new extended (G'/G)-expansion method to find exact traveling wave solutions of nonlinear evolution equations. Mathematics and Statistics. 1(3), 162-166, 2013.

41. M B. Hossen, H. O. Roshid and M. Z. Ali, Modified double sub-equation method for finding complexiton solutions to the (2+1) dimensional nonlinear evolution equations. Int. J. Appl. Comput. Math. 3 (1), 679-697, 2017.

42. M. Safari, D. D. Ganji, and M. Moslemi, Application of He's variational iteration method and Adomian's decomposition method to the fractional KdV-Burgers-KURamoto equation. Computers & Mathematics with Applications. 58, 2091–2097, 2009.

43. M. A. Jafari and A. Aminataei, Improvement of homotopy perturbation method for solving nonlinear diffusion equation. Physica scripta. 82, 015002, 2002.

44. C.B. Wen and B. Zheng, A new fractional sub-equation method for fractional partial differential equations. WSEAS Trans. Math. 12, 564-571, 2013.

45. A.M. Wazwaz, Construction of a hierarchyof negative-order integrable Burgers equations of higher order. Math.Meth. Appl.Sci. 2018, 1-8. Doi no-10.1002/mma.5453.

46. A. M. Wazwaz, A fifth-order Korteweg-deVries equation for shallow water with surface tension: Multiple soliton solution. Acta. Physica Polonica-A. 130,679-682, 2019.

47. K. Hosseini and J. Ayati, Exact solutions of space-time fractional EW and modified EW equations using Kudrayshov method. Nonlinear Sci. Lett. 7(2), 58-66, 2016.

48. .A.M. Wazwaz, Exact soliton and kink solutions for new (3+1)-dimensional nonlinear modified equations of wave propagation. DE GRUYTER, open Eng. 7, 169-174, 2017.

49. T. Benjamin, J. Bona and J. Mohony, Model equations for long waves in nonlinear dispersive system. Phil. Trans. R. Soc, London, Ser-A. 272, 47-78, 1972.

50. N. Laskin, Fractional Schrodinger equation. Phys. Rev. E. 66 (5), 056108, 2002.

51. T. A. Sulaiman, H. Bulut and S. S. Atas, Optical solitons to the fractional Schrödinger-Hirota equation. Appl. Math. Nonl. Sci. 4(2), 535-542, 2019.

52. H. Bateman, Some recent researches on the motion of fluids. Mon Wea Rev. 43(4), 163-170, 1915.

53. G. Jumarie, The Modified Riemann-Liouville derivative and fractional Taylor series of non-differentiable functions further results. Comput. Math. Appl. 51, 1367-1376, 2006.

54. G. Jumarie, Table of some basic fractional calculus formula derived from a modified Riemann-Liiouville derivative for non differentiable function. Appl. Math. Lett. 22, 378-85, 2009.

55. A. R. Seadwya, K, K Ali and R. I Nuruddeene, A variety of soliton solutions for the fractional Wazwaz-Benjamin-Bona-Mahony. Result in Phy. 12, 2234-2241, 2019.

56. S. Zhang and H. Q. Zhang, Fractional sub-equation method and its applications to nonlinear fractional PDEs. Physics Letters A. 375(7), 1069-1073, 2011.

57. K. Hosseini, M. Mirzazadeh, M. Ilie and J. F. Gomez-Aguilar, Biswas-Arshed equation with the beta time derivative: Optical solitons and other solutions, 2020, 217, 164801.

58. A. Atangana and R. T. Alqahtani, Modelling the Spread of River Blindness Disease via the Caputo Fractional Derivative and the Beta-derivative, Entropy. 2016, 18, 40.

59. A. Bekir, O. Guner, and A. C. Cevikel, Fractional complex transform and exp-function methods for fractional differential equations. In M. Bayram (Ed.), Abstract and applied analysis (Vol. 2013, 1–8, 2013). Hindawi Publishing Corporation.

60. B. Lu, Backlund transformation of fractional Riccati equation and its applications to nonlinear fractional partial differential equations. Physics Letters A. 376, 2045–2048, 2012.

61. J. Belmonte-Beitia and G. F. Calvo, Exact solutions for the quintic nonlinear Schrödinger equation with time and space modulated nonlinearities and potentials. Phys. Lett. A. 373, 448, 2009.

62. F. Dalfovo, S. Giorgini, L. P. Pitaevskii and S. Stringari, Theory of Bose Einstein condensation in trapped gases. Rev. Mod. Phys. 71, 463, 1999.

63. E. M. E. Zayed and K. A. E. Alurrfi, A new Jacobi function expansion method for solving a nonlinear PDE describing the nonlinear low-pass electrical lines. Chaos, Solitons & Fractals. 78, 148-155, 2015.

64. D. Kumar, A. R. Seadawy and M. R. Haque, Multiple soliton solutions of the nonlinear partial differential equations describing the wave propagation in nonlinear low-pass electrical transmission lines. Chaos, Solitons & Fractals. 115, 62-76, 2018.

65. J.V.D.C. Sousa and E.C. de Oliveira, A New truncated M-fractional derivative type unifying some fractional derivative types with classical properties. Int. J. Anal. Appl. 16(1), 83-96, 2018.

66. I. Bernstein, E. Zerrad, Q. Zhou, A. Biswas and N. Melikechi, Dispersive optical solitons with Schrodinger-Hirota equation by traveling wave hypothesis. Opto electron, Adv. Mater. Rapid Commun. 9(5-6), 792-797, 2015.

67. I. Bernstein, N. Melikechi, E. Zerrad, A. Biswas and M. Belic, Dispersive optical solitons with Schrodinger-Hirota equation using undetermined coefficients. J. Comput. Theor. Nanosci. 13(8),5288-5293, 2016.

68. M. S. Ullah, H. O. Roshid, M. Z. Ali and Z. Rahman, Novel exact solitary wave solutions for the time fractional generalized Hirota-Satsuma coupled KdV model through the generalized Kudrashov method. Contemporary Mathematics. 1(1), 25-32, 2019

69. Z. Rahman, M. Z.Ali and H. O. Roshid, Closed form soliton solutions of three nonlinear fractional models through a proposed Improved Kudryashov method. Chin.Phys.B, 2021, Vol. 30(5):050202. DOI:10.1088/1674-1056/abd165).

70. Z. Rahman, M. Z. Ali, H. O. Roshid, M. S. Ullah and X. Y. Wen, Dynamical structures of interaction wave solutions for the two extended higher-order KdV equations. *Pramana,* volume 95, Article number: 134 (2021). https://doi.org/10.1007/s12043-021-02155-4.

71. Z. Rahman, M. Z. Ali, H. O. Roshid and M. S. Ullah, Analytical solutions of two space-time fractional nonlinear models using Jacobi elliptic expansion function method. Contemporary Mathematics, Volume 2 Issue 3 (2021), 173-245. **DOI:** https://doi.org/10.37256/cm.232021682.

72. Z. Rahman, H. O. Roshid and M. Z. Ali, New exact solitary wave solutions for two non-linear time fractional evolution equations via the MSE method. (Completed).

73. Z. Rahman, M. Z. Ali and H. O. Roshid , New exact solitary wave solutions for Couple of model through the generalized Kudryshov method. (Completed).

74. Z. Rahman, M. Z. Ali and H. O. Roshid, Analysis the Dynamical structures of fifth order Korteweg-de-Vries (KdV-5) equation. (Completed).

Closed form soliton solutions of three nonlinear fractional models through proposed improved Kudryashov method

Zillur Rahman, M Zulfikar Ali, Harun-Or Roshid

Citation:Chin. Phys. B, 2021, 30 (5): 050202. DOI: 10.1088/1674-1056/abd165
Journal homepage: http://cpb.iphy.ac.cn; http://iopscience.iop.org/cpb

Closed form soliton solutions of three nonlinear fractional models through proposed improved Kudryashov method

Zillur Rahman[1,2], M Zulfikar Ali[2], and Harun-Or Roshid[3,†]

[1] Department of Mathematics, Comilla University, Cumilla-3506, Bangladesh
[2] Department of Mathematics, Rajshahi University, Rajshahi-6205, Bangladesh
[3] Department of Mathematics, Pabna University of Science and Technology, Pabna-6600, Bangladesh

(Received 6 October 2020; revised manuscript received 28 November 2020; accepted manuscript online 8 December 2020)

We introduce a new integral scheme namely improved Kudryashov method for solving any nonlinear fractional differential model. Specifically, we apply the approach to the nonlinear space–time fractional model leading the wave to spread in electrical transmission lines (s-tfETL), the time fractional complex Schrödinger (tfcS), and the space–time M-fractional Schrödinger–Hirota (s-tM-fSH) models to verify the effectiveness of the proposed approach. The implementing of the introduced new technique based on the models provides us with periodic envelope, exponentially changeable soliton envelope, rational rogue wave, periodic rogue wave, combo periodic-soliton, and combo rational-soliton solutions, which are much interesting phenomena in nonlinear sciences. Thus the results disclose that the proposed technique is very effective and straight-forward, and such solutions of the models are much more fruitful than those from the generalized Kudryashov and the modified Kudryashov methods.

Keywords: improved Kudryashov method, fractional electrical transmission line equation, fractional nonlinear complex Schrödinger equation, M-fractional Schrödinger–Hirota (s-tM-fSH)

PACS: 02.30.Jr, 02.30.Ik, 04.20.Jb, 05.45.Yv **DOI:** 10.1088/1674-1056/abd165

1. Introduction

The accurate modeling of nonlinear phenomena related to natural happening is really impossible without fractional derivatives. Nowadays, the fractional calculus has been frequently used to model the nonlinear systems in various fields such as neuron networks,[1] dust acoustic and dense electron–positron–ion wave,[2] plasma physics,[3] quantum mechanics,[4] nonlinear optical fiber communication,[5] superconductivity and Bose–Einstein condensates,[6] electrics signal processing,[7] biological dynamics,[8] water wave dynamics,[9] electro–magnetic waves,[10] nonlinear electric-transmission line,[11] and many other areas. Various types of exact solutions including periodic wave and solitons are essential to realize intrinsic dynamical structure of such models even universe. Up to now, huge improvements have been achieved in the development of techniques to evaluate such exact solutions of the nonlinear models. Several powerful methods are as follows. The $\exp(-\Phi(\eta))$-expansion,[12] Hirota bilinear,[13] Bäklund transformations,[14] modified simple equation,[15] tanh method,[16] $\tan(\Theta/2)$-expansion,[17] soliton ansatz,[18,19] auxiliary equation,[20] sine-cosine,[21] homogeneous balance,[22] Jacobi elliptic function expansion,[23] (G'/G)-expansion,[23,24] modified double sub-equation,[25] exp-function,[26] generalized Kudryashov[26] methods, and many others. It should be pointed out that all the mentioned approaches have some advantages and also a few disadvantages to integrate complex nonlinear systems. As is well known, no approach is suitable for all equations. Thus, we are willing to propose a new and active approach namely improved Kudryashov method (IKM) on the basis of the generalized Kudryashov method[26] by changing its auxiliary equations.

Now, we come to shed light on the nonlinear space–time fractional electrical transmission lines (s-tfETL),[11,27] the time fractional complex Schrödinger (tcFSE),[28] and space–time M-fractional Schrödinger–Hirota (s-tM-fSH)[29] models via the proposed IKM. These models have been widely studied in many aspects for the non-fractional differential case. Abdou and Soliman[11] only solved the fractional transmission line equation thru the generalized $\exp(-\varphi(\xi))$-expansion and generalized Kudryashov methods. But non-fractional transmission line equation has been studied by Zayed and Alurrfi[30] thru using new Jacobi function expansion method, by Kumar *et al.*[31] thru using three schemes as modified Kudryashaov, Sine–Gordon-, and extended Sinh–Gordon-expansion methods, and by Shahoot *et al.*[32] thru using the (G'/G)-expansion scheme. Besides, the time fractional complex Schrödinger equation (FSE) is a vital nonlinear model in solitonic field. The model describes the collision of the adjacent particles of identical mass on a lattice structure through a crystal and demonstrate the fundamental properties of string dynamics with fixed curvature space.[13] This model was first

†Corresponding author. E-mail: harunorroshidmd@gmail.com

developed by Laskin[33] which occurs in many important areas as water wave, fluid dynamics, bio-chemistry, optical pulses propagation into nonlinear fiber, and plasma physics. Few researchers made much more effort to investigate the complex fractional Schrödinger model: Khater[34] studied it by a supplementary equation as well as (G'/G)-schemes, Alam and Li[28] presented wave solutions through modified (G'/G)-expansion technique. In recent years, Sousa and Oliveira invented an M-fractional order derivative.[35] So, we also considered another model namely the space–time truncated M-fractional Schrödinger–Hirota model[29] which frequently arises in quantum Hall effect, optical fibers, heat pulses in solids, and more areas. Sulaiman *et al.*[29] investigated the M-fractional SH model to present optical soliton solutions with the help of a sinh-Gordon technique. But non-fractional SHE is investigated.[36,37]

This research is intended to execute the improved Kudryashov technique to determine abundant exact solitonic solutions as periodic envelope, exponentially changeable soliton envelope, rational, combo periodic-soliton, and combo rational-solitonic solutions of the s-tfETL,[11,27] the tfcSE,[28] and the s-tM-fSH[29] models, which take an essential part in nonlinear complex phenomena of physical sciences.

2. Conformable M-fractional and fractional derivatives with properties

The new M-fractional derivatives are given below.[35]

Let $\wp: [0,\infty) \to \Re$, then M-fractional derivative $\wp$ with order α can be written as follows:

$$ {}_iD_{\mathrm{M}}^{\alpha,\beta}\{(\wp)(t)\} = \lim_{\varepsilon\to 0}\frac{\wp\left(t_i E_\beta(\varepsilon t^{1-\gamma})\right)-\wp(t)}{\varepsilon}, \quad \forall t>0,\ 0<\alpha<1,\ \beta>0, $$

where E_β is a truncated Mittag–Leffler function.[35]

2.1. Properties of new M-fractional derivatives

When $t>0$, $0<\alpha<1$, $\beta>0$, $m,n\in\Re$, Ψ and Ω are α-differentiable, then

(i) ${}_iD_{\mathrm{M}}^{\alpha,\beta}\{(m\Psi+n\Omega)(t)\} = m_iD_{\mathrm{M}}^{\alpha,\beta}\Psi(t)+n_iD_{\mathrm{M}}^{\alpha,\beta}\Omega(t)$, $\forall m,n\in\Re$.

(ii) ${}_iD_{\mathrm{M}}^{\alpha,\beta}(\Psi\cdot\Omega)(t) = \Psi(t)_iD_{\mathrm{M}}^{\alpha,\beta}\Omega(t)+\Omega(t)_iD_{\mathrm{M}}^{\alpha,\beta}\Psi(t)$, $\forall\beta\in\Re$,

(iii) ${}_iD_{\mathrm{M}}^{\alpha,\beta}(\Psi/\Omega)(t) = \left\{\Omega(t)_iD_{\mathrm{M}}^{\alpha,\beta}\Psi(t)-\Psi(t)_iD_{\mathrm{M}}^{\alpha,\beta}\Omega(t)\right\}/\{\Omega(t)\}^2$.

(iv) ${}_iD_{\mathrm{M}}^{\alpha,\beta}(c)=0$, where $\Psi(t)=c$ is a constant.

(v) (Chain rule) If is differentiable, then ${}_iD_{\mathrm{M}}^{\alpha,\beta}\Psi(t) = \dfrac{t^{1-\alpha}}{\Gamma(1+\beta)}\dfrac{\mathrm{d}\Psi(t)}{\mathrm{d}t}$.

If a function defined by $\varphi:(0,\infty)\to\Re$, the conformable fractional derivative with order υ is defined[38] as

$$ \frac{\partial^\upsilon\varphi}{\partial t^\upsilon} = \lim_{\varepsilon\to 0^+}\frac{\varphi(t+\varepsilon t^{1-\upsilon})-\varphi(t)}{\varepsilon},\quad t>0,\ 0<\upsilon\le 1. $$

2.2. Properties of conformable fractional derivative

(I) $\dfrac{\partial^\upsilon}{\partial t^\upsilon}(m\Psi+n\Omega) = m\dfrac{\partial^\upsilon}{\partial t^\upsilon}(\Psi)+n\dfrac{\partial^\upsilon}{\partial t^\upsilon}(\Omega)$, $\forall m,n\in\Re$.

(II) $\dfrac{\partial^\upsilon}{\partial t^\upsilon}(t^\tau) = \tau t^{\tau-\upsilon}$, $\forall\beta\in\Re$ and $\dfrac{\partial^\upsilon}{\partial t^\upsilon}(\nu)=0$, $\nu=$ const.

(III) $\dfrac{\partial^\upsilon}{\partial t^\upsilon}(\Psi\circ\Omega)(t) = t^{1-\upsilon}\Psi'(\Omega(t))\Omega'(t)$.

3. Algorithm of proposed method

The fundamental phases of the technique are as follows.

Step 1 At first, let the subsequent fractional equation with the variables x and t be

$$ N\left(\Upsilon, D_t^\eta\Upsilon, D_x^\alpha\Upsilon, D_t^{2\eta}\Upsilon, D_x^{2\alpha}\Upsilon,\ldots\right)=0, \tag{1} $$

where the function $\Upsilon=\Upsilon(x,t)$ is an unknown wave surface, and N is a function of $\Upsilon(x,t)$ and its highest order fractional derivatives.

Step 2 For complex nonlinear model, take the transformation $\Upsilon(x,t)=\Upsilon(\zeta)\exp(\mathrm{i}\tau)$ with travelling wave variables for space–time fractional model

$$ \zeta = \mathrm{i}k\left(\frac{x^\alpha}{\Gamma(1+\alpha)}+\frac{gt^\eta}{\Gamma(1+\eta)}\right),\quad \tau = \left(\frac{gx^\alpha}{\Gamma(1+\alpha)}+\frac{ht^\eta}{\Gamma(1+\eta)}\right), \tag{2} $$

and for no complex model, adopt the transformation $\Upsilon(x,t)=\Upsilon(\zeta)$ and travelling wave variable for space–time fractional model

$$ \zeta = \frac{k_1}{\Gamma(1+\eta)}t^\eta+\frac{k_2}{\Gamma(1+\alpha)}x^\alpha. \tag{3} $$

Substituting the above Eq. (2) or Eq. (3) into Eq. (1), the resulting equation is reduced to an ordinary differential equation (ODE) with the help of fractional complex transformation producing

$$ \frac{\partial^\eta}{\partial t^\eta} = -\sigma\frac{\partial}{\partial\zeta},\quad \frac{\partial}{\partial x} = \frac{\partial}{\partial\zeta},\quad \frac{\partial^{2\eta}}{\partial t^{2\eta}} = \sigma^2\frac{\partial^{2\eta}}{\partial\zeta^{2\eta}},\ldots, \tag{4} $$

then equation (1) turned into the following form,

$$ \chi(\Upsilon,\Upsilon',\Upsilon'',\ldots)=0. \tag{5} $$

The prime of Υ indicates the usual meaning of derivative.

Step 3 Picking a trial solution for Eq. (5), that is,

$$ \Upsilon(\zeta) = \frac{\sum_{i=0}^{n}\ell_i\varphi^i(\zeta)}{\sum_{j=0}^{m}\wp_j\varphi^j(\zeta)}, \tag{6} $$

where ℓ_i and $\wp_j$ are the real fixed values, and $n > 0$ and $m > 0$ are integers with the restraint $\ell_n, \wp_m \neq 0$.

Here, we just need to take a different auxiliary equation which is satisfied by $\varphi(\zeta)$ and expressed as

$$\varphi'(\zeta) = k - \varphi^2(\zeta), \tag{7}$$

where k is an arbitrary constant. Some special solutions of the Riccati equation, *i.e.*, Eq. (7), are given by

$$\varphi(\zeta) = \begin{cases} \sqrt{k}\tanh(\sqrt{k}\zeta), & k > 0; \\ \sqrt{k}\coth(\sqrt{k}\zeta), & k > 0; \\ 1/\zeta, & k = 0; \\ -\sqrt{-k}\tan(\sqrt{-k}\zeta), & k < 0; \\ \sqrt{-k}\cot(\sqrt{-k}\zeta), & k < 0. \end{cases} \tag{8}$$

Step 4 Combining Eqs. (5), (6), and (7) through computational software, we can get polynomial in $\varphi(\zeta)$. Taking each of coefficients of $\varphi^{\kappa}(\zeta)(\kappa = 0,1,2,3\ldots)$ to be zero and thus some equations are formed in-terms of unknown constants ℓ_κ and $\wp_\kappa$. Solving these unknown constants then putting them into a trial solution together with the solutions Eq. (8), the exact solution of Eq. (1) is obtained.

Remark 1 It is noted that the auxiliary equation in the generalized Kudryashov[11,26] and the modified Kudryashov schemes[31] each are capable to provide only one solution in terms of exponential function. Consequently, the auxiliary Eq. (7) in the proposed IK scheme degenerates five different solutions involving hyperbolic, rational, and trigonometric functions. In the concluding remark, we can say that the introduced scheme will be more useful than the other exiting schemes for different types of solutions.[26,31]

Remark 2 The proposed technique is easier as it takes less calculations than the modified (G'/G)-expansion technique.[28] It is noticed that the modified (G'/G)-expansion method takes double auxiliary equations while we consider only Riccati equation as an auxiliary equation.

4. Applications

4.1. Spatiotemporal fractional electrical transmission line equation (s-tfETLE)

General form of s-tfETLE can be written as follows:[11]

$$\frac{\partial^{2\beta}\varphi}{\partial t^2} - \nu\frac{\partial^{2\beta}}{\partial t^2}(\varphi)^2 + B\frac{\partial^{2\beta}}{\partial t^2}(\varphi)^3 - A^2\frac{\partial^{2\beta}\varphi}{\partial x^2} - \frac{A^4}{12}\frac{\partial^{4\beta}\varphi}{\partial x^4} = 0, \quad 0 < \beta < 1. \tag{9}$$

The s-tfETL equation (9) is one of the important equations in fractional electrical physics. The equation describes data communication and is modified in a telecommunication system.

Considering $\varphi(x,t) = \phi(\zeta)$ and

$$\zeta = \frac{k_1}{\Gamma(1+\beta)}t^\beta + \frac{k_2}{\Gamma(1+\beta)}x^\beta,$$

this nonlinear s-tfETL partial evolution model can be converted into a nonlinear integer order ordinary differential ETL as follows:

$$(k_1^2 - A^2k_2^2)\phi(\zeta) - k_1^2\nu\phi^2(\zeta) + Bk_1^2\phi^3(\zeta) - \frac{A^4k_2^4\beta^2}{12\{\Gamma(1+\beta)\}^2}\phi''(\zeta) = 0. \tag{10}$$

As is well known, the delicate balance between the height derivative and height nonlinear terms gives $n = m + 1$. Consider a trial solution Eq. (6) in the following form ($m = 1, \Rightarrow n = 2$):

$$\phi(\zeta) = \frac{\ell_0 + \ell_1\phi(\zeta) + \ell_2\phi^2(\zeta)}{\wp_0 + \wp_1\phi(\zeta)}, \tag{11}$$

where the auxiliary equation is used

$$\phi'(\zeta) = k - \phi^2(\zeta).$$

Inserting Eq. (11) with Eq. (7) into the reduced nonlinear ordinary differential Eq. (10), we have a polynomial of $\phi^i, (i = 0,1,2,\ldots)$. All the adjacent terms of ϕ^i are equal to zero, and form some equations in terms of unknown constants $\ell_0, \ell_1, \ell_2, \wp_0, \wp_1, k_1$, and k_2. Solving the equations via Maple software, we obtain the five sets of solutions for $L = \Gamma(1+\beta)$.

Set 1 $\ell_0 = \frac{\nu\wp_1\sqrt{-k}}{3\sqrt{2}B}, \ell_1 = \frac{\nu\wp_1}{3B}, \ell_2 = \frac{\nu\wp_1}{3B\sqrt{-2k}}, \wp_0 = 0,$ $k_1 = \frac{3\nu L\sqrt{-3B}}{(9B-2\nu^2)\beta\sqrt{k}}, k_2 = \frac{\sqrt{3}\nu L}{\beta A\sqrt{2k\nu^2 - 9Bk}}$ and $\wp_1$ is const.

Set 2 $\ell_0 = \frac{\nu\wp_1\sqrt{k}}{6B}, \ell_1 = \frac{\nu\wp_1}{3B}, \ell_2 = \frac{\nu\wp_1}{6B\sqrt{k}}, \wp_0 = 0,$ $k_1 = \frac{3\nu L\sqrt{3B}}{(9B-2\nu^2)\beta\sqrt{2k}}, k_2 = \frac{\sqrt{3}\nu L}{\beta A\sqrt{18Bk - 4k\nu^2}}$ and $\wp_1$ is const.

Set 3 $\ell_0 = \frac{\nu\wp_0}{3B}, \ell_1 = \frac{(3Bk\ell_2 + \nu\wp_0)}{3B\sqrt{k}}, \wp_1 = \frac{3B\ell_2\sqrt{k}}{\nu},$ $k_1 = \frac{3\nu L\sqrt{6B}}{(9B-2\nu^2)\beta\sqrt{k}}, k_2 = \frac{\sqrt{6}\nu L}{\beta A\sqrt{9Bk - 2k\nu^2}}$, ℓ_2 and $\wp_0$ are const.

Set 4 $\ell_0 = -k\ell_2, \ell_1 = 0, \wp_0 = -\frac{2\ell_2\nu(A^2\beta^2k_2^2k + 3L^2)}{3\beta^2A^2k_2^2},$ $\wp_1 = \frac{\ell_2\sqrt{2A^2B\beta^2k_2^2k + 6BL^2}}{\beta Ak_2}, k_1 = \frac{k_2A\sqrt{A^2\beta^2k_2^2k + 3L^2}}{\sqrt{3}L}$ and $\ell_2, \wp_2$ are const.

The general solutions of s-tfETL equations for solution **Set 1** are

$$\varphi_{11} = \frac{-\nu + \nu\sqrt{-2}\tanh(\sqrt{k}\zeta) + \nu\tanh^2(\sqrt{k}\zeta)}{3B\sqrt{-2}\tanh(\sqrt{k}\zeta)}, \quad k > 0; \tag{12}$$

$$\varphi_{12} = \frac{-\nu + \nu\sqrt{-2}\coth(\sqrt{k}\zeta) + \nu\coth^2(\sqrt{k}\zeta)}{3B\sqrt{-2}\coth(\sqrt{k}\zeta)}, \quad k > 0; \tag{13}$$

$$\varphi_{13} = \frac{-\nu k\zeta^2 + \nu\sqrt{-2k}\zeta + \nu}{3B\sqrt{-2k}\zeta}, \quad k = 0; \tag{14}$$

$$\varphi_{14} = \frac{\nu - \nu\sqrt{2}\tan(\sqrt{-k}\zeta) + \nu\tan^2(\sqrt{-k}\zeta)}{-3B\sqrt{2}\tan(\sqrt{-k}\zeta)}, \quad k<0; \tag{15}$$

$$\varphi_{15} = \frac{\nu + \nu\sqrt{2}\cot(\sqrt{-k}\zeta) + \nu\cot^2(\sqrt{-k}\zeta)}{3B\sqrt{2}\cot(\sqrt{-k}\zeta)}, \quad k<0; \tag{16}$$

where

$$\zeta = \frac{3\nu L\sqrt{-3B}}{(9B-2\nu^2)\beta\sqrt{k}\Gamma(1+\beta)}t^{\beta} + \frac{\nu L\sqrt{3}}{\sqrt{(2k\nu^2-9Bk)}\beta A\Gamma(1+\beta)}x^{\beta}.$$

The general solutions of s-tfETL equations for solution Set 2 are

$$\varphi_{21} = \frac{\nu + 2\nu\tanh(\sqrt{k}\zeta) + \nu\tanh^2(\sqrt{k}\zeta)}{6B\tanh(\sqrt{k}\zeta)}, \quad k>0; \tag{17}$$

$$\varphi_{22} = \frac{\nu + 2\nu\coth(\sqrt{k}\zeta) + \nu\coth^2(\sqrt{k}\zeta)}{6B\coth(\sqrt{k}\zeta)}, \quad k>0; \tag{18}$$

$$\varphi_{23} = \frac{\nu d\zeta^2 + 2\nu\sqrt{k}\zeta + \nu}{6B\sqrt{k}\zeta}, \quad k=0; \tag{19}$$

$$\varphi_{24} = \frac{\nu - 2\nu\sqrt{-1}\tan(\sqrt{-k}\zeta) - \nu\tan^2(\sqrt{-k}\zeta)}{6B\sqrt{-1}\tan(\sqrt{-k}\zeta)}, \quad k<0; \tag{20}$$

$$\varphi_{25} = \frac{\nu - 2\nu\cot(\sqrt{-k}\zeta)\sqrt{-1} - \nu\cot^2(\sqrt{-k}\zeta)}{6B\cot(\sqrt{-k}\zeta)\sqrt{-1}}, \quad k<0; \tag{21}$$

where

$$\zeta = \frac{3\nu L\sqrt{3B}}{(9B-2\nu^2)\beta\sqrt{2k}\Gamma(1+\beta)}t^{\beta} + \frac{\nu L\sqrt{3}}{\sqrt{(18Bk-2k\nu^2)}\beta A\Gamma(1+\beta)}x^{\beta}.$$

The general solutions of s-tfETL equations for solution **Set 3** are

$$\varphi_{31} = \frac{\nu^2\wp_0 + (3B\nu k\ell_2 + \nu\wp_0)\nu\tanh(\sqrt{k}\zeta) + 3B\ell_2\nu k\tanh^2(\sqrt{k}\zeta)}{3B\nu\wp_0 + 9B^2\ell_2 k\tanh(\sqrt{k}\zeta)}, \quad k>0; \tag{22}$$

$$\varphi_{32} = \frac{\nu^2\wp_0 + (3B\nu k\ell_2 + \nu\wp_0)\nu\coth(\sqrt{k}\zeta) + 3B\ell_2\nu k\coth^2(\sqrt{k}\zeta)}{3B\nu\wp_0 + 9B^2\ell_2 k\coth(\sqrt{k}\zeta)}, \quad k>0; \tag{23}$$

$$\varphi_{33} = \frac{\nu^2\wp_0\sqrt{k}\zeta^2 + (3Bk\ell_2 + \nu\wp_0)\nu\zeta + 3B\nu\sqrt{k}\ell_2}{3B\sqrt{k}\zeta(\nu\wp_0\zeta + 3B\ell_2\sqrt{k})}, \quad k=0; \tag{24}$$

$$\varphi_{34} = \frac{\nu^2\wp_0 - (3B\nu k\ell_2 + \nu\wp_0)\nu\sqrt{-1}\tan(\sqrt{-k}\zeta) - 3B\ell_2\nu k\tan^2(\sqrt{-k}\zeta)}{3B\nu\wp_0 - 9B^2\ell_2 k\sqrt{-1}\tan(\sqrt{-k}\zeta)}, \quad k<0; \tag{25}$$

$$\varphi_{35} = \frac{\nu^2\wp_0 + (3B\nu k\ell_2 + \nu\wp_0)\nu\sqrt{-1}\cot(\sqrt{-k}\zeta) - 3B\ell_2\nu k\cot^2(\sqrt{-k}\zeta)}{3B\nu\wp_0 + 9B^2\ell_2 k\sqrt{-1}\cot(\sqrt{-k}\zeta)}, \quad k<0; \tag{26}$$

where

$$\zeta = \frac{3\nu L\sqrt{6B}}{(9B-2\nu^2)\beta\sqrt{k}\Gamma(1+\beta)}t^{\beta} + \frac{\nu L\sqrt{6}}{\beta A\sqrt{9Bk-2k\nu^2}\Gamma(1+\beta)}x^{\beta}.$$

The general solutions of s-tfETL equations for solution **Set 4** are

$$\varphi_{41} = \frac{3\beta^2A^2k_2^2(-k\ell_2 + \ell_2 k\tanh^2(\sqrt{k}\zeta))}{-2\ell_2\nu(A^2\beta^2kk_2^2 + 3L^2) + 3BA\ell_2\sqrt{2A^2B\beta^2kk_2^2 + 6BL^2}k_2\sqrt{k}\tanh(\sqrt{k}\zeta)}, \quad k>0; \tag{27}$$

$$\varphi_{42} = \frac{3\beta^2A^2k_2^2(-k\ell_2 + \ell_2 k\coth^2(\sqrt{k}\zeta))}{-2\ell_2\nu(A^2\beta^2kk_2^2 + 3L^2) + 3BA\ell_2\sqrt{2A^2B\beta^2kk_2^2 + 6BL^2}k_2\sqrt{k}\coth(\sqrt{k}\zeta)}, \quad k>0; \tag{28}$$

$$\varphi_{43} = \frac{3\beta^2A^2k_2^2(-k\ell_2\zeta^2 + \ell_2)}{-2\ell_2\nu(A^2\beta^2kk_2^2 + 3L^2)\zeta^2 + 3BA\ell_2\sqrt{2A^2B\beta^2kk_2^2 + 6BL^2}\zeta)}, \quad k=0; \tag{29}$$

$$\varphi_{44} = \frac{3\beta^2A^2k_2^2(-k\ell_2 - \ell_2 k\tan^2(\sqrt{-k}\zeta))}{-2\ell_2\nu(A^2\beta^2kk_2^2 + 3L^2) - 3BA\ell_2\sqrt{2A^2B\beta^2kk_2^2 + 6BL^2}k_2\sqrt{-k}\tan(\sqrt{-k}\zeta)}, \quad k<0; \tag{30}$$

$$\varphi_{45} = \frac{3\beta^2A^2k_2^2(-k\ell_2 - \ell_2 k\cot^2(\sqrt{-k}\zeta))}{-2\ell_2\nu(A^2\beta^2kk_2^2 + 3L^2) + 3BA\ell_2\sqrt{2A^2B\beta^2kk_2^2 + 6BL^2}k_2\sqrt{-k}\cot(\sqrt{-k}\zeta)}, \quad k<0; \tag{31}$$

where

$$\zeta = \frac{k_2A\sqrt{A^2\beta^2kk_2^2 + 3L^2}}{\sqrt{3}L\Gamma(1+\beta)}t^{\beta} + \frac{k_2}{\Gamma(1+\beta)}x^{\beta}.$$

4.2. Time fractional complex Schrödinger equation (tfcSE)

The section starts with the tfcSE in the form[31,32]

$$\frac{\partial^\gamma \phi}{\partial t^\gamma}+\mathrm{i}\frac{\partial^2\phi}{\partial x^2}+\frac{\partial}{\partial x}(|\phi|^2\phi)=0,\ \ 0<\gamma<1. \tag{32}$$

For the purpose of mathematical conversion, bring the transformations:

$$\begin{aligned}\phi(x,t) &= \varphi(\xi)\exp(\mathrm{i}\tau),\\ \xi &= \mathrm{i}k\left(x+\frac{2g}{\gamma}t^\gamma\right),\\ \tau &= \left(gx+\frac{h}{\gamma}t^\gamma\right),\end{aligned}$$

and it converts this tfcSE to the one without fractional-order nonlinear SE:

$$\begin{aligned}\frac{\partial^\gamma\phi}{\partial t^\gamma} &= \mathrm{i}(h\varphi+2gk\varphi')\exp(\mathrm{i}\tau),\\ \frac{\partial^2\phi}{\partial x^2} &= -(g^2\varphi+2gk\varphi'+k^2\varphi'')\exp(\mathrm{i}\tau),\\ \frac{\partial}{\partial x}(|\phi|^2\phi) &= \mathrm{i}(g\varphi^3+3k\varphi^2\varphi'')\exp(\mathrm{i}\tau).\end{aligned}$$

We obtain the nonlinear complex PSE by using the above expression,

$$(h-g^2)\varphi-k^2\varphi''+g\varphi^3+3k\varphi^2\varphi'=0. \tag{33}$$

Using the rule of homogenous balance of Eq. (33) (φ'' and $\varphi^2\varphi''$) $\Rightarrow n=m+1/2$ and applying another transformation $\varphi(\xi)=u^{1/2}(\xi)$ in Eq. (33), we obtain the ODEs:

$$4gu^3+4(h-g^2)u^2+6ku^2u'+k^2u'^2-2k^2uu''=0. \tag{34}$$

Again using the rule of homogenous balance on Eq. (34) (uu'' and u^2u), we have $n=m+1$. Therefore, the new form of Eq. (6) is given below by using the auxiliary equation $u'(\zeta)=d-u^2(\zeta)$:

$$u(\xi)=\frac{\ell_0+\ell_1u+\ell_2u^2}{\wp_0+\wp_1u}. \tag{35}$$

Inserting Eqs. (40) and (7) into the reduced nonlinear ordinary differential Eq. (39), we have a polynomial of u^i, ($i=0,1,2,\ldots$). All the adjacent terms of u^i are equal to zero, and form some equations in terms of unknown constants g,h,ℓ_0,ℓ_1, and $\wp_1$ and its solutions are as follows:

Set 1 $h=2dk^2$, $g=\mp k\sqrt{d}$, $\ell_0=\pm\frac{1}{2}\wp_0k\sqrt{d}$, $\ell_1=\frac{1}{2}k(\pm\wp_1\sqrt{d}-\wp_0)$, $\ell_2=-\frac{k\wp_1}{2}$.

Set 2 $h=8dk^2$, $g=\mp 2k\sqrt{d}$, $\ell_0=-\frac{1}{2}d\wp_1k$, $\ell_1=\pm k\wp_1\sqrt{d}$, $\ell_2=-\frac{k\wp_1}{2}$, $\wp_0=0$.

For **Set 1**, the solution sets of the considered equation hold: for $d>0$, we have

$$\phi_1=\left[\frac{\pm\wp_0k\sqrt{d}+k(\pm\wp_1\sqrt{d}-\wp_0)(\sqrt{d}\tanh(\sqrt{d}\xi))-k\wp_1d(\tanh(\sqrt{d}\xi))^2}{2\{\wp_0+\wp_1\sqrt{d}\tanh(\sqrt{d}\xi)\}}\right]^{1/2}\exp(\mathrm{i}\tau), \tag{36}$$

$$\phi_2=\left[\frac{\pm\wp_0k\sqrt{d}+k(\mp\wp_1\sqrt{d}-\wp_0)(\sqrt{d}\coth(\sqrt{d}\xi))-k\wp_1d(\coth(\sqrt{d}\xi))^2}{2\{\wp_0+\wp_1\sqrt{d}\coth(\sqrt{d}\xi)\}}\right]^{1/2}\exp(\mathrm{i}\tau), \tag{37}$$

$$\phi_3=\left[\frac{-k\wp_1\xi-k\wp_1}{2\{\wp_0\xi^2+\wp_1\xi\}}\right]^{1/2}\exp(\mathrm{i}\tau),\ \ d=0; \tag{38}$$

for $d<0$, we have

$$\phi_4=\left[\frac{\pm\wp_0k\sqrt{d}-k(\pm\wp_1\sqrt{d}-\wp_0)(\sqrt{-d}\tan(\sqrt{-d}\xi))+k\wp_1d(\tan(\sqrt{-d}\xi))^2}{2\{\wp_0-\wp_1\sqrt{-d}\tan(\sqrt{-d}\xi)\}}\right]^{1/2}\exp(\mathrm{i}\tau), \tag{39}$$

$$\phi_5=\left[\frac{\pm\wp_0k\sqrt{d}+k(\pm\wp_1\sqrt{d}-\wp_0)(\sqrt{-d}\cot(\sqrt{-d}\xi))+k\wp_1d\left(\cot(\sqrt{-d}\xi)\right)^2}{2\left\{\wp_0+\wp_1\sqrt{-d}\cot(\sqrt{-d}\xi)\right\}}\right]^{1/2}\exp(\mathrm{i}\tau), \tag{40}$$

where

$$\xi=\mathrm{i}k\left(x\mp\frac{2k\sqrt{d}}{\gamma}t^\gamma\right),\quad \tau=\left(\mp k\sqrt{d}x+\frac{2dk^2}{\gamma}t^\gamma\right);$$

for **Set 2**, the solutions of tfcSE hold as follows:

$$\phi_6=\left[\frac{dk\wp_1\pm 2kd\wp_1\tanh(\sqrt{d}\xi)-kd\wp_1(\tanh(\sqrt{d}\xi))^2}{2\wp_1\sqrt{d}\tanh(\sqrt{d}\xi)}\right]^{1/2}\exp(\mathrm{i}\tau),\ \ d>0; \tag{41}$$

$$\phi_7=\left[\frac{dk\wp_1\pm 2kd\wp_1\coth(\sqrt{d}\xi)-kd\wp_1(\coth(\sqrt{d}\xi))^2}{2\wp_1\sqrt{d}\coth(\sqrt{d}\xi)}\right]^{1/2}\exp(\mathrm{i}\tau),\ \ d>0; \tag{42}$$

$$\phi_8=\left[\frac{-k\wp_1}{2\wp_1\xi}\right]^{1/2}\exp(\mathrm{i}\tau),\ \ d=0; \tag{43}$$

$$\phi_9 = \left[\frac{dk\wp_1 \mp 2kd\wp_1\sqrt{-d}\tan(\sqrt{-d}\xi) + kd\wp_1(\tan(\sqrt{-d}\xi))^2}{-2\wp_1\sqrt{-d}\tan(\sqrt{-d}\xi)}\right]^{1/2}\exp(\mathrm{i}\tau),\ d<0; \tag{44}$$

$$\phi_{10} = \left[\frac{dk\wp_1 \pm 2kd\wp_1\sqrt{-d}\cot(\sqrt{-d}\xi) + kd\wp_1(\cot(\sqrt{-d}\xi))^2}{2\wp_1\sqrt{-d}\cot(\sqrt{-d}\xi)}\right]^{1/2}\exp(\mathrm{i}\tau),\ d<0; \tag{45}$$

where

$$\xi = \mathrm{i}k\left(x \mp \frac{4k\sqrt{d}}{\gamma}t^{\gamma}\right),\quad \tau = \left(\mp 2k\sqrt{d}x + \frac{8dk^2}{\gamma}t^{\gamma}\right).$$

4.3. M-fractional Schrödinger–Hirota equation (s-tM-fSH)

This subsection starts with the Schrödinger–Hirota equation[35] with the form

$$\begin{aligned}
&\mathrm{i}D_{\mathrm{M},t}^{\alpha,\beta}\psi + \lambda D_{\mathrm{M},x}^{2\alpha,\beta}\psi + \Xi D_{\mathrm{M},t}^{\alpha,\beta}D_{\mathrm{M},x}^{\alpha,\beta}\psi \\
&+\rho|\psi|^2\psi + \mathrm{i}(AD_{\mathrm{M},x}^{3\alpha,\beta}\psi + B|\psi|^2 D_{\mathrm{M},x}^{\alpha,\beta}\psi) \\
&= \mathrm{i}CD_{\mathrm{M},x}^{\alpha,\beta}\psi + \mathrm{i}\Theta D_{\mathrm{M},x}^{\alpha,\beta}(|\psi|^2\psi) + \mathrm{i}\Omega D_{\mathrm{M},x}^{\alpha,\beta}(|\psi|^2)\psi, \\
&\qquad 0<\alpha<1,\ \beta>0,\ \mathrm{i}=\sqrt{-1},
\end{aligned} \tag{46}$$

where $\psi(x,t)$ is a complex function, coefficients Θ, λ, Ξ, A, and C are the self-steepening, group velocity, spatiotemporal, 3rd dispersion, and inter-modal dispersion terms respectively. Parameters B and Ω are nonlinear dispersions.

Substituting the complex wave transformation

$$\begin{aligned}
\psi(x,t) &= X(\varsigma)\exp(\mathrm{i}\tau), \\
\varsigma &= \frac{\Gamma(1+\beta)}{\alpha}n(x^{\alpha} - vt^{\alpha}), \\
\tau &= \frac{\Gamma(1+\beta)}{\alpha}(-Kx^{\alpha} + wt^{\alpha} + E)
\end{aligned}$$

into Eq. (46), we attain to the ODE with two conditions:

$$\begin{aligned}
&n^2(\lambda - \Xi v + 3AK)X'' - (w + \lambda K^2 - \Xi Kw + AK^3 + CK)X \\
&+(\rho + KB - K\Theta)X^3 = 0,
\end{aligned} \tag{47}$$

with

$$\Omega = \frac{(B-3\Theta)(\lambda - v\Xi) - 3A(2K\Theta + \rho)}{2(3AK + \lambda - \Xi v)},$$

$$C = \frac{A(w + K(-8K\lambda + v(-3+6K\Xi) + 2\Xi w)) - 8A^2K^3 - (\lambda - v\Xi)(v + 2K\lambda - vK\lambda - \Xi w)}{2AK + \lambda - \Xi v}.$$

The homogenous balance provides $n = m+1$. For $m = 1$, we have $n = 2$. So equation (6) reduces to the following equation by using $X'(\zeta) = d - X^2(\zeta)$,

$$\Psi(\xi) = \frac{\ell_0 + \ell_1 X + \ell_2 X^2}{\wp_0 + \wp_1 X}. \tag{48}$$

Inserting Eq. (48) and Eq. (7) into the reduced nonlinear ordinary differential equation (47), we have a polynomial of $X^k, (k = 0,1,2,\ldots)$. All the adjacent terms of X^k are equal to zero, and form some equations with unknown constants ℓ_0, ℓ_1, ℓ_2, $\wp_0$, $\wp_1$, and n. Solving the equations with Maple software, we get three sets of solutions:

Set 1

$$\begin{aligned}
\ell_1 &= \wp_0\sqrt{\frac{wK\Xi - AK^3 - K^2\lambda - CK - w)}{d(\Theta K - BK - \rho)}}, \\
\ell_2 &= \wp_1\sqrt{\frac{wK\Xi - AK^3 - K^2\lambda - CK - w)}{d(\Theta K - BK - \rho)}}, \\
\ell_0 &= 0, \\
n &= \sqrt{\frac{wK\Xi - AK^3 - K^2\lambda - CK - w}{2d(3AK - v\Xi + \lambda)}}.
\end{aligned}$$

Set 2

$$\begin{aligned}
\ell_0 &= -\frac{\wp_1}{2}\sqrt{\frac{d(wK\Xi - K^2\lambda - CK - w - AK^3)}{\Theta K - BK - \rho}}, \\
\ell_2 &= \sqrt{\frac{wK\Xi - K^2\lambda - CK - w - AK^3}{4d(\Theta K - BK - \rho)}}, \\
\ell_1 &= 0, \\
\wp_0 &= 0, \\
n &= \sqrt{\frac{wK\Xi - K^2\lambda - CK - w - AK^3}{8d(3AK - v\Xi + \lambda)}}.
\end{aligned}$$

Set 3

$$\begin{aligned}
\ell_0 &= -\frac{\wp_1}{2}\sqrt{\frac{2d(AK^3 - wK\Xi + K^2\lambda + CK + w)}{\Theta K - BK - \rho}}, \\
\ell_2 &= \sqrt{\frac{AK^3 - wK\Xi + K^2\lambda + CK + w}{2d(\Theta K - BK - \rho)}}, \\
\ell_1 &= 0, \\
\wp_0 &= 0, \\
n &= \sqrt{\frac{AK^3 - wK\Xi + K^2\lambda + CK + w}{4d(3AK - v\Xi + \lambda)}}.
\end{aligned}$$

For **Set 1**, the solutions of spatiotemporal M-fractional SH equation hold:

$$\psi(x,t) = \sqrt{\frac{wK\Xi - AK^3 - K^2\lambda - CK - w}{d(\Theta K - BK - \rho)}} \times \sqrt{d}\tanh(\sqrt{d}\varsigma)\mathrm{e}^{\mathrm{i}\tau}, \quad d > 0; \tag{49}$$

$$\psi(x,t) = \sqrt{\frac{wK\Xi - AK^3 - K^2\lambda - CK - w}{d(\Theta K - BK - \rho)}} \times \sqrt{d}\coth(\sqrt{d}\varsigma)\mathrm{e}^{\mathrm{i}\tau}, \quad d > 0; \tag{50}$$

$$\psi(x,t) = \sqrt{\frac{wK\Xi - AK^3 - K^2\lambda - CK - w}{d(\Theta K - BK - \rho)}} \times \frac{\mathrm{e}^{\mathrm{i}\tau}}{\varsigma}, \quad d = 0; \tag{51}$$

$$\psi(x,t) = -\sqrt{\frac{wK\Xi - AK^3 - K^2\lambda - CK - w}{d(\Theta K - BK - \rho)}} \times \sqrt{-d}\tan(\sqrt{-d}\varsigma)\mathrm{e}^{\mathrm{i}\tau}, \quad d < 0; \tag{52}$$

$$\psi(x,t) = \sqrt{\frac{wK\Xi - AK^3 - K^2\lambda - CK - w}{d(\Theta K - BK - \rho)}} \times \sqrt{-d}\cot(\sqrt{-d}\varsigma)\mathrm{e}^{\mathrm{i}\tau}, \quad d < 0; \tag{53}$$

where

$$\varsigma = \frac{\Gamma(1+\beta)}{\alpha}\sqrt{\frac{wK\Xi - AK^3 - K^2\lambda - CK - w}{2d(3AK - v\Xi + \lambda)}}(x^\alpha - vt^\alpha),$$

$$\tau = \frac{\Gamma(1+\beta)}{\alpha}(-Kx^\alpha + wt^\alpha + E).$$

For **Set 2**, the solutions of spatiotemporal M-fractional SH model hold:

$$\psi(x,t) = \sqrt{\frac{wK\Xi - K^2\lambda - CK - w - AK^3}{4d(\Theta K - BK - \rho)}} \times \left[\frac{-\wp_1 d + d\tanh^2(\sqrt{d}\varsigma)}{\wp_1\sqrt{d}\tanh(\sqrt{d}\zeta)}\right]\mathrm{e}^{\mathrm{i}\tau}, \quad d > 0; \tag{54}$$

$$\psi(x,t) = \sqrt{\frac{wK\Xi - K^2\lambda - CK - w - AK^3}{4d(\Theta K - BK - \rho)}} \times \left[\frac{-\wp_1 d + d\coth^2(\sqrt{d}\varsigma)}{\wp_1\sqrt{d}\coth(\sqrt{d}\varsigma)}\right]\mathrm{e}^{\mathrm{i}\tau}, \quad d > 0; \tag{55}$$

$$\psi(x,t) = \sqrt{\frac{wK\Xi - K^2\lambda - CK - w - AK^3}{4d(\Theta K - BK - \rho)}} \times \left[\frac{\wp_1 d + d\tan^2(\sqrt{-d}\varsigma)}{\wp_1\sqrt{-d}\tan(\sqrt{-d}\zeta)}\right]\mathrm{e}^{\mathrm{i}\tau}, \quad d < 0; \tag{56}$$

$$\psi(x,t) = \sqrt{\frac{wK\Xi - K^2\lambda - CK - w - AK^3}{4d(\Theta K - BK - \rho)}} \times \left[\frac{-\wp_1 d - d\cot^2(\sqrt{-d}\varsigma)}{\wp_1\sqrt{-d}\cot(\sqrt{-d}\varsigma)}\right]\mathrm{e}^{\mathrm{i}\tau}, \quad d < 0; \tag{57}$$

where

$$\varsigma = \frac{\Gamma(1+\beta)}{\alpha}\sqrt{\frac{wK\Xi - K^2\lambda - CK - w - AK^3}{8d(3AK - v\Xi + \lambda)}}(x^\alpha - vt^\alpha),$$

$$\tau = \frac{\Gamma(1+\beta)}{\alpha}(-Kx^\alpha + wt^\alpha + E).$$

For **Set 3**, the solutions of spatiotemporal M-fractional SH equation hold:

$$\psi(\xi) = \sqrt{\frac{AK^3 - wK\Xi + K^2\lambda + CK + w}{2d(\Theta K - BK - \rho)}} \times \left[\frac{-\wp_1 d + d\tanh^2(\sqrt{d}\varsigma)}{\wp_1\sqrt{d}\tanh(\sqrt{d}\varsigma)}\right]\mathrm{e}^{\mathrm{i}\tau}, \quad d > 0; \tag{58}$$

$$\psi(\xi) = \sqrt{\frac{AK^3 - wK\Xi + K^2\lambda + CK + w}{2d(\Theta K - BK - \rho)}} \times \left[\frac{-\wp_1 d + d\coth^2(\sqrt{d}\varsigma)}{\wp_1\sqrt{d}\coth(\sqrt{d}\varsigma)}\right]\mathrm{e}^{\mathrm{i}\tau}, \quad d > 0; \tag{59}$$

$$\psi(\xi) = \sqrt{\frac{AK^3 - wK\Xi + K^2\lambda + CK + w}{2d(\Theta K - BK - \rho)}} \times \left[\frac{\wp_1 d + d\tan^2(\sqrt{-d}\varsigma)}{\wp_1\sqrt{-d}\tan(\sqrt{-d}\varsigma)}\right]\mathrm{e}^{\mathrm{i}\tau}, \quad d < 0; \tag{60}$$

$$\psi(\xi) = \sqrt{\frac{AK^3 - wK\Xi + K^2\lambda + CK + w}{2d(\Theta K - BK - \rho)}} \times \left[\frac{-\wp_1 d - d\cot^2(\sqrt{-d}\varsigma)}{\wp_1\sqrt{-d}\cot(\sqrt{-d}\varsigma)}\right]\mathrm{e}^{\mathrm{i}\tau}, \quad d < 0; \tag{61}$$

where

$$\varsigma = \frac{\Gamma(1+\beta)}{\alpha}\sqrt{\frac{AK^3 - wK\Xi + K^2\lambda + CK + w}{4d(3AK - v\Xi + \lambda)}}(x^\alpha - vt^\alpha),$$

$$\tau = \frac{\Gamma(1+\beta)}{\alpha}(-Kx^\alpha + wt^\alpha + E).$$

5. Graphical representations

5.1. Graphical representation of solutions for stFETL model

The research findings are in the types of hyperbolic, rational, and trigonometric functions. All the results are analyzed and some of them have shown graphically in Figs. 1–3.

5.2. Graphical representations of solutions for tfcSE

Two sets of results are found in the study of the tfcSE. We analyze all results. Five results are graphically shown Figs. 4–7. The three-dimensional (3D) contour, and two-dimensional (2D) plots show the changes of amplitudes, directions, shapes of wave as well as the nature of the solitary waves of gained solutions in space x with time t below.

5.3. Graphical representations of solutions for s-tM-fSH

The derived results are in a variety of hyperbolic, rational, and trigonometric functions. All of the results are analyzed and some of them are shown graphically in Figs. 8–13, where the patterns and natures of the wave surfaces are shown clearly with 3D, 2D, and contour plots.

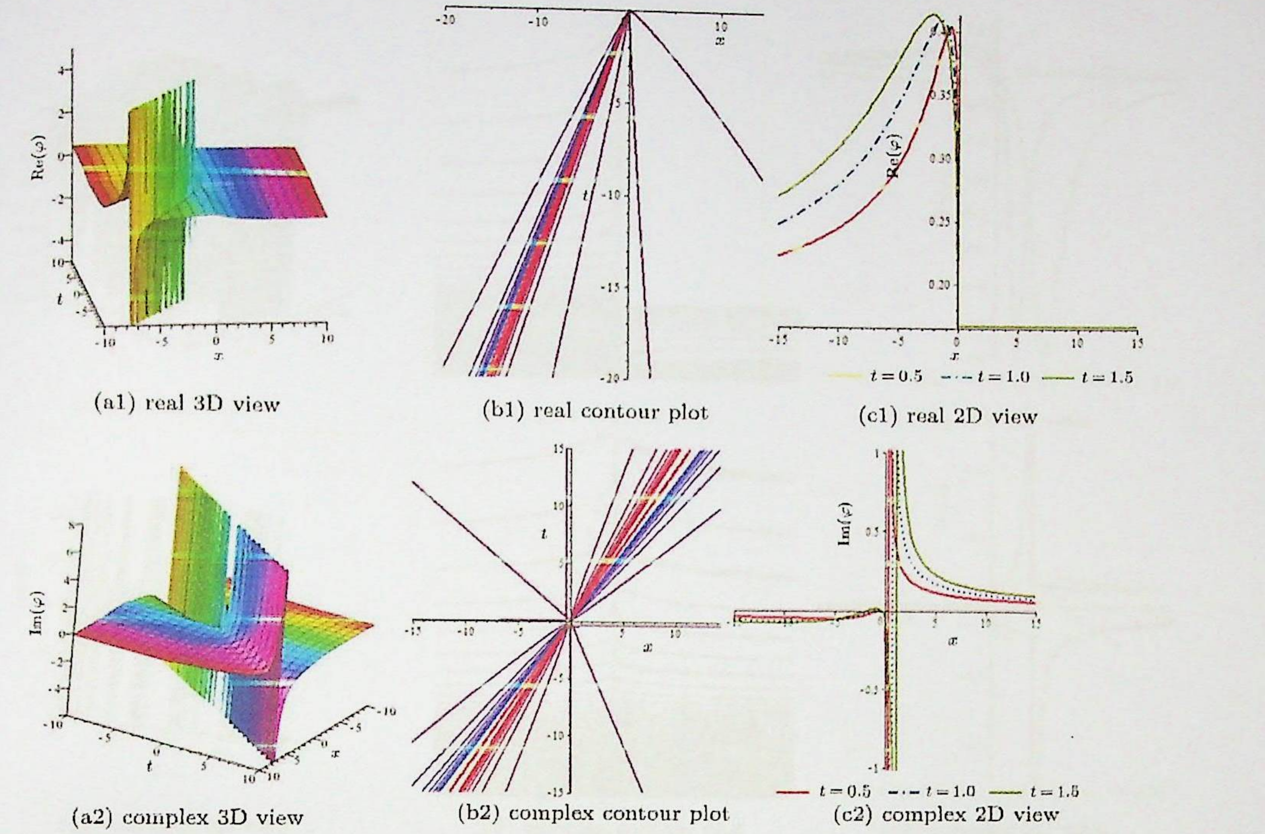

Fig. 1. (a), (b) Real and complex three-dimensional (3D) surface and contour plot of solution $\varphi(x,t)$ of Eq. (12) for $k=2$, $\beta=0.1$, $\nu=0.5$, $A=1$, and $B=-1$, and (c) two-dimensional (2D) plot for $t=0.5$, 1 and 1.5 with parametric values above.

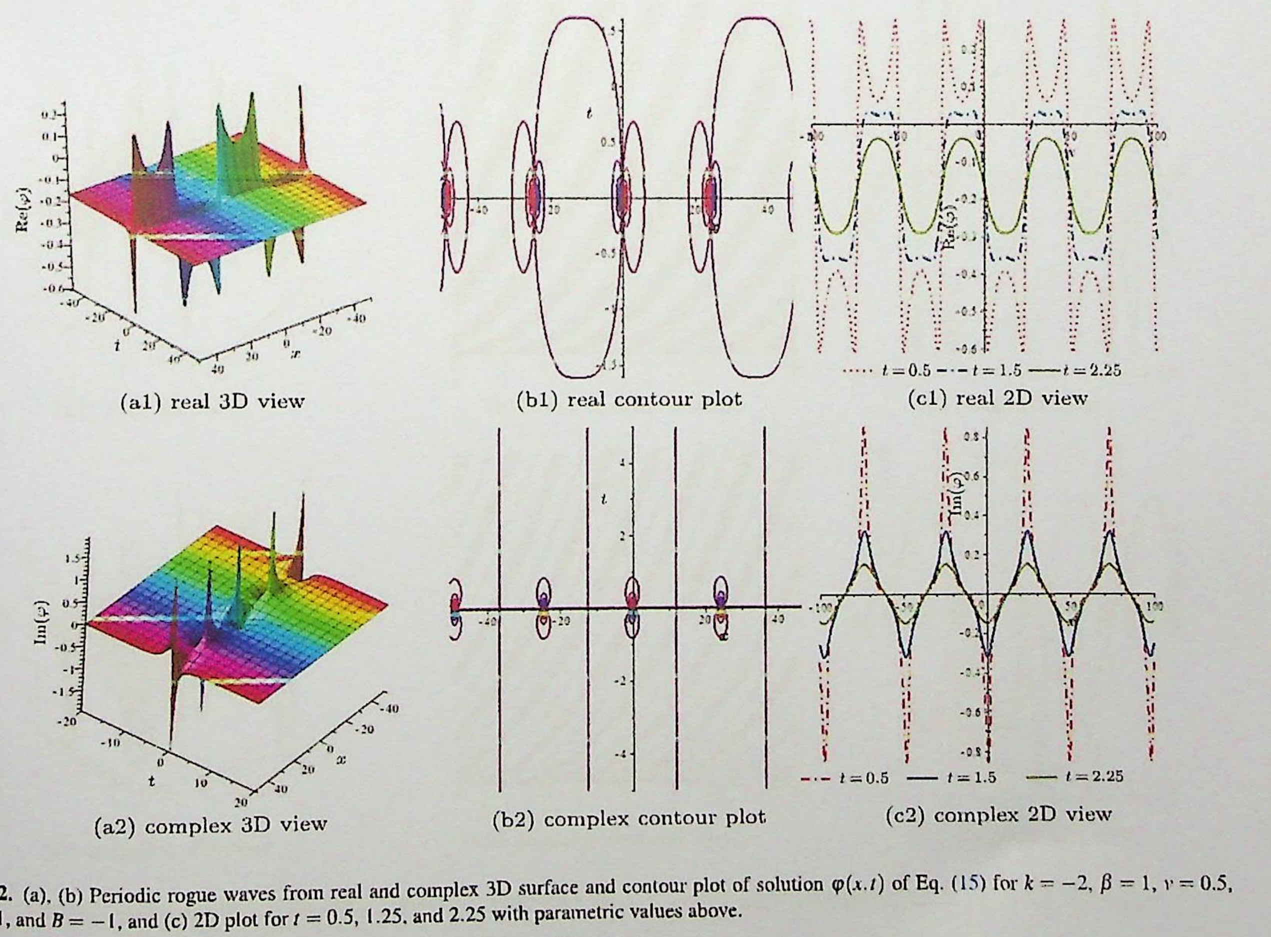

Fig. 2. (a), (b) Periodic rogue waves from real and complex 3D surface and contour plot of solution $\varphi(x,t)$ of Eq. (15) for $k=-2$, $\beta=1$, $\nu=0.5$, $A=1$, and $B=-1$, and (c) 2D plot for $t=0.5$, 1.25, and 2.25 with parametric values above.

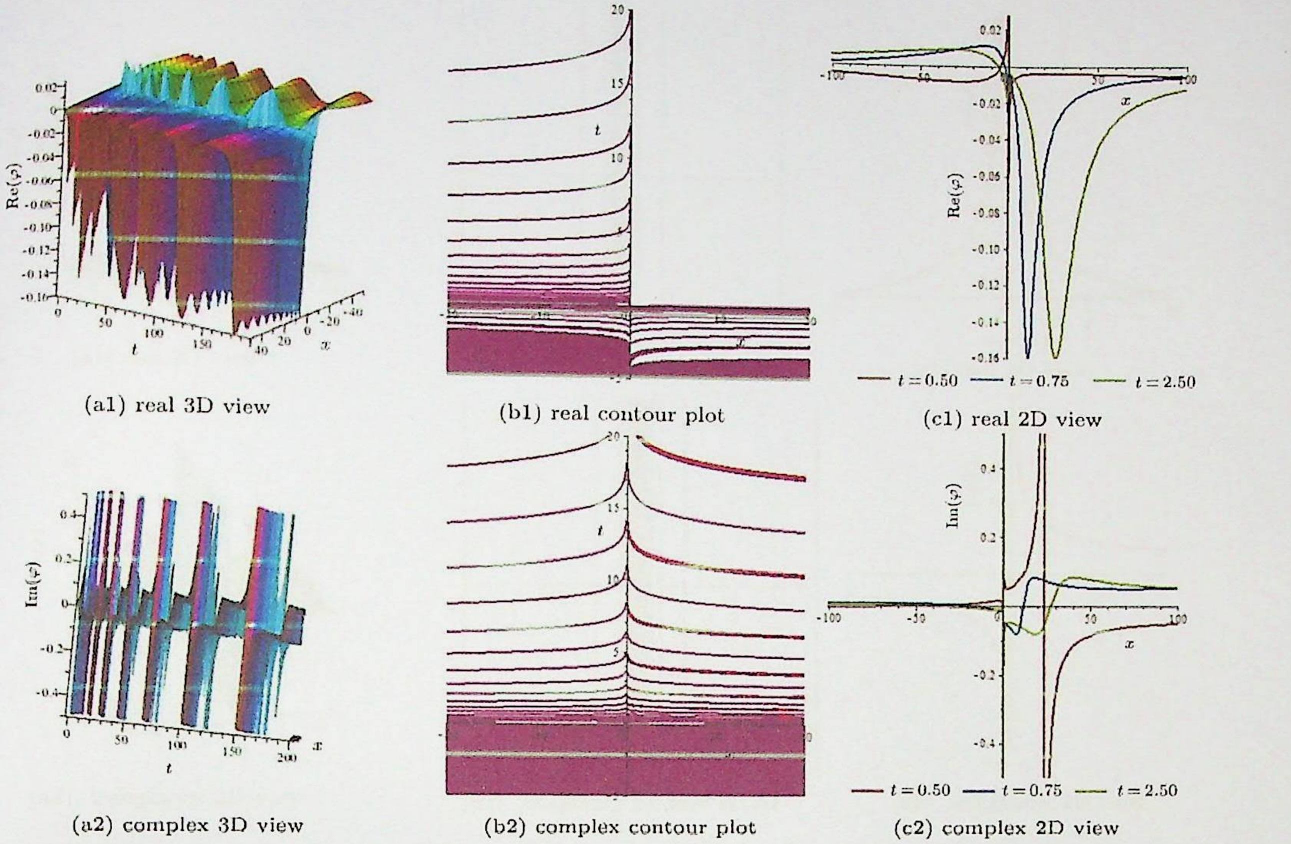

Fig. 3. (a), (b) Real and complex 3D surface and contour plot of solution $\varphi(x,t)$ of Eq. (30) for $k = -2$, $\beta = 0.1$, $\ell_2 = 1$, $\nu = 3$, $A = 2$, $B = -1$, and $k_2 = 2$, and (c) 2D plot for $t = 0.5$, 0.75, and 2.5 with parametric values above.

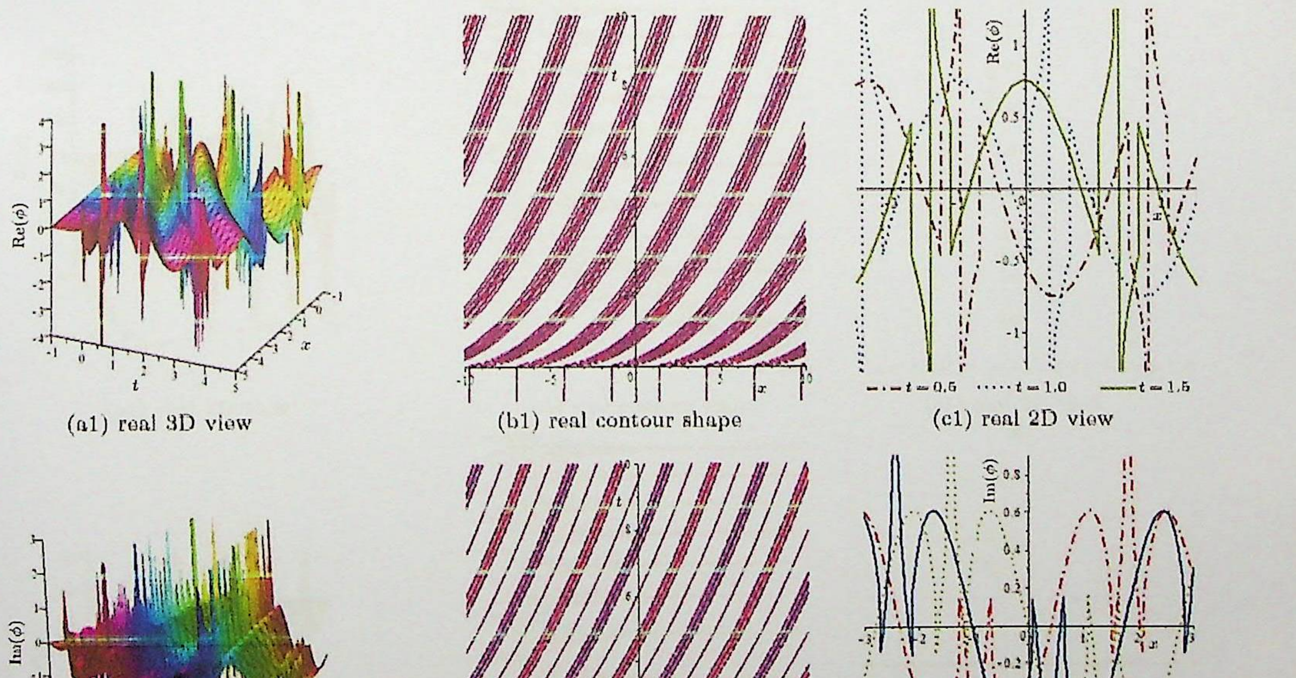

Fig. 4. Solitonic solution $\phi(x,t)$ of Eq. (36) for $d = 2$, $\wp_1 = 0.5$, $\wp_0 = 1$, $\gamma = 0.5$, and $k = 0.8$ and $t = 0.5$, 1, and 1.5 for 2D graph.

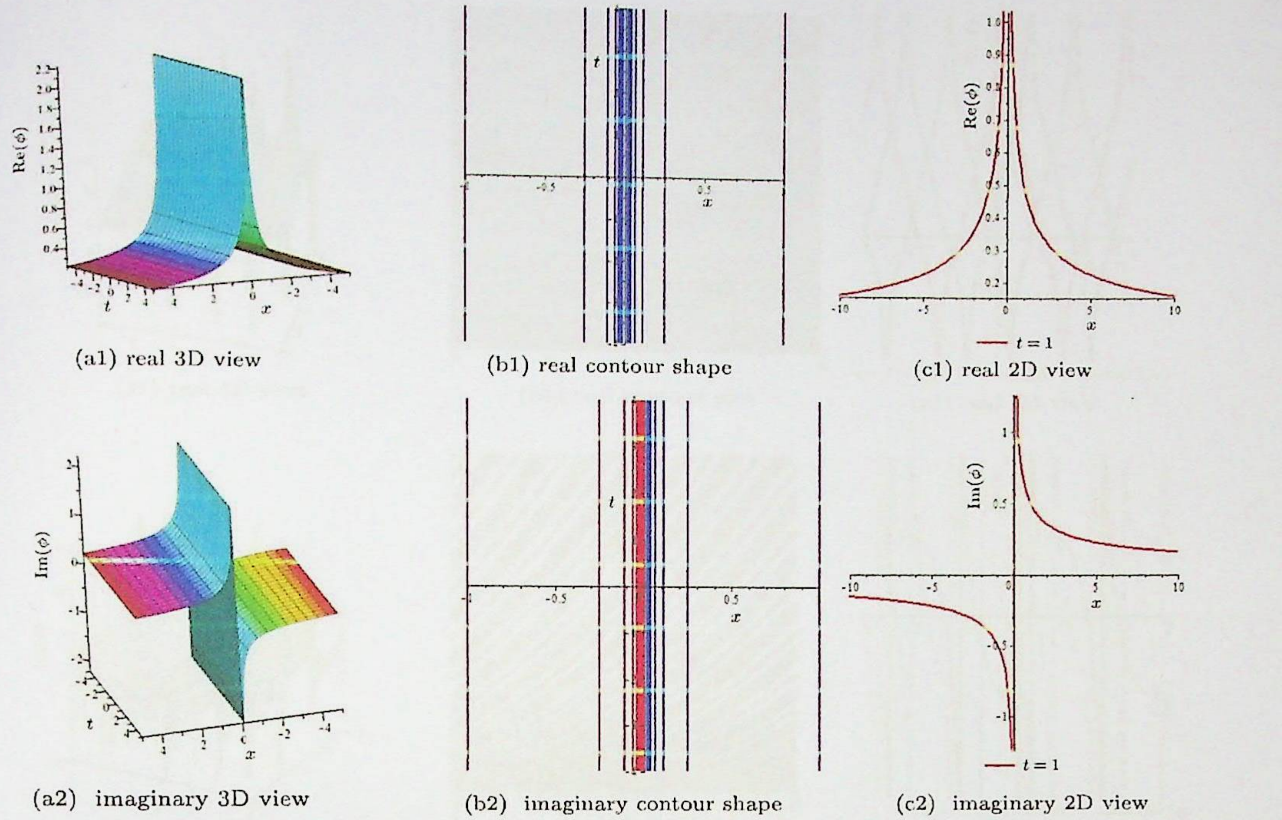

Fig. 5. Plot of solitonic solution $\phi(x,t)$ of Eq. (38) for $d = 0, \wp_1 = 2, \wp_0 = 1, \gamma = 2/3$, and $k = 0.8$ and $t = 1$ for 2D graph.

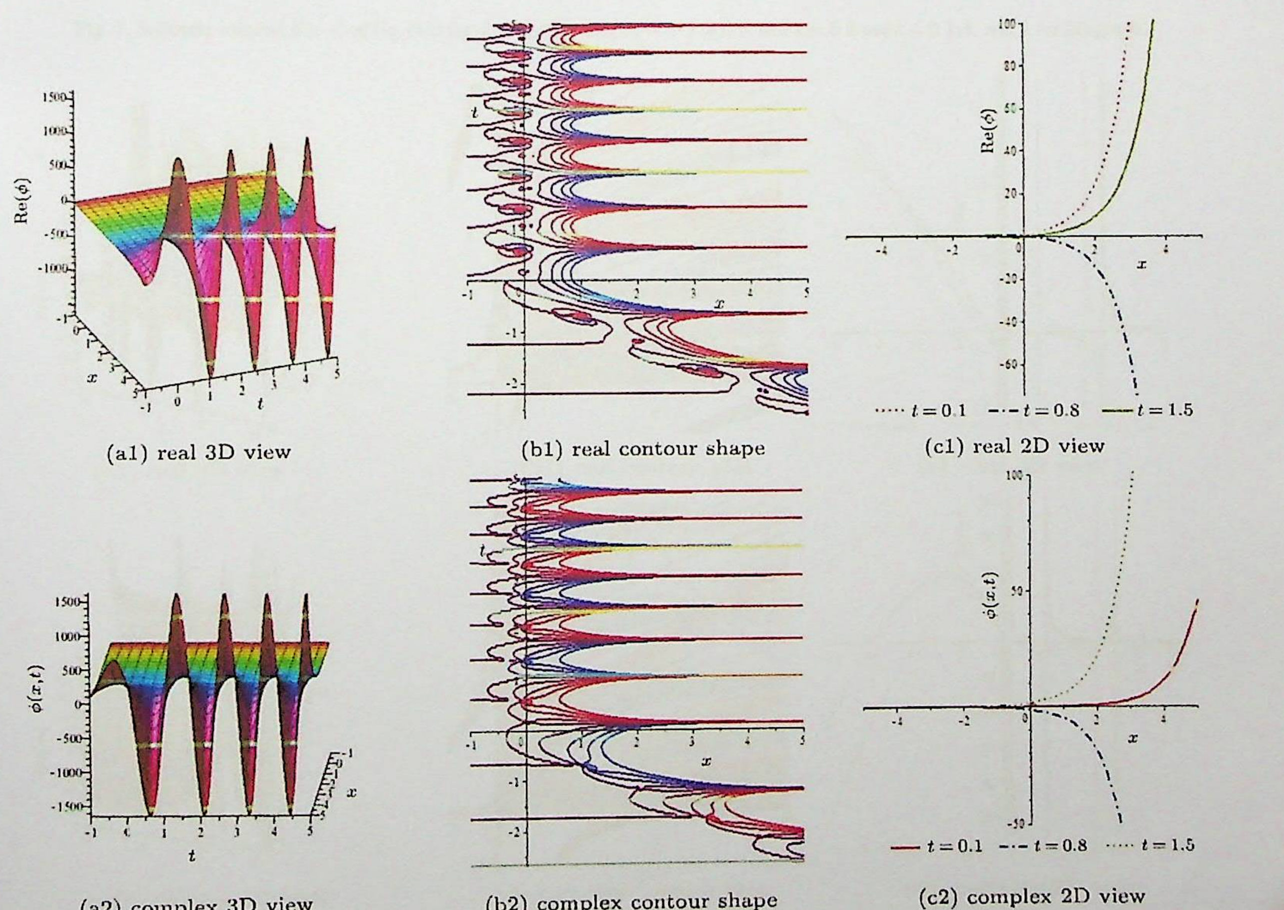

Fig. 6. Solitonic solution $\phi(x,t)$ of Eq. (39) for $d = -2, \wp_1 = 2, \wp_0 = 1, \gamma = 4/5$, and $k = 1$ and $t = 0.1, 0.8$, and 1.5 for 2D graph.

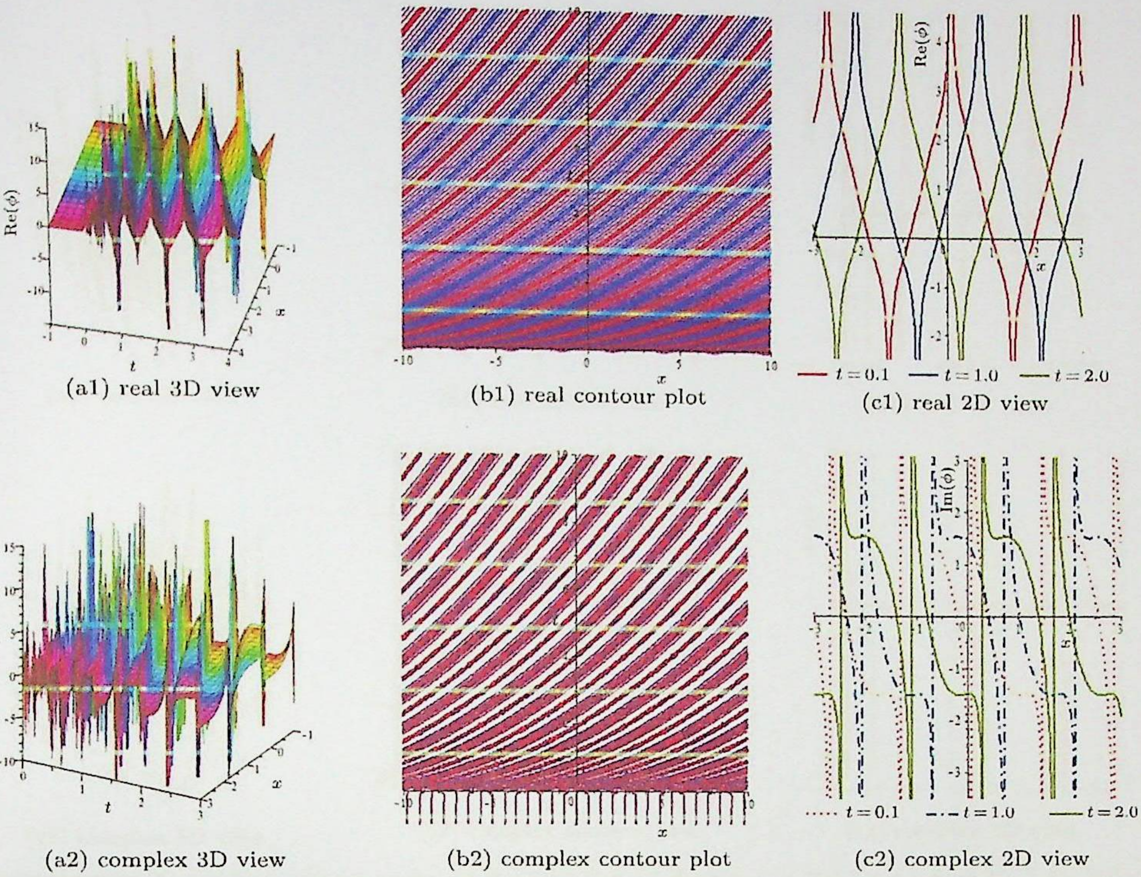

Fig. 7. Solitonic solution $\phi(x,t)$ of Eq. (42) for $d=2$, $\wp_1=0.5$, $\wp_0=1$, $\gamma=0.5$, and $k=0.8$ and $t=0.1, 1$, and 2 for 2D graph.

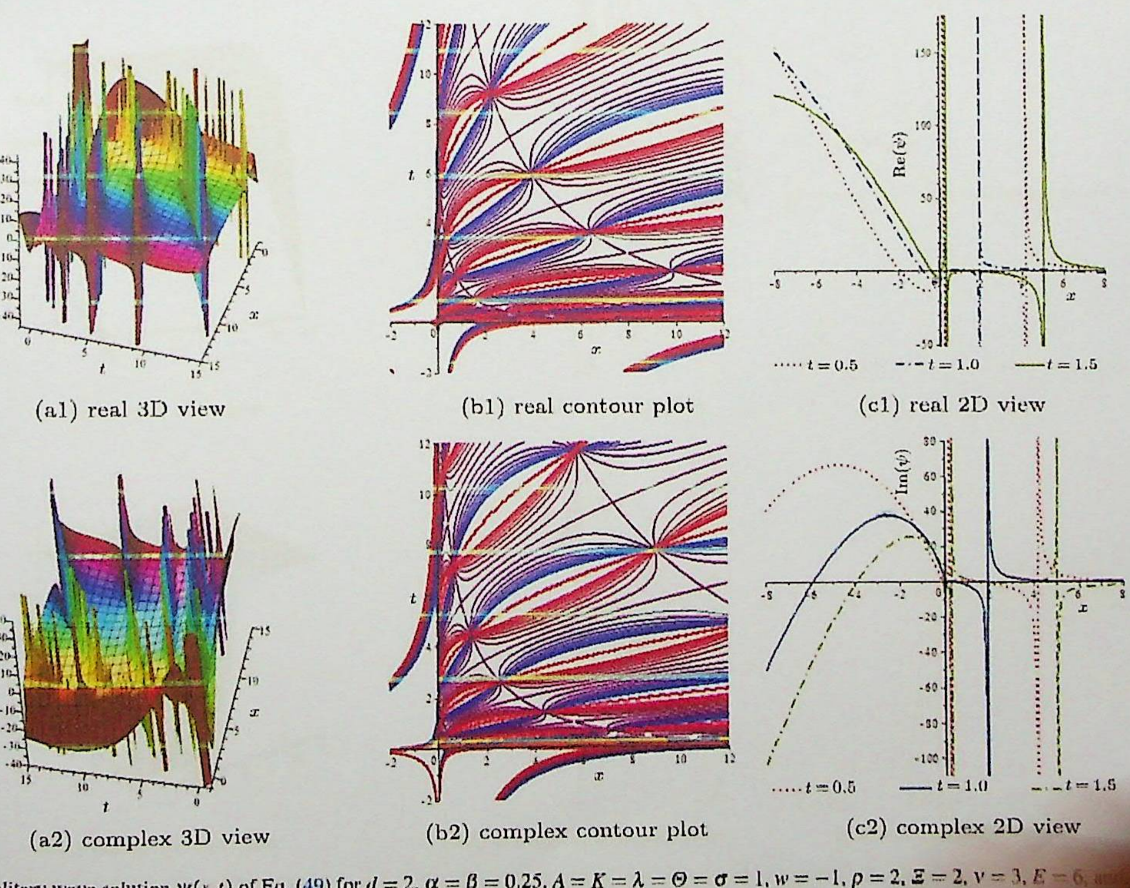

Fig. 8. Solitary wave solution $\psi(x,t)$ of Eq. (49) for $d=2$, $\alpha=\beta=0.25$, $A=K=\lambda=\Theta=\sigma=1$, $w=-1$, $\rho=2$, $\Xi=2$, $\nu=3$, $E=6$, an
1, and 1.5 for 2D graph.

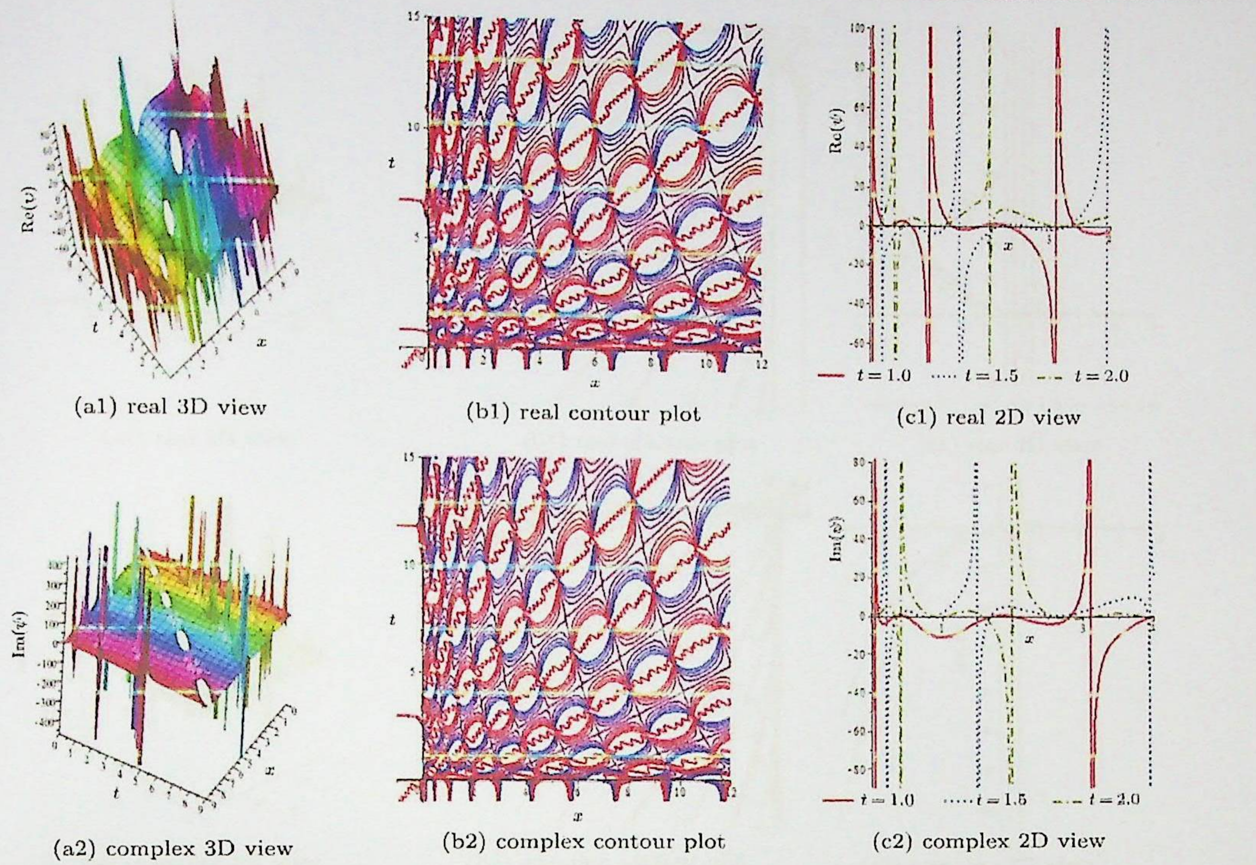

Fig. 9. Solitonic solution $\psi(x,t)$ of Eq. (52) for $d=-2$, $\alpha=0.5$, $\beta=B=0.75$, $A=2$, $K=5$, $w=-1$, $\Theta=3$, $\rho=1$, $\Xi=4$, $\nu=1$, $\lambda=1$, $E=6$, and $\sigma=3$ and $t=1$, 1.5, and 2 for 2D graphs.

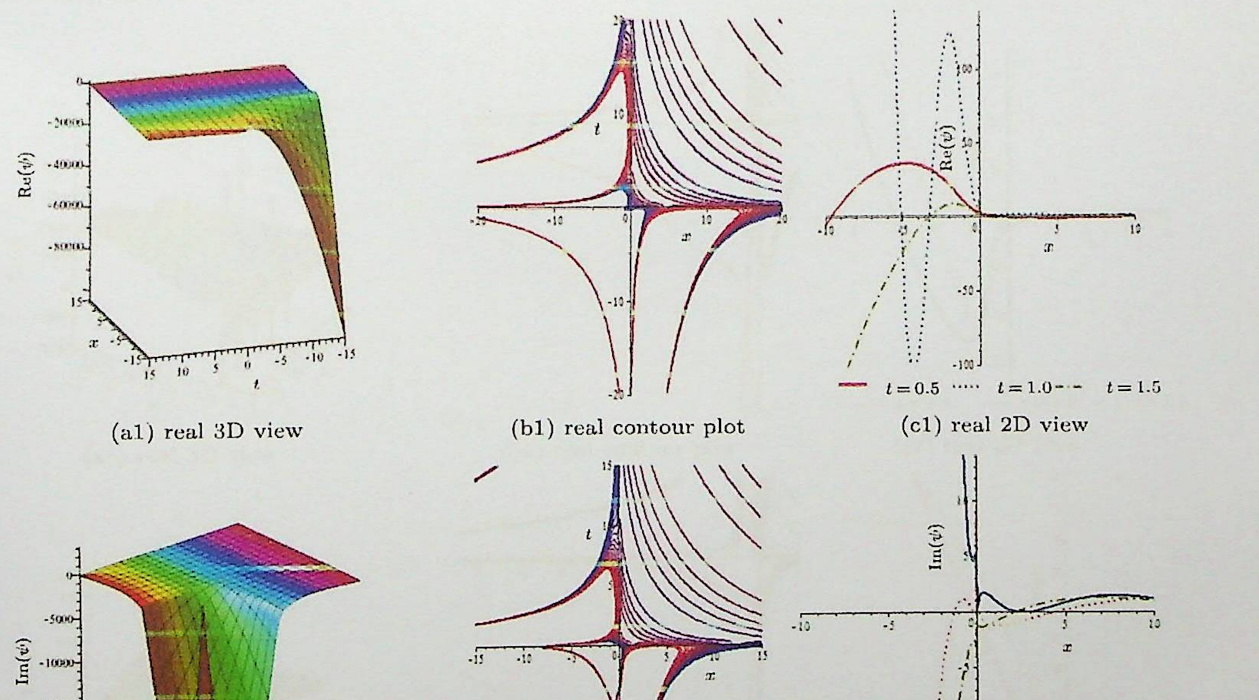

Fig. 10. Solitonic solution $\psi(x,t)$ of Eq. (54) for $\alpha=0/3$, $\beta=B=0.5$, $A=1$, $K=1$, $w=-1$, $\Theta=1$, $\rho=2$, $\Xi=2$, $\nu=0$, $\lambda=1$, and $E=6$ and for 2D graph $t=0.5$, 1, and 1.5.

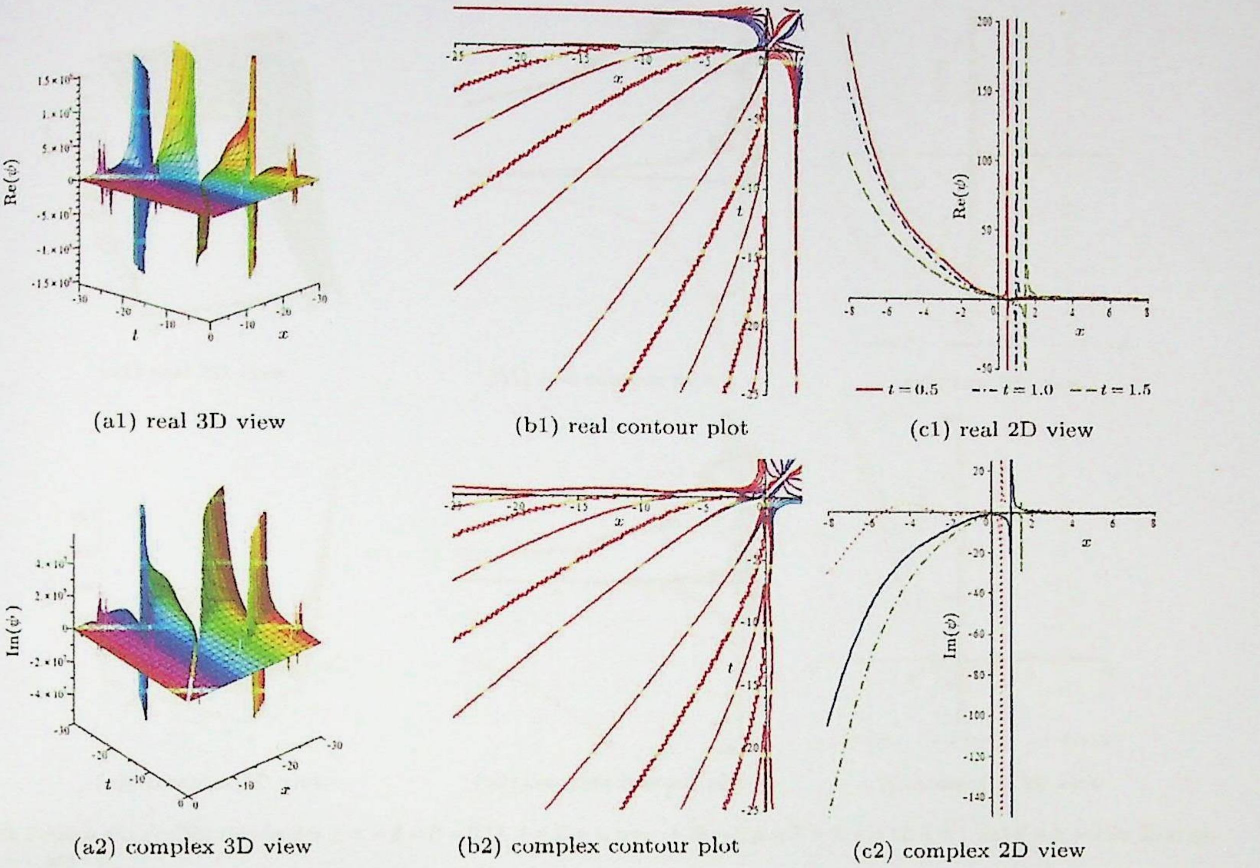

Fig. 11. Wave solution $\psi(x,t)$ of Eq. (56) for $\alpha=\beta=B=0.5$, $A=1$, $K=1$, $w=-1$, $\Theta=1$, $\rho=1$, $\Xi=2$, $\nu=1$, $\lambda=1$, and $E=6$, and for 2D graph $t=0.5$, 1, and 10.5.

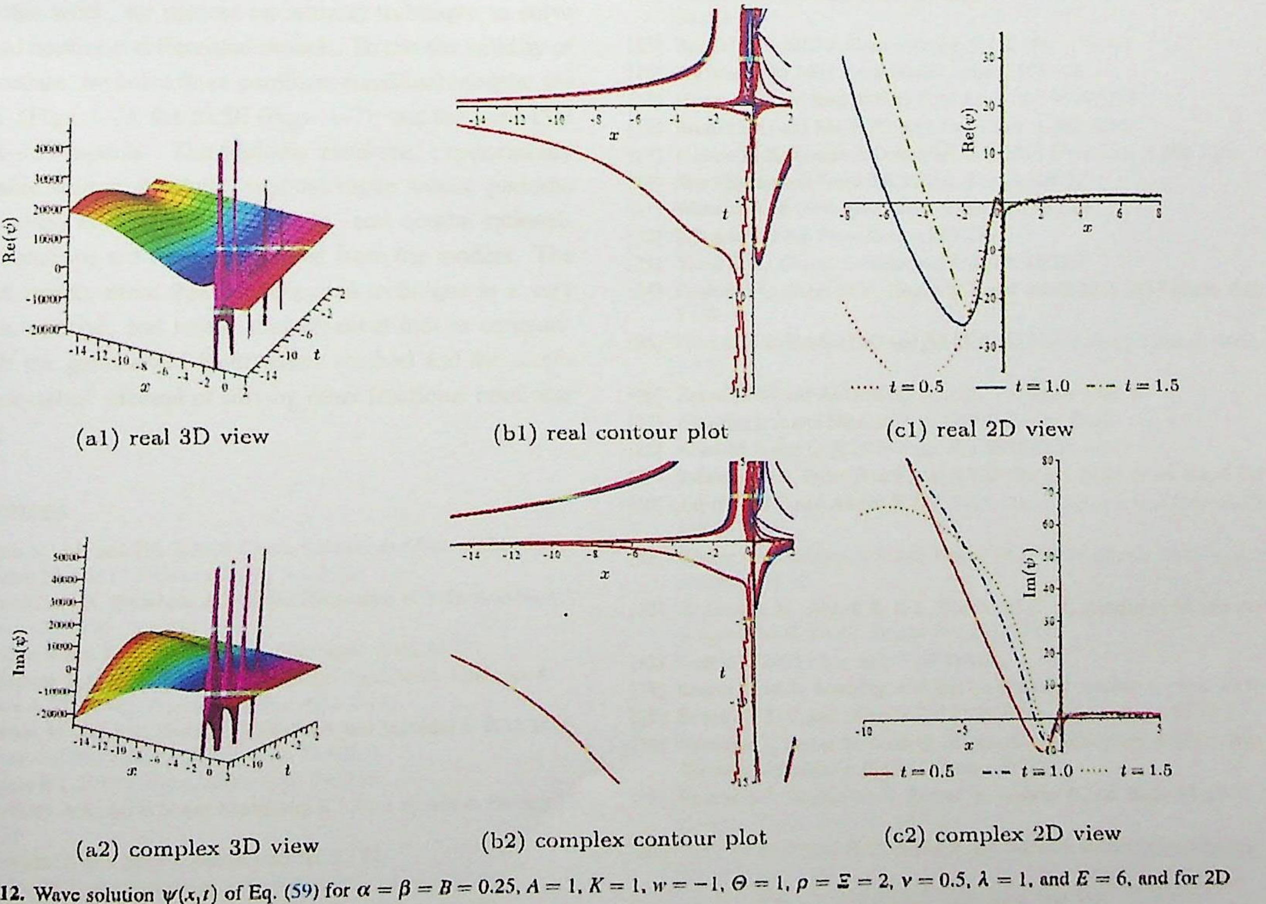

Fig. 12. Wave solution $\psi(x,t)$ of Eq. (59) for $\alpha=\beta=B=0.25$, $A=1$, $K=1$, $w=-1$, $\Theta=1$, $\rho=\Xi=2$, $\nu=0.5$, $\lambda=1$, and $E=6$, and for 2D graph $t=0.5$, 1, 1.5.

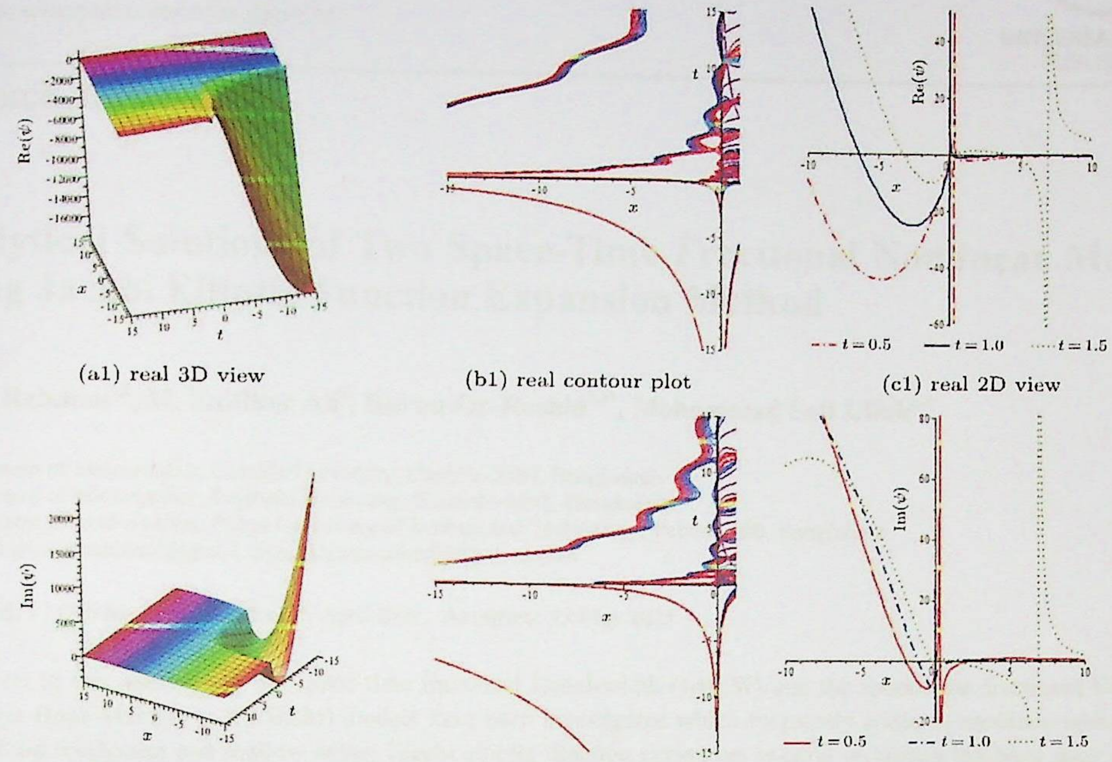

(a1) real 3D view (b1) real contour plot (c1) real 2D view

(a2) complex 3D view (b2) complex contour plot (c2) complex 2D view

Fig. 13. Solution $\psi(x,t)$ of Eq. (61) for $d = 2$, $\alpha = \beta = B = 0.25$, $A = K = 1$, $w = -1$, $\Theta = 1$, $\rho = \Xi = 2$, $\nu = 12$, $\lambda = 1$, and $E = 6$, and for 2D graph, $t = 0.5$, 1, and 1.5.

6. Conclusions

In this work, we present an integral technique to solve fractional nonlinear differential models. To test the validity of the procedure, we solve three nonlinear fractional models: the s-tFETL (Figs. 1–3), the tfcSE (Figs. 4–7), and the s-tM-fSH (Figs. 8–13) models. The periodic envelope, exponentially changeable soliton envelope, rational rogue waves, periodic rogue waves, combo periodic-soliton, and combo rational-soliton solutions are formally derived from the models. The achieved results show that the proposed technique is a very effective, concise, and robust mathematical tool in comparison with the generalized Kudryashov method and the modified Kudryashov method of solving other fractional nonlinear models.

References

[1] Zhou S, Li H and Zhu Z 2008 *Chaos, Solitons and Fractals* **36** 973
[2] Abdou M A 2017 *J. Ocean. Engin. Sci.* **2** 288
[3] Aminikhah H, Sheikhani A H R and Rezazadeh H 2016 *Scientia IUranika* **23** 1048
[4] Saxena R and Kalla S 2010 *Fract. Calc. Appl. Anal.* **13** 177
[5] Sulaiman T A, Bulut H and Atas S S 2019 *Appl. Math. Nonl. Sci.* **4**
[6] Patra A 2019 *Prog. Fractional Differ. Appl.* **5** 125
[7] Salinas M, Salas R, Mellado D, Graria A and Saavedra C 2018 *Modelling and Simulation in Engineering* **72** 80306
[8] Magin R L 2010 *Comput. Math. Appl.* **59** 1586
[9] Seadawy A R, Ali K K and Nuruddeen R I 2019 *Results in Physics* **12** 2234
[10] El-Salam F A A 2013 *J. Taibah Uni. Sci.* **7** 173
[11] Abdou M A and Soliman A A 2018 *Results in Physics* **9** 1497
[12] Roshid H O and Rahman M A 2014 *Results in Physics* **4** 150
[13] Feng L L and Zhang T T 2018 *Appl. Math. Lett.* **78** 133
[14] Zedan A H, Alaidarous E and Shapll S 2013 *Erratum Nonlinear Dyn.* **74** 1153
[15] Roshid H O 2017 *J. Ocean. Engin. Sci.* **2** 196
[16] Wazwaz A M 2005 *Appl. Math.Comput.* **169** 321
[17] Hoque M F and Roshid H O 2020 *Phys. Scr.* **95** 075219
[18] Roshid H O and Ma W X 2018 *Phys. Lett. A* **382** 3262
[19] Hossen M B, Roshid H O and Ali M Z 2018 *Phys. Lett. A* **382** 1268
[20] Sirendaoreji and Sun J 2003 *Phys. Lett. A* **309** 387
[21] Wazwaz A M 2004 *Appl. Math. Comput.* **159** 559
[22] Wang M L 1996 *Phys. Lett. A* **213** 279
[23] Yan Z 2003 *Chaos, Solitons and Fractals* **18** 299
[24] Roshid H O, Alam M N, Hoque M F and Akbar M A 2013 *Math. Stat.* **1** 162
[25] Hossen M B, Roshid H O and Ali M Z 2017 *Int. J. Appl. Comput. Math.* **3** 679
[26] Zayed EME and Al-Nowehy A G 2017 *J. Space Expl.* 6
[27] Alhakim L A and Moussa A A 2019 *J. Ocean. Engin. Sci.* **4** 7
[28] Alam M A and Li X 2020 *Phys. Scr.* **95** 045224
[29] Sulaiman T A, Bulut H and Atas S S 2019 *Appl. Math. Nonl. Sci.* **4** 535
[30] Zayed E M E and Alurrfi K A E 2015 *Chaos, Solitons and Fractals* **78** 148
[31] Kumar D, Seadawy A R and Haque M R 2018 *Chaos, Solitons and Fractals* **115** 62
[32] Shahoot A M, Alurrfi K A E, Elmrid M O M, Almsiri A M and Arwiniya A M H 2019 *J. Taibah Uni. Sci.* **13** 63
[33] Laskin N 2002 *Phys. Rev. E* **66** 056108
[34] Khater M M A, Seadawy A R and Lu D 2018 *Pramana J. Phys.* **90** 59
[35] Sousa J V D C and Oliveira E C D 2018 *Int. J. Anal. Appl.* **16** 83
[36] Bernstein I, Zerrad E, Zhou Q, Biswas A and Melikechi B 2015 *Opto. Electron. Adv. Mater. Rapid Commun.* **9** 792
[37] Bernstein I, Melikechi N, Zerrad E, Aiswas B and Belic M 2016 *J. Comput. Theor. Nanosci.* **13** 5288
[38] Ullah M S, Roshid H O, Ali M Z and Rahman Z 2019 *Contemporary Mathematics* **1** 25
[39] Liu Y and Wen X Y 2019 *Adv. Diff. Equs.* **264** 332

Contemporary Mathematics
http://ojs.wiserpub.com/index.php/CM/

UNIVERSAL WISER
PUBLISHER

Research Article

Analytical Solutions of Two Space-Time Fractional Nonlinear Models Using Jacobi Elliptic Function Expansion Method

Zillur Rahman[1,2], M. Zulfikar Ali[2], Harun-Or-Roshid[2,3*], Mohammad Safi Ullah[1,2]

[1]Department of Mathematics, Comilla University, Cumilla-3506, Bangladesh
[2]Department of Mathematics, Rajshahi University, Rajshahi-6205, Bangladesh
[3]Department of Mathematics, Pabna University of Science and Technology, Pabna-6600, Bangladesh
Email: harunorroshidmd@gmail.com, rahman.zillur54@yahoo.com

Received: 17 October 2020; **Revised:** 7 April 2021; **Accepted:** 13 May 2021

Abstract: In this manuscript, the space-time fractional Equal-width (s-tfEW) and the space-time fractional Wazwaz-Benjamin-Bona-Mahony (s-tfWBBM) models have been investigated which frequently arises in nonlinear optics, solid states, fluid mechanics and shallow water. Jacobi elliptic function expansion integral technique has been used to build more innovative exact solutions of the s-tfEW and s-tfWBBM nonlinear partial models. In this research, fractional beta-derivatives are applied to convert the partial models to ordinary models. Several types of solutions have been derived for the models and performed some new solitary wave phenomena. The derived solutions have been presented in the form of Jacobi elliptic functions initially. Persevering different conditions on a parameter, we have achieved hyperbolic and trigonometric functions solutions from the Jacobi elliptic function solutions. Besides the scientific derivation of the analytical findings, the results have been illustrated graphically for clear identification of the dynamical properties. It is noticeable that the integral scheme is simplest, most conventional and convenient in handling many nonlinear models arising in applied mathematics and the applied physics to derive diverse structural precise solutions.

Keywords: space-time fractional equal width equation, space-time fractional Wazwaz-Benjamin-Bona-Mahony, balance number, fractional beta-derivative, Jacobi elliptic function expansion method, analytical solutions

1. Introduction

In the current world, fractional derivatives have been applied to study the calculus of arbitrary order for modelling of nonlinear happening in different fields like fluid mechanics, signal processing, control theory, astrophysics, dynamical systems, plasma physics, non-linear biological systems, nanotechnology, and engineering. Many real-life problems of the above areas can be modelled by Partial Differential Equation (PDE) relating to the fractional derivatives. The concept of solitons, the top decisive way in applications to such models has played an important role to identify the complex incident in various fields of sciences. Up to days, many techniques have been introduced for deriving exact wave solutions of nonlinear models but the innovation reached is deficient. The precise mathematical methods to derive different classes of exact solutions namely; the inverse variational methods [1], the Darboux Transformation [2], the Exp-function technique [3], tanh method [4], the $\exp(-(\Phi)\eta)$-expansion method [5], first integral scheme [6], the $\tan(\Theta/2)$-expansion approach [7], the Hirota bilinear method [8-9], the sine-cosine analysis [10], the new extended $(G'/$

DOI: https://doi.org/10.37256/cm.232021682

G)-expansion method [11], the modified double sub-equation method [12], the mapping and ansatz methods [13-14], the Jacobi elliptic function expansion method [15-16] as well.

Moreover, it is very problematic to derive the exact solution of nonlinear fractional PDE via the best possible method. So, it is significant to arise the explicit solutions which are exact for advanced study of these nonlinear fractional models and have to realize the nonlinear phenomena. Many powerful and useful ways have been introduced to solve the exact solution of nonlinear fractional equations [17-18]. The Jacobi elliptic function expansion method [15-16] is an excellent way to integrate fractional nonlinear differential models.

In this research work, we start the research with s-tfEW [18] and s-WBBM [19-21] models to analyse the nonlinear phenomena Hosseini and Ayati [18] presented exact solutions of the s-tfEW with the help of Kudrayshov method. Benjamin-Bona-Mohony introduces the BBM equation [19]. Then Wazwaz modified this equation to WBBM [20]. This script considers the Jacobi elliptic function expansion method to integrate the s-tfEW and s-tfWBBM models for deriving exact solutions. This technique also bases on the homogeneous balance method which is an influential procedure for achieving solutions of fractional PDE introduced by Zhang and Zhang [17]. According to this method, fractional complex transform and some useful formulas of fractional beta-derivative [21-25] are applied to transform the nonlinear s-tfEW equation to ordinary differential equation.

2. Beta-fractional derivative

Let us review the beta-derivative [21-25] as follows:

Definition 1 Let $\phi : [a, \infty) \to \Re$, then the fractional beta-derivative of ϕ of order β is defined as

$D^{\eta}(\phi)(x) = \lim_{\varepsilon \to 0} \dfrac{\phi(x+\varepsilon(x+\frac{1}{\Gamma(\beta)})^{1-\beta}) - \phi(x)}{\varepsilon}$, for all $x \geq a$, $\beta \in (0, 1]$. If the limit of the above exists, then $\phi(x)$ is said to be beta-differentiable.

Some properties of the derivative for the functions $\phi(x)$ and $\psi(x)$

(i). $D^{\beta}(m\phi(x)+n\psi(x)) = mD^{\beta}\phi(x)+nD^{\beta}\psi(x)$, where a and b are constants.

(ii). $D^{\beta}x^{\alpha} = \alpha(x+\frac{1}{\Gamma(\beta)})^{\alpha-\beta}$. $\alpha \in \Re$.

(iii). $D^{\beta}(\phi\psi) = \phi D^{\beta}(\psi)+\psi D^{\beta}(\phi)$.

(iv). $D^{\beta}(\frac{\phi}{\psi}) = \dfrac{\psi D^{\beta}(\phi)-\phi D^{\beta}(\psi)}{\psi^{2}}$, where $\psi \neq 0$.

(v). $D^{\beta}(c) = 0$, where c is a constant.

Here $D^{\beta}(\psi(x)) = (x+\frac{1}{\Gamma(\beta)})^{1-\beta}\frac{d\psi}{dx}$.

Definition 2 Let $\phi : [0, \infty) \to \Re$ such that ϕ is differentiable. Let $\psi(x)$ be another function defined the same range of $\phi(x)$ and also differentiable. Then, the two functions satisfied the following rule [19]:

$$D^{\beta}(\phi o \psi) = (x+\frac{1}{\Gamma(\beta)})^{1-\beta}\psi(x)'\phi'(\psi(x)).$$

3. The Jacobi elliptic function expansion method

Consider a given nonlinear wave equation

$$\mathrm{N}(\varphi, D_t^{\gamma_2}\varphi, D_x^{\gamma_1}\varphi, D_t^{2\gamma_2}\varphi, D_x^{2\gamma_1}\varphi....) = 0. \tag{1}$$

The function $\varphi = \varphi(x, t)$ is unknown wave surface and N is a function of $\varphi = \varphi(x, t)$ and its highest order fractional derivatives.

We seek its wave transformation

$$\varphi = \varphi(\xi),\ \xi = \frac{k}{\Gamma(\gamma_1)}x^{\gamma_1} - \frac{c}{\Gamma(\gamma_2)}t^{\gamma_2}. \tag{2}$$

The symbols k the wave number and c wave speed.

By using the above transformation Eq. (2), the fractional nonlinear Eq. (1) is converted to the following ordinary differential equation;

$$P(\varphi,\ \varphi',\ \varphi'',\ \varphi''' \ldots\ldots\ldots). \tag{3}$$

In [17], $\varphi(\xi)$ is a trail solution in the form of Jacobi elliptic sine function $sn(\xi)$,

$$\varphi(\xi) = a_0 + \sum_{i=1}^{n} a_i sn^i(\xi) + \sum_{i=1}^{n} b_i sn^{-i}(\xi). \tag{4}$$

$sn(\xi)$ is Jacobi elliptic sine function, and its highest degree is

$$\mathrm{P}(\varphi(\xi)) = n. \tag{5}$$

$$\mathrm{P}(\frac{d\varphi}{d\xi}) = n+1,\ \mathrm{P}(\varphi\frac{d\varphi}{d\xi}) = 2n+1,\ \mathrm{P}(\frac{d^2\varphi}{d\xi^2}) = n+2, \text{ and } \mathrm{P}(\frac{d^3\varphi}{d\xi^3}) = n+3. \tag{6}$$

Thus, we can consider n in Eq. (4) to homogenous balance from the terms of the highest order of derivative term and nonlinear.

Here, $cn(\xi)$ and $dn(\xi)$ are the Jacobi elliptic cosine function and the Jacobi elliptic functions respectively.

And

$$cn^2(\xi) = 1 - sn^2(\xi),\ dn^2(\xi) = 1 - m^2 sn^2(\xi), \text{ where } m\,(0 < m < 1). \tag{7}$$

$$\frac{d}{d\xi}(sn(\xi)) = cn(\xi)dn(\xi),\ \frac{d}{d\xi}(cn(\xi)) = -sn(\xi)dn(\xi). \tag{8}$$

$$\frac{d}{d\xi}(dn(\xi)) = -m^2 sn(\xi)cn(\xi). \tag{9}$$

We know that, when $m \to 1$, and $m \to 0$, then $sn(\xi) \to \tanh(\xi)$ and $sn(\xi) \to \sin(\xi)$ respectively. Thus, using Eq. (4) and its derivatives along with Eq. (7) and Eq. (8) into Eq. (3), we achieve a set of equations with unknown parameters. Solve the system for the unknown parameters. Using the parameters, the series solution of Eq. (4) is determined in terms of Jacobi elliptic functions.

We can convert the Jacobi elliptic sine function to solitonic and periodic function by selecting the conditions $m \to 1$, and $m \to 0$ respectively.

4. Application of the method

In this section, we apply Jacobi Elliptic Expansion function method to the s-tfEW and the s-tfWBBM models.

4.1 *Solutions of s-tfEW equation*

The space-time fractional EW(s-tfEW) equation [18] read as:

$$D_t^{\beta}\varphi(x,t)+\varepsilon D_x^{\beta}\varphi^2(x,t)-\delta D_{xxt}^{3\beta}\varphi(x,t)=0,\ t>0,\ 0<\beta\le 1. \tag{10}$$

Introducing a travelling wave transformation for s-tfEW model Eq. (10)

$$\varphi(x,t)=f(\xi),\ \xi=\frac{k}{\Gamma(\beta)}x^{\beta}-\frac{c}{\Gamma(\beta)}t^{\beta}. \tag{11}$$

Eq. (11) converts nonlinear partial differential Eq. (10) to the following nonlinear ordinary differential equation (ODE),

$$-cf'+\varepsilon k(f^2)'+\delta ck^2f'''=0. \tag{12}$$

Integrating Eq. (12) with respect to ξ, then the equation converted to the nonlinear ODE Eq. (13),

$$-cf+\varepsilon kf^2+\delta ck^2f''=0. \tag{13}$$

Using the balancing role (f^2 with f'') in Eq. (13) gives $n=2$. Now, choose an auxiliary solution for the balance number.

$$f(\xi)=a_0+a_1sn(\xi)+a_2sn^2(\xi)+b_1sn^{-1}(\xi)+b_2sn^{-2}(\xi). \tag{14}$$

Inserting $f(\xi)$ from Eq. (14) to the Eq. (13), then equating adjacent terms of $sn^i(\xi)$ to zero and solve these terms for a_0, a_1, a_2, b_1 and b_2, we get

Case-1:

$$k=\frac{1}{2\sqrt{d}\sqrt[4]{m^4+14m^2+1}},\ a_0=\frac{c\sqrt{d}(m^2+1-2\sqrt{(m^4+14m^2+1)})}{\varepsilon\sqrt[4]{m^4+14m^2+1}},$$

$$a_2=-\frac{3c\sqrt{d}m^2}{\sqrt[4]{m^4+14m^2+1}},\ b_2=-\frac{3c\sqrt{d}}{\varepsilon\sqrt[4]{m^4+14m^2+1}},\ a_1=0,\ b_1=0.$$

Case-2:

$$k=-\frac{1}{2\sqrt{d}\sqrt[4]{m^4+14m^2+1}},\ a_0=-\frac{c\sqrt{d}(m^2+1-2\sqrt{(m^4+14m^2+1)})}{\varepsilon\sqrt[4]{m^4+14m^2+1}},$$

$$a_2 = \frac{3c\sqrt{d}m^2}{\sqrt[4]{m^4+14m^2+1}},\ b_2 = \frac{3c\sqrt{d}}{\varepsilon\sqrt[4]{m^4-m^2+1}},\ a_1 = 0,\ b_1 = 0.$$

Case-3:

$$k = \frac{1}{2\sqrt{d}\sqrt[4]{m^4-m^2+1}},\ a_0 = \frac{c\sqrt{d}(m^2+1-2\sqrt{(m^4-m^2+1)})}{\varepsilon\sqrt[4]{m^4-m^2+1}},$$

$$b_2 = -\frac{3c\sqrt{d}}{\varepsilon\sqrt[4]{m^4-m^2+1}},\ a_1 = 0,\ a_2 = 0,\ b_1 = 0.$$

Case-4:

$$k = -\frac{1}{2\sqrt{d}\sqrt[4]{m^4-m^2+1}},\ a_0 = -\frac{c\sqrt{d}(m^2+1-2\sqrt{(m^4-m^2+1)})}{\varepsilon\sqrt[4]{m^4-m^2+1}},$$

$$b_2 = \frac{3c\sqrt{d}}{\varepsilon\sqrt[4]{m^4-m^2+1}},\ a_1 = 0,\ a_2 = 0,\ b_1 = 0.$$

Case:-5:

$$k = \frac{1}{2\sqrt{d}\sqrt[4]{m^4-m^2+1}},\ a_0 = \frac{c\sqrt{d}(m^2+1-2\sqrt{(m^4-m^2+1)})}{\varepsilon\sqrt[4]{m^4-m^2+1}},$$

$$a_2 = -\frac{3c\sqrt{d}m^2}{\varepsilon\sqrt[4]{m^4-m^2+1}},\ a_1 = 0,\ b_1 = 0,\ b_2 = 0.$$

Case-6:

$$k = -\frac{1}{2\sqrt{d}\sqrt[4]{m^4-m^2+1}},\ a_0 = -\frac{c\sqrt{d}(m^2+1-2\sqrt{(m^4-m^2+1)})}{\varepsilon\sqrt[4]{m^4-m^2+1}},$$

$$a_2 = \frac{3c\sqrt{d}m^2}{\varepsilon\sqrt[4]{m^4-m^2+1}},\ a_1 = 0,\ b_1 = 0,\ b_2 = 0.$$

Eq. (10) are reduced the following exact solutions by using (case-1-6)

$$\varphi(x,t)=\frac{c\sqrt{d}\,(m^2+1-2\sqrt{m^4+14m^2+1})}{\varepsilon\sqrt[4]{m^4+14m^2+1}}-\frac{3c\sqrt{d}\,m^2}{\sqrt[4]{m^4+14m^2+1}}sn^2\Big(\frac{1}{2\sqrt{d}\sqrt[4]{m^4+14m^2+1}}\frac{1}{\Gamma(\beta)}x^{\beta}-\frac{c}{\Gamma(\beta)}t^{\beta}\Big)$$

$$-\frac{3c\sqrt{d}}{\varepsilon\sqrt[4]{m^4+14m^2+1}}sn^{-2}\Big(\frac{1}{2\sqrt{d}\sqrt[4]{m^4+14m^2+1}}\frac{1}{\Gamma(\beta)}x^{\beta}-\frac{c}{\Gamma(\beta)}t^{\beta}\Big). \tag{15}$$

$$\varphi(x,t)=-\frac{c\sqrt{d}\,(m^2+1-2\sqrt{m^4+14m^2+1})}{\varepsilon\sqrt[4]{m^4+14m^2+1}}+\frac{3c\sqrt{d}\,m^2}{\sqrt[4]{m^4+14m^2+1}}sn^2\Big(-\frac{1}{2\sqrt{d}\sqrt[4]{m^4+14m^2+1}}\frac{1}{\Gamma(\beta)}x^{\beta}-\frac{c}{\Gamma(\beta)}t^{\beta}\Big)$$

$$+\frac{3c\sqrt{d}}{\varepsilon\sqrt[4]{m^4+14m^2+1}}sn^{-2}\Big(-\frac{1}{2\sqrt{d}\sqrt[4]{m^4+14m^2+1}}\frac{1}{\Gamma(\beta)}x^{\beta}-\frac{c}{\Gamma(\beta)}t^{\beta}\Big). \tag{16}$$

$$\varphi(x,t)=\frac{c\sqrt{d}\,(m^2+1-2\sqrt{m^4-m^2+1})}{\varepsilon\sqrt[4]{m^4-m^2+1}}-\frac{3c\sqrt{d}}{\varepsilon\sqrt[4]{m^4-m^2+1}}sn^{-2}\Big(\frac{1}{2\sqrt{d}\sqrt[4]{m^4-m^2+1}}\frac{1}{\Gamma(\beta)}x^{\beta}-\frac{c}{\Gamma(\beta)}t^{\beta}\Big). \tag{17}$$

$$\varphi(x,t)=-\frac{c\sqrt{d}\,(m^2+1-2\sqrt{m^4-m^2+1})}{\varepsilon\sqrt[4]{m^4-m^2+1}}+\frac{3c\sqrt{d}}{\varepsilon\sqrt[4]{m^4-m^2+1}}sn^{-2}\Big(-\frac{1}{2\sqrt{d}\sqrt[4]{m^4-m^2+1}}\frac{1}{\Gamma(\beta)}x^{\beta}-\frac{c}{\Gamma(\beta)}t^{\beta}\Big). \tag{18}$$

$$\varphi(x,t)=\frac{c\sqrt{d}\,(m^2+1+\sqrt{m^4-m^2+1})}{\varepsilon\sqrt[4]{m^4-m^2+1}}-\frac{3c\sqrt{d}\,m^2}{\varepsilon\sqrt[4]{m^4-m^2+1}}sn^{2}\Big(\frac{1}{2\sqrt{d}\sqrt[4]{m^4-m^2+1}}\frac{1}{\Gamma(\beta)}x^{\beta}-\frac{c}{\Gamma(\beta)}t^{\beta}\Big). \tag{19}$$

$$\varphi(x,t)=-\frac{c\sqrt{d}\,(m^2+1+\sqrt{m^4-m^2+1})}{\varepsilon\sqrt[4]{m^4-m^2+1}}+\frac{3c\sqrt{d}\,m^2}{\varepsilon\sqrt[4]{m^4-m^2+1}}sn^{2}\Big(-\frac{1}{2\sqrt{d}\sqrt[4]{m^4-m^2+1}}\frac{1}{\Gamma(\beta)}x^{\beta}-\frac{c}{\Gamma(\beta)}t^{\beta}\Big). \tag{20}$$

Eq. (15-20) represent the solutions in term of Jacobi elliptic function.
When $m\to 1$, the solutions Eq. (15-20) convert in the form,

$$\varphi(x,t)=-\frac{3c\sqrt{d}}{\varepsilon}-\frac{3c\sqrt{d}}{2}\tanh^2\Big(\frac{1}{4\sqrt{d}}\frac{1}{\Gamma(\beta)}x^{\beta}-\frac{c}{\Gamma(\beta)}t^{\beta}\Big)-\frac{3c\sqrt{d}}{2\varepsilon}\tanh^{-2}\Big(\frac{1}{4\sqrt{d}}\frac{1}{\Gamma(\beta)}x^{\beta}-\frac{c}{\Gamma(\beta)}t^{\beta}\Big). \tag{21}$$

$$\varphi(x,t)=\frac{3c\sqrt{d}}{\varepsilon}+\frac{3c\sqrt{d}}{2}\tanh^2\Big(-\frac{1}{4}\frac{1}{\Gamma(\beta)}x^{\beta}-\frac{c}{\Gamma(\beta)}t^{\beta}\Big)+\frac{3c\sqrt{d}}{2\varepsilon}\tanh^{-2}\Big(-\frac{1}{4\sqrt{d}}\frac{1}{\Gamma(\beta)}x^{\beta}-\frac{c}{\Gamma(\beta)}t^{\beta}\Big). \tag{22}$$

$$\varphi(x,t) = -\frac{3c\sqrt{d}}{\varepsilon}\tanh^{-2}(\frac{1}{2\sqrt{d}}\frac{1}{\Gamma(\beta)}x^{\beta} - \frac{c}{\Gamma(\beta)}t^{\beta}). \tag{23}$$

$$\varphi(x,t) = \frac{3c\sqrt{d}}{\varepsilon}\tanh^{-2}(-\frac{1}{2\sqrt{d}}\frac{1}{\Gamma(\beta)}x^{\beta} - \frac{c}{\Gamma(\beta)}t^{\beta}). \tag{24}$$

$$\varphi(x,t) = -\frac{3c\sqrt{d}}{\varepsilon}\tanh^{2}(\frac{1}{2\sqrt{d}}\frac{1}{\Gamma(\beta)}x^{\beta} - \frac{c}{\Gamma(\beta)}t^{\beta}). \tag{25}$$

$$\varphi(x,t) = \frac{3c\sqrt{d}}{\varepsilon}\tanh^{2}(-\frac{1}{2\sqrt{d}}\frac{1}{\Gamma(\beta)}x^{\beta} - \frac{c}{\Gamma(\beta)}t^{\beta}). \tag{26}$$

Solitary wave solutions Eq. (21-26) come in terms of hyperbolic functions form.
When $m \to 0$, the solutions Eq. (15-20) convert in the form,

$$\varphi(x,t) = -\frac{c\sqrt{d}}{\varepsilon} - \frac{3c\sqrt{d}}{\varepsilon}\sin^{-2}(\frac{1}{2\sqrt{d}}\frac{1}{\Gamma(\beta)}x^{\beta} - \frac{c}{\Gamma(\beta)}t^{\beta}). \tag{27}$$

$$\varphi(x,t) = \frac{c\sqrt{d}}{\varepsilon} + \frac{3c\sqrt{d}}{\varepsilon}\sin^{-2}(-\frac{1}{2\sqrt{d}}\frac{1}{\Gamma(\eta)}x^{\eta} - \frac{c}{\Gamma(\eta)}t^{\eta}). \tag{28}$$

$$\varphi(x,t) = -\frac{c\sqrt{d}}{\varepsilon} - \frac{3c\sqrt{d}}{\varepsilon}\sin^{-2}(\frac{1}{2\sqrt{d}}\frac{1}{\Gamma(\beta)}x^{\beta} - \frac{c}{\Gamma(\beta)}t^{\beta}). \tag{29}$$

$$\varphi(x,t) = \frac{c\sqrt{d}}{\varepsilon} + \frac{3c\sqrt{d}}{\varepsilon}\sin^{-2}(-\frac{1}{2\sqrt{d}}\frac{1}{\Gamma(\beta)}x^{\beta} - \frac{c}{\Gamma(\beta)}t^{\beta}). \tag{30}$$

These are periodic wave solutions of the nonlinear-tfEW model and the other two solutions (19), (20) give constants only.

4.2 *Solutions of the WBBM model*

The space-time fractional WBBM equation [21] read as:

$$D_t^{\beta}\varphi(x,y,z,t) + D_x^{\beta}\varphi(x,y,z,t) + D_y^{\beta}\varphi(x,y,z,t) - D_{xzt}^{3\beta}\varphi(x,y,z,t) = 0,\ t > 0,\ 0 < \beta \le 1. \tag{31}$$

Considering a travelling wave transformation for space-time fractional 3D WBBM model Eq. (31)

$$\varphi(x,t) = \varphi(\zeta),\ \zeta = \frac{1}{\Gamma(\beta)}(\ell x^{\beta} + \wp y^{\beta} + cz^{\beta} - wt^{\beta}). \tag{32}$$

Eq. (32) transform the WBBM Eq. (31) to the following nonlinear ODE,

$$(-w+\ell)\phi' + \wp(\phi^3)' + \ell cw\phi''' = 0. \tag{33}$$

Integrating Eq. (33) with respect to ζ, then Eq. (31) converted to the nonlinear ODE Eq. (34),

$$(-w+\ell)\phi + \wp\phi^3 + \ell cw\phi'' = 0. \tag{34}$$

Using the balancing role (ϕ^2 with ϕ'') in Eq. (34) gives $n = 1$. Now, choose an auxiliary solution for the balance number.

$$\phi(\zeta) = a_0 + a_1 sn(\zeta) + b_1 sn^{-1}(\zeta). \tag{35}$$

Plugging $\phi(\zeta)$ from Eq. (35) to the Eq. (34), then comparing the adjacent terms of $sn^i(\zeta)$ to zero and solving these algebraic equations for a_0, a_1, w and b_1, we get four sets of solutions.

Case-1:

$$w = \frac{\ell}{\ell cm^2 - 6\ell cm + \ell c + 1},\ a_0 = 0,\ a_1 = \pm\ell m\sqrt{\frac{-2c}{\wp(\ell cm^2 - 6\ell cm + \ell c + 1)}},\ b_2 = \pm\ell\sqrt{\frac{-2c}{\wp(\ell cm^2 - 6\ell cm + \ell c + 1)}}.$$

Case-2:

$$w = \frac{\ell}{\ell cm^2 + 6\ell cm + \ell c + 1},\ a_0 = 0,\ a_1 = \pm\ell m\sqrt{\frac{-2c}{\wp(\ell cm^2 + 6\ell cm + \ell c + 1)}},\ b_2 = \pm\ell\sqrt{\frac{-2c}{\wp(\ell cm^2 + 6\ell cm + \ell c + 1)}}.$$

Case-3:

$$w = \frac{\ell}{\ell cm^2 + \ell c + 1},\ a_0 = 0,\ a_1 = 0,\ b_2 = \pm\ell\sqrt{\frac{-2c}{\wp(\ell cm^2 + \ell c + 1)}}.$$

Case-4:

$$w = \frac{\ell}{\ell cm^2 + \ell c + 1},\ a_0 = 0,\ b_1 = 0,\ a_1 = \pm\ell m\sqrt{\frac{-2c}{\wp(\ell cm^2 + \ell c + 1)}}.$$

The exact solutions of Eq. (31) by using (case-1-4)

$$\varphi_{11}(x,t) = \ell\sqrt{\frac{-2c}{\wp(\ell cm^2 - 6\ell cm + \ell c + 1)}}\left\{\begin{array}{l} -msn\left(\frac{1}{\Gamma(\beta)}(\ell x^\beta + \wp y^\beta + cz^\beta - wt^\beta)\right) \\ +sn^{-1}\left(\frac{1}{\Gamma(\beta)}(\ell x^\beta + \wp y^\beta + cz^\beta - wt^\beta)\right) \end{array}\right\}. \tag{36}$$

$$\varphi_{12}(x,t)=\ell\sqrt{\frac{-2c}{\wp(\ell cm^2-6\ell cm+\ell c+1)}}\begin{Bmatrix} msn(\frac{1}{\Gamma(\beta)}(\ell x^\beta+\wp y^\beta+cz^\beta-wt^\beta)) \\ -sn^{-1}(\frac{1}{\Gamma(\beta)}(\ell x^\beta+\wp y^\beta+cz^\beta-wt^\beta)) \end{Bmatrix}. \quad (37)$$

In Eq. (36) and Eq. (37), $w=\frac{\ell}{\ell cm^2-6\ell cm+\ell c+1}$.

$$\varphi_{13}(x,t)=\ell\sqrt{\frac{-2c}{\wp(\ell cm^2+6\ell cm+\ell c+1)}}\begin{Bmatrix} msn(\frac{1}{\Gamma(\beta)}(\ell x^\beta+\wp y^\beta+cz^\beta-wt^\beta)) \\ +sn^{-1}(\frac{1}{\Gamma(\beta)}(\ell x^\beta+\wp y^\beta+cz^\beta-wt^\beta)) \end{Bmatrix}. \quad (38)$$

$$\varphi_{14}(x,t)=-\ell\sqrt{\frac{-2c}{\wp(\ell cm^2+6\ell cm+\ell c+1)}}\begin{Bmatrix} msn(\frac{1}{\Gamma(\beta)}(\ell x^\beta+\wp y^\beta+cz^\beta-wt^\beta)) \\ +sn^{-1}(\frac{1}{\Gamma(\beta)}(\ell x^\beta+\wp y^\beta+cz^\beta-wt^\beta)) \end{Bmatrix}. \quad (39)$$

In Eq. (38) and Eq. (39), $w=\frac{\ell}{\ell cm^2+6\ell cm+\ell c+1}$.

$$\varphi_{15}(x,t)=\ell\sqrt{\frac{-2c}{\wp(\ell cm^2+\ell c+1)}}sn^{-1}(\frac{1}{\Gamma(\beta)}(\ell x^\beta+\wp y^\beta+cz^\beta-wt^\beta)). \quad (40)$$

$$\varphi_{16}(x,t)=-\ell\sqrt{\frac{-2c}{\wp(\ell cm^2+\ell c+1)}}sn^{-1}(\frac{1}{\Gamma(\beta)}(\ell x^\beta+\wp y^\beta+cz^\beta-wt^\beta)). \quad (41)$$

$$\varphi_{17}(x,t)=\ell m\sqrt{\frac{-2c}{\wp(\ell cm^2+\ell c+1)}}sn(\frac{1}{\Gamma(\beta)}(\ell x^\beta+\wp y^\beta+cz^\beta-wt^\beta)). \quad (42)$$

$$\varphi_{18}(x,t)=-\ell m\sqrt{\frac{-2c}{\wp(\ell cm^2+\ell c+1)}}sn(\frac{1}{\Gamma(\beta)}(\ell x^\beta+\wp y^\beta+cz^\beta-wt^\beta)). \quad (43)$$

In Eq. (40), Eq. (41), Eq. (42) and Eq. (43), $w=\frac{\ell}{\ell cm^2+\ell c+1}$.

Eq. (36-43) represent the Jacobi elliptic function solutions of Eq. (31).

When $m\to 1$, the solutions Eq. (36-43) convert to the following form,

$$\varphi_{19}(x,t)=\ell\sqrt{\frac{-2c}{\wp(1-4\ell c)}}\left\{\begin{array}{l}-\tanh(\frac{1}{\Gamma(\beta)}(\ell x^{\beta}+\wp y^{\beta}+cz^{\beta}-wt^{\beta}))\\+\coth(\frac{1}{\Gamma(\beta)}(\ell x^{\beta}+\wp y^{\beta}+cz^{\beta}-wt^{\beta}))\end{array}\right\}. \tag{44}$$

$$\varphi_{19}(x,t)=\ell\sqrt{\frac{-2c}{\wp(1-4\ell c)}}\left\{\begin{array}{l}\tanh(\frac{1}{\Gamma(\beta)}(\ell x^{\beta}+\wp y^{\beta}+cz^{\beta}-wt^{\beta}))\\-\coth(\frac{1}{\Gamma(\beta)}(\ell x^{\beta}+\wp y^{\beta}+cz^{\beta}-wt^{\beta}))\end{array}\right\}. \tag{45}$$

In Eq. (44) and Eq. (45), $w=\frac{\ell}{(1-4\ell c)}$.

$$\varphi_{20}(x,t)=\ell\sqrt{\frac{-2c}{\wp(1+8\ell cm)}}\left\{\begin{array}{l}\tanh(\frac{1}{\Gamma(\beta)}(\ell x^{\beta}+\wp y^{\beta}+cz^{\beta}-wt^{\beta}))\\+\coth(\frac{1}{\Gamma(\beta)}(\ell x^{\beta}+\wp y^{\beta}+cz^{\beta}-wt^{\beta}))\end{array}\right\}. \tag{46}$$

$$\varphi_{21}(x,t)=-\ell\sqrt{\frac{-2c}{\wp(1+8\ell c)}}\left\{\begin{array}{l}\tanh(\frac{1}{\Gamma(\beta)}(\ell x^{\beta}+\wp y^{\beta}+cz^{\beta}-wt^{\beta}))\\+\coth(\frac{1}{\Gamma(\beta)}(\ell x^{\beta}+\wp y^{\beta}+cz^{\beta}-wt^{\beta}))\end{array}\right\}. \tag{47}$$

In Eq. (46) and Eq. (47) carry the value of $w=\frac{\ell}{(1+8\ell c)}$.

$$\varphi_{22}(x,t)=\ell\sqrt{\frac{-2c}{\wp(1+2\ell c)}}\coth(\frac{1}{\Gamma(\beta)}(\ell x^{\beta}+\wp y^{\beta}+cz^{\beta}-wt^{\beta})). \tag{48}$$

$$\varphi_{23}(x,t)=-\ell\sqrt{\frac{-2c}{\wp(1+2\ell c)}}\coth(\frac{1}{\Gamma(\beta)}(\ell x^{\beta}+\wp y^{\beta}+cz^{\beta}-wt^{\beta})). \tag{49}$$

$$\varphi_{25}(x,t)=-\ell\sqrt{\frac{-2c}{\wp(1+2\ell c)}}\tanh(\frac{1}{\Gamma(\beta)}(\ell x^{\beta}+\wp y^{\beta}+cz^{\beta}-wt^{\beta})). \tag{50}$$

In Eq. (48), Eq. (49) and Eq. (50), $w=\frac{\ell}{(1+2\ell c)}$.

Solitary wave solutions come from the hyperbolic functions Eq. (44-50).
When $m\to 0$, the solutions Eq. (36-43) convert to the form,

$$\varphi_{25}(x,t) = \ell\sqrt{\frac{-2c}{\wp(1+\ell c)}}\left\{\cos ec\left(\frac{1}{\Gamma(\beta)}(\ell x^{\beta} + \wp y^{\beta} + cz^{\beta} - wt^{\beta})\right)\right\}. \tag{51}$$

$$\varphi_{26}(x,t) = \ell\sqrt{\frac{-2c}{\wp(1+\ell c)}}\left\{-\cos ec\left(\frac{1}{\Gamma(\beta)}(\ell x^{\beta} + \wp y^{\beta} + cz^{\beta} - wt^{\beta})\right)\right\}. \tag{52}$$

$$\varphi_{27}(x,t) = -\ell\sqrt{\frac{-2c}{\wp(1+\ell c)}}\left\{\cos ec\left(\frac{1}{\Gamma(\beta)}(\ell x^{\beta} + \wp y^{\beta} + cz^{\beta} - wt^{\beta})\right)\right\}. \tag{53}$$

In Eq. (51), Eq. (52) and Eq. (53), $w = \frac{\ell}{(1+\ell c)}$.

Eq. (36)-Eq. (43) are Jacobi functions solution of the nonlinear WBBM model. Out of the eight Jacobi elliptic functions, three of them are repeated and two results give zero solution. So, these five solutions are neglected.

5. Graphical representation

In this section, we will provide some graphical representations of the exact solutions of the space-time fractional Equal Width(s-tfEW) equation (Eq. (10)) and the space-time fractional Wazwaz-Benjamin-Bona-Mahony (s-tfWBBM) model (Eq. (31)). Graphical representations are portrayed below using the selected exact solutions of EW and WBBM model.

5.1 *Graphics of the solutions of s-tfEW equation*

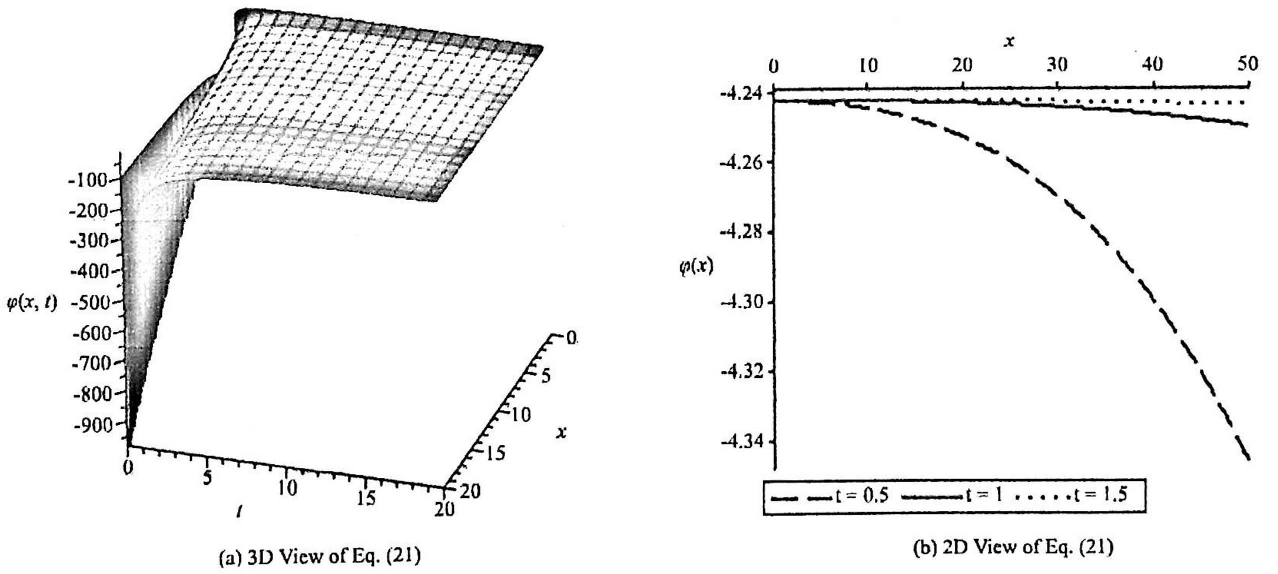

(a) 3D View of Eq. (21)

(b) 2D View of Eq. (21)

Figure 1. Represent the solitary wave $\varphi(x, t)$ in Eq. (21) for the physical parametric values, $d = 0.5$, $\beta = 1/6$, $c = 1$, $\varepsilon = 1$: (a) 3D surface, (b) 2D graphs at $t = 0.5, 1, 1.5$.

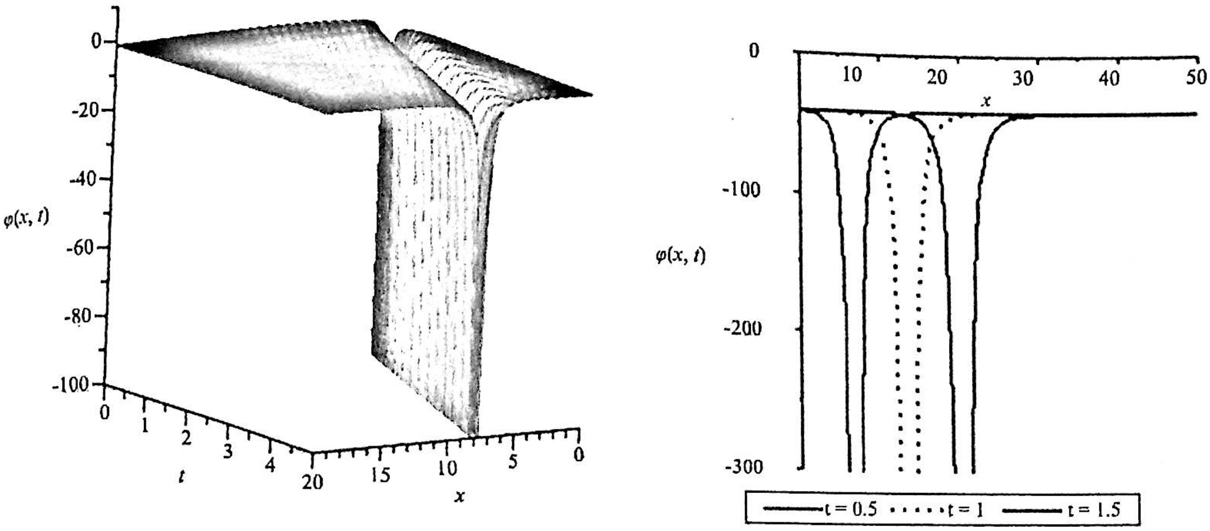

(a) 3D View of Eq. (23)

(b) 2D View of Eq. (23)

Figure 2. Represent the solitary wave $\varphi(x, t)$ in Eq. (23) for the physical parametric values, $d = 0.5$, $\beta = 3/4$, $c = 5$, $\varepsilon = 2$: (a) 3D surface and (b) 2D graphs at $t = 0.5, 1, 1.5$.

Three types of results are achieved for EW equation. All of the results are analysed and some of them are depicted in Figures (1-4). The graphs signify the change of amplitude, direction, shape of the derived wave solutions to identify the intrinsic nature of the model. The solution $\varphi(x, t)$ in Eq. (15-20) represents the Jacobi elliptic functions Eq. (21-26) shows the solitonic nature comes from hyperbolic function and Eq. (27-30) are trigonometric function exhibit as periodic waves.

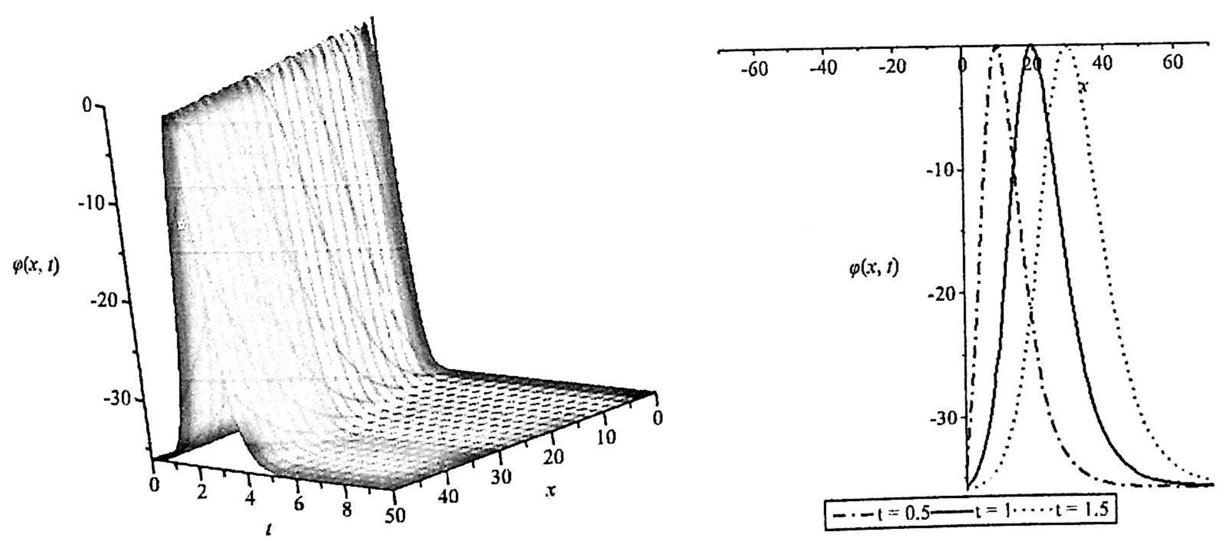

(b) 2D View of Eq. (25)

(a) 3D View of Eq. (25)

Figure 3. Represent the bell type solitary wave $\varphi(x, t)$ in Eq. (25) for the physical parametric values, $d = 1$, $\beta = 3/5$, $c = 3$, $\varepsilon = 0.25$: (a) 3D surface and (b) 2D graphs for and $t = 0.5, 1, 1.5$.

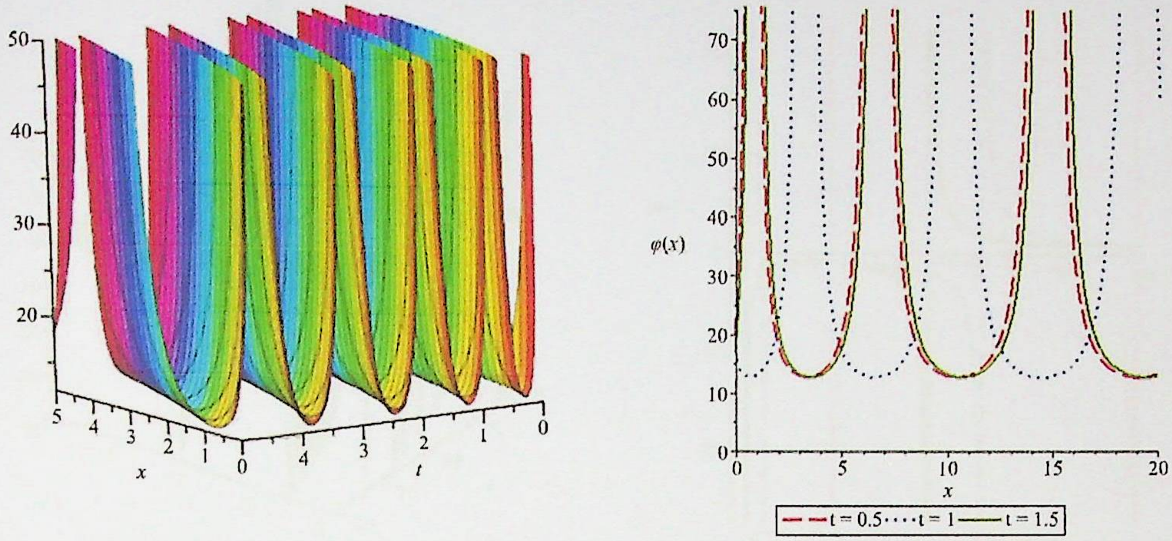

(a) 3D View of Eq. (27)

(b) 2D View of Eq. (27)

Figure 4. Represent the periodic wave of $\varphi(x, t)$ in Eq. (27) for the physical parametric values, $d = 0.5$, $\beta = 3/4$, $c = -3$, $\varepsilon = 1$: (a) 3D surface and (b) 2D graphs at $t = 0.5, 1, 1.5$.

5.2 *Graphics of the equation WBBM*

The findings of the research on WBBM model are in the types of hyperbolic (Eq. (44-51)) and trigonometric (Eq. (52-55)) functions. Hyperbolic and trigonometric functions represent solitonic and periodic solutions. All the results are analysed and two types of function have been shown graphically in Figure 5 to Figure 6.

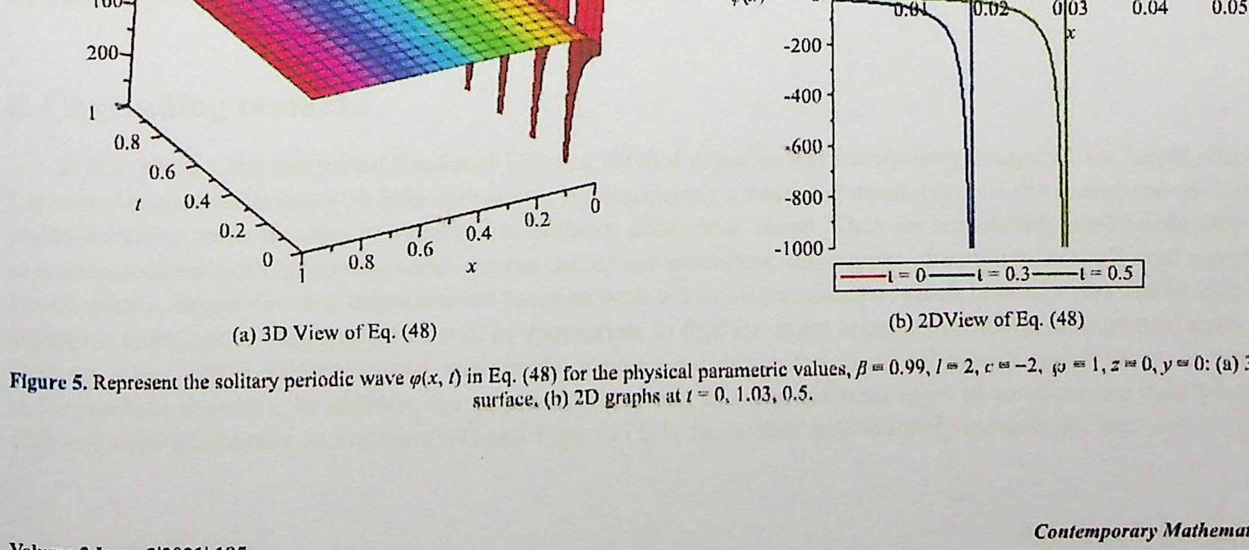

(a) 3D View of Eq. (48)

(b) 2DView of Eq. (48)

Figure 5. Represent the solitary periodic wave $\varphi(x, t)$ in Eq. (48) for the physical parametric values, $\beta = 0.99$, $l = 2$, $c = -2$, $\wp = 1$, $z = 0$, $y = 0$: (a) 3D surface, (b) 2D graphs at $t = 0, 1.03, 0.5$.

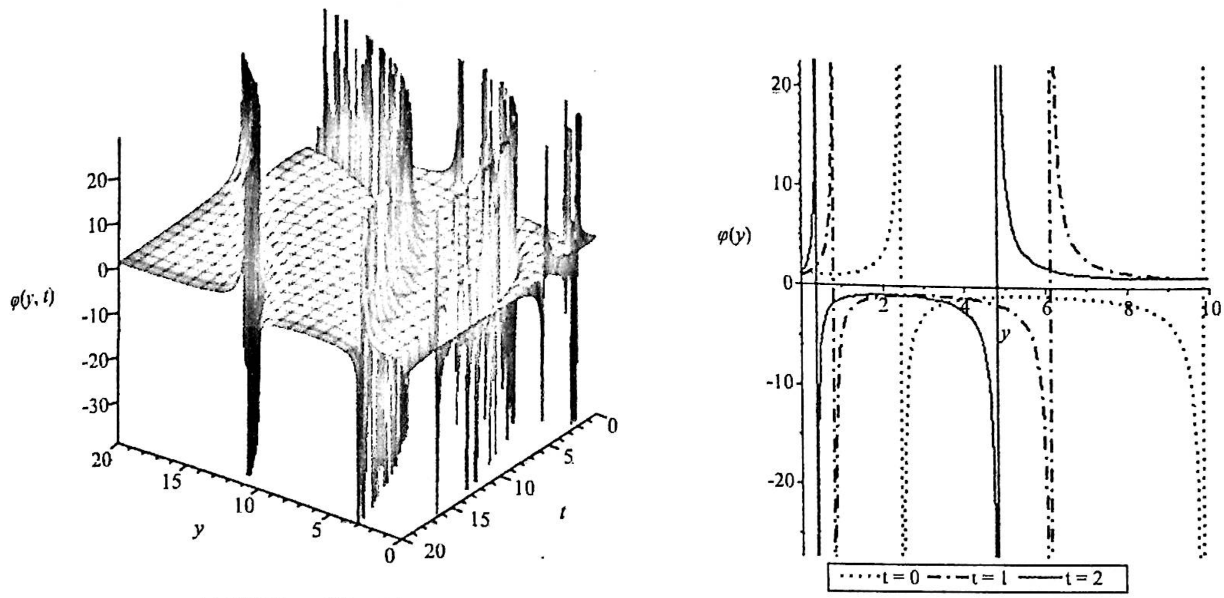

(a) 3D View of Eq. (52)

(b) 3D View of Eq. (52)

Figure 6. Represent the periodic wave $\varphi(x, t)$ in Eq. (52) for the physical parametric values, $\beta = 0.5, l = 2, c = -2, \wp = 1, z = 0, x = 0$: (a) 3D surface, (b) 2D graphs at $t = 0, 1.2$.

Remarks More other Jacobi function solutions to the s-tfEW and WBBM equation are derivable by keeping the trial solution in terms of the Jacobi functions $cn(\xi)$ and $dn(\xi)$ as below;

$$u(\xi) = a_0 + \sum_{i \to 1}^{n} a_i cn^i(\xi) + \sum_{i \to 1}^{n} a_{-i} cn^{-i}(\xi). \tag{54}$$

And

$$u(\xi) = a_0 + \sum_{i \to 1}^{n} a_i dn^i(\xi) + \sum_{i \to 1}^{n} a_{-i} dn^{-i}(\xi). \tag{55}$$

In view of Eq. (54) and Eq. (55), we can add soliton and non-solitonic solutions describe via cnoidal, dnoidal waves and trigonometric functions.

6. Concluding remarks

In this portion, the space-time fractional EW and WBBM equation has successfully integrated via Jacobi elliptic function expansion technique with beta-derivatives. By introducing a fractional transformation, the considered nonlinear partial travelling wave equation was reduced to ordinary differential model. Then we successfully used Jacobi elliptic expansion method to integrate the model. At the end of our procedure, three types of solutions are achieved namely, Jacobi elliptic, hyperbolic and trigonometric function with unknown parameters, which indicates that Jacobi elliptic expansion technique is very fruitful as well as appropriate to find the exact solutions of nonlinear fractional models. Here we, successfully derived cnoidal and dnoidal waves solutions to the fractional models which were not found in the previous literature. In addition, the graphical illustration of some different types of solutions has been plotted with unknown parameters in Figures (1-4) and Figures (5-6) for s-tfEW and WBBM respectively. Researchers can undoubtedly use the technique to analyse the internal mechanism of nonlinear physical systems.

Conflict of interest

Authors declared that they have no conflict of interest.

References

[1] Kara AH, Khalique CM. Nonlinear evolution-type equations and their exact solutions using inverse variational methods. *Journal of Physics A: Mathematical and General*. 2005; 38: 4629-4636.

[2] Matveev VB, Salle MA. *Darboux Transformation and Solitons*. Berlin: Springer; 1991.

[3] Ma WX, Huang T, Zhang Y. A multiple exp-function method for nonlinear differential equations and its application. *Physica Scripta*. 2010; 82: 065003.

[4] Malfliet W, Hereman W. The tanh method: I. Exact solutions of nonlinear evolution and wave equations. *Physica Scripta*. 1996; 54(6): 563-568.

[5] Rashid HO, Rahman MA. The exp$-\Phi(\eta)$-expansion method with application in the (1+1)-dimensional classical Boussinesq equation. *Result in Physics*. 2014; 4: 150-155.

[6] Feng Z. The first integral method to study the Burgers-Korteweg-de vries equation. *Journal of Physics A: Mathematical and General*. 2002; 35: 343-349.

[7] Hoque MF, Roshid HO. Optical soliton solutions of the Biswas-Arshed model by the tan(Θ/2)-expansion approach. Physica. *Scripta*. 2020; 95(7): 075219.

[8] Roshid HO, Ma WX. Dynamics of mixed lump-solitary waves of an extended (2+1)-dimensional shallow water wave model. *Physics Letter A*. 2018; 382(45): 3262-3268.

[9] Hossen MB, Roshid HO, Ali MZ. Characteristics of the solitary waves and rogue waves with interaction phenomena in a (2+1)-dimensional Breaking soliton equation. *Physics Letter A*. 2018; 382: 1268-1274.

[10] Wazwaz AM. *A* sine-cosine method for handling nonlinear wave equations. *Mathematical Computer Modelling*. 2004; 40: 499-508.

[11] Roshid HO, Alam MN, Hoque MF, Akbar MA. A new extended (G'/G)-expansion method to find exact traveling wave solutions of nonlinear evolution equations. *Mathematics and Statistics*. 2013; 1(3): 162-166.

[12] Hossen MB, Roshid HO, Ali MZ. Modified double sub-equation method for finding complexiton solutions to the (2+1)-dimensional nonlinear evolution equations. *International Journal of Applied Computational Mathematics*. 2017; 3(1): 679-697.

[13] Krishnan EV, Biswas A. Solutions to the Zakharov-Kuznetsov equation with higher order nonlinearity by mapping and ansatz methods. *Physics of Wave Phenomena*. 2010; 18(4): 256-261.

[14] Roshid HO, Khan MH, Wazwaz AM. Lump, multi-lump, cross kinky-lump and manifold periodic-soliton solutions for the (2+1)-D Calogero-Bogoyavlenskii-Schiff equation. *Heliyon*. 2020; 6(4): 03701.

[15] Dai CQ, Zhang JF. Jacobian elliptic function method for nonlinear differential-difference equations. *Chaos Soiton and Fractals*. 2006; 27: 1042-1049.

[16] Liu SK, Fu ZT, Liu SD. Jacobi elliptic function expansion method and periodic wave solutions of nonlinear wave equations. *Physics Letters A*. 2001; 289: 69-74.

[17] Zhang S, Zhang HQ. Fractional sub-equation method and its applications to nonlinear fractional PDEs. *Physics Letters A*. 2011; 375(7): 1069-1073.

[18] Hosseini K, Ayati J. Exact solutions of space-time fractional EW and modified EW equations using Kudrayshov method. *Nonlinear Science. Letter*. 2016; 7(2): 58-66.

[19] Benjamin TB, Bona JL, Mohony JJ. Model equations for long waves in nonlinear dispersive system. *Philosophical Transaction of Royel Society B Biological Sciences*. 1972; 272(1220): 47-78.

[20] Wazwaz AM. Exact soliton and kink solutions for new (3+1)-dimensional nonlinear modified equations of wave propagation. *Open Engineering*. 2017; 7: 169-174.

[21] Hosseini K, Mirzazadeh M, Ilie M, Gomez-Aguila JF. Biswas-Arshed equation with the beta time derivative: Optical solitons and other solutions. *Optik*. 2020; 217: 164801.

[22] Atangana A, Alqahtani RT. Modelling the spread of river blindness disease via the caputo fractional derivative and the beta-derivative. *Entropy*. 2016; 18: 40.

[23] Atangana A, Goufo EFD. Extension of matched asymptotic method to fractional boundary layers problems. *Mathematical Problem and Engineering*. 2014; 2014: 7. Available from: https://doi.org/10.1155/2014/107535.
[24] Hosseini K, Gomez-Aguilar JF. Soliton solutions of the sasa-satsuma equation in the monomode optical fibers including the beta-derivatives. *Optik*. 2020; 224: 165425.
[25] Hosseini K, Kaur L, Mirzazadeh M, Baskonus HM. 1-Soliton solutions of the (2+1)-dimensional Heisenberg ferromagnetic spin chain model with the beta-derivative. *Optical and Quantum Electrinics*. 2021; 53: 125.

Contemporary Mathematics
http://ojs.wiserpub.com/index.php/CM/

UNIVERSAL WISER
PUBLISHER

Research Article

Analytical Solutions of Two Space-Time Fractional Nonlinear Models Using Jacobi Elliptic Function Expansion Method

Zillur Rahman[1,2], M. Zulfikar Ali[2], Harun-Or-Roshid[2,3*], Mohammad Safi Ullah[1,2]

[1]Department of Mathematics, Comilla University, Cumilla-3506, Bangladesh
[2]Department of Mathematics, Rajshahi University, Rajshahi-6205, Bangladesh
[3]Department of Mathematics, Pabna University of Science and Technology, Pabna-6600, Bangladesh
Email: harunorroshidmd@gmail.com, rahman.zillur54@yahoo.com

Received: 17 October 2020; **Revised:** 7 April 2021; **Accepted:** 13 May 2021

Abstract: In this manuscript, the space-time fractional Equal-width (s-tfEW) and the space-time fractional Wazwaz-Benjamin-Bona-Mahony (s-tfWBBM) models have been investigated which frequently arises in nonlinear optics, solid states, fluid mechanics and shallow water. Jacobi elliptic function expansion integral technique has been used to build more innovative exact solutions of the s-tfEW and s-tfWBBM nonlinear partial models. In this research, fractional beta-derivatives are applied to convert the partial models to ordinary models. Several types of solutions have been derived for the models and performed some new solitary wave phenomena. The derived solutions have been presented in the form of Jacobi elliptic functions initially. Persevering different conditions on a parameter, we have achieved hyperbolic and trigonometric functions solutions from the Jacobi elliptic function solutions. Besides the scientific derivation of the analytical findings, the results have been illustrated graphically for clear identification of the dynamical properties. It is noticeable that the integral scheme is simplest, most conventional and convenient in handling many nonlinear models arising in applied mathematics and the applied physics to derive diverse structural precise solutions.

Keywords: space-time fractional equal width equation, space-time fractional Wazwaz-Benjamin-Bona-Mahony, balance number, fractional beta-derivative, Jacobi elliptic function expansion method, analytical solutions

1. Introduction

In the current world, fractional derivatives have been applied to study the calculus of arbitrary order for modelling of nonlinear happening in different fields like fluid mechanics, signal processing, control theory, astrophysics, dynamical systems, plasma physics, non-linear biological systems, nanotechnology, and engineering. Many real-life problems of the above areas can be modelled by Partial Differential Equation (PDE) relating to the fractional derivatives. The concept of solitons, the top decisive way in applications to such models has played an important role to identify the complex incident in various fields of sciences. Up to days, many techniques have been introduced for deriving exact wave solutions of nonlinear models but the innovation reached is deficient. The precise mathematical methods to derive different classes of exact solutions namely; the inverse variational methods [1], the Darboux Transformation [2], the Exp-function technique [3], tanh method [4], the exp(−(Φ)η)-expansion method [5], first integral scheme [6], the tan(Θ/2)-expansion approach [7], the Hirota bilinear method [8-9], the sine-cosine analysis [10], the new extended (G'/

DOI: https://doi.org/10.37256/cm.232021682

G)-expansion method [11], the modified double sub-equation method [12], the mapping and ansatz methods [13-14], the Jacobi elliptic function expansion method [15-16] as well.

Moreover, it is very problematic to derive the exact solution of nonlinear fractional PDE via the best possible method. So, it is significant to arise the explicit solutions which are exact for advanced study of these nonlinear fractional models and have to realize the nonlinear phenomena. Many powerful and useful ways have been introduced to solve the exact solution of nonlinear fractional equations [17-18]. The Jacobi elliptic function expansion method [15-16] is an excellent way to integrate fractional nonlinear differential models.

In this research work, we start the research with s-tfEW [18] and s-WBBM [19-21] models to analyse the nonlinear phenomena Hosseini and Ayati [18] presented exact solutions of the s-tfEW with the help of Kudrayshov method. Benjamin-Bona-Mohony introduces the BBM equation [19]. Then Wazwaz modified this equation to WBBM [20]. This script considers the Jacobi elliptic function expansion method to integrate the s-tfEW and s-tfWBBM models for deriving exact solutions. This technique also bases on the homogeneous balance method which is an influential procedure for achieving solutions of fractional PDE introduced by Zhang and Zhang [17]. According to this method, fractional complex transform and some useful formulas of fractional beta-derivative [21-25] are applied to transform the nonlinear s-tfEW equation to ordinary differential equation.

2. Beta-fractional derivative

Let us review the beta-derivative [21-25] as follows:

Definition 1 Let $\phi : [a, \infty) \rightarrow \Re$, then the fractional beta-derivative of ϕ of order β is defined as

$D^{\eta}(\phi)(x) = \lim_{\varepsilon \to 0} \dfrac{\phi(x+\varepsilon(x+\frac{1}{\Gamma(\beta)})^{1-\beta}) - \phi(x)}{\varepsilon}$, for all $x \geq a$, $\beta \in (0, 1]$. If the limit of the above exists, then $\phi(x)$ is said to be beta-differentiable.

Some properties of the derivative for the functions $\phi(x)$ and $\psi(x)$

(i). $D^{\beta}(m\phi(x)+n\psi(x)) = mD^{\beta}\phi(x)+nD^{\beta}\psi(x)$, where a and b are constants.

(ii). $D^{\beta}x^{\alpha} = \alpha(x+\dfrac{1}{\Gamma(\beta)})^{\alpha-\beta}$. $\alpha \in \Re$.

(iii). $D^{\beta}(\phi\psi) = \phi D^{\beta}(\psi)+\psi D^{\beta}(\phi)$.

(iv). $D^{\beta}(\dfrac{\phi}{\psi}) = \dfrac{\psi D^{\beta}(\phi)-\phi D^{\beta}(\psi)}{\psi^{2}}$, where $\psi \neq 0$.

(v). $D^{\beta}(c) = 0$, where c is a constant.

Here $D^{\beta}(\psi(x)) = (x+\dfrac{1}{\Gamma(\beta)})^{1-\beta}\dfrac{d\psi}{dx}$.

Definition 2 Let $\phi : [0, \infty) \rightarrow \Re$ such that ϕ is differentiable. Let $\psi(x)$ be another function defined the same range of $\phi(x)$ and also differentiable. Then, the two functions satisfied the following rule [19]:

$$D^{\beta}(\phi o\psi) = (x+\frac{1}{\Gamma(\beta)})^{1-\beta}\psi(x)'\phi'(\psi(x)).$$

3. The Jacobi elliptic function expansion method

Consider a given nonlinear wave equation

$$\mathrm{N}(\varphi, D_t^{\gamma_2}\varphi, D_x^{\gamma_1}\varphi, D_t^{2\gamma_2}\varphi, D_x^{2\gamma_1}\varphi....) = 0. \tag{1}$$

The function $\varphi = \varphi(x, t)$ is unknown wave surface and N is a function of $\varphi = \varphi(x, t)$ and its highest order fractional derivatives.

We seek its wave transformation

$$\varphi = \varphi(\xi),\ \xi = \frac{k}{\Gamma(\gamma_1)} x^{\gamma_1} - \frac{c}{\Gamma(\gamma_2)} t^{\gamma_2}. \tag{2}$$

The symbols k the wave number and c wave speed.

By using the above transformation Eq. (2), the fractional nonlinear Eq. (1) is converted to the following ordinary differential equation;

$$P(\varphi,\ \varphi',\ \varphi'',\ \varphi''' \ldots\ldots). \tag{3}$$

In [17], $\varphi(\xi)$ is a trail solution in the form of Jacobi elliptic sine function $sn(\xi)$,

$$\varphi(\xi) = a_0 + \sum_{i=1}^{n} a_i sn^i(\xi) + \sum_{i=1}^{n} b_i sn^{-i}(\xi). \tag{4}$$

$sn(\xi)$ is Jacobi elliptic sine function, and its highest degree is

$$\mathrm{P}(\varphi(\xi)) = n. \tag{5}$$

$$\mathrm{P}(\frac{d\varphi}{d\xi}) = n+1,\ \mathrm{P}(\varphi\frac{d\varphi}{d\xi}) = 2n+1,\ \mathrm{P}(\frac{d^2\varphi}{d\xi^2}) = n+2, \text{ and } \mathrm{P}(\frac{d^3\varphi}{d\xi^3}) = n+3. \tag{6}$$

Thus, we can consider n in Eq. (4) to homogenous balance from the terms of the highest order of derivative term and nonlinear.

Here, $cn(\xi)$ and $dn(\xi)$ are the Jacobi elliptic cosine function and the Jacobi elliptic functions respectively.

And

$$cn^2(\xi) = 1 - sn^2(\xi),\ dn^2(\xi) = 1 - m^2 sn^2(\xi), \text{ where } m\,(0 < m < 1). \tag{7}$$

$$\frac{d}{d\xi}(sn(\xi)) = cn(\xi)dn(\xi),\ \frac{d}{d\xi}(cn(\xi)) = -sn(\xi)dn(\xi). \tag{8}$$

$$\frac{d}{d\xi}(dn(\xi)) = -m^2 sn(\xi)cn(\xi). \tag{9}$$

We know that, when $m \to 1$, and $m \to 0$, then $sn(\xi) \to \tanh(\xi)$ and $sn(\xi) \to \sin(\xi)$ respectively. Thus, using Eq. (4) and its derivatives along with Eq. (7) and Eq. (8) into Eq. (3), we achieve a set of equations with unknown parameters. Solve the system for the unknown parameters. Using the parameters, the series solution of Eq. (4) is determined in terms of Jacobi elliptic functions.

We can convert the Jacobi elliptic sine function to solitonic and periodic function by selecting the conditions $m \to 1$, and $m \to 0$ respectively.

4. Application of the method

In this section, we apply Jacobi Elliptic Expansion function method to the s-tfEW and the s-tfWBBM models.

4.1 *Solutions of s-tfEW equation*

The space-time fractional EW(s-tfEW) equation [18] read as:

$$D_t^{\beta}\varphi(x,t)+\varepsilon D_x^{\beta}\varphi^2(x,t)-\delta D_{xxt}^{3\beta}\varphi(x,t)=0,\ t>0,\ 0<\beta\le 1. \tag{10}$$

Introducing a travelling wave transformation for s-tfEW model Eq. (10)

$$\varphi(x,t)=f(\xi),\ \xi=\frac{k}{\Gamma(\beta)}x^{\beta}-\frac{c}{\Gamma(\beta)}t^{\beta}. \tag{11}$$

Eq. (11) converts nonlinear partial differential Eq. (10) to the following nonlinear ordinary differential equation (ODE),

$$-cf'+\varepsilon k(f^2)'+\delta ck^2 f'''=0. \tag{12}$$

Integrating Eq. (12) with respect to ξ, then the equation converted to the nonlinear ODE Eq. (13),

$$-cf+\varepsilon kf^2+\delta ck^2 f''=0. \tag{13}$$

Using the balancing role (f^2 with f'') in Eq. (13) gives $n=2$. Now, choose an auxiliary solution for the balance number.

$$f(\xi)=a_0+a_1 sn(\xi)+a_2 sn^2(\xi)+b_1 sn^{-1}(\xi)+b_2 sn^{-2}(\xi). \tag{14}$$

Inserting $f(\xi)$ from Eq. (14) to the Eq. (13), then equating adjacent terms of $sn^i(\xi)$ to zero and solve these terms for a_0, a_1, a_2, b_1 and b_2, we get

Case-1:

$$k=\frac{1}{2\sqrt{d}\sqrt[4]{m^4+14m^2+1}},\ a_0=\frac{c\sqrt{d}\,(m^2+1-2\sqrt{(m^4+14m^2+1)})}{\varepsilon\sqrt[4]{m^4+14m^2+1}},$$

$$a_2=-\frac{3c\sqrt{d}\,m^2}{\sqrt[4]{m^4+14m^2+1}},\ b_2=-\frac{3c\sqrt{d}}{\varepsilon\sqrt[4]{m^4+14m^2+1}},\ a_1=0,\ b_1=0.$$

Case-2:

$$k=-\frac{1}{2\sqrt{d}\sqrt[4]{m^4+14m^2+1}},\ a_0=-\frac{c\sqrt{d}\,(m^2+1-2\sqrt{(m^4+14m^2+1)})}{\varepsilon\sqrt[4]{m^4+14m^2+1}},$$

$$a_2 = \frac{3c\sqrt{d}m^2}{\sqrt[4]{m^4+14m^2+1}},\ b_2 = \frac{3c\sqrt{d}}{\varepsilon\sqrt[4]{m^4-m^2+1}},\ a_1 = 0,\ b_1 = 0.$$

Case-3:

$$k = \frac{1}{2\sqrt{d}\sqrt[4]{m^4-m^2+1}},\ a_0 = \frac{c\sqrt{d}(m^2+1-2\sqrt{(m^4-m^2+1)})}{\varepsilon\sqrt[4]{m^4-m^2+1}},$$

$$b_2 = -\frac{3c\sqrt{d}}{\varepsilon\sqrt[4]{m^4-m^2+1}},\ a_1 = 0,\ a_2 = 0,\ b_1 = 0.$$

Case-4:

$$k = -\frac{1}{2\sqrt{d}\sqrt[4]{m^4-m^2+1}},\ a_0 = -\frac{c\sqrt{d}(m^2+1-2\sqrt{(m^4-m^2+1)})}{\varepsilon\sqrt[4]{m^4-m^2+1}},$$

$$b_2 = \frac{3c\sqrt{d}}{\varepsilon\sqrt[4]{m^4-m^2+1}},\ a_1 = 0,\ a_2 = 0,\ b_1 = 0.$$

Case:-5:

$$k = \frac{1}{2\sqrt{d}\sqrt[4]{m^4-m^2+1}},\ a_0 = \frac{c\sqrt{d}(m^2+1-2\sqrt{(m^4-m^2+1)})}{\varepsilon\sqrt[4]{m^4-m^2+1}},$$

$$a_2 = -\frac{3c\sqrt{d}m^2}{\varepsilon\sqrt[4]{m^4-m^2+1}},\ a_1 = 0,\ b_1 = 0,\ b_2 = 0.$$

Case-6:

$$k = -\frac{1}{2\sqrt{d}\sqrt[4]{m^4-m^2+1}},\ a_0 = -\frac{c\sqrt{d}(m^2+1-2\sqrt{(m^4-m^2+1)})}{\varepsilon\sqrt[4]{m^4-m^2+1}},$$

$$a_2 = \frac{3c\sqrt{d}m^2}{\varepsilon\sqrt[4]{m^4-m^2+1}},\ a_1 = 0,\ b_1 = 0,\ b_2 = 0.$$

Eq. (10) are reduced the following exact solutions by using (case-1-6)

$$\varphi(x,t)=\frac{c\sqrt{d}(m^2+1-2\sqrt{m^4+14m^2+1})}{\varepsilon\sqrt[4]{m^4+14m^2+1}}-\frac{3c\sqrt{d}m^2}{\sqrt[4]{m^4+14m^2+1}}sn^2(\frac{1}{2\sqrt{d}\sqrt[4]{m^4+14m^2+1}}\frac{1}{\Gamma(\beta)}x^\beta-\frac{c}{\Gamma(\beta)}t^\beta)$$

$$-\frac{3c\sqrt{d}}{\varepsilon\sqrt[4]{m^4+14m^2+1}}sn^{-2}(\frac{1}{2\sqrt{d}\sqrt[4]{m^4+14m^2+1}}\frac{1}{\Gamma(\beta)}x^\beta-\frac{c}{\Gamma(\beta)}t^\beta). \tag{15}$$

$$\varphi(x,t)=-\frac{c\sqrt{d}(m^2+1-2\sqrt{m^4+14m^2+1})}{\varepsilon\sqrt[4]{m^4+14m^2+1}}+\frac{3c\sqrt{d}m^2}{\sqrt[4]{m^4+14m^2+1}}sn^2(-\frac{1}{2\sqrt{d}\sqrt[4]{m^4+14m^2+1}}\frac{1}{\Gamma(\beta)}x^\beta-\frac{c}{\Gamma(\beta)}t^\beta)$$

$$+\frac{3c\sqrt{d}}{\varepsilon\sqrt[4]{m^4+14m^2+1}}sn^{-2}(-\frac{1}{2\sqrt{d}\sqrt[4]{m^4+14m^2+1}}\frac{1}{\Gamma(\beta)}x^\beta-\frac{c}{\Gamma(\beta)}t^\beta). \tag{16}$$

$$\varphi(x,t)=\frac{c\sqrt{d}(m^2+1-2\sqrt{m^4-m^2+1})}{\varepsilon\sqrt[4]{m^4-m^2+1}}-\frac{3c\sqrt{d}}{\varepsilon\sqrt[4]{m^4-m^2+1}}sn^{-2}(\frac{1}{2\sqrt{d}\sqrt[4]{m^4-m^2+1}}\frac{1}{\Gamma(\beta)}x^\beta-\frac{c}{\Gamma(\beta)}t^\beta). \tag{17}$$

$$\varphi(x,t)=-\frac{c\sqrt{d}(m^2+1-2\sqrt{m^4-m^2+1})}{\varepsilon\sqrt[4]{m^4-m^2+1}}+\frac{3c\sqrt{d}}{\varepsilon\sqrt[4]{m^4-m^2+1}}sn^{-2}(-\frac{1}{2\sqrt{d}\sqrt[4]{m^4-m^2+1}}\frac{1}{\Gamma(\beta)}x^\beta-\frac{c}{\Gamma(\beta)}t^\beta). \tag{18}$$

$$\varphi(x,t)=\frac{c\sqrt{d}(m^2+1+\sqrt{m^4-m^2+1})}{\varepsilon\sqrt[4]{m^4-m^2+1}}-\frac{3c\sqrt{d}m^2}{\varepsilon\sqrt[4]{m^4-m^2+1}}sn^2(\frac{1}{2\sqrt{d}\sqrt[4]{m^4-m^2+1}}\frac{1}{\Gamma(\beta)}x^\beta-\frac{c}{\Gamma(\beta)}t^\beta). \tag{19}$$

$$\varphi(x,t)=-\frac{c\sqrt{d}(m^2+1+\sqrt{m^4-m^2+1})}{\varepsilon\sqrt[4]{m^4-m^2+1}}+\frac{3c\sqrt{d}m^2}{\varepsilon\sqrt[4]{m^4-m^2+1}}sn^2(-\frac{1}{2\sqrt{d}\sqrt[4]{m^4-m^2+1}}\frac{1}{\Gamma(\beta)}x^\beta-\frac{c}{\Gamma(\beta)}t^\beta). \tag{20}$$

Eq. (15-20) represent the solutions in term of Jacobi elliptic function.
When $m\to 1$, the solutions Eq. (15-20) convert in the form,

$$\varphi(x,t)=-\frac{3c\sqrt{d}}{\varepsilon}-\frac{3c\sqrt{d}}{2}\tanh^2(\frac{1}{4\sqrt{d}}\frac{1}{\Gamma(\beta)}x^\beta-\frac{c}{\Gamma(\beta)}t^\beta)-\frac{3c\sqrt{d}}{2\varepsilon}\tanh^{-2}(\frac{1}{4\sqrt{d}}\frac{1}{\Gamma(\beta)}x^\beta-\frac{c}{\Gamma(\beta)}t^\beta). \tag{21}$$

$$\varphi(x,t)=\frac{3c\sqrt{d}}{\varepsilon}+\frac{3c\sqrt{d}}{2}\tanh^2(-\frac{1}{4}\frac{1}{\Gamma(\beta)}x^\beta-\frac{c}{\Gamma(\beta)}t^\beta)+\frac{3c\sqrt{d}}{2\varepsilon}\tanh^{-2}(-\frac{1}{4\sqrt{d}}\frac{1}{\Gamma(\beta)}x^\beta-\frac{c}{\Gamma(\beta)}t^\beta). \tag{22}$$

$$\varphi(x,t)=-\frac{3c\sqrt{d}}{\varepsilon}\tanh^{-2}(\frac{1}{2\sqrt{d}}\frac{1}{\Gamma(\beta)}x^{\beta}-\frac{c}{\Gamma(\beta)}t^{\beta}). \quad (23)$$

$$\varphi(x,t)=\frac{3c\sqrt{d}}{\varepsilon}\tanh^{-2}(-\frac{1}{2\sqrt{d}}\frac{1}{\Gamma(\beta)}x^{\beta}-\frac{c}{\Gamma(\beta)}t^{\beta}). \quad (24)$$

$$\varphi(x,t)=-\frac{3c\sqrt{d}}{\varepsilon}\tanh^{2}(\frac{1}{2\sqrt{d}}\frac{1}{\Gamma(\beta)}x^{\beta}-\frac{c}{\Gamma(\beta)}t^{\beta}). \quad (25)$$

$$\varphi(x,t)=\frac{3c\sqrt{d}}{\varepsilon}\tanh^{2}(-\frac{1}{2\sqrt{d}}\frac{1}{\Gamma(\beta)}x^{\beta}-\frac{c}{\Gamma(\beta)}t^{\beta}). \quad (26)$$

Solitary wave solutions Eq. (21-26) come in terms of hyperbolic functions form.
When $m \longrightarrow 0$, the solutions Eq. (15-20) convert in the form,

$$\varphi(x,t)=-\frac{c\sqrt{d}}{\varepsilon}-\frac{3c\sqrt{d}}{\varepsilon}\sin^{-2}(\frac{1}{2\sqrt{d}}\frac{1}{\Gamma(\beta)}x^{\beta}-\frac{c}{\Gamma(\beta)}t^{\beta}). \quad (27)$$

$$\varphi(x,t)=\frac{c\sqrt{d}}{\varepsilon}+\frac{3c\sqrt{d}}{\varepsilon}\sin^{-2}(-\frac{1}{2\sqrt{d}}\frac{1}{\Gamma(\eta)}x^{\eta}-\frac{c}{\Gamma('\eta)}t^{\eta}). \quad (28)$$

$$\varphi(x,t)=-\frac{c\sqrt{d}}{\varepsilon}-\frac{3c\sqrt{d}}{\varepsilon}\sin^{-2}(\frac{1}{2\sqrt{d}}\frac{1}{\Gamma(\beta)}x^{\beta}-\frac{c}{\Gamma(\beta)}t^{\beta}). \quad (29)$$

$$\varphi(x,t)=\frac{c\sqrt{d}}{\varepsilon}+\frac{3c\sqrt{d}}{\varepsilon}\sin^{-2}(-\frac{1}{2\sqrt{d}}\frac{1}{\Gamma(\beta)}x^{\beta}-\frac{c}{\Gamma(\beta)}t^{\beta}). \quad (30)$$

These are periodic wave solutions of the nonlinear-tfEW model and the other two solutions (19), (20) give constants only.

4.2 *Solutions of the WBBM model*

The space-time fractional WBBM equation [21] read as:

$$D_t^{\beta}\varphi(x,y,z,t)+D_x^{\beta}\varphi(x,y,z,t)+D_y^{\beta}\varphi(x,y,z,t)-D_{xzt}^{3\beta}\varphi(x,y,z.t)=0,\ t>0,\ 0<\beta\le 1. \quad (31)$$

Considering a travelling wave transformation for space-time fractional 3D WBBM model Eq. (31)

$$\varphi(x,t)=\varphi(\zeta),\ \zeta=\frac{1}{\Gamma(\beta)}(\ell x^{\beta}+\wp y^{\beta}+cz^{\beta}-wt^{\beta}). \quad (32)$$

Eq. (32) transform the WBBM Eq. (31) to the following nonlinear ODE,

$$(-w+\ell)\phi' + \wp(\phi^3)' + \ell c w \phi''' = 0. \tag{33}$$

Integrating Eq. (33) with respect to ζ, then Eq. (31) converted to the nonlinear ODE Eq. (34),

$$(-w+\ell)\phi + \wp\phi^3 + \ell c w \phi'' = 0. \tag{34}$$

Using the balancing role (ϕ^2 with ϕ'') in Eq. (34) gives $n = 1$. Now, choose an auxiliary solution for the balance number.

$$\phi(\zeta) = a_0 + a_1 sn(\zeta) + b_1 sn^{-1}(\zeta). \tag{35}$$

Plugging $\phi(\zeta)$ from Eq. (35) to the Eq. (34), then comparing the adjacent terms of $sn^i(\zeta)$ to zero and solving these algebraic equations for a_0, a_1, w and b_1, we get four sets of solutions.

Case-1:

$$w = \frac{\ell}{\ell cm^2 - 6\ell cm + \ell c + 1},\ a_0 = 0,\ a_1 = \pm \ell m\sqrt{\frac{-2c}{\wp(\ell cm^2 - 6\ell cm + \ell c + 1)}},\ b_2 = \pm \ell\sqrt{\frac{-2c}{\wp(\ell cm^2 - 6\ell cm + \ell c + 1)}}.$$

Case-2:

$$w = \frac{\ell}{\ell cm^2 + 6\ell cm + \ell c + 1},\ a_0 = 0,\ a_1 = \pm \ell m\sqrt{\frac{-2c}{\wp(\ell cm^2 + 6\ell cm + \ell c + 1)}},\ b_2 = \pm \ell\sqrt{\frac{-2c}{\wp(\ell cm^2 + 6\ell cm + \ell c + 1)}}.$$

Case-3:

$$w = \frac{\ell}{\ell cm^2 + \ell c + 1},\ a_0 = 0,\ a_1 = 0,\ b_2 = \pm \ell\sqrt{\frac{-2c}{\wp(\ell cm^2 + \ell c + 1)}}.$$

Case-4:

$$w = \frac{\ell}{\ell cm^2 + \ell c + 1},\ a_0 = 0,\ b_1 = 0,\ a_1 = \pm \ell m\sqrt{\frac{-2c}{\wp(\ell cm^2 + \ell c + 1)}}.$$

The exact solutions of Eq. (31) by using (case-1-4)

$$\varphi_{11}(x,t) = \ell\sqrt{\frac{-2c}{\wp(\ell cm^2 - 6\ell cm + \ell c + 1)}}\left\{\begin{array}{l} -m\,sn\left(\frac{1}{\Gamma(\beta)}(\ell x^\beta + \wp y^\beta + cz^\beta - wt^\beta)\right) \\ +sn^{-1}\left(\frac{1}{\Gamma(\beta)}(\ell x^\beta + \wp y^\beta + cz^\beta - wt^\beta)\right) \end{array}\right\}. \tag{36}$$

$$\varphi_{12}(x,t)=\ell\sqrt{\frac{-2c}{\wp(\ell cm^2-6\ell cm+\ell c+1)}}\left\{\begin{array}{l} msn(\frac{1}{\Gamma(\beta)}(\ell x^{\beta}+\wp y^{\beta}+cz^{\beta}-wt^{\beta})) \\ -sn^{-1}(\frac{1}{\Gamma(\beta)}(\ell x^{\beta}+\wp y^{\beta}+cz^{\beta}-wt^{\beta})) \end{array}\right\}. \quad (37)$$

In Eq. (36) and Eq. (37), $w=\dfrac{\ell}{\ell cm^2-6\ell cm+\ell c+1}$.

$$\varphi_{13}(x,t)=\ell\sqrt{\frac{-2c}{\wp(\ell cm^2+6\ell cm+\ell c+1)}}\left\{\begin{array}{l} msn(\frac{1}{\Gamma(\beta)}(\ell x^{\beta}+\wp y^{\beta}+cz^{\beta}-wt^{\beta})) \\ +sn^{-1}(\frac{1}{\Gamma(\beta)}(\ell x^{\beta}+\wp y^{\beta}+cz^{\beta}-wt^{\beta})) \end{array}\right\}. \quad (38)$$

$$\varphi_{14}(x,t)=-\ell\sqrt{\frac{-2c}{\wp(\ell cm^2+6\ell cm+\ell c+1)}}\left\{\begin{array}{l} msn(\frac{1}{\Gamma(\beta)}(\ell x^{\beta}+\wp y^{\beta}+cz^{\beta}-wt^{\beta})) \\ +sn^{-1}(\frac{1}{\Gamma(\beta)}(\ell x^{\beta}+\wp y^{\beta}+cz^{\beta}-wt^{\beta})) \end{array}\right\}. \quad (39)$$

In Eq. (38) and Eq. (39), $w=\dfrac{\ell}{\ell cm^2+6\ell cm+\ell c+1}$.

$$\varphi_{15}(x,t)=\ell\sqrt{\frac{-2c}{\wp(\ell cm^2+\ell c+1)}}sn^{-1}(\frac{1}{\Gamma(\beta)}(\ell x^{\beta}+\wp y^{\beta}+cz^{\beta}-wt^{\beta})). \quad (40)$$

$$\varphi_{16}(x,t)=-\ell\sqrt{\frac{-2c}{\wp(\ell cm^2+\ell c+1)}}sn^{-1}(\frac{1}{\Gamma(\beta)}(\ell x^{\beta}+\wp y^{\beta}+cz^{\beta}-wt^{\beta})). \quad (41)$$

$$\varphi_{17}(x,t)=\ell m\sqrt{\frac{-2c}{\wp(\ell cm^2+\ell c+1)}}sn(\frac{1}{\Gamma(\beta)}(\ell x^{\beta}+\wp y^{\beta}+cz^{\beta}-wt^{\beta})). \quad (42)$$

$$\varphi_{18}(x,t)=-\ell m\sqrt{\frac{-2c}{\wp(\ell cm^2+\ell c+1)}}sn(\frac{1}{\Gamma(\beta)}(\ell x^{\beta}+\wp y^{\beta}+cz^{\beta}-wt^{\beta})). \quad (43)$$

In Eq. (40), Eq. (41), Eq. (42) and Eq. (43), $w=\dfrac{\ell}{\ell cm^2+\ell c+1}$.

Eq. (36-43) represent the Jacobi elliptic function solutions of Eq. (31).
When $m\rightarrow 1$, the solutions Eq. (36-43) convert to the following form,

$$\varphi_{19}(x,t)=\ell\sqrt{\frac{-2c}{\wp(1-4\ell c)}}\begin{Bmatrix}-\tanh(\frac{1}{\Gamma(\beta)}(\ell x^{\beta}+\wp y^{\beta}+cz^{\beta}-wt^{\beta}))\\+\coth(\frac{1}{\Gamma(\beta)}(\ell x^{\beta}+\wp y^{\beta}+cz^{\beta}-wt^{\beta}))\end{Bmatrix}. \tag{44}$$

$$\varphi_{19}(x,t)=\ell\sqrt{\frac{-2c}{\wp(1-4\ell c)}}\begin{Bmatrix}\tanh(\frac{1}{\Gamma(\beta)}(\ell x^{\beta}+\wp y^{\beta}+cz^{\beta}-wt^{\beta}))\\-\coth(\frac{1}{\Gamma(\beta)}(\ell x^{\beta}+\wp y^{\beta}+cz^{\beta}-wt^{\beta}))\end{Bmatrix}. \tag{45}$$

In Eq. (44) and Eq. (45), $w=\frac{\ell}{(1-4\ell c)}$.

$$\varphi_{20}(x,t)=\ell\sqrt{\frac{-2c}{\wp(1+8\ell cm)}}\begin{Bmatrix}\tanh(\frac{1}{\Gamma(\beta)}(\ell x^{\beta}+\wp y^{\beta}+cz^{\beta}-wt^{\beta}))\\+\coth(\frac{1}{\Gamma(\beta)}(\ell x^{\beta}+\wp y^{\beta}+cz^{\beta}-wt^{\beta}))\end{Bmatrix}. \tag{46}$$

$$\varphi_{21}(x,t)=-\ell\sqrt{\frac{-2c}{\wp(1+8\ell c)}}\begin{Bmatrix}\tanh(\frac{1}{\Gamma(\beta)}(\ell x^{\beta}+\wp y^{\beta}+cz^{\beta}-wt^{\beta}))\\+\coth(\frac{1}{\Gamma(\beta)}(\ell x^{\beta}+\wp y^{\beta}+cz^{\beta}-wt^{\beta}))\end{Bmatrix}. \tag{47}$$

In Eq. (46) and Eq. (47) carry the value of $w=\frac{\ell}{(1+8\ell c)}$.

$$\varphi_{22}(x,t)=\ell\sqrt{\frac{-2c}{\wp(1+2\ell c)}}\coth(\frac{1}{\Gamma(\beta)}(\ell x^{\beta}+\wp y^{\beta}+cz^{\beta}-wt^{\beta})). \tag{48}$$

$$\varphi_{23}(x,t)=-\ell\sqrt{\frac{-2c}{\wp(1+2\ell c)}}\coth(\frac{1}{\Gamma(\beta)}(\ell x^{\beta}+\wp y^{\beta}+cz^{\beta}-wt^{\beta})). \tag{49}$$

$$\varphi_{25}(x,t)=-\ell\sqrt{\frac{-2c}{\wp(1+2\ell c)}}\tanh(\frac{1}{\Gamma(\beta)}(\ell x^{\beta}+\wp y^{\beta}+cz^{\beta}-wt^{\beta})). \tag{50}$$

In Eq. (48), Eq. (49) and Eq. (50), $w=\frac{\ell}{(1+2\ell c)}$.

Solitary wave solutions come from the hyperbolic functions Eq. (44-50).
When $m\longrightarrow 0$, the solutions Eq. (36-43) convert to the form,

$$\varphi_{25}(x,t) = \ell\sqrt{\frac{-2c}{\wp(1+\ell c)}}\left\{\cos ec\left(\frac{1}{\Gamma(\beta)}(\ell x^{\beta} + \wp y^{\beta} + cz^{\beta} - wt^{\beta})\right)\right\}. \tag{51}$$

$$\varphi_{26}(x,t) = \ell\sqrt{\frac{-2c}{\wp(1+\ell c)}}\left\{-\cos ec\left(\frac{1}{\Gamma(\beta)}(\ell x^{\beta} + \wp y^{\beta} + cz^{\beta} - wt^{\beta})\right)\right\}. \tag{52}$$

$$\varphi_{27}(x,t) = -\ell\sqrt{\frac{-2c}{\wp(1+\ell c)}}\left\{\cos ec\left(\frac{1}{\Gamma(\beta)}(\ell x^{\beta} + \wp y^{\beta} + cz^{\beta} - wt^{\beta})\right)\right\}. \tag{53}$$

In Eq. (51), Eq. (52) and Eq. (53), $w = \frac{\ell}{(1+\ell c)}$.

Eq. (36)-Eq. (43) are Jacobi functions solution of the nonlinear WBBM model. Out of the eight Jacobi elliptic functions, three of them are repeated and two results give zero solution. So, these five solutions are neglected.

5. Graphical representation

In this section, we will provide some graphical representations of the exact solutions of the space-time fractional Equal Width(s-tfEW) equation (Eq. (10)) and the space-time fractional Wazwaz-Benjamin-Bona-Mahony (s-tfWBBM) model (Eq. (31)). Graphical representations are portrayed below using the selected exact solutions of EW and WBBM model.

5.1 *Graphics of the solutions of s-tfEW equation*

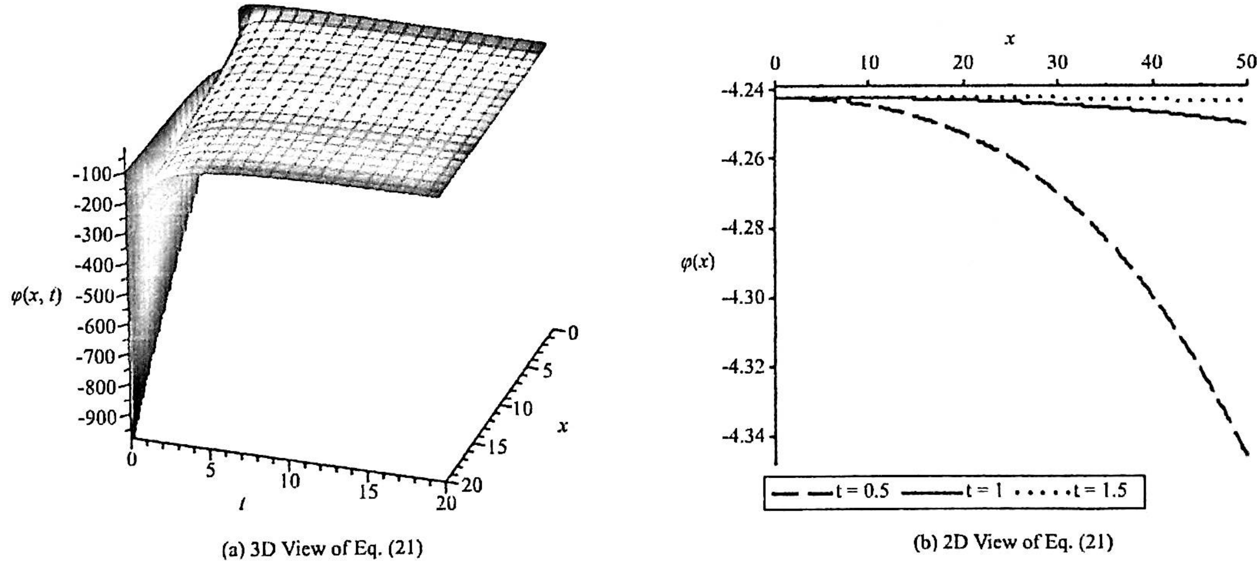

(a) 3D View of Eq. (21) (b) 2D View of Eq. (21)

Figure 1. Represent the solitary wave $\varphi(x, t)$ in Eq. (21) for the physical parametric values, $d = 0.5$, $\beta = 1/6$, $c = 1$, $\varepsilon = 1$: (a) 3D surface, (b) 2D graphs at $t = 0.5$, 1, 1.5.

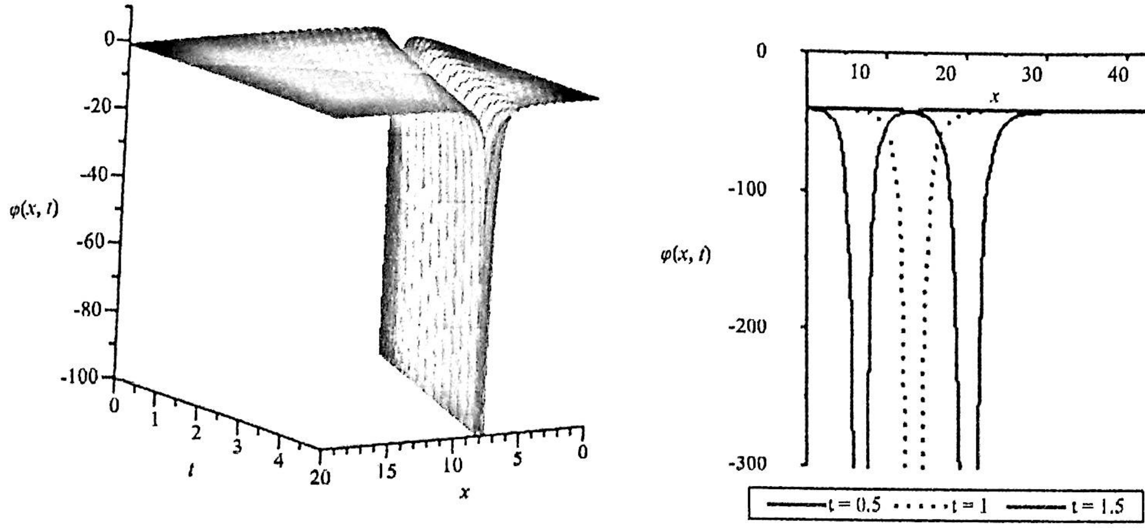

(a) 3D View of Eq. (23)

(b) 2D View of Eq. (23)

Figure 2. Represent the solitary wave $\varphi(x, t)$ in Eq. (23) for the physical parametric values, $d = 0.5$, $\beta = 3/4$, $c = 5$, $\varepsilon = 2$: (a) 3D surface and (b) 2D graphs at $t = 0.5, 1, 1.5$.

Three types of results are achieved for EW equation. All of the results are analysed and some of them are depicted in Figures (1-4). The graphs signify the change of amplitude, direction, shape of the derived wave solutions to identify the intrinsic nature of the model. The solution $\varphi(x, t)$ in Eq. (15-20) represents the Jacobi elliptic functions Eq. (21-26) shows the solitonic nature comes from hyperbolic function and Eq. (27-30) are trigonometric function exhibit as periodic waves.

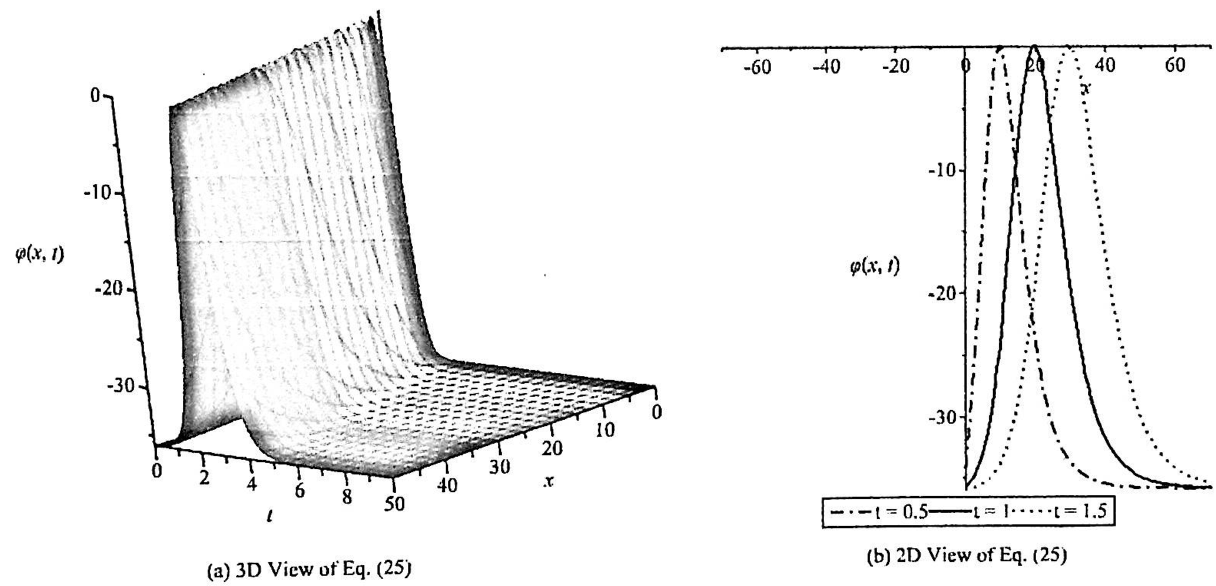

(a) 3D View of Eq. (25)

(b) 2D View of Eq. (25)

Figure 3. Represent the bell type solitary wave $\varphi(x, t)$ in Eq. (25) for the physical parametric values, $d = 1$, $\beta = 3/5$, $c = 3$, $\varepsilon = 0.25$: (a) 3D surface and (b) 2D graphs for and $t = 0.5, 1, 1.5$.

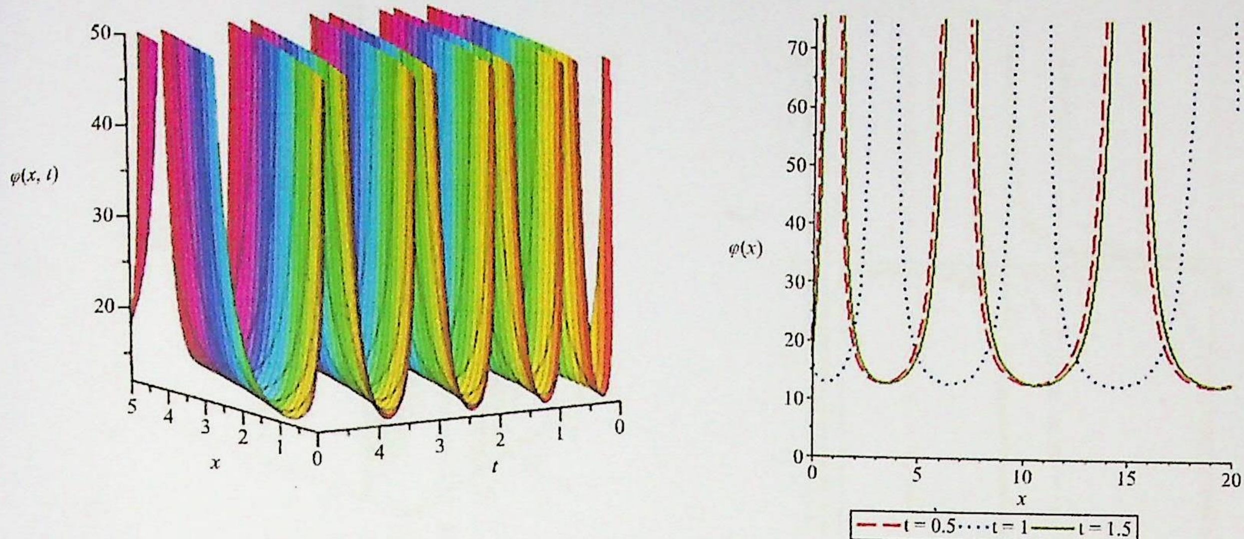

(a) 3D View of Eq. (27)

(b) 2D View of Eq. (27)

Figure 4. Represent the periodic wave of $\varphi(x, t)$ in Eq. (27) for the physical parametric values, $d = 0.5$, $\beta = 3/4$, $c = -3$, $\varepsilon = 1$: (a) 3D surface and (b) 2D graphs at $t = 0.5, 1, 1.5$.

5.2 *Graphics of the equation WBBM*

The findings of the research on WBBM model are in the types of hyperbolic (Eq. (44-51)) and trigonometric (Eq. (52-55)) functions. Hyperbolic and trigonometric functions represent solitonic and periodic solutions. All the results are analysed and two types of function have been shown graphically in Figure 5 to Figure 6.

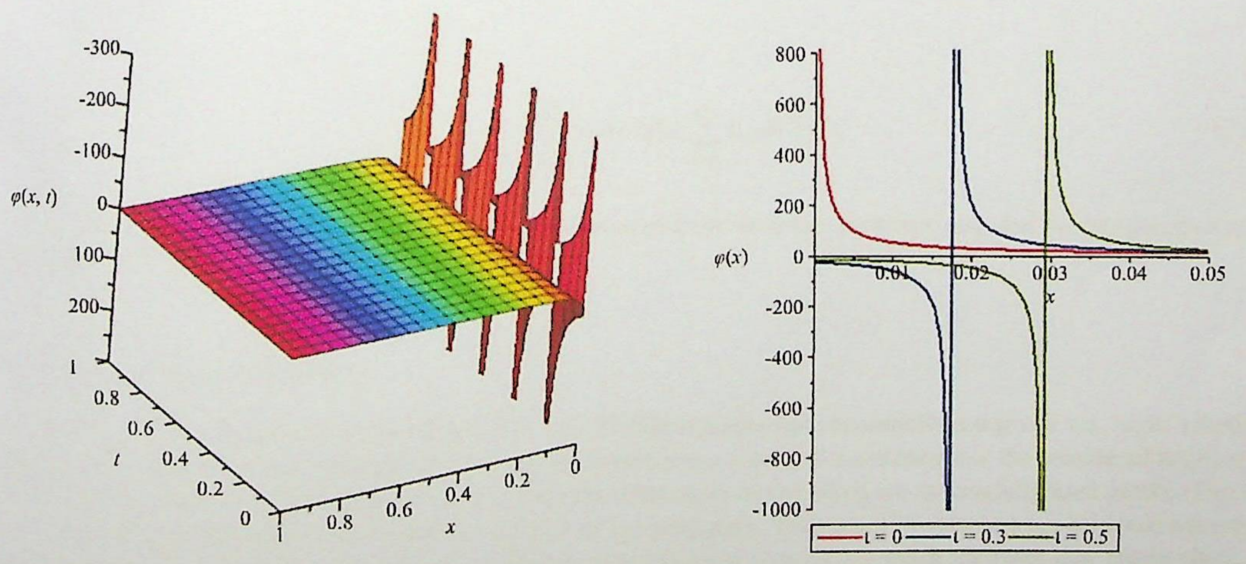

(a) 3D View of Eq. (48)

(b) 2DView of Eq. (48)

Figure 5. Represent the solitary periodic wave $\varphi(x, t)$ in Eq. (48) for the physical parametric values, $\beta = 0.99$, $l = 2$, $c = -2$, $\wp = 1$, $z = 0$, $y = 0$: (a) 3D surface, (b) 2D graphs at $t = 0$, 1.03, 0.5.

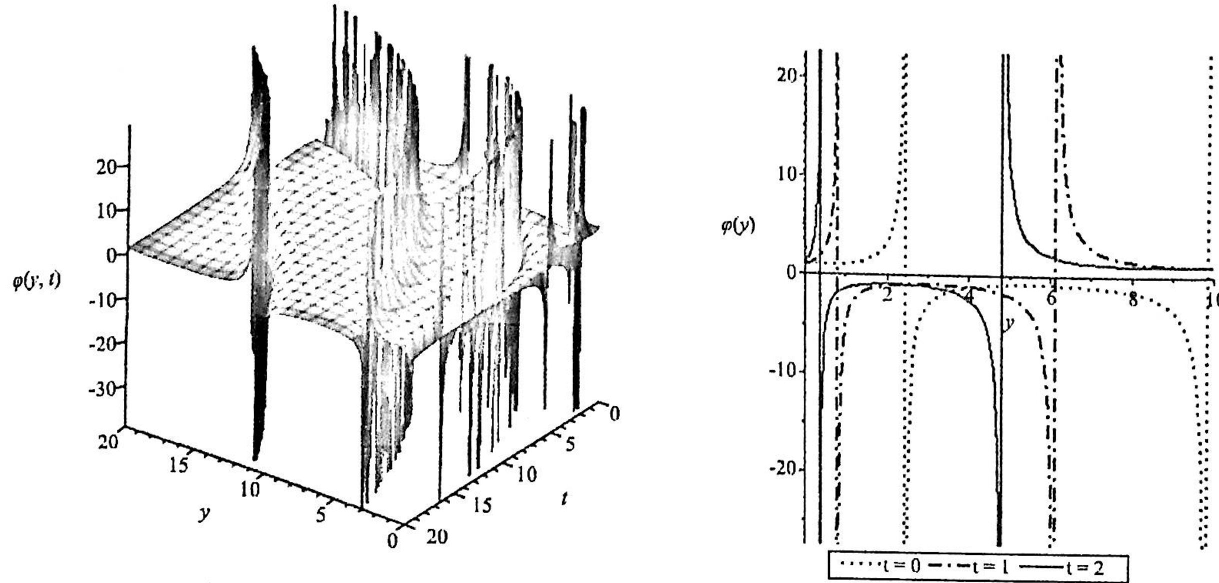

(a) 3D View of Eq. (52)

(b) 3D View of Eq. (52)

Figure 6. Represent the periodic wave $\varphi(x, t)$ in Eq. (52) for the physical parametric values, $\beta = 0.5$, $l = 2$, $c = -2$, $\wp = 1$, $z = 0$, $x = 0$: (a) 3D surface, (b) 2D graphs at $t = 0, 1.2$.

Remarks More other Jacobi function solutions to the s-tfEW and WBBM equation are derivable by keeping the trial solution in terms of the Jacobi functions $cn(\xi)$ and $dn(\xi)$ as below;

$$u(\xi) = a_0 + \sum_{i \to 1}^{n} a_i cn^i(\xi) + \sum_{i \to 1}^{n} a_{-i} cn^{-i}(\xi). \tag{54}$$

And

$$u(\xi) = a_0 + \sum_{i \to 1}^{n} a_i dn^i(\xi) + \sum_{i \to 1}^{n} a_{-i} dn^{-i}(\xi). \tag{55}$$

In view of Eq. (54) and Eq. (55), we can add soliton and non-solitonic solutions describe via cnoidal, dnoidal waves and trigonometric functions.

6. Concluding remarks

In this portion, the space-time fractional EW and WBBM equation has successfully integrated via Jacobi elliptic function expansion technique with beta-derivatives. By introducing a fractional transformation, the considered nonlinear partial travelling wave equation was reduced to ordinary differential model. Then we successfully used Jacobi elliptic expansion method to integrate the model. At the end of our procedure, three types of solutions are achieved namely, Jacobi elliptic, hyperbolic and trigonometric function with unknown parameters, which indicates that Jacobi elliptic expansion technique is very fruitful as well as appropriate to find the exact solutions of nonlinear fractional models. Here we, successfully derived cnoidal and dnoidal waves solutions to the fractional models which were not found in the previous literature. In addition, the graphical illustration of some different types of solutions has been plotted with unknown parameters in Figures (1-4) and Figures (5-6) for s-tfEW and WBBM respectively. Researchers can undoubtedly use the technique to analyse the internal mechanism of nonlinear physical systems.

Conflict of interest

Authors declared that they have no conflict of interest.

References

[1] Kara AH, Khalique CM. Nonlinear evolution-type equations and their exact solutions using inverse variational methods. *Journal of Physics A: Mathematical and General*. 2005; 38: 4629-4636.

[2] Matveev VB, Salle MA. *Darboux Transformation and Solitons*. Berlin: Springer; 1991.

[3] Ma WX, Huang T, Zhang Y. A multiple exp-function method for nonlinear differential equations and its application. *Physica Scripta*. 2010; 82: 065003.

[4] Malfliet W, Hereman W. The tanh method: I. Exact solutions of nonlinear evolution and wave equations. *Physica Scripta*. 1996; 54(6): 563-568.

[5] Rashid HO, Rahman MA. The exp$-\Phi(\eta)$-expansion method with application in the (1+1)-dimensional classical Boussinesq equation. *Result in Physics*. 2014; 4: 150-155.

[6] Feng Z. The first integral method to study the Burgers-Korteweg-de vries equation. *Journal of Physics A: Mathematical and General*. 2002; 35: 343-349.

[7] Hoque MF, Roshid HO. Optical soliton solutions of the Biswas-Arshed model by the tan(Θ/2)-expansion approach. Physica. *Scripta*. 2020; 95(7): 075219.

[8] Roshid HO, Ma WX. Dynamics of mixed lump-solitary waves of an extended (2+1)-dimensional shallow water wave model. *Physics Letter A*. 2018; 382(45): 3262-3268.

[9] Hossen MB, Roshid HO, Ali MZ. Characteristics of the solitary waves and rogue waves with interaction phenomena in a (2+1)-dimensional Breaking soliton equation. *Physics Letter A*. 2018; 382: 1268-1274.

[10] Wazwaz AM. *A* sine-cosine method for handling nonlinear wave equations. *Mathematical Computer Modelling*. 2004; 40: 499-508.

[11] Roshid HO, Alam MN, Hoque MF, Akbar MA. A new extended *(G'/G)*-expansion method to find exact traveling wave solutions of nonlinear evolution equations. *Mathematics and Statistics*. 2013; 1(3): 162-166.

[12] Hossen MB, Roshid HO, Ali MZ. Modified double sub-equation method for finding complexiton solutions to the (2+1)-dimensional nonlinear evolution equations. *International Journal of Applied Computational Mathematics*. 2017; 3(1): 679-697.

[13] Krishnan EV, Biswas A. Solutions to the Zakharov-Kuznetsov equation with higher order nonlinearity by mapping and ansatz methods. *Physics of Wave Phenomena*. 2010; 18(4): 256-261.

[14] Roshid HO, Khan MH, Wazwaz AM. Lump, multi-lump, cross kinky-lump and manifold periodic-soliton solutions for the (2+1)-D Calogero-Bogoyavlenskii-Schiff equation. *Heliyon*. 2020; 6(4): 03701.

[15] Dai CQ, Zhang JF. Jacobian elliptic function method for nonlinear differential-difference equations. *Chaos Soiton and Fractals*. 2006; 27: 1042-1049.

[16] Liu SK, Fu ZT, Liu SD. Jacobi elliptic function expansion method and periodic wave solutions of nonlinear wave equations. *Physics Letters A*. 2001; 289: 69-74.

[17] Zhang S, Zhang HQ. Fractional sub-equation method and its applications to nonlinear fractional PDEs. *Physics Letters A*. 2011; 375(7): 1069-1073.

[18] Hosseini K, Ayati J. Exact solutions of space-time fractional EW and modified EW equations using Kudrayshov method. *Nonlinear Science. Letter*. 2016; 7(2): 58-66.

[19] Benjamin TB, Bona JL, Mohony JJ. Model equations for long waves in nonlinear dispersive system. *Philosophical Transaction of Royel Society B Biological Sciences*. 1972; 272(1220): 47-78.

[20] Wazwaz AM. Exact soliton and kink solutions for new (3+1)-dimensional nonlinear modified equations of wave propagation. *Open Engineering*. 2017; 7: 169-174.

[21] Hosseini K, Mirzazadeh M, Ilie M, Gomez-Aguila JF. Biswas-Arshed equation with the beta time derivative: Optical solitons and other solutions. *Optik*. 2020; 217: 164801.

[22] Atangana A, Alqahtani RT. Modelling the spread of river blindness disease via the caputo fractional derivative and the beta-derivative. *Entropy*. 2016; 18: 40.

[23] Atangana A, Goufo EFD. Extension of matched asymptotic method to fractional boundary layers problems. *Mathematical Problem and Engineering*. 2014; 2014: 7. Available from: https://doi.org/10.1155/2014/107535.

[24] Hosseini K, Gomez-Aguilar JF. Soliton solutions of the sasa-satsuma equation in the monomode optical fibers including the beta-derivatives. *Optik*. 2020; 224: 165425.

[25] Hosseini K, Kaur L, Mirzazadeh M, Baskonus HM. 1-Soliton solutions of the (2+1)-dimensional Heisenberg ferromagnetic spin chain model with the beta-derivative. *Optical and Quantum Electrinics*. 2021; 53: 125.